Novel technologies applied to flavoromics and sensory evaluation of foods

Edited by
Geraldine M. Dowling and Michel Aliani

Published in
Frontiers in Nutrition

About Frontiers

Frontiers is more than just an open access publisher of scholarly articles: it is a pioneering approach to the world of academia, radically improving the way scholarly research is managed. The grand vision of Frontiers is a world where all people have an equal opportunity to seek, share and generate knowledge. Frontiers provides immediate and permanent online open access to all its publications, but this alone is not enough to realize our grand goals.

Frontiers journal series

The Frontiers journal series is a multi-tier and interdisciplinary set of open-access, online journals, promising a paradigm shift from the current review, selection and dissemination processes in academic publishing. All Frontiers journals are driven by researchers for researchers; therefore, they constitute a service to the scholarly community. At the same time, the *Frontiers journal series* operates on a revolutionary invention, the tiered publishing system, initially addressing specific communities of scholars, and gradually climbing up to broader public understanding, thus serving the interests of the lay society, too.

Dedication to quality

Each Frontiers article is a landmark of the highest quality, thanks to genuinely collaborative interactions between authors and review editors, who include some of the world's best academicians. Research must be certified by peers before entering a stream of knowledge that may eventually reach the public – and shape society; therefore, Frontiers only applies the most rigorous and unbiased reviews. Frontiers revolutionizes research publishing by freely delivering the most outstanding research, evaluated with no bias from both the academic and social point of view. By applying the most advanced information technologies, Frontiers is catapulting scholarly publishing into a new generation.

What are Frontiers Research Topics?

Frontiers Research Topics are very popular trademarks of the *Frontiers journals series*: they are collections of at least ten articles, all centered on a particular subject. With their unique mix of varied contributions from Original Research to Review Articles, Frontiers Research Topics unify the most influential researchers, the latest key findings and historical advances in a hot research area.

Find out more on how to host your own Frontiers Research Topic or contribute to one as an author by contacting the Frontiers editorial office: frontiersin.org/about/contact

Novel technologies applied to flavoromics and sensory evaluation of foods

Topic editors

Geraldine M. Dowling — Atlantic Technological University, Ireland

Michel Aliani — University of Manitoba, Canada

Table of
contents

*CORRESPONDENCE
Geraldine M. Dowling
✉ Geraldine.Dowling@atu.ie
Michel Aliani
✉ Michel.Aliani@Umanitoba.ca

Editorial: Novel technologies applied to flavoromics and sensory evaluation of foods

Geraldine M. Dowling[1,2,3]* and Michel Aliani[4,5]*

[1]Department of Life Sciences, School of Science, Atlantic Technological University, Sligo, Ireland,
[2]Cameron Forensic Medical Sciences, William Harvey Research Institutes, Barts and The London
School of Medicine and Dentistry, Queen Mary University of London, London, United Kingdom,
[3]Department of Analytical, Environmental and Forensic Sciences, School of Cancer and
Pharmaceutical Sciences, Faculty of Life Sciences and Medicine, King's College London, London,
United Kingdom, [4]Department of Food and Human Nutritional Sciences, Faculty of Agriculture and
Food Sciences, University of Manitoba, Winnipeg, MB, Canada, [5]The Division of Neurodegenerative
Disorders, St. Boniface Hospital Research Centre, Winnipeg, MB, Canada

Editorial on the Research Topic
Novel technologies applied to flavoromics and sensory evaluation
of foods

Flavoromics, an emerging field that combines chemometrics and progressive analytical techniques, aims to understand the complex processes behind flavor formation in foods. By using data from diverse samples, it helps address challenges such as distinguishing similar food products and ensuring authenticity.

Flavoromics

Flavoromics has the potential to transform various disciplines by providing a deeper understanding of the chemical compounds responsible for flavor. It can enhance food quality, support the development of functional foods and beverages and expand product formulations across industries. In the herbal and medicinal fields, flavoromics helps isolate bioactive compounds, supporting the discovery of new therapeutic properties. Flavoromics has promising applications in medicine, particularly by enhancing the sensory experience of food, supporting personalized nutrition, and hypothetically aiding in therapeutic and pharmaceutical applications. Its interdisciplinary applications extend to agriculture, biotechnology, and even environmental sciences, offering valuable insights for improving flavors, health benefits, and sustainability in diverse products and processes into the future.

Sensory evaluation, a key component of flavoromic studies, is defined as the scientific discipline dedicated to assessing the eating quality of food by systematically measuring human responses to its sensory attributes, including aroma, appearance, texture and flavor. This field relies on both qualitative and quantitative methods to capture how consumers perceive and interact with food products.

While sensory evaluation provides direct insights into human perception, it is often complemented by analytical and instrumental techniques. These tools are essential for identifying and quantifying the formation of specific chemical compounds responsible for the sensory characteristics detected by the olfactory (smell) and gustatory (taste) systems.

In complex food systems, the generation of flavor compounds is influenced by a wide range of chemical and biochemical reactions. These reactions can involve the breakdown of proteins, carbohydrates, and fats, as well as the interaction of enzymes, heat and pH conditions during food processing. Understanding these intricate processes is crucial for

optimizing product quality, enhancing sensory appeal and ensuring consistency in food production. Ultimately, sensory evaluation, combined with analytical techniques, provides a holistic approach to understanding and improving the overall sensory experience of food.

Advanced analytical techniques, including chromatography, mass spectrometry and spectroscopy, play a crucial role in dissecting the complex chemical profiles that define the flavor, aroma, and texture of food products. These methods enable precise identification and quantification of volatile and non-volatile compounds, providing a detailed understanding of the molecular components that contribute to sensory perception.

Several original research manuscripts presented here offer some key sensory methods and/or analytical tools used in flavoromics studies of orange juice, raw and pasteurized honey, tilapia by products, Fritillaria, rhubarb, steamed beef with rice flour, herbs, Zheng'an Bai tea and Saskatoon berry fortified Greek style frozen yogurt. Five of these studies included sensory evaluation methods and a range of instrumental measurements such as gas chromatography, mass spectrometry, nuclear magnetic resonance (NMR) spectroscopy, and electronic nose and electronic tongue.

Kardas, Kiciak et al., assessed the color of orange juice in the context of dietitian's food preferences. The research demonstrated that dietitian's preferred bright juices with a vibrant orange hue while product packaging influences the dietitian choice regardless of the content.

Ren et al., identified 16 novel salty peptides from hydrolysates of tilapia by products by batch molecular docking. They were predominately salty with a threshold of 0.256–0.379 mmol/L with some sourness and astringency where HLDDALR had the highest salty intensity.

Kardas, Staśkiewicz-Bartecka et al., studied the quality of selected raw and pasteurized honeys based on their sensory profiles and consumer preferences demonstrating consumer preference for the taste of pasteurized honeys.

Dai et al., explored the rapid detection of Fritillaria using gas chromatography ion mobility spectrometry to identify 67 volatile organic compounds which may be used for identification and authenticity determination of varieties of Fritillaria.

Liu T. et al., optimized a traditional method of rhubarb processing by combining flavor analysis with anthraquinone content. The results showed SDR-6 and SDR-9 in terms of smell, taste and composition indicating that the steaming and sun-drying cycles can be reduced from 9 to 6.

Wang et al., characterized the flavor profile of steamed beef with rice flour (SBD) using gas chromatography ion mobility spectrometry combined with electronic nose and tongue offering valuable insights into the industrial scale production and flavor regulation of SBD products.

Wu et al., developed an ic-CLEIA for precise detection of 3-CQA in herbs and patent medicines ensuring quality control and therapeutic efficiency with significant potential for diverse therapeutic milieus and applications.

Liu L. et al., used targeted metabolomics and SPME-GC-MS analysis to reveal the quality characteristics of non-volatile/volatile compounds in Zheng'an Bai tea which provided the foundation for further processing improvement.

Ryland et al., employed a flavoromics approach to investigate the effect of saskatoon berry powder on sensory attributes, acceptability, volatile components and electronic nose responses of a low-fat frozen yogurt with potential to fortified dairy products.

Together, these advanced technologies and studies facilitate a deeper understanding of the molecular basis of flavor and enable the development of innovative, high-quality food products tailored to consumer preferences. By integrating traditional analytical techniques with AI-driven data analysis, flavoromics provides a powerful framework for advancing sensory science and food innovation.

We hope this Research Topic will serve as a potential template for food scientists, researchers, food, and nutraceutical companies. Flavoromics has diverse applications. It could be used in medicine to improve the taste of medicines, particularly liquid medications or those intended for children or people with swallowing difficulties. By enhancing the flavor profile of medications, patient compliance and overall medication adherence can be improved. In addition, understanding the chemical components that contribute to flavor, food scientists can develop appealing, nutritious foods to inspire better dietary habits. The use of flavoromics in conjunction with genomics can help tailor dietary recommendations based on an individual's genetic makeup and flavor preferences. This can potentially lead to personalized nutrition plans that enhance health outcomes and prevent disease. More research in flavoromics can also contribute to the development of functional foods developed to prevent or manage conditions such as cardiovascular disease, diabetes, and obesity by understanding how specific flavor compounds influence biological systems, like metabolism and blood sugar regulation.

Author contributions

GD: Writing – original draft, Writing – review & editing. MA: Writing – original draft, Writing – review & editing.

Acknowledgments

Conflict of interest

The authors declare that the research was conducted in the absence of any commercial or financial relationships that could be construed as a potential conflict of interest.

Publisher's note

All claims expressed in this article are solely those of the authors and do not necessarily represent those of their affiliated organizations, or those of the publisher, the editors and the reviewers. Any product that may be evaluated in this article, or claim that may be made by its manufacturer, is not guaranteed or endorsed by the publisher.

Identification and virtual screening of novel salty peptides from hydrolysate of tilapia by-product by batch molecular docking

Hongjun Ren[1], Jingxuan Zhou[1], Huixian Fu[1], Qiaohui Feng[1], Jionghao Wang[1], Chuan Li[1,2,3], Guanghua Xia[1,2,3], Wenting Shang[1] and Yanfu He[1,2,3]*

[1]College of Food Science and Engineering, Hainan University, Haikou, China, [2]Hainan Provincial Engineering Research Centre of Aquatic Resources Efficient Utilization in the South China Sea, Haikou, China, [3]Key Laboratory of Seafood Processing of Haikou, Haikou, China

Introduction: Tilapia produces a large number of by-products during processing, which contain potentially flavorful peptides.

Methods: The application of PyRx software enabled batch molecular docking andscreening of 16 potential salty peptides from 189 peptides identified in the enzymaticdigestion of tilapia by-products.

Results: According to sensory analysis, all 16 peptides werepredominantly salty with a threshold of 0.256 - 0.379 mmol/L with some sournessand astringency, among which HLDDALR had the highest salty intensity, followedby VIEPLDIGDDKVR, FPGIPDHL, and DFKSPDDPSRH.I addition, moleculardocking results showed these four core peptides with high salt intensity bound to thesalt receptor TRPV1 mainly via van der Waals interactions, hydrogen bonds, andhydrophobic forces; Arg491, Tyr487, VAL441, and Asp708 were the key sites for thebinding of salty peptides to TRPV1. Therefore, the application of batch moleculardocking using PyRx is effective and economical for the virtual screening of saltypeptides.

KEYWORDS
tilapia by-product hydrolysate, salty peptide, salt receptor, TRPV1, virtual screening, molecular docking

1 Introduction

As standards of living improve, people are becoming increasingly concerned about the health of their diets. Many diseases such as hypertension, kidney disease, cardiovascular disease, and osteoporosis are associated with excessive salt intake, so there is a need to develop salt substitutes that reduce sodium intake while maintaining the saltiness of foods. Many researchers have proposed different solutions to reduce sodium chloride (NaCl) content in foods without altering the original salty taste, such as substitution with other metallic salts, the addition of flavor enhancers, and improvement of NaCl taste perception by taste contrast, and several salt substitutes have been reported to reduce dietary salt levels in foods; however, the successful implementation of salt reduction strategies depends on several factors, including their effects on food taste. Alio et al. (1) used KCl, CaCl$_2$, and MgCl$_2$ as partial substitutes for NaCl in dry-cured ham; better dehydration and curing were observed with KCl replacing 50% of NaCl, whereas CaCl$_2$ and MgCl$_2$ partially replacing NaCl resulted in a burnt taste quality defect. However, too high of a replacement with KCl can lead to bitter and metallic flavors,

e.g., replacing 50% NaCl with KCl in bread making is organoleptically acceptable but leaves a poor aftertaste and flavor as the potassium salt itself may give a bitter/metallic off-flavor (2). Flavor enhancers, such as monosodium glutamate (MSG), inorganic phosphate nucleotides (IMP/GMP), herb and spice blends, certain alkaline amino acids, and salty peptides (3), are another important salt reduction strategy that can increase the perception of salt when mixed with salt, but not their salty taste. However, MSG and IMP/GMP still contain a certain amount of Na ions and carry some risk of harm to the body.

Although they have a salty taste, salty peptides do not contain Na ions, and their nutritional and functional characteristics have received widespread attention. They can replace salt for food cooking or processing to a certain extent. Their use, development, and application prospects are broad (3). Zheng et al. (4) discovered five salty peptides of ASP-Asp, Glu-ASP, ASP-Asp-Asp, Ser-PRO-Glu, and PHE-DILE from yeast extracts. Mushroom fungi are the main source of microbial salty peptides, and (5) isolated pyroglutamine dipeptide from mushroom protein hydrolysate, which can improve the salty taste of a solution. A polypeptide EDEGEQPRPF was separated and purified from commercial soy by Chen et al. (6), which not only has a salty taste, but also has a synergistic effect with NaCl, that is, the salty strength of 0.4 mg/mL salt peptide added to 50 mmol/L NaCl solution is equivalent to 63 mmol/L NaCl solution, and the salty flavor strength is increased by 26%.

Tilapia, scientifically known as *Oreochromis mossambicus*, is a tropical fish of African origin that is capable of living in highly saline waters. Numerous by-products containing potentially bioactive proteins are produced during the processing of tilapia, of which the rational exploitation provides abundant high-quality protein resources for humans, and the preparation of protein hydrolyzed flavor peptides using aquatic by-products has been a hot research topic.

Salinity receptors include both transient receptor potential cation channel subfamily V member 1 (TRPV1) and epithelial Na$^+$ channels (ENaCs) (7, 8). ENaCs play a major role in Na$^+$-triggered salt signaling and are highly sensitive to amiloride administration, whereas TRPV1 is a cation non-selective pathway that is insensitive to one or more amilorides (9). TRPV1 is best known as the capsaicin receptor, but can also be activated by calmodulin, peptides, endogenous lipids, ATP, acidity (pH <5.9), and temperature (>43°C), suggesting that it is a pleiotropic receptor (10). Investigation of the TRPV1 receptor structure revealed that its three-dimensional structure resembles the homotetramer of a voltage-gated ion channel (VGIC) with six highly conserved transmembrane (TM) structural domains (S1 ± S6), with transmembrane helices S5 and S6 forming the ion permeation pathway and transmembrane helices S1 to S4 forming the central pore ring region (11). Salty peptides can generate cations by ionization, some of which are used in taste transduction processes to convert chemical signals into molecular second messengers, causing the interaction between cations and taste receptor cells, activating ion channels on taste receptor cells' surfaces, and triggering depolarization

and Ca^{2+} release from taste receptor cells, which in turn transmits the "salty" signal to the brain (12).

The identification of flavor peptides from food constituents is an important challenge. Although traditional multiplex chromatographic purification methods can identify small amounts of peptides, they are time-consuming and may affect the accuracy of the results (13). Currently, gel filtration, ion exchange, and reversed-phase high-performance liquid chromatography (HPLC) are commonly used to determine peptide fractions in hydrolysis products or aqueous extracts, followed by tandem mass spectrometry for peptide identification (5, 6, 14). Therefore, the identification of salt peptides requires high throughput, high sensitivity, and high accuracy methods. Virtual screening is a class of screening techniques consisting of bioinformatics, molecular docking, and other techniques (15). Many studies have accurately screened peptides with different flavors using molecular docking techniques (16–19).

Consequently, in the present study, we propose to use tilapia by-products to prepare taste-active peptides by enzymatic digestion, identify salty taste peptides using a high-throughput screening method based on peptidomics and virtual screening, and further evaluate the binding mechanism of salty peptides to the TRPV1 receptor to lay the foundation for the application of developing salty substances of natural origin.

2 Materials and methods

2.1 Materials

Tilapia by-products were purchased from Hainan Xiangtai Fishery Co, Ltd. (Chengmai County, Hainan Province, China), boiled in water for 15 min to inactivate the endogenous protease activity, then stirred, portioned, and stored at −20°C. The potential salt peptides were synthesized by Nanjing Peptide Biotechnology Co. Ltd. (Nanjing, Jiangsu Province, China), with a purity of 98%. Papain was purchased from Henan Shengsted Industrial Company (Zhengzhou, Henan Province, China). All chemicals and solvents were analytical grades.

2.2 Preparation of salty peptide component by hydrolyzing tilapia by-product

A previous study by our group found that tilapia by-products hydrolyzed with papain had the highest salty taste score. Therefore, the preparation of enzymatic hydrolysate of tilapia by-products was based on the method of Gan et al. (20). By-products were added to distilled water at a solid–liquid ratio of 1:3 and homogenized in an ice bath. After being pH-adjusted with 1 mol/L NaOH or HCl solution, the mixture was shaken in a constant temperature and shaker water bath. Based on the results of our previous study, the optimal enzymatic conditions for papain are as follows: 0.8% enzyme addition, 50°C enzymatic temperature, pH 7.5, and 6 h enzymatic time. Enzymatic products were inactivated at 95°C for 15 min.

Enzyme hydrolysate was centrifuged and ultrafiltered at 4°C using an ultrafiltration tube (Millipore, Massachusetts, United States) with a cut-off relative molecular weight (MW) of 2.0 kDa. Fractions with a MW less than 2.0 kDa were retained for subsequent peptide identification.

2.3 Peptide identification

Liquid chromatography-tandem mass spectrometry (LC-MS/MS) detection: After desalting, each sample was separated by the nanoUPLC liquid phase system EASY-nLC1200 and data were collected using a mass spectrometer equipped with a nanoliter ion source. The mobile phase was an acetonitrile-water-formic acid system, where mobile phase A contained 2% acetonitrile, 98% H_2O, and 0.1% formic acid, and phase B contained 80% acetonitrile, 20% H_2O, and 0.1% formic acid. After equilibration of the column with 100% phase A, the sample was injected through an autosampler and separated by a column gradient at a flow rate of 300 nL/min and a gradient duration of 120 min. The mobile phase B ratio was: 2%–5% for 2 min, 5%–22% for 88 min, 22%–45% for 26 min, 45%–95% for 2 min, and 95% for 2 min. Mass spectrometry (MS) was performed in data-dependent acquisition mode with positive ion detection, 120k resolution, automatic gain control (AGC) of 3E6, max IT 50 ms, and a primary scan range of 350–1,600 m/z. The 20 most intense ions in the primary scan were screened by a four-stage rod and then scanned for fragment ions using high-energy induced cleavage with 15k resolution and an AGC of 1E5, max IT 50 ms. The dynamic exclusion time was set to 45 s according to the peak width; the secondary scan was not performed for single-charged and >6-valent ions.

Identification of library searches and protein quantification: raw data files were first converted to the common mzML file format using ProteoWizard software (version 3.0.18299). The MS data were matched to the corresponding species-level database sequence (uniprotOreochromis+Niloticus.fasta) using MSFragger software, and the main search parameters were according to the developer's recommendations. Enzyme specificity was set to: non-specific; allowed peptide length range: 7–25; variable modifications included: 15.994915 [M], 42.010565 [nterm]; [C] without alkylation modification; parent ion mass accuracy: +/20 ppm; fragment ion accuracy: +/20 ppm. MSFragger library search results were then analyzed using the Philosopher (v3.3.11) toolset for subsequent analysis, primarily including PeptideProphet (v5.2.1) for peptide false discovery rate (1%) control and ProteinProphet (v5.2.1) for protein false discovery rate (1%) control. Quantification analysis was performed using the frequent module, and additional maxLFQ analysis was performed using IonQuant with a min ratio count of 1.

2.4 Homology modeling of salty taste receptor

The crystal structure of TRPV1 as a human salt receptor remains unclear, therefore, homology modeling was used to construct its three-dimensional (3D) structure. The amino acid sequence of TRPV1 was obtained from the UniProt database at https://www.UniProt.org/ (protein accession number Q8NER1). The template (PDB: 7LQY) was selected and homology modeling was performed using SwissModel.[1] To further assess the quality of the model, the modeling was performed using SAVES,[2] and the optimized homology model was evaluated using the residual percentage of Ramachandran plots (PROCHECK). The validated homology model was further used for molecular docking.

2.5 Virtual screening of salty peptides by molecular docking

Peptide structures were drawn using Chem Draw 14.0 (Cambridge soft, Cambridge, United States) and hydrogen atoms were added to the CHARMM force field in PyMOL (Schrödinger, LLC., New York, NY, United States). Batch energy minimization and format conversion of 3D peptide structures using PyRx (SourceForge, San Diego, United States) and batch molecular docking of 3D peptide structures to receptors accelerated the virtual peptide screening process and reduced operational complexity (21). The AutoDock Vina docking software (Scripps Research Institute Molecular Graphics Laboratory, La Jolla, CA, United States) included with PyRx was used to perform molecular docking. A semi-flexible docking method was chosen for the docking process. Peptides with docking energy < −8 kcal/mol were further synthesized and verified.

2.6 Validation of salty peptides

2.6.1 Sensory evaluation

Sensory evaluation was based on the method proposed by Gan et al. (20) with some modifications. The sensory evaluation team consisted of eight sensory evaluators, aged 20–25 years, four males and four females, who were uniformly screened and professionally trained. The evaluators were trained in advance using 50 mg/mL NaCl as a reference solution for salty taste. The salty taste of each synthetic peptide was rated at room temperature (25 ± 1°C) using the 10-point method, with 0–3 being weak, 4–6 being standard, and 7–10 being strong.

2.6.2 Taste dilution analysis

To further understand the flavor properties, the taste dilution analysis (TDA) method was used to assess the flavor recognition thresholds of the synthetic peptides and to define their palatability. Taste peptides were prepared at a concentration of 1 mg/mL and diluted in a 1:1 series with deionized water until just separated from the blank control. The maximum dilution concentration that could be accurately judged by trained sensory panel members was used as the salty taste detection threshold for the peptide.

2.6.3 Electronic tongue analysis

According to the method of Zhang et al. (15), the peptides were prepared at a concentration of 0.5 mg/mL, loaded into special beakers for the electronic tongue, and placed on an autosampler and analyzer. Each sample was repeated four times and the data from the first time were removed. The response characteristics of the Insent SA402B electronic tongue sensors AAE, CT0, CA0, C00, and AE1 were fresh,

---

1 https://swissmodel.expasy.org/

2 https://SAVES.mbi.UCLA.edu/

salty, sour, bitter, and astringent flavors. The sensor and reference probes were immersed in the sample solution for 30 s to detect membrane potential changes and the same concentration of KCl solution was used as a standard control.

2.7 Statistical analysis

SPSS 23.0 was used to process the relevant data for ANOVA and significance testing, and each group of experiments was repeated three times to calculate the mean; Origin 2022 was used for graphing.

3 Results and discussion

3.1 Identification of salty peptides from hydrolysate of tilapia by-product by nano-HPLC-MS/MS

Previous studies found that the MW of peptides with high flavor activity was mainly concentrated in the range of <1,500 Da (22). Therefore, in this study, hydrolysate with a strong salty flavor was ultrafiltered and the AA sequences of peptides in the ultrafiltered fractions were determined by nano-UPLC-MS/MS.

A total of 189 peptides (Supplementary Table S1) were detected in three parallel samples, 85.6% of which had molecular weights <1,500 Da, and the sequence length distribution of the identified peptides was analyzed (Supplementary Figure S1), which mainly consisted of 12–14 AAs, followed by 10–11 AAs, with a smaller distribution of peptides with less than 10 AAs. Subsequently, 189 peptide sequences were used for the virtual screening of potential salty peptides.

3.2 Homology modeling of TRPV1 receptor

Although TRPV1 is associated with salty taste sensitivity (23), few studies have elucidated the mechanism of salty taste by molecular docking between salty taste receptor TRPV1 and salty substances. There is currently no definitive 3D structure of TRPV1 in the Protein Structure Data Bank (PDB); therefore, a model of the TRPV1 receptor must be obtained via homology modeling. The AA sequence of TRPV1 was searched in the Protein Data Bank (Uniprot) and the homologous sequence obtained, Q8NER1, was used as a template for TRPV1 to be submitted to the SwissModel server for homology modeling analysis. TRPV1 with PDB ID 7LQY was selected as the template to construct the best model. The analysis results showed that the sequence similarity of TRPV1 was 85.35%. Meanwhile, the Ramachandran plot calculated by SVAE showed that 100% of the AA residues were within a reasonable range, where the optimal region was 86.5%, the acceptable region was 12.9%, the generally acceptable region was 0.7%, the disagreed region was 0.00% (Figure 1A). It is generally accepted that the sequence similarity between the target and template is 30% (24) and the AA residues in the disallowed region are <5% (25). Thus, the homologous model was successfully used to predict the protein structure. Since TRPV1 is a homotetramer protein consisting of four monomers, the A chain of TRPV1 was extracted as an acceptor (TRPV1 A) for molecular docking (Figure 1B). These

results suggest that the TRPV1 model constructed in this study can be used as a receptor for further docking analysis.

3.3 Virtual screening of potential salty peptides by molecular docking and their taste characteristics

After establishing a reasonable homology model, the binding pocket of the salty receptor TRPV1 was predicted by Discovery Studio as shown in Figure 2, where the predicted pocket is composed of red spheres and the green represents the binding sites in the binding pocket. Similar to the binding pocket of TRPV1 as a capsaicin or cannabinoid receptor (19, 26), the binding pocket is formed by S3, S4, and S4–S5 junctions in the membrane (27). However Li et al. (26), found that endogenous cannabinoids can also bind to TRPVl, but the details of the ligand-TRPVl interaction are different from those of capsaicinoids; hydrogen bonds between capsaicinoids and T551 are important for their binding, but no hydrogen bonds are formed between endogenous cannabinoids and T551. They suggested that van der Waals interactions between the tail of the ligand and the receptor channel protein are the main factors affecting the binding conformation of endogenous cannabinoids to TRPVl. Thus, differences in the binding pocket in terms of key AA residues, ligand structure, and the forces formed by the AA residues with the ligand may be important for the different tastes perceived by TRPV1 as a receptor. The binding pocket was, therefore, used to further investigate the binding mechanism between the salty peptide and TRPV1 and red balls form the active binding pockets of the salty receptor TRPV1.

Batch molecular docking of the ligand to the TRPV1 receptor was performed by generating 189 peptide 3D structure files and using AutoDockVina under PyRx. The docking energies of the 189 peptides are listed in Supplementary Table S1. Docking energy is the main reference indicator for screening ligand-receptor interactions, and the value of the docking energy indicates the strength of affinity between the ligand and receptor. Sixteen of 189 peptides were screened according to the docking energy, as shown in Supplementary Table S2, and their docking energies are less than −8 kcal/mol; docking energy less than −7.0 kcal/mol indicates a strong binding activity between ligand and receptor, and the lower the docking energy, the more stable the receptor-ligand complex (28). As more than 60 of the 189 peptides had docking energies less than −7 kcal/mol (Supplementary Table S1), we selected 16 peptides with docking energies less than −8 kcal/mol for further analysis.

To further understand the taste properties of the salty peptides, the taste recognition thresholds of 16 synthetic peptides were evaluated using TDA, and their taste ability was defined. As shown in Supplementary Table S2, the taste recognition thresholds of the 16 peptides ranged from 0.256–0.379 mmol/L, and their salty taste thresholds were all lower than that of salt, indicating that the synthetic peptides were highly salty, but many of them also had some sour and astringent tastes. Chen et al. (6) identified the taste active peptides from Chinese curd; Glu-Asp-Glu-Gly-Glu-Gln-Pro-Arg-Pro-Phe was the most promising salt-tasting peptide and a 50 mmol/L NaCl solution containing 0.4 mg/mL of the peptide was equivalent to the salt-tasting level of a 63 mmol/L NaCl solution. Shan et al. (29) reported that four peptides, PKLLLLPKP,
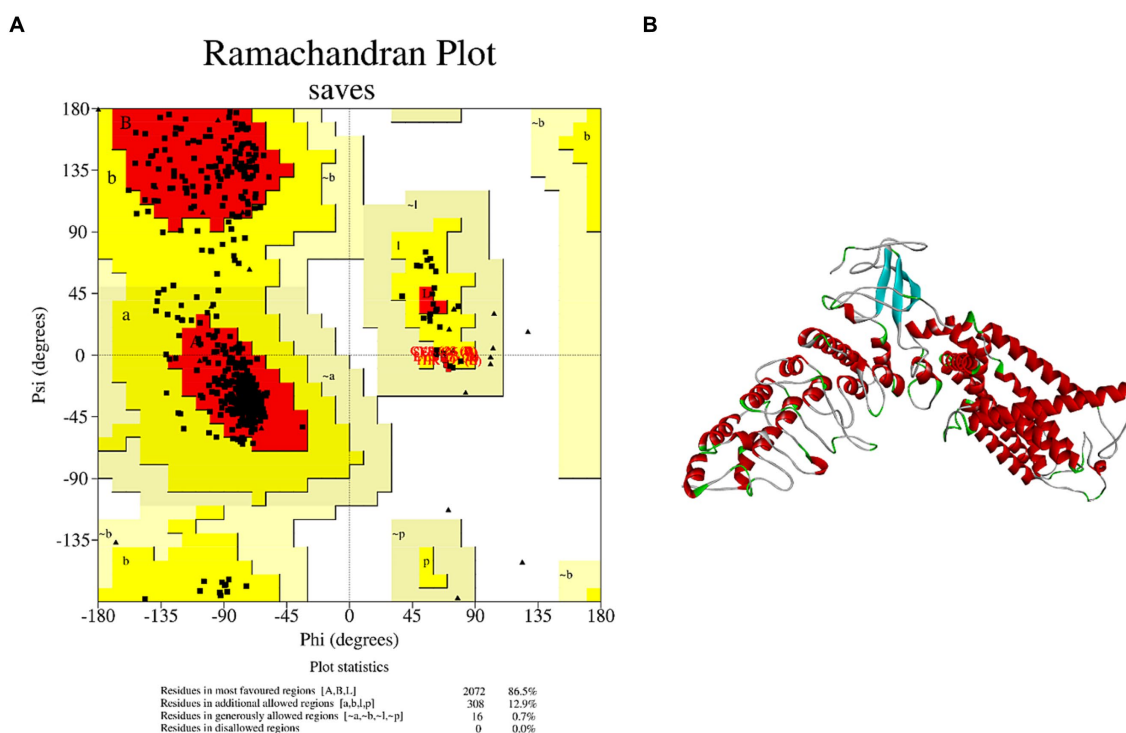
FIGURE 1
Homology modeling of TRPV1 and its reliability. **(A)** Ramachandran plot of TRPV1. **(B)** 3D structure of salty receptor TRPV1 subunit.
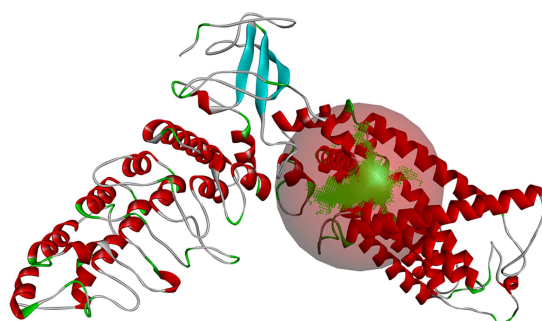
FIGURE 2
The predicted binding pocket of salty receptor TRPV1. The green area and red balls form the active binding pockets of the salty receptor TRPV1.

GGISTGNLN, LVKGGLIP, and SSAVK isolated from yeast extract had high salt-taste enhancing effects with their thresholds ranging from 0.18–0.59 mmol/L.

The 16 potential salty peptides identified from the enzymatic digestion of tilapia by-products were synthesized and their salty taste characteristics were verified using the electronic tongue system. The principal component analysis (PCA) and taste radar plots of the 16 synthesized peptides by e-tongue analysis are shown in Figures 3A,B. The taste characteristics of the 16 synthetic peptides had the same trend, where salty was the strongest, followed by sour and astringent; moreover, the 16 peptides had the same intensity of astringency, fresh taste, and richness, bitter aftertaste (aftertaste-A)

and astringent aftertaste (aftertaste-B) were not prominent, and bitter was the weakest, with their intensities lower than that of KCl (Figure 3A). Among the 16 synthetic peptides, HLDDALR had the highest salty taste intensity score (11.56), followed by VIEPLDIGDDKVR (9.47), FPGIPDHL (9.30), and DFKSPDDPSRH (9.17). However, as shown in Supplementary Table S2, the peptides with the lowest docking energies were FPGDFTPEVH and VIEPLDIGDDKVR, both at −9 (kcal/mol), followed by GEIDEFLPAPR and VFDISNADRLG, both at −8.6 (kcal/mol). The salt intensity of several of the 16 peptides, except VIEPLDIGDDKVR, was not particularly prominent, suggesting that the docking energies were not consistent with the salt intensity. Therefore, we speculated that although molecular docking can be used to predict the taste characteristics of salty peptides, the intensity of salty taste cannot be predicted by the docking energy alone and this must be combined with sensory evaluation and e-tongue. This is similar to the results of previous studies (30, 31).

To further analyze the differences between the different peptides, the e-tongue response scores of freshness, saltiness, sourness, bitterness, bitter aftertaste, and astringent aftertaste in the samples were selected for PCA, and the contributions of PC1 and PC2 were 41.7% and 31.8%, respectively (Figure 3B). Salty aftertaste had the greatest effect on PC1, followed by astringent and bitter aftertaste, while sourness and richness had a greater effect on PC2. Sixteen peptides were separated mainly along PC1 and four peptides, HLDDALR, VIEPLDIGDDKVR, FPGIPDHL, and DFKSPDDPSRH, were similarly distributed and close to the salty taste. It was further confirmed that the four salty peptides had a relatively high salty taste intensity.

FIGURE 3
Taste radar map **(A)** and principal component analysis (PCA) plot **(B)** of the 16 potential salty peptides analyzed by e-tongue.
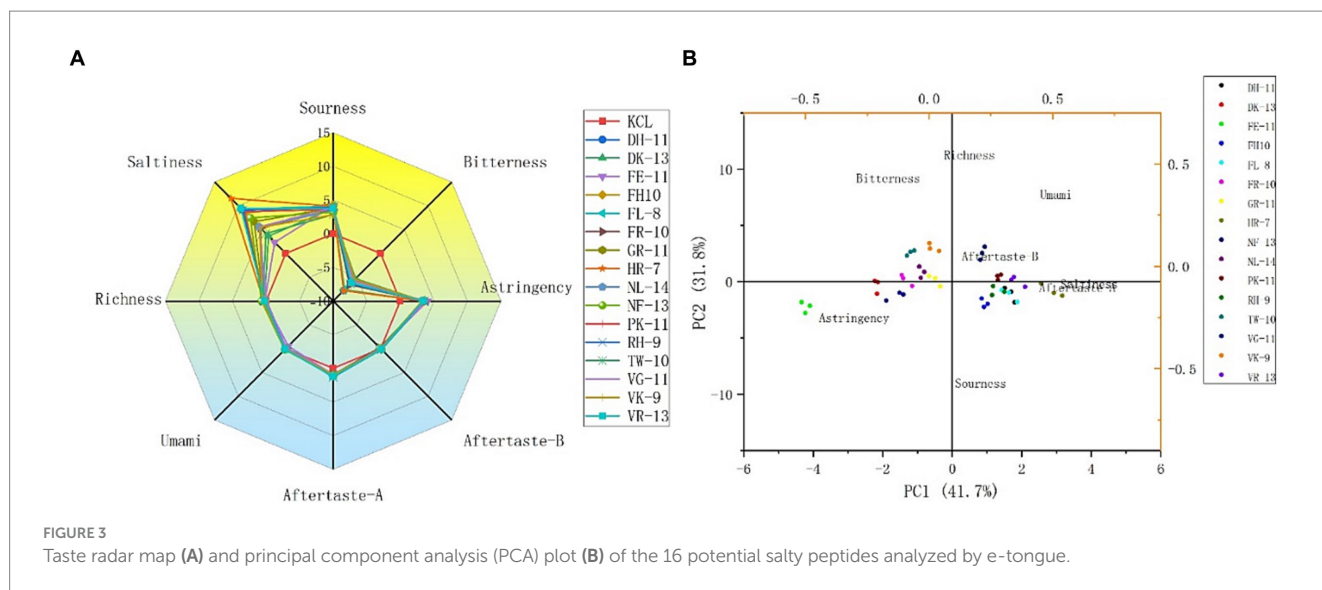
3.4 Energy interaction and surface force between TRPV1 receptor and salty peptides

Understanding the key active sites of flavor peptides is important for understanding ligand and receptor recognition patterns (15). To explore the mechanism of taste presentation of salty peptides, we further investigated the interaction between TRPV1 and four salty peptides. Molecular docking is a process in which two or more molecules recognize each other through assembly and energy matching to obtain the optimal binding pattern between the molecules (32). The optimal binding conformation of the four salty peptides in the active pocket of TRPV1 is shown in Figures 4A–D and the 2D plot of the interaction between the four peptides and the active residues of TRPV1 is presented in Figures 4E–H. The results showed that the four salty peptides were successfully inserted into the active site of the TRPV1 subunit and were locked in the active pocket of TRPV1.

The binding forces of ligand-receptor interactions in the spatial structure have a strong influence on taste, including electrostatic interactions, hydrogen bonding, hydrophobic interactions, π-alkyl, π-sulfur, salt bridges, and van der Waals force interactions (15). As shown in Figures 4E–H, the binding of the four salty peptides to TRPV1 mainly involves non-covalent interactions, such as van der Waals interactions, hydrogen bonding, and hydrophobic forces (alkyl or π-alkyl). In addition to van der Waals forces, the conventional hydrogen bond and alkyl or π-alkyl are the main interaction forces between the four salty peptides and TRPV1, while π-stacked is only present in DFKSPDDPSRH and FPGIPDHL, and the attractive charge is only present in HLDDALR and VIEPLDIGDDKVR. The most bindings between VIEPLDIGDDKVR and TRPV1 included 13 alkyl or π-alkyl and 12 conventional hydrogen bonds, two π-stacked, and the rest were two unfavorable donor–donor, one attractive charge, and one π-sigma. π-alkyl is a hydrophobic force. Hydrophobic interactions, as well as the balance between hydrophobic and hydrophilic forces, are the main forces that maintain structural stability between peptides and receptors (30); hydrogen bonding also plays an important role in biological macromolecules, being one of the main driving forces for protein-ligand interactions and playing an indispensable role in stabilizing protein-ligand complexes. Conventional hydrogen bonds

were also as high as 12 and 15 in DFKSPDDPSRH and HLDDALR, respectively, while there was only one conventional hydrogen bond in FPGIPDHL. However, another five alkyl or π-alkyl interactions, two π-π stacked and one π-Sigma interaction, in which residue VAL441 formed both π-π stacked and π-Sigma interactions with FPGIPDHL, made us speculate that VAL441 may be a key AA for the binding of FPGIPDHL to the salty receptor TRPV1 residues. It is possible that the differences in molecular structure led to the differences in receptor-ligand interactions, which ultimately led to the differences in the affinity of the peptides for TRPV1, which is similar to the findings of Xiao et al. (19), and these strong interactions may lead to a better salty taste of the salty peptide.

In this study, four salty peptides exhibited binding to 37 AA residues of the TRPV1 subunit, the major AA residues being Arg491, Tyr487, VAL441, Asp708, Arg557, Asp509, Arg410, Arg499, Arg500, Tyr445, and Phe488, with Arg491 appearing frequently in DFKSPDDPSRH and VIEPLDIGDDKVR; Tyr487 and VAl441 occurred in DFKSPDDPSRH, FPGIPDHL, and VIEPLDIGDDKVR; and Asp708 occurred in HLDDALR and VIEPLDIGDDKVR. These results suggest that Arg491, Tyr487, VAL441, and Asp708 are important binding sites that play a crucial role in the interaction between salty peptides and TRPV1 subunits. TRPV1 has been extensively studied as a capsaicin receptor, and Domene et al. (33) reported that the binding of TRPV1 to capsaicin is mediated by hydrogen bonding and van der Waals interactions and that residue Y511 is essential for stabilizing the binding state and during the binding process. Xiao et al. (19) reported that some amide bonds and similar groups, or even benzene rings in spicy compounds, play a key role in spicy taste perception, with Glu570 in the active pocket of TRPV1 playing an important role in spice detection. There are similarities but also differences in the binding modes of TRPV1 and ligands as receptors for different tastes and perceptions. The similarities lie in the binding modes of different ligands to TRPV1 being mainly hydrogen bonds and van der Waals forces, while the differences lie in the different binding AA residues.

Figure 5 shows the details of the surface forces between the salty peptides and TRPV1. The HLDDALR and VIEPLAIGDDKVR
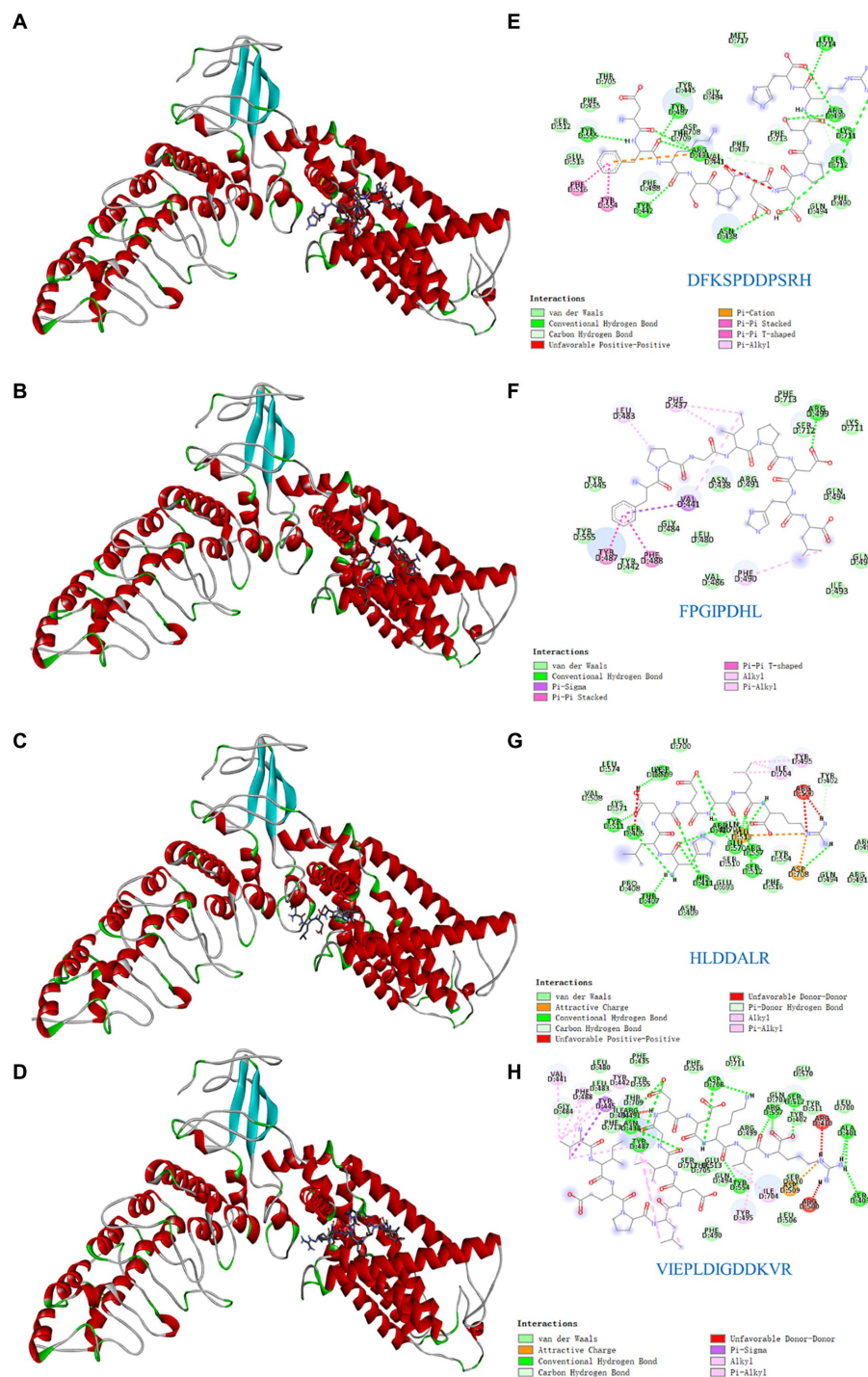
FIGURE 4
Molecular docking of the TRPV1 receptor and salty peptides. **(A–D)** 3D docking complex diagrams between TRPV1 and four salty peptides. **(E–H)** 2D diagrams between TRPV1 and four salty peptides.

structures are mostly wrapped in the lumen of the receptor TRPV1 active pocket, while DFKSPDDPSRH and FPGIPDHL are located on the surface of the receptor TRPV1 active pocket. All four salty peptides interact with TRPV1 through three main surface forces: aromatic interactions, hydrogen bonding, and hydrophobicity. In this study, the electrostatic interaction between the protons on the edge ring of TRPV1 and the salty peptide was stronger than the π-electron

density on the face ring; this result is similar to the surface interaction between umami peptides and umami receptor T1R1/T1R3 (34). All four salty peptides were able to form strong hydrogen bonds with TRPV1; in terms of hydrophobicity, all four salty peptides were significantly hydrophilic, which may be attributed to the abundance of hydrophilic groups such as $-NH_2$, $-COOH$, and $-OH$ in TRPV1 and the salty peptide.

FIGURE 5
Surface force analysis of TRPV1 interaction with four salty peptides.
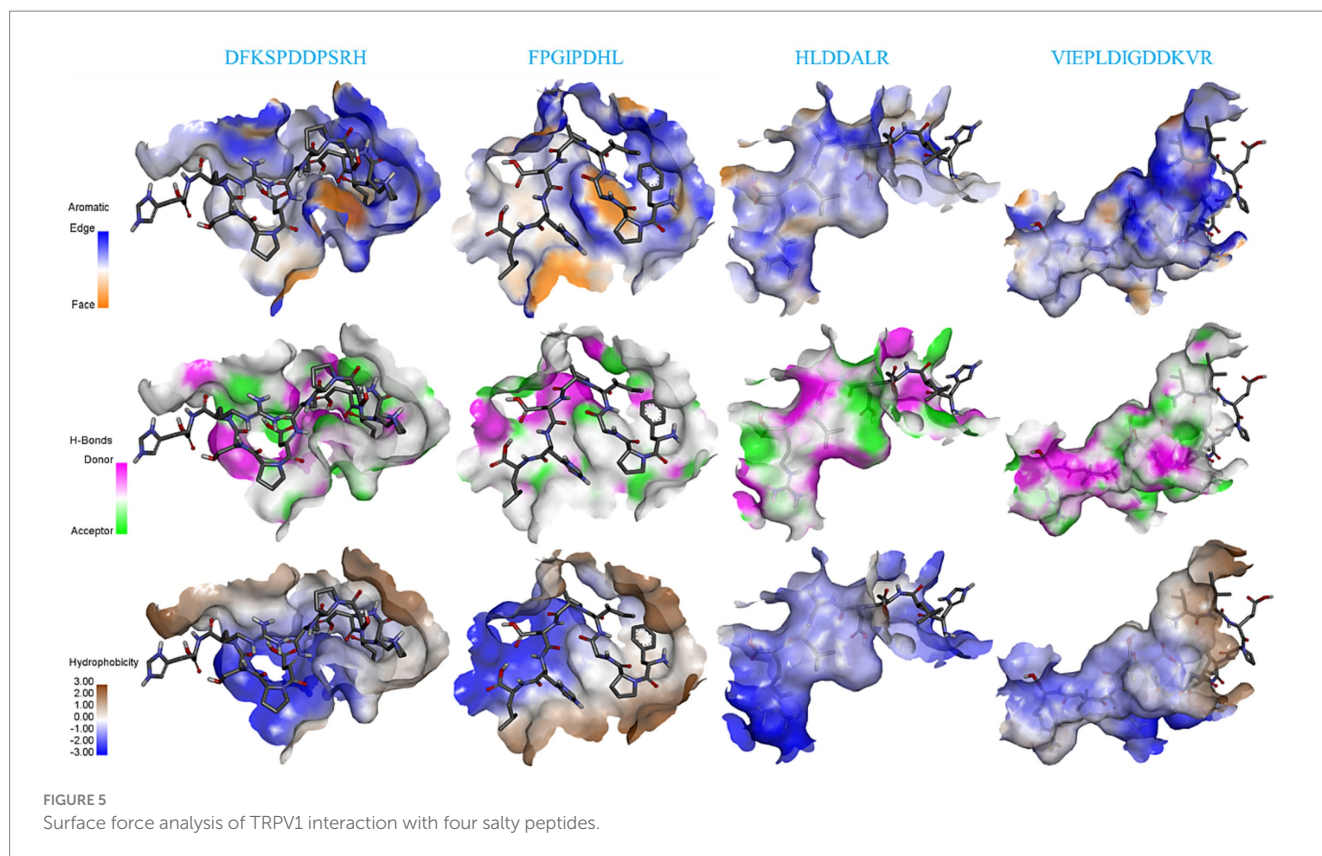
4 Conclusion

In this study, the major salty components of the enzymatic hydrolysate of tilapia by-products were obtained and identified to 189 peptides by nano-HPLC-MS/MS. Batch molecular docking of 189 peptides with the salty receptor TRPV1 was performed using Python script to obtain 16 potential salty peptides with low docking energy, which were further synthesized and subjected to taste identification and threshold analysis by sensory evaluation, TDA, and e-tongue. It was found that all 16 potential salty peptides had a significant salty taste with salty threshold values in the range of 0.256–0.379 mmol/L, which was lower than the salty threshold of NaCl. The highest salinity score was obtained for HLDDALR, followed by VIEPLDIGDDKVR, FPGIPDHL, and DFKSPDDPSRH. Further analysis of the binding forces and binding sites of these four salty peptides to TRPV1 revealed that van der Waals interactions, hydrogen bonding, and hydrophobic forces were the main binding forces. Aromatic interactions, hydrogen bonding, and hydrophobicity were the main surface forces and Arg491, Tyr487, VAL441, and Asp708 were the key sites for binding the salty peptides to TRPV1.

In summary, our work accomplished the preparation of enzymatic digests of tilapia by-products, virtual screening of salty peptides, and receptor binding analysis, which may provide a valuable research basis for the utilization of salty peptides from natural sources as well as salt reduction strategies.

The mass spectrometry proteomics data have been deposited to the ProteomeXchange Consortium[3] via the iProX partner repository (35, 36) with the dataset identifier PXD047590.

---

3 http://proteomecentral.proteomexchange.org

Data availability statement

The original contributions presented in the study are publicly available. This data can be found here: http://proteomecentral.proteomexchange.org, PXD047590.

Author contributions

HR: Data curation, Investigation, Software, Writing – original draft. JZ: Investigation, Methodology, Software, Writing – review & editing. HF: Investigation, Methodology, Software, Writing – review & editing. QF: Conceptualization, Methodology, Writing – review & editing. JW: Methodology, Software, Writing – review & editing. CL: Resources, Visualization, Writing – review & editing. GX: Resources, Writing – review & editing. WS: Conceptualization, Resources, Writing – review & editing. YH: Formal analysis, Supervision, Writing – review & editing.

Funding

Conflict of interest

The authors declare that the research was conducted in the absence of any commercial or financial relationships that could be construed as a potential conflict of interest.

Publisher's note

All claims expressed in this article are solely those of the authors and do not necessarily represent those of their affiliated organizations, or those of the publisher, the editors and the reviewers. Any product that may be evaluated in this article, or claim that may be made by its manufacturer, is not guaranteed or endorsed by the publisher.

Supplementary material

The Supplementary material for this article can be found online at: https://www.frontiersin.org/articles/10.3389/fnut.2023.1343209/full#supplementary-material

References

1. Alio M, Grau R, Toldr F, Barat JM. Physicochemical changes in dry-cured hams salted with potassium, calcium and magnesium chloride as a partial replacement for sodium chloride. *Meat Sci.* (2010) 86:331–6. doi: 10.1016/j.meatsci.2010.05.003

2. Braschia A, Gilla L, Naismith DJ. Partial substitution of sodium with potassium in white bread: feasibility and bioavailability. *Int J Food Sci Nutr.* (2009) 60:507–21. doi: 10.1080/09637480701782118

3. Le B, Yu B, Amin MS, Liu R, Zhang N, Soladoye OP, et al. Salt taste receptors and associated salty/salt taste-enhancing peptides: a comprehensive review of structure and function. *Trends Food Sci Technol.* (2022) 129:657–66. doi: 10.1016/j.tifs.2022.11.014

4. Zheng Y, Tang L, Yu M, Li T, Song H, Li P, et al. Fractionation and identification of salty peptides from yeast extract. *J Food Sci Technol.* (2021) 58:1199–208. doi: 10.1007/s13197-020-04836-1

5. Moore A, Luckett CR, Munafo JP. Taste-active dipeptides from hydrolyzed mushroom protein enhance saltiness. *J Agric Food Chem.* (2021) 69:11947–59. doi: 10.1021/acs.jafc.1c04479

6. Chen Y, Wang M, Blank I, Xu J, Chung HY. Saltiness-enhancing peptides isolated from the Chinese commercial fermented soybean curds with potential applications in salt reduction. *J Agric Food Chem.* (2021) 69:10272–80. doi: 10.1021/acs.jafc.1c03431

7. Oka YA, Butnaru MA, Von Buchholtz LB, Ryba NJPB, Zuker CSA. High salt recruits aversive taste pathways. *Nature.* (2013) 494:472–5. doi: 10.1038/nature11905

8. Tapanee P, Tidwell DK, Schilling MW, Peterson DG, Tolar-Peterson T. Genetic variation in taste receptor genes (SCNN 1 B, TRPV 1) and its correlation with the perception of saltiness in normotensive and hypertensive adults. *Int J Hypertens.* (2021) 2021:1–7. doi: 10.1155/2021/5559831

9. Smith K, Treesukosol Y, Paedae A, Contreras R, Spector A. Contribution of the TRPV1 channel to salt taste quality in mice as assessed by conditioned taste aversion generalization and chorda tympani nerve responses. *Am J Physiol Regul Integr Comp Physiol.* (2012) 303:R1195–205. doi: 10.1152/ajpregu.00154.2012

10. Nilius B. TRP channels in disease. *Biochim Biophys Acta.* (2007) 1772:805–12. doi: 10.1016/j.bbadis.2007.02.002

11. Liao M, Cao E, Julius D, Cheng Y. Structure of the TRPV1 ion channel determined by electron cryo-microscopy. *Nature.* (2013) 504:107–12. doi: 10.1038/nature12822

12. Liman ER. Salty taste: from transduction to transmitter release, hold the calcium. *Neuron.* (2020) 106:709–11. doi: 10.1016/j.neuron.2020.05.012

13. Liu R, Zhu Y, Chen J, Wu H, Shi L, Wang X, et al. Characterization of ACE inhibitory peptides from *Mactra veneriformis* hydrolysate by nano-liquid chromatography electrospray ionization mass spectrometry (Nano-LC-ESI-MS) and molecular docking. *Mar Drugs.* (2014) 12:3917–28. doi: 10.3390/md12073917

14. Shen D, Pan F, Yang ZC, Song HL, Zou T, Xiong J, et al. Identification of novel saltiness-enhancing peptides from yeast extract and their mechanism of action for transmembrane channel-like 4 (TMC4) protein through experimental and integrated computational modeling. *Food Chem.* (2022) 388:132993. doi: 10.1016/j.foodchem.2022.132993

15. Zhang T, Hua Y, Zhou C, Xiong Y, Pan D, Liu Z, et al. Umami peptides screened based on peptidomics and virtual screening from *Ruditapes philippinarum* and *Mactra veneriformis* clams. *Food Chem.* (2022) 394:133504. doi: 10.1016/j.foodchem.2022.133504

16. Ruan S, Sun L, Sun X, He J, Zhuang Y. Novel umami peptides from tilapia lower jaw and molecular docking to the taste receptor T1R1/T1R3. *Food Chem.* (2021) 362:130249. doi: 10.1016/j.foodchem.2021.130249

17. Liang L, Zhou C, Zhang J, Huang Y, Zhao J, Sun BG, et al. Characteristics of umami peptides identified from porcine bone soup and molecular docking to the taste receptor T1R1/T1R3. *Food Chem.* (2022) 387:132870. doi: 10.1016/j.foodchem.2022.132870

18. Wang W, Yang L, Ning M, Liu Z, Liu Y. A rational tool for the umami evaluation of peptides based on multi-techniques. *Food Chem.* (2022) 371:131105. doi: 10.1016/j.foodchem.2021.131105

19. Xiao S, Song P, Bu F, Pang G, Zhou A, Zhang Y, et al. The investigation of detection and sensing mechanism of spicy substance based on human TRPV1 channel protein-cell membrane biosensor. *Biosens Bioelectron.* (2021) 172:112779. doi: 10.1016/j.bios.2020.112779

20. Gan R, He Y, Li Y. Structural characteristics of taste active peptides in protein hydrolysates from tilapia by-products. *J Food Meas Charact.* (2022) 16:1674–87. doi: 10.1007/s11694-022-01302-8

21. Zhang J, Zhang J, Liang L, Sun B, Zhang Y. Identification and virtual screening of novel umami peptides from chicken soup by molecular docking. *Food Chem.* (2022) 404:134414. doi: 10.1016/j.foodchem.2022.134414

22. Fu Y, Liu J, Hansen ET, Bredie W, Lametsch R. Structural characteristics of low bitter and high umami protein hydrolysates prepared from bovine muscle and porcine plasma. *Food Chem.* (2018) 257:163–71. doi: 10.1016/j.foodchem.2018.02.159

23. Dias AG, Rousseau D, Duizer L, Cockburn M, Chiu W, Nielsen D, et al. Genetic variation in putative salt taste receptors and salt taste perception in humans. *Chem Senses.* (2013) 38:137–45. doi: 10.1093/chemse/bjs090

24. Singh KD, Muthusamy K. Molecular modeling, quantum polarized ligand docking and structure-based 3D-QSAR analysis of the imidazole series as dual AT1 and ETA receptor antagonists. *Acta Pharmacol Sin.* (2013) 34:1592–606. doi: 10.1038/aps.2013.129

25. Shrivastav A, Srivastava S. Human sweet taste receptor: complete structure prediction and evaluation. *Int J Chem Anal Sci.* (2013) 4:24–32. doi: 10.1016/j.ijcas.2013.03.002

26. Li Y, Chen X, Nie Y. Endocannabinoid activation of the TRPV1 ion channel is distinct from activation by capsaicin. *J Biol Chem.* (2021) 297:101022. doi: 10.1016/j.jbc.2021.101022

27. Yang F, Zheng J. Understand spiciness: mechanism of TRPV1 channel activation by capsaicin. *Protein Cell.* (2017) 8:169–77. doi: 10.1007/s13238-016-0353-7

28. Dang Y, Gao X, Xie A, Wu X, Ma F. Interaction between umami peptide and taste receptor T1R1/T1R3. *Cell Biochem Biophys.* (2014) 70:1841–8. doi: 10.1007/s12013-014-0141-z

29. Shan Y, Pu D, Zhang J, Zhang L, Huang Y, Li P, et al. Decoding of the saltiness enhancement taste peptides from the yeast extract and molecular docking to the taste receptor T1R1/T1R3. *J Agric Food Chem.* (2022) 70:14898–906. doi: 10.1021/acs.jafc.2c06237

30. Gao B, Hu X, Xue H, Li R, Liu H, Han T, et al. Isolation and screening of umami peptides from preserved egg yolk by nano-HPLC-MS/MS and molecular docking. *Food Chem.* (2022) 377:131996. doi: 10.1016/j.foodchem.2021.131996

31. Dang Y, Hao L, Cao J, Sun Y, Zeng X, Wu Z, et al. Molecular docking and simulation of the synergistic effect between umami peptides, monosodium glutamate and taste receptor T1R1/T1R3. *Food Chem.* (2019) 271:697–706. doi: 10.1016/j.foodchem.2018.08.001

32. Sanjukta S, Padhi S, Sarkar P, Singh SP, Sahoo D, Rai AK. Production, characterization and molecular docking of antioxidant peptides from peptidome of kinema fermented with proteolytic Bacillus spp. *Food Res Int.* (2021) 141:110161. doi: 10.1016/j.foodres.2021.110161

33. Domene C, Darré L, Oakes V, Gonzalez-Resines S. A potential route of capsaicin to its binding site in the TRPV1 ion channel. *J Chem Inf Model.* (2022) 62:2481–9. doi: 10.1021/acs.jcim.1c01441

34. Yang D, Li C, Li L, Chen S, Hu X, Xiang H. Taste mechanism of umami peptides from Chinese traditional fermented fish (Chouguiyu) based on molecular docking using umami receptor T1R1/T1R3. *Food Chem.* (2022) 389:133019. doi: 10.1016/j.foodchem.2022.133019

35. Ma J, Chen T, Wu S, Yang C, Bai M, Shu K, et al. iProX: an integrated proteome resource. *Nucleic Acids Res.* (2019) 47:D1211–7. doi: 10.1093/nar/gky869

36. Chen T, Ma J, Liu Y, Chen Z, Xiao N, Lu Y, et al. iProX: connecting proteomics data sharing with big data. *Nucleic Acids Res.* (2021) 50:D1522–7. doi: 10.1093/nar/gkab1081

Assessment of the color of orange juice in the context of dietitians' food preferences

Marek Kardas[1], Agata Kiciak[1], Kamila Szynal[2], Barbara Sitkiewicz[1], Wiktoria Staśkiewicz-Bartecka[1]* and Agnieszka Bielaszka[1]

[1]Department of Food Technology and Quality Evaluation, Department of Dietetics, Faculty of Public Health in Bytom, Medical University of Silesia in Katowice, Zabrze, Poland, [2]Doctoral School of the Medical University of Silesia in Katowice, Department of Human Nutrition, Faculty of Public Health in Bytom, Medical University of Silesia in Katowice, Zabrze, Poland

Introduction: Color is an integral part of product selection and is used to assess its attractiveness and quality. Dietitians are a group that influences the dietary choices of the population through education and promotion of rational eating behavior. The purpose of this study was to evaluate the color of selected juices in the context of dietitians' food preferences.

Methods: In the first stage of the research, the color of orange juices was measured using a spectrophotometer. In the second stage, sensory analysis was carried out using the ranking method. Participants were asked to assess the attractiveness of the color of juices through glasses and bottles without the original label and with the label. The juice with the best color turned out to be the juice which, according to the L * a * b * parameters, was relatively dark and had an intense orange tint.

Results: As the juice with the worst color, they chose the juice that was colored green and blue. When assessing the color without and with the original label, the respondents indicated which one was significantly brighter and more yellow compared to the others. Dietitians prefer bright juices with a vibrant orange hue. Product packaging influences dieticians' choices regardless of the content.

Discussion: Instrumental control of color during product production and selection of packaging elements for attractive synergy are determinants of the perceived attractiveness of juices in the study group.

KEYWORDS

color, dietitian, food preference, dietary choice, spectrophotometer, juice, consumer preference

1 Introduction

Orange juices are popular products on the food market in Poland and Europe, not only because of their taste but also because of the health benefits resulting from the content of vitamins, minerals, and antioxidants. According to World Health Organization (WHO) recommendations, a glass of such juice can replace one portion of vegetables and/or fruit on a given day. Nutritionists who promote healthy foods may lean toward juices with colors associated with the maturity and quality of raw materials. Dietitians' preferences for juice color stem from their understanding that color is related to nutrient content and influences

sensory perception, which can affect fluid intake and the overall nutritional value of the product. Dietitians are the people who influence and modify their patients' food choices, so the aspect of evaluating their consumer preferences is important (1–3). So, what makes a dietitian prefer a particular brand of juice?

Sensory senses such as taste, smell, texture, and color play an important role in the choice of a specific product. In addition to the brand, price, and type of packaging, the most important sense determining its purchase is the sense of sight. It provides information about the size, shape, and color of the product, which proves its freshness and attractiveness (1, 2). The visual appearance of food in terms of color has a great influence on the perception of food quality. Color may be correlated with other quality features, such as sensory, nutritional, and visual or non-visual defects, and its changes enable them to be controlled immediately (3, 4).

Integrating dieters' preferences with CIELAB's color assessment allows for a holistic analysis, combining health aspects with precise and objective color measurements, which can be important both for effective nutrition communication and for maintaining the high sensory quality of food products (5).

CIELAB is one of the most common color spaces for measuring the color of objects and is widely used in the color control and management industry (6). The CIELAB method, an international standard in color analysis, enjoys widespread use in scientific research on fruit juice color because of its standardization and accurate representation of human color perception. The CIELAB color space is based on a three-coordinate system: $L*$ (brightness), $a*$ (green-red tones), and $b*$ (blue-yellow tones), enabling precise quantification of color intensity, brightness, and hue. Its international nature facilitates the comparability of measurement results between different laboratories on a global scale. The adoption of this method also stems from its consideration of human color perception, making it particularly useful in the context of sensory analysis of food products such as fruit juices. The choice of CIELAB stems from its ability to directly address fundamental aspects of color perception, such as brightness, saturation, and hue. In addition, the CIELAB space allows monitoring of color changes over time, which is crucial for food products subject to natural oxidation or enzymatic browning processes. Thanks to the intuitive nature of CIELAB coordinates, measurement results are easy to understand and interpret, facilitating analysis and data presentation in the context of scientific research on fruit juice colors (7, 8).

Sensory analysis techniques are also used to optimize sales, which show the preferences of potential consumers about the examined factor (1, 9). One of these methods is the scheduling method. It is an intermediate between the differential methods and the scaling methods. It consists of arranging several samples, given in random order, in terms of the selected quality feature (e.g., from the worst to the best color). The scale of the difficulty of the task depends on the size of the differences between the samples. Its advantages are simple tasks and speed of the assessment (10).

Packaging at the point of sale is the manufacturer's last chance to convince the customer of their product. Research suggests that the inclusion of shape and color elements in the packaging design may affect the perception of quality by consumers, their emotional reactions related to the brand/product, and, consequently, general preferences (11–13). Moreover, the sensory stimuli contained in the packaging help to distract the customer from routine purchasing activities, attracting their attention through novelty and mediating product categorization (14).

The main objective of the study was to evaluate the color of selected food products in the context of dieters' food preferences. The specific objectives were the measurement of the color of selected orange juices using the spectrophotometric method in the CIELAB color system, the consumer assessment of the attractiveness of selected orange juices using the scheduling method, and the assessment of the relationship between the appearance of the packaging and the consumer assessment of the color of selected orange juices.

2 Materials and methods

2.1 Study design

The research covered six pasteurized orange juices (100% juice) from various producers (sample designations: RJ, VF, LI, SN, SO, and ON), available on the Polish market. The study was carried out in a sensory analysis laboratory designed according to the PN-EN ISO 8589: 2017 standard. The Declaration of Helsinki of the World Medical Association guided the conduct of this study. The study protocol (KNW-0022/KB1/73/I/16) was reviewed by the Bioethics Committee of the Silesian Medical University in Katowice and was approved. Each person participating in the study gave informed consent to participate in the study and was informed about the anonymity of the results.

2.2 Color measurements

Color measurements were made with a Tri-Color SF80 spectrophotometer calibrated according to the $L*$ 90.08, $a*$ −0.74, and $b*$ 0.70 standards, in the SCI3 measurement geometry, with a D654 light source and an observation angle of 10°. Further, 30 ml of a given orange juice was poured into a cuvette to measure the liquid and 15 measurements were made, from which the arithmetic mean was then calculated. Before measuring the color of a juice from another manufacturer, the cuvette was washed under running water and wiped dry.

2.3 Sensory analysis

Sensory analysis was conducted among 71 female dietetics students at the Medical University of Silesia in Katowice in the laboratory of sensory analysis. All the students were active in the dietetics profession. The analysis was carried out in three stages. In the first station, the color was assessed through 50 ml plastic glasses with 30 ml of juice. On the second stand, the juice was assessed through the original bottle without the manufacturer's label. At the last stand, the color of the juice was assessed through the original bottle with the manufacturer's label. The samples were numbered with three-digit random numbers. The evaluation was performed using the scheduling method prepared by the PN-ISO 5497: 1998 standard.

2.4 Statistical analysis

The results of color measurements were compiled using Color QC and Microsoft Office Excel 2019.

Statistical calculations were made in Statistica 13.3 (StatSoft 2017). To statistically analyze the results of the conducted sensory analysis using the scheduling method, the Friedman test was used and the Kendall coefficient of concordance was used. To calculate the correlation between the studied discriminants and the significance of differences between the mean values, the one-way ANOVA and a *post-hoc* test, the method of least significant differences (NIR), were used.

A correlation analysis was conducted between rank scores and color measurements in CIELAB space. Pearson's r correlation coefficients were used to determine whether there is a relationship between the two variables.

The criterion for statistical significance was $p < 0.05$.

3 Results

3.1 Instrumental analysis of orange juice color using the spectrophotometric method in the CIELAB color system

The RJ orange juice color measurements in terms of the L * parameter ranged from 39.77 to 39.93. In terms of the a * parameter, the values were from −0.39 to −0.42, and in the case of the b * parameter, the values were from 15.75 to 15.90.

The L * parameter measurements for VF orange juice ranged from 39.32 to 39.35. For the a * parameter, the values were from −1.40 to −1.44, and for the b * parameter, the values were from 12.95 to 13.00.

For LI orange juice, the color measurements in terms of the L * parameter ranged from 40.77 to 40.98. In terms of the a * parameter, the values were from −1.37 to −1.52, and in the case of the b * parameter, the values were from 12.70 to 13.03.

SN orange juice obtained the following measurement results: parameter L * values between 43.14 and 43.37; parameter a * values from −0.46 to −0.49; parameter b * values from 15.81 to 16.05.

The SO orange juice color measurements in terms of the L * parameter ranged from 43.89 to 44.09. In terms of the a * parameter, the values were from −0.88 to −0.94, and for the b * parameter, the values were from 17.68 to 17.86.

For ON orange juice, the color measurements in terms of the L * parameter ranged from 41.13 to 41.33. In terms of the a * parameter, the values were from −0.58 to −0.62, and for the b * parameter, the values were from 14.99 to 15.05.

Comparing the arithmetic means of the measurements, the orange juice SO had the highest L * value and VF juice the lowest. In turn, the highest value of a * was for SN juice and the lowest LI. SO juice showed the highest value of the b * parameter and LI juice had the lowest (Table 1).

The average values of juice color measurement are also presented in the chromaticity graphs (Figure 1).

Based on these results, it can be concluded that SO juice was the brightest and that its color deviated the most toward yellow. On the other hand, the juice values differ the most between green and blue

TABLE 1 Comparison of the mean values of the measurements.

Juice name	L * ($\bar{x} \pm$ SD)	a * ($\bar{x} \pm$ SD)	b * ($\bar{x} \pm$ SD)	*p*
RJ	39.87 ± 0.04	−0.41 ± 0.01	15.83 ± 0.04	0.13
VF	39.34 ± 0.01	−1.41 ± 0.01	12.97 ± 0.02	**0.02***
LI	40.92 ± 0.07	−1.47 ± 0.04	12.79 ± 0.1	0.33
SN	43.32 ± 0.06	0.47 ± 0.01	15.91 ± 0.07	0.12
SO	43.98 ± 0.05	−0.92 ± 0.02	17.77 ± 0.07	0.12
ON	41.23 ± 0.04	−0.59 ± 0.01	15.03 ± 0.02	**0.04***

L *, brightness; a *, green-red tones; b *, blue-yellow tones; $\bar{x}$, average; SD, standard deviation.
*$p < 0.05$.

in comparison to other juices. VF juice was the darkest among the subjects and SN juice was the closest to the shades of red. Detailed information on the color of the sap in the CIE L * a * b * color space is shown in Figure 2.

3.2 Sensory analysis of the color of orange juices by the serialization method

The female students taking part in the survey were between 18 and 30 years old. The average age of the respondents was 22.69 ± 2.16.

When assessing the color of orange juice by glass, statistically significant differences were found in the respondents' assessments ($p < 0.05$). In addition, the raters show poor agreement in their ratings because the Kendall coefficient of agreement is 0.13. The study showed that the group of 71 dieticians did not find significant differences in desirability between the samples of RJ, SN, SO, and ON juices. The VF and LI juice samples were different, with a significantly lower desirability than all other juice samples, but not statistically different and the least was LI juice (2.63 ± 1.55). Comparing these results to spectrophotometric measurements, RJ juice showed low brightness and a considerable approximation to the red and yellow colors compared to other juices. On the other hand, the LI juice was the most abnormal in comparison to the others and turned green and blue in color.

When assessing the color of orange juice using bottles without the original manufacturer's label, statistically significant differences were also found in the respondents' assessments ($p < 0.05$). Again, the raters showed poor agreement in their ratings (Kendall's coefficient of agreement = 0.03). The study showed no statistically significant differences in color desirability between RJ and VF juices in a bottle without the original manufacturer's label. The SN and SO juices were different, but they were not statistically different. LI and ON juices were statistically similar to the two groups mentioned. In the case of color evaluation using unlabeled bottles, SN juice (3.87 ± 1.87) was the most desirable and VF juice (3.27 ± 1.70) the least. Compared to the results of the color assessment by glass, the respondents chose a very light juice with a color closest to red as the best in comparison to other samples. The last place was a darker juice, closer to green and blue on the axis.

When assessing the color of orange juice using bottles with the original manufacturer's label, no statistically significant differences were found in the respondents' assessments ($p > 0.05$). Thus, no statistically significant differences between individual juices
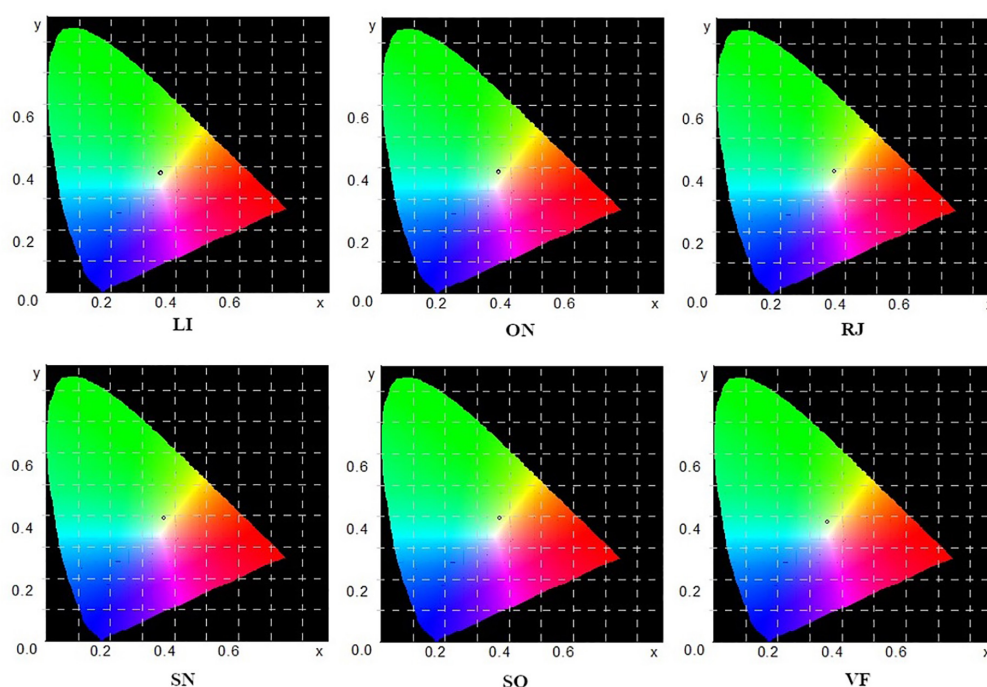
FIGURE 1
Juice color measurement values are located on chromaticity charts.
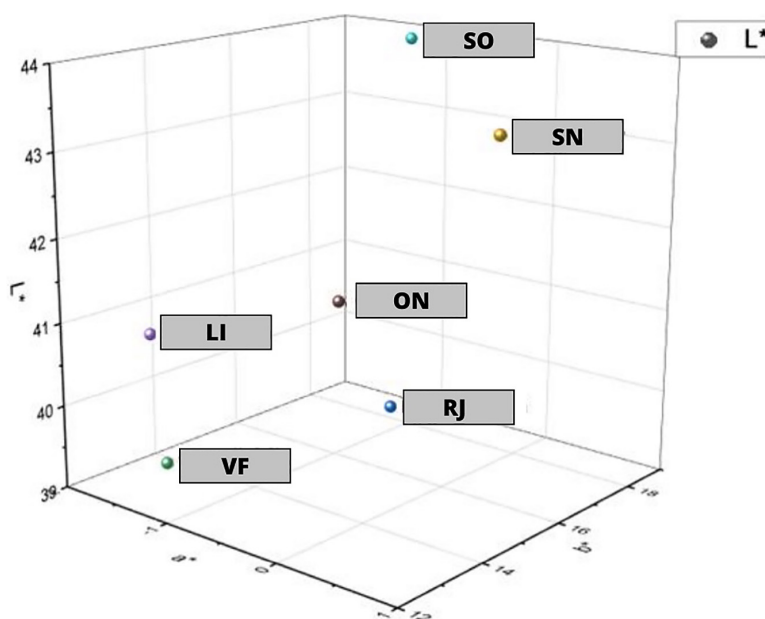
FIGURE 2
Juice color in the color space in the CIE L*a*b* system.

were found. In assessing the color through the bottle with the manufacturer's label, the respondents again chose SN juice (3.69 ± 1.69) as the one with the most desirable color for orange juice. On the other hand, ON juice was rated the worst (3.37 ± 1.82). In terms of color parameters in the L * a * b * system, it does not stand out in particular from other juices. As in the case of the evaluation via unlabeled bottles, VF juice was ranked low again (3.38 ± 1.67).

A collective summary of the results of the assessment of the color of juices by the glass, a bottle without a label, and a bottle with a label are presented in Table 2.

Comparing the above results, the most desirable color of orange juice, when the original manufacturer's packaging had no impact on the assessment, was RJ juice, and the least – was LI juice. RJ has anthropomorphic packaging with a white label and black cap. LI

TABLE 2 Summary of the results of the assessment of the color of juices by the glass, a bottle without a label, and a bottle with a label.

Name	Glass			Unlabeled bottle			Bottle with label		
	Sum of ranks	Rank average ($\bar{x} \pm$ SD)	Significance of differences (a = 0.05*)	Sum of ranks	Rank average ($\bar{x} \pm$ SD)	Significance of differences (a = 0.05*)	Sum of ranks	Rank average ($\bar{x} \pm$ SD)	Significance of differences (a = 0.05*)
RJ	292	4.11 ± 1.47	b	232	3.27 ± 1.70	a	259	3.65 ± 1.79	a
VF	190	2.68 ± 1.76	a	218	3.07 ± 1.50	a	240	3.38 ± 1.67	a
LI	187	2.63 ± 1.55	a	253	3.56 ± 1.25	ab	244	3.44 ± 1.69	a
SN	286	4.03 ± 2.12	b	275	3.87 ± 1.87	b	262	3.69 ± 1.69	a
SO	268	3.77 ± 1.56	b	274	3.86 ± 1.81	b	247	3.48 ± 1.63	a
ON	268	3.77 ± 0.93	b	239	3.37 ± 1.93	ab	239	3.37 ± 1.82	a

$\bar{x}$, average; SD, standard deviation. *Sums of ranks or rank averages marked with the same letters do not differ significantly.

juice is round in shape with a transparent label and a black cap. During the evaluation by the original manufacturer's bottle with and without a label, SN juice was selected for the best color juice, and VF juice was selected for the worst color. SN juice has a small, slim bottle with a white label and an orange cap. VF juice is round in shape with a predominantly black color (label and cap). Bottle designs are presented in Figure 3.

3.3 Correlation analysis between orange juice color evaluated using the CIELAB method and dieticians color evaluation by serialization method

A correlation analysis was conducted between dieticians' evaluations of the color of the juice in the glass and color measurements in the CIELAB space. Pearson's r correlation coefficients were used to determine whether there was a relationship between the variables. Detailed information is presented in Table 3.

The value of the correlation coefficient between dieticians' preference and the L * coordinate was 0.14, suggesting that orange juice brightness (measured in the CIELAB space) has a moderately low positive correlation with dieticians' visual evaluation. However,

TABLE 3 Ranks given to L*, a*, b* coordinate values and consumer preference assessment.

Juice name	L* (brightness)	a* (green-red tones)	b* (blue-yellow tones)	Consumer assessment
RJ	2	5	4	6
VF	1	2	2	2
LI	3	1	1	1
SN	5	6	5	5
SO	6	3	6	3
ON	4	4	3	4

this correlation is not strong, meaning that changes in brightness are not strongly related to dieticians' preference. The Pearson correlation coefficient value of 0.94 between dieticians' preference and the a * coordinate indicates a strong positive correlation. This means that changes in the red-green component of the CIELAB color space are highly related to dieticians' preferences. In practice, this may suggest that more intense colors in the red-green range may be preferred by dieticians. The Pearson correlation coefficient value of 0.6 between dieticians' preference and the b * coordinate indicates a moderate positive correlation. This means that changes in the yellow-blue component of the CIELAB color space are moderately related to dieticians' preference. In practice, this could mean that certain shades of yellow and blue are more attractive to dieticians. In summary, Pearson's correlation analysis between dieticians' preference and individual coordinates of the CIELAB color space provides an understanding of which color components of orange juice are more relevant to consumer taste. A stronger correlation may suggest that a particular component has a greater influence on dieticians' visual evaluation preferences.

4 Discussion

Due to the topic and characteristics of this research article, there are few similar studies and new scientific reports from the last 10 years. Available studies usually address the dietary choices and consumer preferences of specific groups of people, but the dietary preferences of dieticians are not a frequent subject of research.
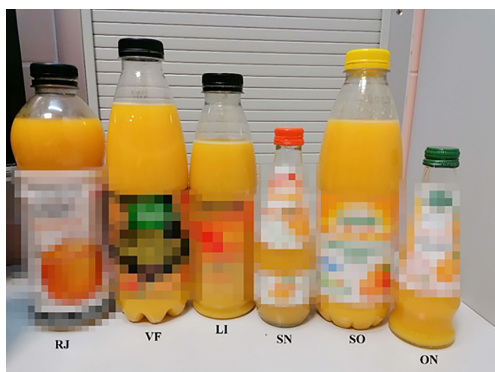

FIGURE 3
The design of the bottles.

In the Suwała (4) study, the colors of carrot juices were determined spectrophotometrically and the results were compared to consumer preferences. Color measurements were made in the CIELAB system and the assessment of consumer preferences was made using the 5-point method. As a result, it was concluded that the most desirable juice is the one with parameters $L^* = 24.98$; $a^* = 38.76$; $b^* = 42.89$, which the human eye perceives as an intense orange color, with a hue tending more toward red than yellow. In our study, the juice with the most desirable color was the juice with the values $L^* = 43.32$; $a^* = 0.47$; $b^* = 15.91$, where, similarly to the Suwała study, the values of the b^* parameter are higher than the values of the a^* parameters, but at the same time the value of the L^* parameter is the highest among all tested juices. This may be helpful for producers of juices whose color is commonly considered to be orange (orange, carrot), as they may try to control the color during the technological process to adjust to the preferences of consumers. A similar study was carried out by Fernandez-Vazquez et al. (15), this time on orange juices from five different varieties of this fruit. They were freshly squeezed through a juicer, then frozen at $-21°C$ until testing, and thawed at room temperature for 24 h. Color measurement values ranged between 56.48 and 60.66 for L^*, 12.40 and 24.60 for a^*, and 58.12 and 64.66 for b^*. Similar results were also obtained by Melendez-Martinez et al. (16), who measured the color of juices from the Valencia orange variety. They were frozen and stored at -18 to $-21°C$ until distributed. The results they obtained were $L^* = 63.23$, $a^* = 16.18$, and $b^* = 64.64$, indicating a deep, intense orange color. Compared to our study, where the results were between 39.34 and 43.98 for L^*, -1.47 and 0.47 for a^*, and 12.79 and 17.77 for b^*, it can be hypothesized that the method of juice production and its storage may influence the color differences. Moreover, the results probably indicate that pasteurized juices show a lower color intensity than freshly squeezed juices fixed by deep freezing.

In the study by Fernandez-Vazquez et al. (15), the consumer assessment of juices was also carried out and these results were compared to the values of instrumental measurements. It was concluded that the most desirable juice was the one with the most orange color ($L^* = 57.41$; $a^* = 18.29$; $b^* = 60.98$) and the least yellowish juice among all the tested samples ($L^* = 60.66$; $a^* = 12.40$; $b^* = 64.66$). In our study, similar results were obtained. If the manufacturer's packaging was excluded, the respondents rated the dark orange juice best ($L^* = 39.87$; $a^* = -0.41$; $b^* = 15.83$) and the worst assessment was the lighter juice falling into tones blue and green ($L^* = 40.92$; $a^* = -1.47$; $b^* = 12.79 \pm 0.10$). In the next two studies, the color of juice from the Valencia orange variety was measured. Sánchez-Moreno et al. (17) squeezed the juice through a domestic juicer and filtered it through steel sieves. The color measurement results obtained are $L^* = 34.76$; $a^* = -2.48$; and $b^* = 35.37$. On the other hand, Pérez-López et al. (18) tested freshly squeezed juice which was then subjected to a temperature of 98°C for 20 s and obtained the results of $L^* = 52.99$; $a^* = 5.50$; and $b^* = 33.83$. Compared to our research, this is a significant difference in values despite the similar method of juice preservation (high-temperature pasteurization) and a similar research methodology. In the works mentioned earlier in this section, a higher value of parameters was found in freshly squeezed juices than in those given in thermal treatment. In this case, it is the other way around. This leaves the topic open for discussion and further research to clarify what might have contributed to this discrepancy in the results.

Color measurements using the spectrophotometric method are not only used to monitor food quality or adjust product characteristics to the preferences of consumers. Pérez-López et al. (18) investigated the effect of the addition of mandarin orange juice on the improvement of the quality and desirability of orange juice. Thanks to CIELAB measurements combined with consumer sensory analysis, the first result they obtained was that among 100% of respondents, the color of mandarin juice was more desirable than the color of orange juice. Following this lead, they investigated whether consumers saw a difference between pure orange juice and juice with an addition of 3%, 6%, 9%, and 10% mandarin juice. They found that the differences were noticeable. This shows that instrumental color measurement may be necessary to control food additives to obtain the most desirable color.

The obtained results indicate that the product packaging may influence the consumer's assessment of the color. The color assessment using a glass was the most reliable because each juice was served in the same vessel. Nothing disturbed the judgment. In this case, the juice with the best color turned out to be RJ juice. However, when judging the color through the unlabeled original manufacturer's bottle, this juice dropped significantly in the ranking. In both cases, i.e., the bottles without and with the original manufacturer's label, the SN juice was rated the best. The difference can be found in the shape and color of the bottle. Color plays an important role in increasing sales. Red has been associated with excitement, but also with danger. In contrast, blue is often used to represent openness and a peaceful imagination. When considering emotional responses, light colors often evoke positive associations, while dark colors primarily evoke negative ones. Black, for example, causes negative emotions such as sadness, depression, fear, and anger, mainly because it is also associated with the concept of death. At the other end of the spectrum, bright colors such as red, orange, and yellow can cause euphoria. Among different perceptions, red has been shown to produce feelings of warmth and intimacy, while some other shades are irritating (19). As with color, it has been observed that the shape of the packaging, especially for bottles, also has a significant impact on the perception of the brand among consumers as it can communicate the apparent advantages and disadvantages of the product. In addition, consumers tend to judge product volume and comfort based on sight or touch, especially for food packaging, which helps to identify color, shape, and size as key dimensions of packaging design (20). Consumers perceive products in attractive packaging as having higher quality than in less attractive packaging. The design and color of the product can also be used as an indicator of the price range. More expensive products tend to have darker colors, while less expensive products tend to have lighter shades. Additionally, it has been shown that the shape of the package influences the perception of volume, for example, elongated shapes are seen as offering better value for money (21). The studies by Mehta et al. (22) showed that the expectations for the product (orange juice) formed during the first contact with the packaging affect the sensory experience, as consumers expected that the juice from the glass bottle would be fresher than from other packaging materials. According to Chittur et al. (21), the most important thing is the synergy between the shape and color of the bottle. The white color of the cap seemed to have the most positive effect compared to black, red, and blue. However, this hypothesis was only applicable to the combination of a black-capped round bottle, as the combination

of a square bottle with a black cap had already obtained a much higher preference index. In our study, the most desirable juice was the one in a glass bottle with an elongated shape, with a white label with orange elements, and an orange cap. According to Wolniak and Zadura (23), respondents chose packages with warm and light (bright) colors. This is related to attracting attention. Moreover, warm colors stimulate the imagination and evoke a feeling of happiness. In this case, a small glass bottle could also have influenced consumers' choices. It seems that this type of packaging is perceived as more luxurious, expensive, fresh, home-made, produced on a small scale, and more valuable. However, these are only the researcher's own thoughts and are undoubtedly worth exploring in subsequent research (21).

However, the study has its limitations. The study focused only on orange juices, which may limit the generalizability of its results. Dieticians' color preferences can vary widely depending on the type of juice. While the study analyzes the importance of color in product choice, it does not delve into other factors that may influence consumer choices, such as taste, price, or brand reputation. A more comprehensive analysis would provide a more nuanced understanding of consumer behavior. The sensory analysis included participants evaluating juices without the original label and with the label. This setting may not fully reflect the actual experiences of dieters, where branding and labeling play a significant role in product perception. In addition, only female dietitians between the ages of 18 and 30 participated in the study. Age and gender may be important determinants of sensory evaluation. The strengths of this study should also be mentioned. The study used a combination of objective and subjective methods to evaluate the color of selected juices, providing a comprehensive picture. The use of a spectrophotometer in the first stage ensured precise and unbiased color measurement. The inclusion of sensory analysis using a ranking method included consumer preferences, adding a practical aspect to the research. This approach can help bridge the gap between scientific measurements and actual consumer choices. The study found a clear preference among dieticians for bright juices with a vibrant orange hue. This finding could be valuable for product development and marketing strategies, as it underscores the importance of color in consumer choices. The study confirmed the influence of product packaging on consumer choices, highlighting the synergy between color and packaging elements. This recognition can guide product design and marketing efforts. The use of objective color measurement techniques, such as the L * a * b * parameters, increases the reproducibility of the study's results, making it easier for other researchers to validate or use the results. It should be mentioned that there are no other comparative studies that assess the consumer preferences of dietitians and this is a group that influences and shapes the public's dietary choices.

5 Conclusion

Based on spectrophotometric measurements, there was significant variation in the color parameters of orange juices. The results of sensory tests indicate that dieticians are more likely to reach for bright juices with an intense orange hue. In addition, the product's packaging influences dieticians' dietary choices regardless of its content. When choosing orange juice, the synergy between

packaging elements is also important. Instrumental color control during product manufacturing is justified, as well as the selection of packaging elements to achieve an attractive synergy.

Data availability statement

The raw data supporting the conclusions of this article will be made available by the authors, without undue reservation.

Ethics statement

Author contributions

MK: Methodology, Project administration, Writing – review & editing, Funding acquisition. AK: Resources, Writing – original draft. KS: Conceptualization, Data curation, Methodology, Writing – review & editing. BS: Formal Analysis, Software, Writing – review & editing. WS-B: Validation, Visualization, Writing – review & editing. AB: Investigation, Supervision, Writing – original draft.

Funding

Conflict of interest

The authors declare that the research was conducted in the absence of any commercial or financial relationships that could be construed as a potential conflict of interest.

Publisher's note

References

1. Baryłko-Piekielna N, Matuszewska I, Szczecińska A, Radzanowska J, Jeruszka M. Jakość sensoryczna rynkowych soków jabłkowych i pomarańczowych. *Żywność Nauka Technol Jakość.* (2002) 1:34–51.

2. Malinowska E, Wiśniewska M, Szymańska-Brałkowska M. *Ocena Sensoryczna Jakości Produktów Żywnościowych. Zakład Zarządzania Jakością i Środowiskiem.* Sopot: Wydział Zarządzania Uniwersytetu Gdańskiego (2014). p. 1–9.

3. Nisha P, Singhal RS, Pandit AB. Kinetic modelling of colour degradation in tomato puree (Lycopersicon esculentum L.). *Food Bioproc Tech.* (2011) 4:781–7. doi: 10.1007/s11947-009-0300-1

4. Suwała G. Porównanie preferencji konsumenckich barwy soków marchwiowych z wynikami oznaczeń spektofotometrycznych. *Zeszyty Naukowe Akad Ekon Krakowie.* (2003) 623:35–44.

5. Kazimierska M. Obiektywna ocena barwy wyrobów użytkowych. *Techn Jak Wyr.* (2014) 59:44–7.

6. Pathare PB, Opara L, Al-Said FA. Colour measurement and analysis in fresh and processed foods: a review. *Food Bioproc Tech.* (2013) 6:36–60. doi: 10.1007/s11947-012-0867-9

7. Zahir SA, Yahaya O, Omar AF. Correlating the natural color of tropical fruit juice with its pH. *Color Res Appl.* (2020) 46:467–76. doi: 10.1002/col.22575

8. Pecho OE, Ghinea R, Alessandretti R, Pérez MM, Della Bona A. Visual and instrumental shade matching using CIELAB and CIEDE2000 color difference formulas. *Dental materials.* (2016) 32:82–92.

9. Budsławski J, Drabant Z. *Metody Analizy Żywności.* Warszawa: WNT (1972).

10. ISO. *ISO 8587:2006. Sensory analysis — Methodology — Ranking.* (2006). Available online at: https://www.iso.org/standard/36172.html (accessed October 20, 2023).

11. Ahmed RR, Parnar V, Amin MA. Impact of product packaging on consumer's buying behavior. *Eur J Sci Res.* (2014) 120:145–57. doi: 10.13140/2.1.2343.4885

12. Kuvykaite R, Dovaliene A, Navickiene L. Impact of package elements on consumer's purchase decision. *Econ Manag.* (2009) 14:441–7.

13. Schifferstein HN, Lemke M, de Boer A. An exploratory study using graphic design to communicate consumer benefits on food packaging. *Food Qual Prefer.* (2022) 97:104458. doi: 10.1016/j.foodqual.2021.104458

14. Koutsimanis G, Behe K, Harte J, Almenar E. Influences of packaging attributes on consumer purchase decisions for fresh produce. *Appetite.* (2012) 59:270–80. doi: 10.1016/j.appet.2012.05.012

15. Fernandez-Vazquez R, Stincio C, Melendez-Martinez A, Heredia F, Vicario I. Visual and instrumental evaluation of orange juice color: a consumers' preference study. *J Sens Stud.* (2011) 6:436–44. doi: 10.1111/j.1745-459X.2011.00360.x

16. Meléndez-Martínez A, Vicario I, Heredia F. Application of tristimulus colorimetry to estimate the carotenoids content in ultrafrozen orange juices. *J Agric Food Chem.* (2003) 25:7266–70. doi: 10.1021/jf034873z

17. Sánchez-Moreno C, Plaza L, De Ancos B, Cano MP. Vitamin C, provitamin A carotenoids, and other carotenoids in high-pressurized orange juice during refrigerated storage. *J Agric Food Chem.* (2003) 51:647–53. doi: 10.1021/jf020795o

18. Pérez-López A, Beltran F, Serrano-Megías M, López D, Carbonell-Barrachina G. Changes in orange juice color by addition of mandarin juice. *Eur Food Res Technol.* (2006) 222:516–20. doi: 10.1007/s00217-005-0099-6

19. Naz K, Epps H. Relationship between color and emotion: a study of college students. *Coll Stud J.* (2004) 38:396.

20. Parise CV, Spence C. Assessing the associations between brand packaging and brand attributes using an indirect performance measure. *Food Qual Prefer.* (2012) 24:17–23. doi: 10.1016/j.foodqual.2011.08.004

21. Chitturi R, Londono JC, Amezquita CA. The influence of color and shape of package design on consumer preference: the case of orange juice. *Int J Innov Econ Dev.* (2019) 5:42–56. doi: 10.18775/ijied.1849-7551-7020.2015.52.2003

22. Mehta A, Serventi L, Kumar L, Viejo CG, Fuentes S, Torrico DD. Influence of expectations and emotions raised by packaging characteristics on orange juice acceptability and choice. *Food Packag Shelf Life.* (2022) 33:100926. doi: 10.1016/j.fpsl.2022.100926

23. Wolniak R, Zadura M. Wpływ opakowania na wybór produktu przez konsumenta na przykładzie zabawek. *Zeszyty Naukowe Organ Zarządzanie.* (2012) 1891:111–24.

frontiers | Frontiers in Nutrition

The quality of selected raw and pasteurized honeys based on their sensory profiles and consumer preferences

Marek Kardas[1], Wiktoria Staśkiewicz-Bartecka[1]*,
Katarzyna Sołtys[1], Lechowsław Dul[2], Anna-Maria Sapała[1],
Agata Kiciak[1], Agnieszka Bielaszka[1] and Justyna Kardas[3]

[1]Department of Food Technology and Quality Evaluation, Department of Dietetics, Faculty of Public
Health in Bytom, Medical University of Silesia in Katowice, Zabrze, Poland, [2]Department of
Biostatistics, Faculty of Public Health in Bytom, Medical University of Silesia, Bytom, Poland, [3]Doctoral
School of the Medical University of Silesia in Katowice, Department of Human Nutrition, Faculty of
Public Health in Bytom, The Medical University of Silesia in Katowice, Zabrze, Poland

The purpose of this study was to determine the sensory profile of honeys based on the method of quantitative descriptive analysis and principal component analysis and assess consumer preferences of raw and pasteurized honeys. Samples of multi-floral honeys (from the store and apiary) were subjected to sensory analysis based on the method of ranking for taste preference, the method of scaling based on color, aroma, taste, and texture, and the method of differential descriptive analysis using 11 quality descriptors. The results were subjected to statistical analysis using the Principal Component Analysis method. The taste was found to be a descriptor that differentiates honey by origin. Consumers prefer the taste of pasteurized honeys. As a result of assessing the quality of honeys using the scaling method, it was found that: raw honeys are characterized by a lighter color than pasteurized honeys, store-bought honeys have a less noticeable aroma than honeys obtained from beekeepers, while samples of pasteurized honeys were judged to have a consistency more like that of typical honey. The sensory profiles obtained highlight the differences between pasteurized honeys and raw honeys.

KEYWORDS

quantitative descriptive analysis (QDA), principal components analysis (PCA), honey, sensory quality, consumer preferences

1 Introduction

Due to its composition and properties, honey is one of the most valuable animal products used by humans (1). It is a naturally sweet substance produced by bees, it is synthesized from the nectar of flowers, from the excretions of living parts of plants, or from the secretions of insects sucking the juices of living parts of plants, which bees collect, carry, and combine with specific substances of their own, deposit and leave to mature in honeycombs (2, 3). This substance is known as a food product, due to its flavorful qualities it has applications in culinary technology: for spreading bread, as a sweetener, as the base of sweet sauces, and as an ingredient in various desserts. On the other hand, honey is also used as a remedy for many ailments; herbal drinks, ointments, and medicinal patches are made from it (1, 4, 5). It is

valued for its multidirectional properties. The components of honey have bactericidal and bacteriostatic effects. In addition to its nutritional value, it also has phytochemical, anti-inflammatory, antimicrobial, and antioxidant effects (6). The factors that provide the antibiotic effect of honey can be divided into three main groups: physical, such as high osmotic pressure and acidic reaction; enzymatic, such as the content of glucose oxidase and lysozyme; and chemicals, such as the content of essential oils, flavonoids, organic acids, and tannins (5). Protein and enzymatic factors have antibiotic properties. An important substance is glucose oxidase, which in honey in the course of a chemical reaction leads to the formation of gluconolactone, which combined with water gives gluconic acid and hydrogen peroxide, with antibacterial and antifungal activity (5, 7–9). Another compound that affects antibiotic activity is lysozyme, a small-molecule, a thermostable protein that is responsible for the phenomenon of lysis of the cell walls of Gram-positive bacteria (10, 11). There are also other thermostable substances in honey, such as essential oils, flavonoids, and tannins. Storing honey under unsuitable conditions and heating it to temperatures above 45°C causes it to lose its enzymatic properties (8, 10). Honey has strong antioxidant properties, for which enzymes, vitamins, and polyphenols are responsible, whose content ranges from 0.01 to tens of mg/kg (12–14). Thanks to all these properties, honey is used in cosmetics, the production of medicines, as well as in the prevention of diseases. Its multidirectional use in the treatment of diseases is so important that it has received its own name apitherapy. Ancient civilizations considered honey a gift, so its importance is described in all religions. (5, 15–17). Thanks to the development of science, there are various means to evaluate the composition and biological and therapeutic properties of honey. There are different types of honey, which differ in composition, physicochemical properties, and biological effects (18).

Based on its origin, honey is divided into nectar, honeydew, and nectar-honeydew. In addition, the Polish Standard also distinguishes varieties of nectar honey, such as acacia, lime, buckwheat, heather, and multi-flower (19).

Nectar honey is produced by bees from the nectar of plants. Honeydew honey is honey made mainly from the excretions of insects sucking the juices of living plant parts or their secretions. On the other hand, nectar-honeydew honey is a mixture of these two varieties (19).

Color, flavor, aroma, and texture are features that characterize the different varieties of honey and make it possible to differentiate them (19). The peculiar organoleptic properties of honey are determined primarily by the type and species of the plant from which the pollen was collected. Among honeys, a wide variety is observed in terms of color. Individual varieties of honey can range in color from light cream to brown (19, 20). The color of honey is determined by factors such as the type of forage, environmental factors (temperature, soil, humidity), and storage time (19, 21). Honey color is also influenced by the content of natural pigments: carotenoid compounds, xanthophyll, chlorophyll and its derivatives, flavonoids, and anthocyanins (5, 20). The different varieties differ significantly in palatability. The main component determining the flavor of honey is sugars; those with a higher fructose content than glucose are considered sweeter (15, 16, 22). Other compounds that determine the taste of a particular variety of honey are organic acids (gluconic acid, citric acid, malic acid, acetic acid), tannins, glycosides, and alkaloidal substances (5). The consistency of honey depends on the advancement of the crystallization process. Honey can have a liquid, viscous, partially or completely crystallized consistency. The storage temperature of the product has a significant effect on the crystallization process of honey and consistency (5, 15).

Today, interest in honey is very high, as there is a growing interest in natural medicine, healthy eating, and taking care of appearance. However, it is important to distinguish raw honey, which, through the absence of technological processes, is a product with greater biological value than honey subjected to pasteurization.

The sensory qualities of a product play an important role in its acceptance. This is because consumers do not want to buy and consume products that do not meet their expectations. Evaluation of consumer preferences is very important and valuable information for food manufacturers, but it is not enough. After all, a producer needs to know not only how his product is rated by consumers, but also why it received a certain rating. Quantitative descriptive analysis (QDA) provides valuable answers to this question.

The purpose of this study was to determine the sensory profile of honeys based on the method of quantitative descriptive analysis, and principal component analysis, and to assess consumer preferences and the quality of raw and pasteurized honeys.

2 Materials and methods

2.1 Sample collection

The study material consisted of 16 samples of nectar, multifloral honeys of various origins obtained in the second quarter of 2022. The honey samples were divided into two categories. The first category consisted of samples of raw, unprocessed honey obtained from beekeepers from two apiaries located in Poland, in Silesia Province (Raw Samples). The honeys were classified as spring honeys, which were produced from spring-flowering plants in various proportions: lime, turnip, sunflower, buckwheat. All honey samples were not heated by producers and were taken no later than 4 weeks after extraction from the hives, the batches showed no signs of fermentation or crystallization. The honey samples were stored at room temperature until use. Both apiaries used bees of one subspecies, *Apis mellifera carnica*. The second category consisted of nectar, multifloral, pasteurized honeys purchased from two shopping centers in the city of Katowice (Silesia Province, Poland), these honeys were a mixture of honeys from EU and non-EU member states (Pasteurized Samples). Honey producers did not declare detailed information on the time of harvesting honey and the species of bees. According to the producers, the honeys were pasteurized, heated at 80°C for 3 min, then immediately cooled to 45°C. Four samples were taken from each sample acquisition point, which were then mixed to obtain a representative sample for further analysis before proceeding. Samples were combined under laboratory conditions at 21 degrees C with full sterility of methods. The samples of multifloral honeys used in the study were coded and labeled with symbols (according to the place of origin): Raw Sample 1, Raw Sample 2, Pasteurized Sample 1 and Pasteurized Sample 2.

The honeys were stored in a dry, dark, and cool place. Prior to sensory testing, honey was recrystallized and samples of one origin were combined in a water bath at 40°C ± 1°C to standardize consistency.

TABLE 1 Border markings of the 5-point scale.

Sample characteristic	1	5
Color	Bright, cream-colored	Dark, pale yellow color
Smell	Impalpable	Very palpable
Taste	Impalpable	Very palpable
Texture	Adequate for honey	Inadequate for honey

The evaluation group consisted of people who participated in the serialization method and were properly trained for the described evaluation.

TABLE 2 Discriminators used in the QDA assessment.

Characteristic	Definition
Color	Typical for honey: from bright, cream-colored to dar, pale yellow colour.
Smell of beeswax	The smell is characteristic of beeswax.
Sweet-nectar smell	Mild, sweet, nectar-like smell.
Sweet taste	The basic quality of a sweet taste does not need to be defined.
Honey taste	The taste is characteristic of honey.
Burning-irritating taste	A slight burning sensation in the mouth and throat, irritation of the taste buds.
Acerbic taste	A tightening sensation, especially felt at the edges of the tongue and the walls of the mouth.
Foreign taste	Taste to stray from the typical honey taste
Smoothness	Uniform structure of the sample when spreading it through the mouth.
Stickiness	A feeling of sticking the surface of the tongue to the top of the mouth.
Dissolving in the mouth	A feeling that the sample is melting in the mouth.

2.2 Study design

Appropriately coded and prepared samples were subjected to sensory analysis using 3 methods. The research was carried out in the sensory laboratory of the Department of Dietetics of the Department of Food Technology and Quality Evaluation, Medical University of Silesia, designed in accordance with the standard: PN-EN ISO 8589: 2010 (23). The laboratory had 6 separate workstations, providing the assessors with appropriate conditions to conduct the test (elimination of disturbing factors; noise, bright light, etc.). The samples for evaluation were administered in odorless, colorless, plastic containers intended for contact with food.

The study was conducted with the approval of the Bioethics Committee of the Silesian Medical University in Katowice (KNW/0022/KB/16–1/14).

2.3 Evaluation by serialization method

In the first stage of the research, the honey samples were assessed by the serialization method, using the author's assessment card. The samples had to be ranked from most to least palatable by writing the sample codes in the correct order. The evaluation group consisted of 75 people (36 women and 29 men) trained in the scheduling method. The evaluators ranged in age from 18 to 30, with an average age of 23.43 ± 2,43.

2.4 Evaluation by scaling method

In the second stage, the honey samples were assessed by the scaling method, using the proprietary five-point scale, assessing the samples on the basis of four differentiators: color, smell, taste, and consistency. The evaluators were asked to evaluate the samples using a 5-point hedonic scale. The boundary values of the scale are shown in the table below (Table 1). The values from 2 to 4 corresponded to the intermediate intensity of the examined feature.

2.5 Quantitative descriptive analysis

The last method was the quantitative descriptive analysis (QDA) in accordance with the executive procedure described in ISO 13299:2016–05 (24). To conduct the study, an original questionnaire was used, for the preparation of which the qualitative attributes for the evaluation of honey were selected and defined. The study used 10 descriptors for odor, taste, smoothness, viscosity, and mouthfeel. The descriptors are summarized in Table 2.

For the quantification of the descriptors, a linear scale with the given boundary terms was used. The intensity of the descriptors assessed increased from left to right in order to minimize the possibility of error.

The sensory characteristics of the samples were performed by a 10-person evaluation team (in two independent repetitions), properly trained, and prepared methodically in accordance with the PN-ISO 4121: 1998 (25) and PN-ISO 6564: 1999 standards (26).

2.6 Statistical analysis

The obtained data were developed using Statistica v.13.3 (Stat Soft Polska) and R v. 225 4.0.0 package (2020) under the GNU GPL license (The R Foundation for Statistical Com-226 puting).

To present quantitative data, mean values, and standard deviations were calculated - $X \pm S$. For qualitative data, percentage notation was used. Qualitative data were expressed as numerical values determined by mathematical methods to make statistical inferences. The Friedeman test (the non-parametric equivalent of one-way analysis of variance) was used to analyze the variation in rank sums. In order to check the compliance of the assessments of tested products, the W Kendall coefficient of conformity (WK) and the Spearman similarity coefficient (rS) was used. Kendall's W coefficient of concordance is the arithmetic mean of Spearman's rank correlation coefficients calculated for each pair of subjects evaluating the samples analyzed. Spearman's similarity coefficient was used to test the correlation between the

ratings (more precisely, the ranks) given to each sample by the respondents. The more the ordering of the honey samples differed for a pair of subjects, the closer rS was to 0. Kendall's W concordance coefficient takes values between 0 and 1, where 0 means there is a complete lack of concordance between the ratings assigned to the honey samples by the subjects, while 1 means that all subjects assigned the same ranks to the honey samples.

Principal Component Analysis (PCA) is a method used to interpret sensory profiling results. The extensive use of PCA in QDA is based on the concept of a spatial n-dimensional model of a product's sensory quality (or its single modality, such as aroma, texture, or palatability) determined by a set of discriminants, or descriptors.

Principal Component Analysis makes it possible to study a large number of data, taking into account the interdependencies between them. The results of PCA are presented in graphical form (the so-called PCA projection of differences and similarities in sensory quality of the food products studied). In Principal Component Analysis, a coordinate system was created, the axes of which are the so-called principal components, and by analyzing the correlation between the primary variables (i.e., the values of the relevant differentiators for the tested honey samples) and the obtained principal components, the primary variables (i.e., the differentiators, descriptors describing the tested products) were reduced and the differentiators and the tested products were clustered.

A value of $p < 0.05$ was used as a criterion for statistical significance.

3 Results

The analysis of the results from the honey sample analysis by the ranking method was started by summing up the ranking positions of individual samples on each evaluation sheet. A scaling method was also used based on four discriminants: color, smell, taste, and texture. After assigning each of the ratings a numerical value and summing them up by counting the ranks, the results presented in Table 3 were obtained.

On the basis of the obtained sums of ranks, it was found that the pasteurized honeys were rated as tastier than the raw honeys. According to the evaluators, the Pasteurized Sample 1 turned out to be the tastiest sample, while the Raw Sample 1 was the least tasty. In order to assess the agreement of the respondents' ranking of the samples of honey analyzed, Kendall's W coefficient of agreement (WK = 0.12) and Spearman's similarity coefficient (rS = 0.11) were calculated. The obtained values indicate very low agreement of consumers' ratings of the analyzed honey samples. Details of the ranks awarded are shown in Figure 1.

The results indicate that raw honeys are much lighter. According to the evaluators, the lightest sample was Raw Sample 2, then Raw Sample 1, Pasteurized Sample 1, and the darkest one - Pasteurized Sample 2, there was good agreement in the rater responses. Based on the calculated Kendall's W coefficient of concordance (WK = 0.84) and similarity coefficient (rS = 0.84), it can be concluded that the concordance of the evaluators' responses was high. The statement that the color of the samples depends on their origin is plausible.

Based on the results, differences can be seen between the smells of pasteurized honeys and those obtained from apiaries. As the sample with the least noticeable odor, the evaluators considered the sample Pasteurized Sample 2, followed by Pasteurized Sample 1, Raw Sample 1, and Raw Sample 2. The calculated coefficient of concordance W Kendall (WK = 0.39) and the coefficient of similarity (rS = 0.39) indicate low concordance of the evaluators' answers.

As the sample with the most intense taste, the evaluators selected the sample of Raw Sample 2, then Pasteurized Sample 1 and Pasteurized Sample 2. The sample of Raw Sample 1 was selected as the sample with the least palpable taste. As a result of the analysis of the obtained data, the Kendall W concordance value (WK = 0.18) and the coefficient of similarity (rS = 0.17) were obtained. The obtained values indicate a low agreement of the evaluators' answers, although higher than with the scheduling method for the same discriminant.

As the sample with the consistency most similar to that suitable for honey, the evaluators indicated the sample Pasteurized Sample 1, then Pasteurized Sample 2, Raw Sample 1, and Raw Sample 2. Analyzing the above data, the following values were obtained: WK = 0.35 and rS = 0.34, which indicates a low concordance of the evaluators' answers. Figure 2 presents the obtained results graphically.

As a result of the evaluation of the honeys, in duplicate, using the QDA method, the mean scores were obtained, which are summarized in Table 4.

On the basis of the averages obtained, the intensity of individual descriptors was presented graphically (Figure 3).

The data obtained as a result of tests of honey samples carried out by the scaling method and the QDA method were analyzed by the PCA principal components method. The results of the analysis are presented in Figure 4.

Based on the PCA analysis, the honey samples were classified based on two factors explaining the variability of the original data. In a study by respondents evaluating honey samples using the scaling method, component 1 explains 93.6%, while component 2 explains 5.4% of the variability of all the discriminants used in the study.

As can be seen from the graphic PCA projection of the similarities and differences in the sensory quality of the samples of the tested honeys, two groups of samples of similar sensory

TABLE 3 Assessment of the intensity of the examined honey features (rank sums) by the ranking method ($N = 75$).

Honey sample	RANK SUMS				
	Color	Smell	Taste	Consistency	General
Raw Sample 1	152[b]	240[b]	152[b]	258[b]	214[b]
Pasteurized Sample 1	271[a]	175[a]	236[a]	149[a]	142[a]
Raw Sample 2	108[b]	283[b]	244[c]	264[b]	212[b]
Pasteurized Sample 2	309[c]	142[a]	208[a]	169[a]	182[a]

The values of the sum of the ranks within the ratings of the individual distinguishing factors marked with different letters are statistically significantly different ($p < 0.05$).

The values of the sum of ranks within the ratings of individual discriminants marked with different letters significantly differ statistically.
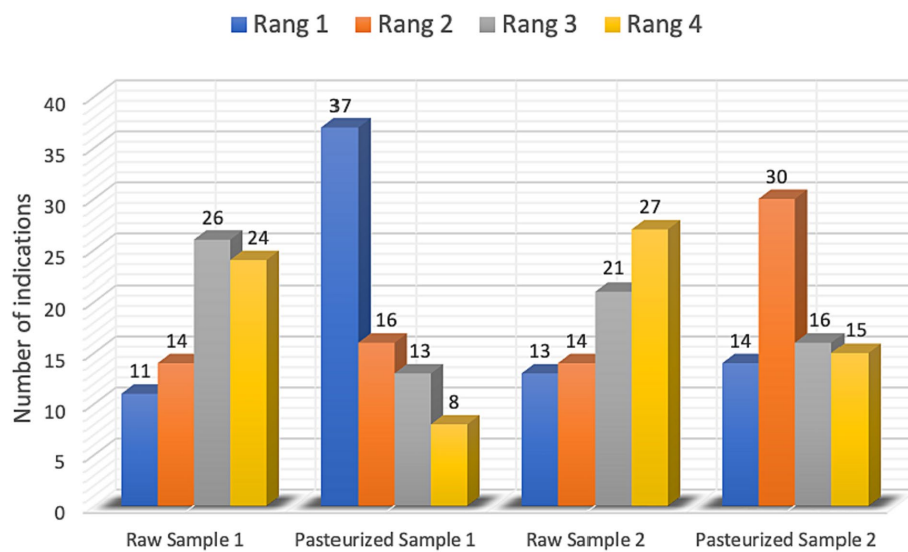
FIGURE 1
Number of indications in the serialization survey. Rang 1 rated as "the best" to rang 4 classified as "the worst," according to the researchers' assessment.
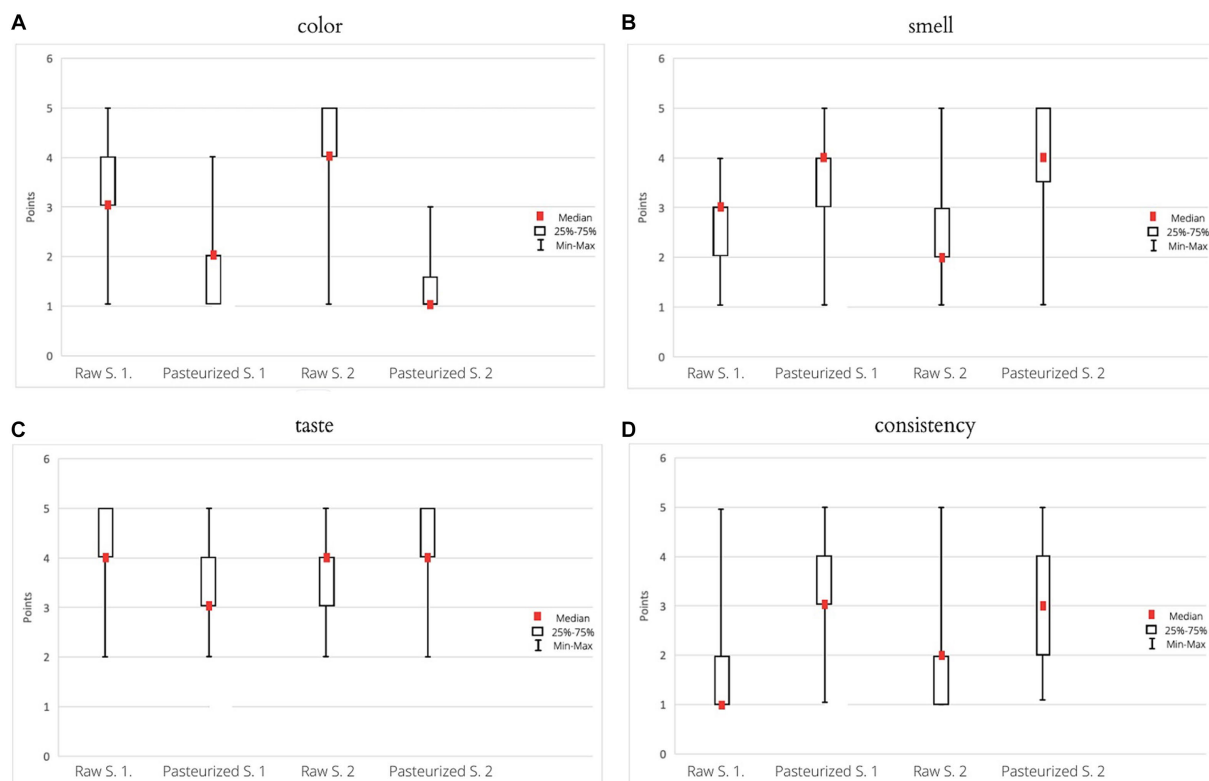
FIGURE 2
Results of evaluation of the intensity of the color **(A)**, smell **(B)**, taste **(C)**, and consistency **(D)**.

quality were created. The groups discussed are located in different halves of the graph, which correspond to the different signs of the factor axis.

The length of the vector, which corresponds to the "taste" descriptor, in relation to component 1 is very small, which means that

this feature has a very weak effect on the differentiation of both examined groups of honeys. Pasteurized honey samples clearly differ in color from samples of raw honeys. On the other hand, honey samples from apiaries have a more intense smell and consistency compared to honey samples from stores.

Subjecting the data obtained by QDA tests were subjected to statistical analysis using the PCA method, on this basis, the classification of the tested honey samples was made based on 2 factors explaining the variability of descriptors.

In the first study, component 1 explains 57.2%, while component 2 explains 37.6%, while in the second repetition, component 1 explains 57.8%, and component 2 explains 35% of the variability of all discriminants used in the study (Figure 5).

The analysis of the results from the first repetition of the QDA test shows the presence of three groups of samples of the tested honeys: Pasteurized 1 and Pasteurized 2, Raw 1, and Raw 2.

Pasteurized honeys samples are characterized by a high similarity in their sensory quality. Color and smoothness are the descriptors that

clearly distinguish the pasteurized-samples of honey from raw-samples of honey (27).

The sample of Raw 1 honey has a more intense, burning-irritating taste compared to the other samples. On the other hand, the honey sample of Raw 2 is characterized by a more intense honey flavor and a sweet-nectar aroma compared to other samples.

The results of the PCA statistical analysis of the results obtained in the second replication of the QDA study are presented in Figure 6.

The results of the repeated tests, presented on the graphic PCA projection of the similarities and differences in sensory quality of the samples of the tested honeys (Figure 6), confirm the conclusions obtained in the first study.

4 Discussion

All the honeys tested were multiflorous honeys. Nevertheless, differences in the assessment of the tested honey sensory features and the perception of individual descriptors were visible. This may be due to differences in the botanical regions of the samples. Multi flower honeys can differ significantly from one another depending on the origin of the nectar collected and used by bees.

The apiaries from which the honey was obtained, Raw Sample 1 and Raw Sample 2, were located in the Silesian Province. The labels honeys' samples Pasteurized 1 and Pasteurized 2 contained the information - "A mixture of honeys from EU and non-EU Member States.," Which indicates that the exact origin of the honey is unknown. The composition of honey blends can be very diverse. The information on the label that the product is such a mixture is a gateway for producers to market honey of unknown origin, without adequate information for consumers.

The research on preferences regarding the choice of the place of honey supply shows that buyers prefer honeys from private apiaries. Aldona Gontarz et al., analyzing the consumer preferences of students regarding honey, showed that 67.1% of respondents prefer to buy honey directly from the producer (28). Similar conclusions were

TABLE 4 QDA ratings of honeys with standard deviation in two replicates.

Sample	Raw 1 X ± SD	Raw 2 X ± SD	Pasteurized 1 X ± SD	Pasteurized 2 X ± SD
C	4.90 ± 0,3	6.15 ± 0.25	8.00 ± 0.14	8.30 ± 0.00
SB	5.00 ± 0,3	7.25 ± 0.07	6.85 ± 0.07	5.80 ± 0.28
SNS	4.45 ± 0.35	8.20 ± 0.14	6.90 ± 0.28	6.40 ± 0.28
ST	8.70 ± 0.14	9.35 ± 0.07	8.30 ± 0.28	9.20 ± 0.14
HT	7.35 ± 0.21	9.25 ± 0.07	6.65 ± 0.07	6.40 ± 0.21
BIT	3.70 ± 0.14	1.55 ± 0.35	1.90 ± 0.00	0.85 ± 0.05
AT	2.30 ± 0.14	1.55 ± 0.07	1.65 ± 0.21	1.30 ± 0.00
FT	1.10 ± 0.28	0.65 ± 0.07	2.40 ± 0.43	1.80 ± 0.14
SM	6.20 ± 0.00	6.40 ± 0.07	8.40 ± 0.43	7.80 ± 0.14
S	6.75 ± 0.21	8.85 ± 0.07	8.70 ± 0.00	8.50 ± 0.28
DM	7.70 ± 0.00	8.50 ± 0.42	8.25 ± 0.64	8.60 ± 0.42
G	7.75 ± 0.21	8.50 ± 0.42	7.25 ± 0.21	7.25 ± 0.21

C – color, SB – the smell of beeswax, SNS – sweet-nectar smell, ST – sweet taste, HT – honey taste, BIT – burning-irritating taste, AT – acerbic taste, FT – foreign taste, SM – smoothness, S – stickiness, DM – dissolving in the mouth, G – general.
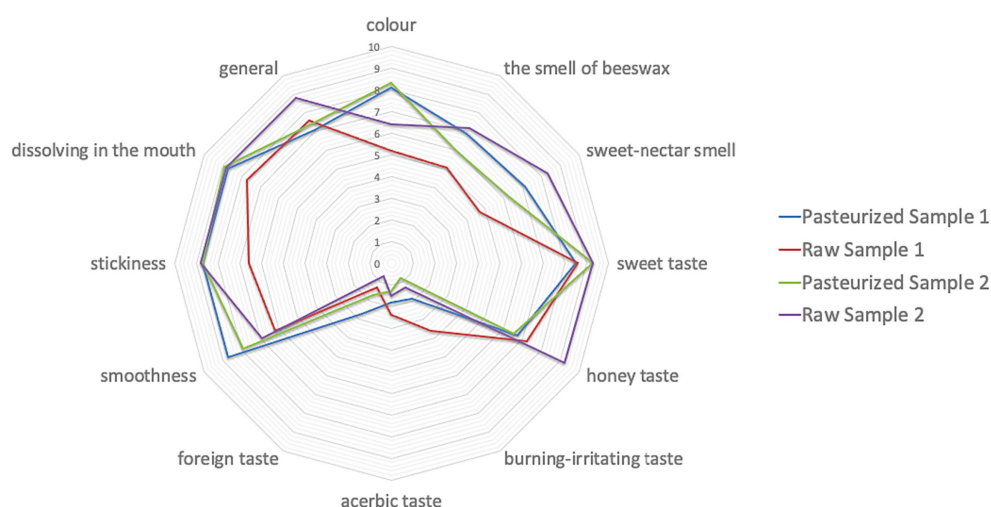

FIGURE 3
Radar plot showing the intensity of individual descriptors in duplicate QDA tests.
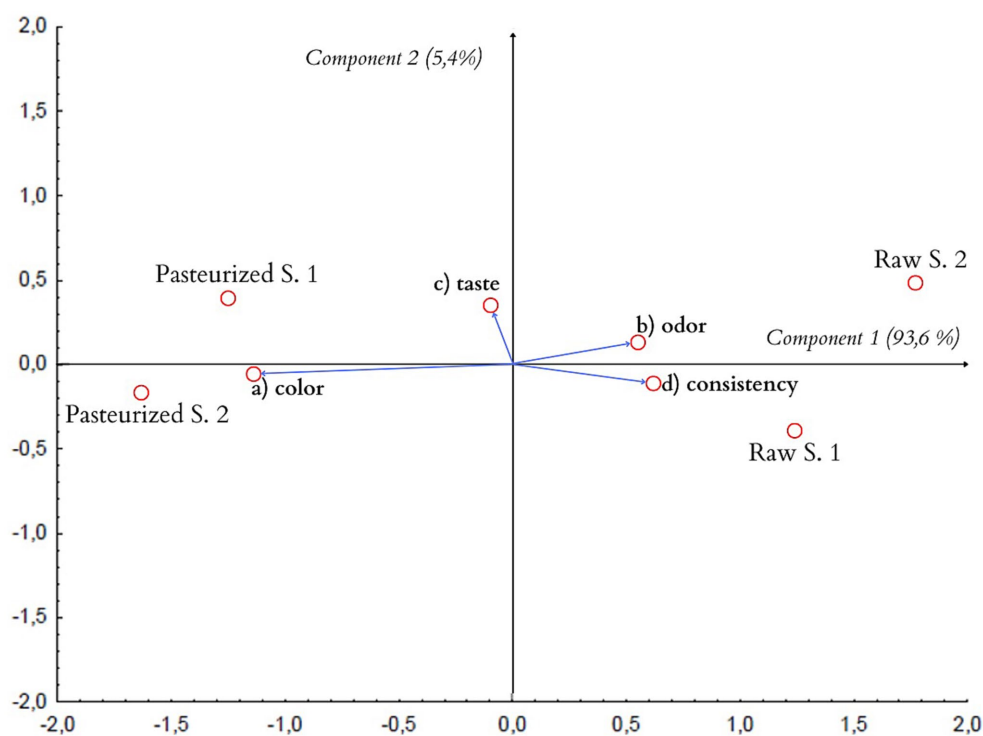
FIGURE 4
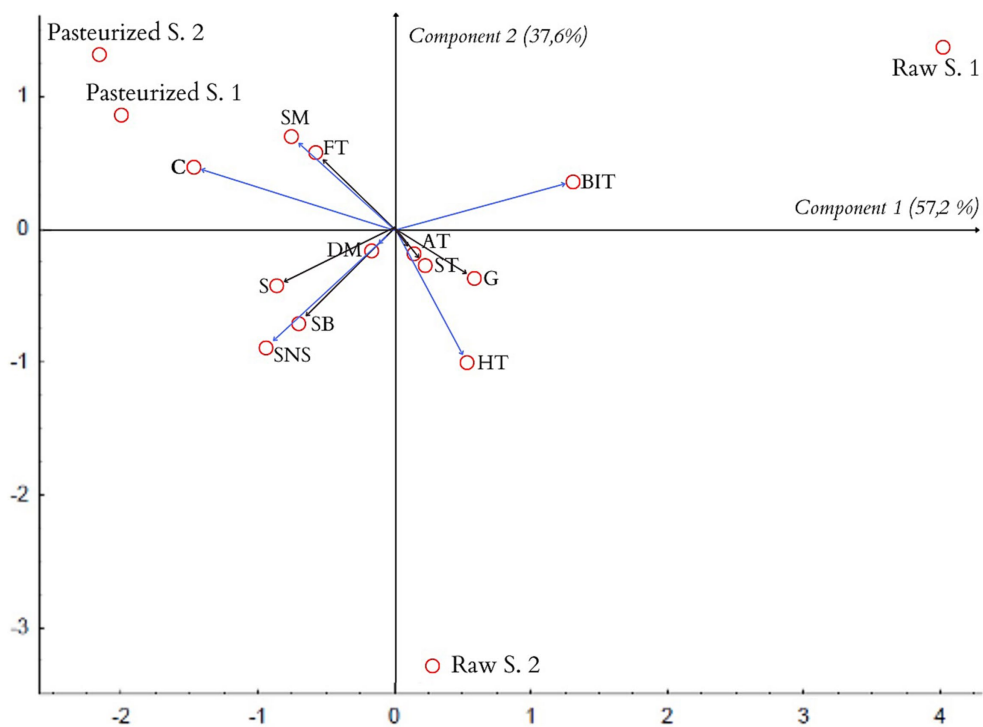PCA projection of similarities and differences in sensory quality of the tested honeys (biplot).

FIGURE 5
PCA projection of the similarities and differences in sensory quality of the tested honeys in the first study (biplot).
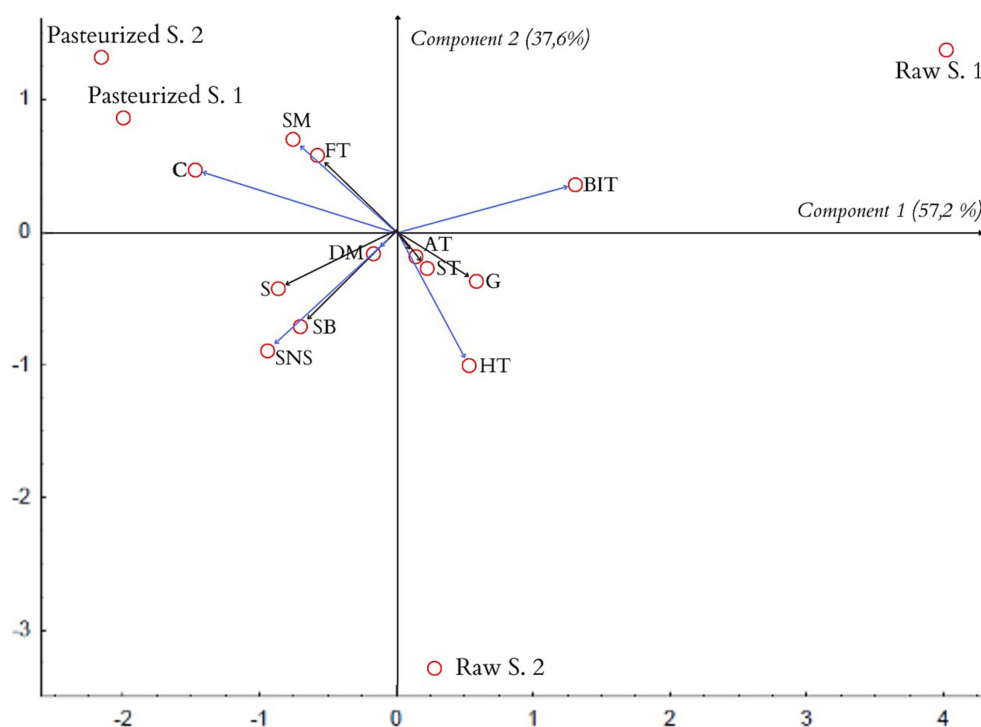
FIGURE 6
PCA projection of the similarities and differences in sensory quality of the tested honeys in the second study (biplot).

obtained on the basis of research carried out by Bratkowski et al., in which as many as 84.8% declared that they most willingly obtain honey directly at the beekeeper's house (29). This form of selling honey allows the customer to contact the beekeeper directly. The consumer has the opportunity to obtain the necessary information which increases the awareness of the buyer.

The consumer assessment using the ranking method showed differences in the preferences of respondents regarding the taste of honey. Honey from shopping malls was rated as tastier. Comparing the assessment of taste preferences in the conducted study to the questionnaire research on the declared preferences regarding the place of honey purchase, it can be concluded that it is contradictory. This is due to the fact that the samples were encoded and the place of origin was unknown to the respondents.

As a result of the evaluation of the color intensity of the tested samples, raw honeys were considered darker. Color variation within one variety may depend on the degree of consistency. Pasteurized honeys were poured, while the consistency of the honeys from the apiaries was a bit dense. Differences in color may also result from differences in the type of fruit used in the production of honey and the period of its production. Raw honey obtained from apiaries turned out to be sampled with a more intense smell. The results indicate that the evaluators noticed significant differences in the perception of smell between the tested honey samples.

Sensory evaluation, next to chemical, physical, and microbiological tests, is an important element of all kinds of food analysis and evaluation. The scheduling method requires the evaluator to rank the samples according to appropriate guidance. It is not possible to evaluate two samples equally. In the study, the evaluators had to rank the honey samples from the most delicious to the least

tasty according to their preferences. This method allowed for greater differentiation between the assessed samples than in the scaling method, where respondents could assign the same number of points to a different sample of honey.

The data obtained as a result of the scaling methods were analyzed with the PCA method. The charts included in the work, obtained as a result of the PCA analysis, have the form of a "qualitative map." They allow to assess the similarities of the sensory quality of the tested honey samples on the basis of their location in relation to each other in the system of main components - the closer the honey samples are, the greater the similarity of their sensory quality. The distance between the samples of the tested honeys on the PCA projection allows for assessing the differences between the samples.

Creating a biplot of the analyzed descriptors allows for a fairly simple indication of which descriptors and to what extent the examined honey samples differentiate. Based on the vectors created in the system of principal components, which begin at the beginning of the coordinate system and end at the point of the analyzed discriminant, it is possible to assess the degree of differentiation of the honey samples - the greater length of the vector means that the given descriptor differentiates the examined honey samples more strongly. The distribution of honey samples on the biplot diagram, concerning the QDA method used in the first repetition, indicates the division of the tested samples into groups. This division suggests a sensory similarity of pasteurized honeys from stores. Also, the results for the sensory evaluation at the consumer level indicated that the "color" discriminant clearly distinguished the tested samples of pasteurized honeys from samples of raw honeys.

The obtained graphs (Figures 4, 5) show that the conclusions obtained on the basis of the scaling method concerning the color

intensity coincide. They show that the color of pasteurized honeys is the feature that distinguishes them most from the other samples.

Raw honey samples were smooth. In the scaling method, the respondents indicated the above samples as having a consistency more suitable for honey. In consumer research on the preferences of bee honeys (30, 31), as many as 48.78% of respondents declared that they prefer liquid honeys.

The QDA method used in the study characterizes the analyzed samples in detail. It is used for sensory analysis of bee honey, which is considered an important tool for determining its floral origin. Ciappini et al. (32) tested samples of Argentine honeys using QDA. In order to determine the sensory profile, clover and eucalyptus honey were assessed. Significant differences in perceived descriptors were shown. Clover honey was characterized by a fruity and floral taste of low intensity, while eucalyptus honey had a more intense flavor, with a floral note and an aromatic scent (30, 31, 33).

Indian honeys were also analyzed using the QDA method (32). The study included 11 samples of multiflorous honeys, which were grouped using PCA according to sensory variables and physicochemical parameters in order to analyze the relationship between the groups. The usefulness of the QDA method in the sensory tests of honey in combination with the use of physicochemical tests can be used to distinguish the floral origin and the fruit used by bees in order to differentiate the tested samples, as well as to characterize the individual varieties of honey.

Where honey is bought is an important factor in determining the quality of honey and its health-promoting qualities. In recent years, a number of producers have appeared in the retail chain, buying honey from apiaries, packaging it, and selling it. Such honey requires careful veterinary inspection for quality, as it is one of the food products that are often adulterated, and it is almost impossible for the consumer to distinguish a quality product from an imitation on his own. Adulterated honey is characterized by a lower content of compounds that have a positive effect on human health (34, 35).

The study by Kędzierska-Matysek et al. analyzed the mineral content of honeys purchased from apiaries and stores available on the Polish market. Honeys purchased directly from the producer contained more K, Mg, and Mn (36). A study by Balzan et al. analyzed the microbiota of honeys, it can provide information on production in a contaminated environment and failure to follow good beekeeping and production practices, which may be less dangerous in terms of food safety and affect product quality. Honeys from market sales presented inferior quality. Honeys obtained from beekeepers are characterized by very low amounts of contaminating microorganisms, and beneficial spore-forming bacteria may be present (37).

There are some limitations of the current study. The samples analyzed came from 2 apiaries and 2 stores, it would be reasonable to increase the number of places from which honey samples were obtained. It would also be worth considering expanding the study to include chemical analysis of the samples and comparing it with consumer preferences. On the other hand, an important value of this work is to obtain practical results that can provide important information for beekeepers about the preferred characteristics of this product. Obtaining honey with desirable characteristics by beekeepers can increase the interest of potential consumers, this phenomenon is also important with regard to the possible health-promoting effects on the health of honey obtained from apiaries.

5 Conclusion

Based on the results, it was concluded that the analysis of sensory characteristics of honey samples showed significant differences between honeys taken from different points. Taste is a descriptor that differentiates honey in terms of its origin. Consumers prefer the taste of pasteurized honeys purchased in stores to those raw from apiaries. In addition, raw honeys are characterized by a lighter color than pasteurized honeys, store honeys have a less noticeable aroma than honeys obtained from beekeepers, and samples of pasteurized honeys according to respondents have a texture more suitable for honey. The sensory profiles obtained highlight the differences between pasteurized honeys and raw honeys. Honeys from stores are characterized by high similarity in sensory quality. Distinguishing characteristics of raw honeys obtained from apiaries include honey taste, burning-irritating taste, and sweet-nectar aroma. Obtaining a sensory profile of raw honeys similar to pasteurized honeys can increase their consumption, which may have health-promoting value.

Data availability statement

The raw data supporting the conclusions of this article will be made available by the authors, without undue reservation.

Ethics statement

The studies involving humans were approved by Komisja Bioetyczna przy Śląskim Uniwersytecie Medycznym w Katowicach. The studies were conducted in accordance with the local legislation and institutional requirements. The participants provided their written informed consent to participate in this study. Written informed consent was obtained from the individual(s) for the publication of any potentially identifiable images or data included in this article.

Author contributions

MK: Funding acquisition, Methodology, Project administration, Writing – review & editing. WS-B: Methodology, Resources, Writing – original draft. KS: Conceptualization, Data curation, Methodology, Writing – review & editing. LD: Fomal analysis, Software, Writing – review & editing. A-MS: Validation, Visualization, Writing – review & editing. AK: Investigation, Supervision, Writing – original draft. AB: Resources, Writing – original draft. JK: Writing – original draft.

Funding

Conflict of interest

The authors declare that the research was conducted in the absence of any commercial or financial relationships that could be construed as a potential conflict of interest.

Publisher's note

All claims expressed in this article are solely those of the authors and do not necessarily represent those of their affiliated organizations, or those of the publisher, the editors and the reviewers. Any product that may be evaluated in this article, or claim that may be made by its manufacturer, is not guaranteed or endorsed by the publisher.

References

1. Baryłko-Piekielna N, Matuszewska I, Szczecińska A, Radzanowska J, Jeruszka M. Jakość sensoryczna rynkowych soków jabłkowych i pomarańczowych. *Żywność Nauka Technologia Jakość*. (2002) 1:34–51.

2. Miguel MG, Antunes MD, Faleiro ML. Honey as a complementary medicine. *Integr Med Insights*. (2017) 12:1178633717702869. doi: 10.1177/1178633717702869

3. Council of the European Union. *Council Directive 2001/110/WE of 20 December 2001 relating to honey*. (2001).

4. Siddiqui AJ, Musharraf SG, Choudhary M. Application of analytical methods in authentication and adulteration of honey. *Food Chem*. (2017) 21:687–98. doi: 10.1016/j.foodchem.2016.09.001

5. AyoubMeo S, Ahmad Al-Asiri S, Latief Mahesar A, Javed AM. Role of honey in modern medicine Saudi. *Saudi J Biol Sci*. (2017) 24:975–8. doi: 10.1016/j.sjbs.2016.12.010

6. Jones R. Honey and healing through the ages. *Journal of Api Product and Api Medical Science*. (2009) 1:2–5. doi: 10.3896/IBRA.4.01.1.02

7. Samarghandian S, Farkhondeh T, Samini F. Honey and health: a review of recent clinical research. *Pharm Res*. (2017) 9:121–7. doi: 10.4103/0974-8490.204647

8. Cianciosi D, Forbes-Hernández TY, Afrin S, Gasparrini M, Reboredo-Rodriguez P, Manna PP, et al. Phenolic compounds in honey and their associated health benefits: a review. *Molecules*. (2018) 23:2322. doi: 10.3390/molecules23092322

9. Albaridi NA. Antibacterial potency of honey. *Int J Microbiol*. (2019) 2:2464507. doi: 10.1155/2019/2464507

10. Brudzynski K, Miotto D, Kim L, Sjaarda C, Maldonado-Alvarez L, Fukś H. Active macromolecules of honey form colloidal particles essential for honey antibacterial activity and hydrogen peroxide production. *Sci Rep*. (2017) 7:7637. doi: 10.1038/s41598-017-08072-0

11. Vică ML, Glevitzky M, Tit DM, Behl T, Heghedűş-Mîndru RC, Zaha DC, et al. The antimicrobial activity of honey and propolis extracts from the central region of Romania. *Food Biosci*. (2021) 41:101014. doi: 10.1016/j.fbio.2021.101014

12. Ranneh Y, Akim AM, Hamid HA, Khazaai H, Fadel A, Zakaria ZA, et al. Honey and its nutritional and anti-inflammatory value. *BMC Complement Med Ther*. (2021) 21:1–17. doi: 10.1186/s12906-020-03170-5

13. Monggudal MB, Radzi MNFM, Ismail MM, Ismail WW. Effect of six month storage on physicochemical analysis and antioxidant activity of several types of honey. *IOP Conf Ser Mater Sci Eng*. (2018) 440:012047. doi: 10.1088/1757-899X/440/1/012047

14. Zarei M, Fazlara A, Tulabifard N. Effect of thermal treatment on physicochemical and antioxidant properties of honey. *Heliyon*. (2019) 5:e01894. doi: 10.1016/j.heliyon.2019.e01894

15. Wantusiak P, Piszcz M, Skwarek M, Głód B. Właściwości antyoksydacyjne miodów wyznaczone metodami chromatograficznymi. *Camera Separatoria*. (2011) 3:297–317.

16. Mohammed MEA. Factors affecting the physicochemical properties and chemical composition of bee's honey. *Food Rev Int*. (2022) 38:1330–41. doi: 10.1080/87559129.2020.1810701

17. Koszowska A, Dittfeld A, Nowak J, Ziora K. Pszczoły i ich produkty – znaczenie dla zrównoważonego rozwoju. *Med Środ*. (2013) 16:79–84.

18. Khan SU, Anjum SI, Rahman K, Ansari MJ, Khan WU, Kamal S, et al. Honey: single food stuff comprises many drugs. *Saudi J Biol Sci*. (2018) 25:320–5. doi: 10.1016/j.sjbs.2017.08.004

19. Gropoşilă-Constantinescu D, Popa G, Vişan V, Mărgărit GL, Toma R, Barba D. Comparative study of the quality of traditional honey and industrial honey. *Scientific Bulletin Series F Biotechnologies*. (2020) 24:50–4.

20. PN-88/A-77626. *Bee honey polish Committee for Standardization, measures and quality*. Warsaw, Poland: Wydawnictwa Normalizacyjne alfa. (1988).

21. Geisa MG, Ciappini MC, Hilgert NI. Sensory attributes of native stingless bee honey (*Plebeia molesta*): first approaches to the characterization and preference of local consumers. *Ethnobiol Conserv*. (2021):10. doi: 10.15451/ec2021-06-10.27-1-15

22. Azman KF, Zakaria R. Honey as an antioxidant therapy to reduce cognitive ageing. *Iran J Basic Med Sci*. (2019) 22:1368. doi: 10.22038/IJBMS.2019.14027

23. Al-Farsi M, Al-Belushi S, Al-Amri A, Al-Hadhrami A, Al-Rusheidi M, Al-Alawi A. Quality evaluation of Omani honey. *Food Chem*. (2018) 262:162–7. doi: 10.1016/j.foodchem.2018.04.104

24. PN-EN ISO. *8589:2010/A1:2014–07*. Sensory Analysis-General Guidelines for Designing a Sensory Analysis Laboratory: Geneva, Switzerland. (2007).

25. *Sensory analysis – methodology – method of investigating sensitivity of taste*. Warszawa, Poland: Polish Normalization Committee (2016).

26. Sensory analysis - methodology - evaluation of food products by methods using scales In: *Polish normalization committee*. Warszawa, Poland: (1998)

27. Sensory analysis - methodology - flavour profile methods In: *Polish normalization committee*. Warszawa, Poland: (1999)

28. *Rozporządzenie Ministra Rolnictwa i Rozwoju Wsi z dnia 14 stycznia 2009r. w sprawie metod analiz związanych z dokonywaniem oceny miodu*. Available at: https://isap.sejm.gov.pl/isap.nsf/DocDetails.xsp?id=WDU20090170094 [Accessed online 7.12.2023r.]

29. Gontarz A, Błońska I, Socha S. Analiza preferencji konsumenckich dotycząca miodow pszczelich. *Wiad Zootech*. (2016) 54:61–76.

30. Bratkowski J, Wilde J, Miećkowska A. Wymagania konsumentów stawiane gospodarstwom pasiecznym prowadzącym sprzedaż detaliczną miodu. *Biuletyn Naukowy*. (2008) 28:37–43.

31. Kopała E, Kuźnicka E, Balcerak M. Survey of consumer preferences on the bee product market. Part 1. Honey. Ann Warsaw Univ of life Sci - SGGW. *Anim Sci*. (2019) 58:153–8. doi: 10.22630/AAS.2019.58.2.16

32. Ciappini MC, Di Vito MV, Gatti MB, Calviño AB. Development of a quantitative descriptive sensory honey analysis: application to eucalyptus and clover honeys. *J Food Sci Technol*. (2013) 5:829–38. doi: 10.19026/ajfst.5.3169

33. Roman A, Popiela-Pleban E, Kozak M. Factors influencing consumer behavior relating to the purchasing of honey part 1. The buying process and the level of consumption. *J Apicult Sci*. (2013) 57:159–72. doi: 10.2478/jas-2013-0026

34. Anupama D, Bhat K, Sapna VK. Sensory and physicochemical properties of commercial samples of honey. *Food Res Int*. (2003) 36:183–91. doi: 10.1016/S0963-9969(02)00135-7

35. Skrypka HA, Khimych MS, Salata VZ, Naidich OV, Gorobei OM, Matviishyn TS. Monitoring of compliance of quality and safety of sunflower honey with the requirements of the national standard. *Scientific Messenger of LNU of Veterinary Medicine and Biotechnologies*. (2021) 23:162–7. doi: 10.32718/nvlvet10323

36. Kędzierska-Matysek M, Florek M, Wolanciuk A, Barłowska J, Litwińczuk Z. Concentration of minerals in nectar honeys from direct sale and retail in Poland. *Biol Trace Elem Res*. (2018) 186:579–88. doi: 10.1007/s12011-018-1315-0

37. Balzan S, Carraro L, Merlanti R, Lucatello L, Capolongo F, Fontana F. Microbial metabarcoding highlights different bacterial and fungal populations in honey samples from local beekeepers and market in North-Eastern Italy. *Int J Food Microbiol*. (2020) 334:108806. doi: 10.1016/j.ijfoodmicro.2020.108806

frontiers | Frontiers in Nutrition

Explorative study for the rapid detection of Fritillaria using gas chromatography-ion mobility spectrometry

Yuping Dai[1,2,3†], Shanshuo Liu[1†], Li Yang[4], Ye He[1], Xiao Guo[1], Yang Ma[1], Shunxiang Li[1,3,5]* and Dan Huang[1,3,5]*

[1]State Key Laboratory of Chinese Medicine Powder and Medicine Innovation in Hunan (Incubation), Science and Technology Innovation Center, Hunan University of Chinese Medicine, Changsha, China, [2]Hunan Fenghuang Lanke Traditional Chinese Medicine Co., Ltd., Changsha, China, [3]Hunan Engineering Technology Research Center for Bioactive Substance Dis-covery of Chinese Medicine, School of Pharmacy, Hunan University of Chinese Medicine, Changsha, China, [4]Chongqing Healn Drug Sales Co., Ltd., Chongqing, China, [5]Hunan Province Sino-US International Joint Research Center for Therapeutic Drugs of Senile Degenerative Diseases, Changsha, China

Fritillaria is a well-known health-promoting food, but it has many varieties and its market circulation is chaotic. In order to explore the differences in volatile organic compounds (VOCs) among different varieties of Fritillaria and quickly and accurately determine the variety of Fritillaria, this study selected six varieties of Fritillaria and identified and analyzed their volatile components using gas chromatography-ion mobility spectrometry (GC-IMS), establishing the characteristic fingerprints of VOCs in Fritillaria. In all samples, a total of 76 peaks were detected and 67 VOCs were identified. It was found that the composition of VOCs in different varieties of Fritillaria was similar, but the content was different. Combined with chemometric analysis, the differences between VOCs were clearly shown after principal component analysis, cluster analysis, and partial least-squares discriminant analysis. This may provide theoretical guidance for the identification and authenticity determination of different varieties of Fritillaria.

1 Introduction

Fritillaria is a well-known health-promoting food. Popular Fritillaria -based foods including Fritillaria chicken soup, Fritillaria pear paste and Fritillaria wine, have been gradually developed in the world. It belongs to the Liliaceae family, and there are about 130 species around the world; it is widely distributed in temperate regions of the northern hemisphere, especially in Central Asia, North America, and the Mediterranean region. There are about 40 species of Fritillaria in China, mainly distributed in Sichuan, Zhejiang, Gansu, Xinjiang, and Hubei and other places. It was recorded in the classis Chinese medicine work "*Shen nong's Herbal Classis*" more than 2,000 years ago. Fritillaria tastes hot and flat, and is mainly used to treat cold and fever, drenching, hernia paralysis, laryngeal paralysis, lactation, and wind spasms. Modern research shows that it has antitumor (1, 2), antioxidant (3, 4), and antibacterial effects (5), and prevents neuropathies such as Alzheimer's disease (6).

The current 2020 edition of the Chinese Pharmacopoeia contains eight herbs of the genus Fritillaria, which are categorized as Fritillariae cirrhosae bulbus, Fritillariae thunbergh bulbus, Fritillariae ussuriensis bulbus, Fritillariae pallidiflorae bulbus, and Fritillariae

hupehensis bulbus (7). General Fritillariae cirrhosae bulbus is bittersweet and slightly cold, mostly used for deficiency coughs (8–12); Fritillariae thunbergh bulbus is bitter cold, mostly used for external coughs (13), which, in the clinical sense, is labeled "Chuanbeimu" and "Zhebeimu" according to the corresponding evidence; and Fritillariae ussuriensis bulbus (14) and Fritillariae pallidiflorae bulbus have the same efficacy as Fritillariae cirrhosae bulbus (15). Fritillariae hupehensis bulbus is used for coughs due to heat-phlegm, and for subcutaneous nodule scrofula. It can be seen that different varieties of fritillaria directly affect its quality, thus affecting its clinical efficacy (16).

Due to the special growth environment of Fritillariae cirrhosae bulbus, its growth is slow, and existing wild resources have been overharvested; however, there has been no breakthrough in artificial planting technology, resulting in the scarcity of genuine Fritillariae cirrhosae bulbus which cannot meet the market demand, prompting prices to soar. In addition, the market contains a wide range of Fritillaria medicinal materials with complex sources and similar appearances. In some cases, the cheaper species of Fritillaria (such as Fritillariae thunbergh bulbus,Fritillariae ussuriensis bulbus,Fritillariae pallidiflorae bulbus,Fritillariae hupehensis bulbus, and so on) are adulterated or sold as Fritillariae cirrhosae bulbus in order to obtain higher profits. This seriously affects the market order, jeopardizes the interests of consumers, and affects the safety and efficacy of medication. Therefore, it is very meaningful to establish an objective, scientific, accurate, and rapid method to identify different species of Fritillaria and adulteration problems (17).

At present, research into Fritillaria identification mostly uses feature and microscopic identification, DNA barcoding technique, high-performance liquid chromatography fingerprinting, etc. feature identification and microscopic identification is fast, but requires skill, and it is subjective, while DNA barcoding technique identification and high-performance liquid chromatography fingerprinting is precise and accurate, but the process is cumbersome and demanding on operators, takes a lot of time, and is expensive (18, 19).

Gas chromatography-ion mobility spectrometry (GC-IMS) is a fast and highly efficient analytical instrument that can operate under ambient pressure and temperature. It combines the strong separation capability of GC with the advantages of the high sensitivity and high resolution of IMS, which provides richer chemical information and more comprehensive analysis of compounds, as well as fast analysis speed with less sample dosage, and provides convenient conditions for the detection of samples with only trace amounts. Highly efficient and convenient conditions are provided for the detection of samples that can only be obtained in minute quantities (20). GC-IMS is now used in the fields of foods, odor analysis and environmental testing (21–24). In addition, GC-IMS technology is used to provide certain theoretical references for the identification, quality evaluation and production of medicinal herbs (25–28). Different varieties have certain differences in the types and contents of their compounds. Fritillaria contains a variety of VOCs, given that GC-IMS technology has the ability to efficiently analyze volatile substances, we predict that the type of Fritillaria can be quickly identified by analyzing the distribution and relative content of various VOCs in caladium by GC-IMS. In addition, identification accuracy is further improved by effectively identifying and quantifying various compounds. However, few studies have been reported on the identification of different species of Fritillaria using GC-IMS with Chemometric. Therefore, it is necessary to systematically

and comprehensively analyze VOCs in different types Fritillaria under new technologies.

In this study, VOCs in different species of Fritillaria were studied with GC-IMS. Principal component analysis (PCA), cluster analysis (CA), and Partial least-squares discriminant analysis (PLS-DA) were used to analyze the differences of VOC odor fingerprints in different varieties of Fritillaria. The characteristic VOCs in different varieties of Fritillaria were displayed in a visual form, thus laying a certain foundation for rapid identification of Fritillaria in different species. This will be helpful to ensure the quality of Fritillaria and ensure the safety and effectiveness of medication for patients.

2 Materials and methods

2.1 Materials

The powders of the six kinds of Fritillaria were purchased from the National Institutes for Food and Drug Control, Beijing, China: Tendrilleaf Fritillary Bulb (the dried bulb of Fritillaria cirrhosa D. Don, No. 121757-202101, named CBM-01; the dried bulb of Fritillaria unibracteata Hsiao et K. C. Hsia, No. 121000-201609, named CBM-02); Thunberg Fritillary Bulb (the dried bulb of Fritillaria thunbergii Miq, No. 120972-201906, named ZBM-02); Ussuri Fritillary Bulb (the dried bulb of Fritillaria ussuriensis Maxim., No. 120924-201711, named PBM-01); Sinkiang Fritillary Bulb (the dried bulb of Fritillaria walujewii Regel, No. 121739-201701, named YBM-01); and Hubei Fritillary Bulb (the dried bulb of Fritillaria hupehensis Hsiao et K. C. Hsia, No. 120962-201005, named HBBM-01).

2.2 GC–IMS methods

2.2.1 Sample preparation
The powders of the samples were accurately weighed out to 1 g and placed into a 20 mL headspace vial, then incubated at 80°C for 15 min.

2.2.2 Headspace conditional
Static headspace autosampler unit (CTC-PAL 3), (CTC Analytics AG, Zwingen, Switzerland); injection volume: 500 μL; non-shunt injection; speed: rotation speed of 500 rpm for 20 min; injection needle temperature: 85°C.

2.2.3 GC conditional
A chromatographic column of MXT-WAX (15 m × 0.53 mm, 1.0 μm, Restek Inc., United States) was used. Column temperature: 60°C; carrier gas: high-purity N_2 (purity ≥99.999%); programmed boosting: initial flow rate of 2.00 mL/min was held for 2 min, linearly increased to 10.00 mL/min within 8 min, linearly increased to 100.00 mL/min within 10 min, and held for 10 min. Chromatographic runtime: 30 min; injection temperature: 80°C. Run time: 30 min; inlet temperature: 80°C.

2.2.4 IMS conditional
GC-IMS instrument: FlavourSpec® Gas Phase Ion Mobility Spectrometer, G.A.S. (Dortmund, Germany); ionization source:

tritium source (3H); drift tube length: 53 mm; electric field strength: 500 V/cm; drift tube temperature: 45°C; drift gas: high-purity N_2 (purity ≥99.999%); flow rate: 150 mL/min; positive ion mode.

2.3 Statistical analysis

Preliminarily, the peaks of the samples were chosen and compared using the Laboratory Analytical Viewer (v.2.2.1, G.A.S.) and Reporter analysis (v.1.2.12, G.A.S.). We performed quantitative analysis using Gallery Plot Analysis (v.1.0.7, G.A.S.) on selected signal peaks. The principal component analysis (PCA) was performed in Origin software (Northampton, Massachusetts, United States), TBtools was used for cluster analysis and partial least-squares discriminant analysis (PLS-DA) of volatile profiles was performed in SIMCA software (Umea, Sweden).

To compare VOCs among samples, Reporter, Gallery Plot, and other plug-ins in VOCal data processing software were used to generate three-dimensional spectra, two-dimensional spectra, difference spectra, and fingerprints.

3 Results and discussion

3.1 Qualitative analysis of Fritillaria samples from different species

The three-dimensional(3D) GC-IMS spectra of different varieties of Fritillaria are shown in Figure 1. The three coordinates represent the drift time, retention time, and signal peak intensity, respectively, from which we can visualize the differences in VOCs of different varieties of Fritillaria. Figure 2 shows a comparison of the differences: the background of the whole image is blue, the red vertical line at 1.0 of the horizontal coordinates represents the RIP (reactive ion peak: represents the total amount of available ions formed), each point on both sides of the RIP represents one VOC, and the color represents the peak intensity of the substance. From blue to red, the darker the color, the greater the peak intensity, and it can be seen that there are certain differences in the VOCs from the samples of different types of

Fritillaria. In order to further visualize and compare the differences in volatile components, the spectrum of the CBM-1 sample was selected as a reference, and the spectra of other samples were deducted from the reference to obtain a comparison of the differences between different samples, as shown in Figure 3. If the VOC contents in the target sample and the reference were the same, the background after deduction was white, while a red color means that the concentration of the substance was higher than the reference in the target sample, and a blue color means that the concentration of the substance was lower than the reference in the target sample.

3.1.1 Comparison of differences in volatile components of CBM-01 and CBM-02 samples

Using the comparison chart of the difference in VOCs of the CBM-01 and CBM-02 samples, it can be seen that there was also a significant difference in the VOCs. Although they are all named Tendrilleaf Fritillary Bulb, different origins, cultivation methods, and storage times may affect the content of some volatile substances.

3.1.2 Comparison of the differences in VOCs between Tendrilleaf Fritillary Bulb and other varieties of Fritillaria

The VOCs in all varieties of Fritillaria were analyzed using GC-IMS and well separated. The composition of the VOCs in different varieties of Fritillaria was similar, but there were significant differences in the contents. This may also be related to the fact that different varieties of Fritillaria can exert different medicinal effects.

3.2 Identification of VOCs in different Fritillaria samples

After GC-IMS analysis, a total of 76 substances were detected, and two-dimensional characterization was carried out using the NIST2020 gas-phase retention index database built in the Practical Vocal software and the IMS drift time database of G.A.S. The results of the GC-IMS analysis are shown in Table 1 and Figure 4.

According to Table 1, it can be seen that the content of the same VOCs differed significantly in different varieties of Fritillaria samples.
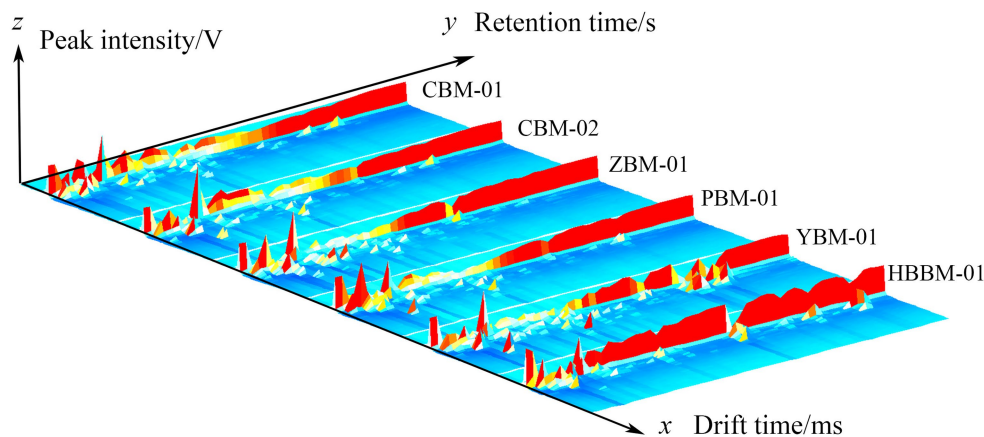
FIGURE 1
GC-IMS three-dimensional spectra of different varieties of Fritillaria.
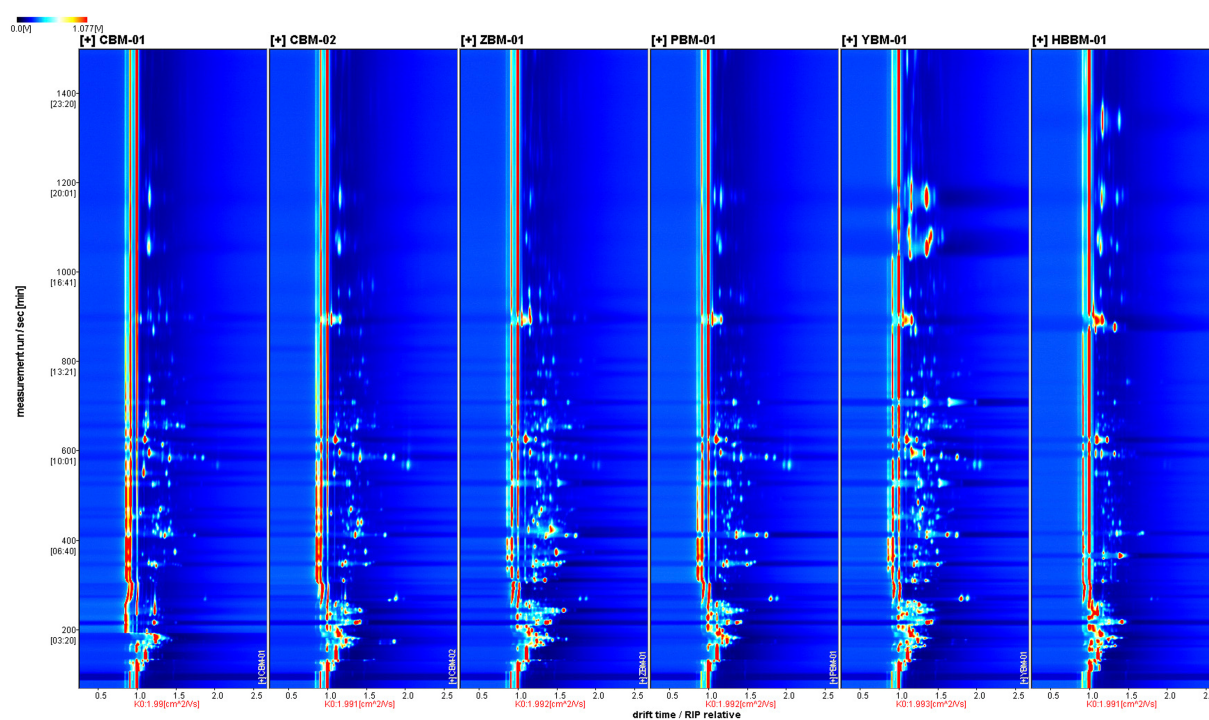
FIGURE 2
GC-IMS two-dimensional spectra of different varieties of Fritillaria.
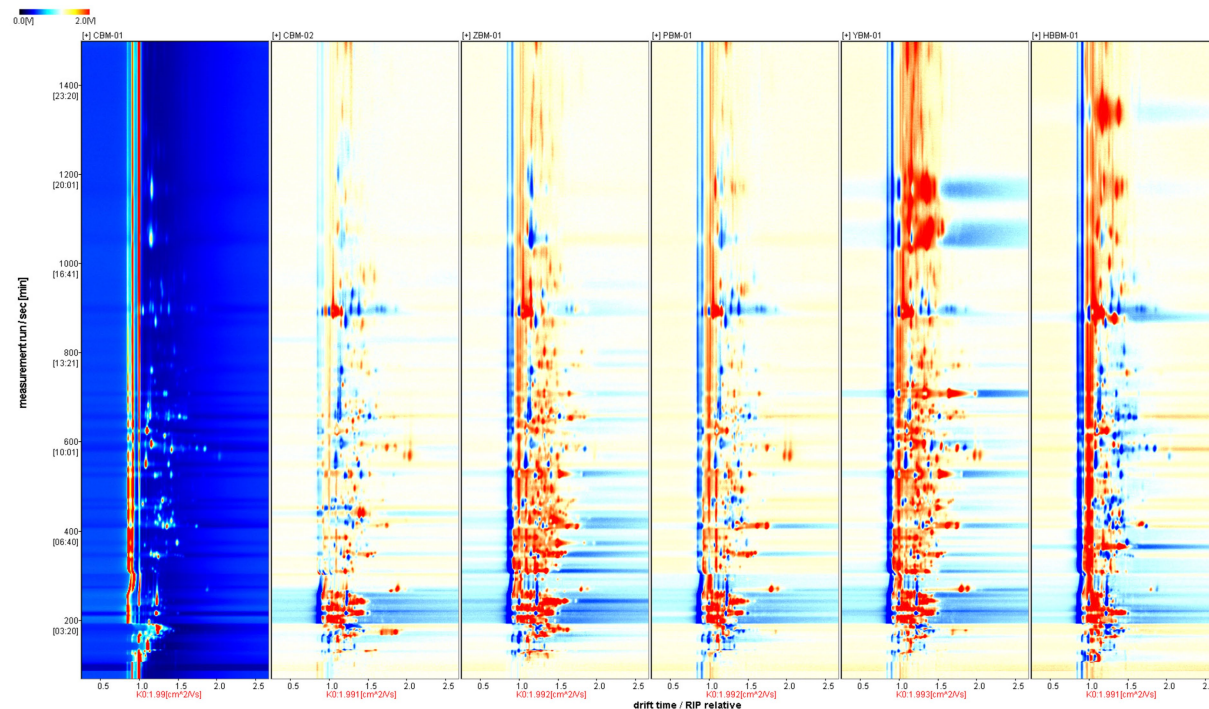
FIGURE 3
GC-IMS difference comparison chart of different varieties of Fritillaria.

Combined with the analysis of Table 1 and Figure 4, it can be concluded that a total of 67 VOCs were detected in six varieties of Fritillaria samples, including acids, ketones, esters, alcohols, aldehydes, furans, and pyrazine.

This includes the monomers and dimers of some of the substances, in which the monomers and dimers identified had the same chemical formulas and CAS numbers, and only differed in their morphology.

TABLE 1 Results of component analysis of different varieties of Fritillaria.

Count	Compound	CAS	Molecular formula	RI	Rt (sec)	Dt (a.u.)	Comment
1	1-Butanoic acid D	C107926	$C_4H_8O_2$	1,649	1340.216	1.3959	Dimers
2	1-Butanoic acid M	C107926	$C_4H_8O_2$	1650.1	1343.799	1.16474	Monomers
3	2-Methyl propanoic acid D	C79312	$C_4H_8O_2$	1587.4	1161.106	1.36183	Dimers
4	2-Methyl propanoic acid M	C79312	$C_4H_8O_2$	1588.1	1162.897	1.15744	Monomers
5	Methyl 2-furoate	C611132	$C_6H_6O_3$	1547.2	1057.221	1.14527	–
6	Propanoic acid M	C79094	$C_3H_6O_2$	1554.1	1074.349	1.10932	Monomers
7	Propanoic acid D	C79094	$C_3H_6O_2$	1551.8	1068.667	1.28382	Dimers
8	Benzaldehyde	C100527	C_7H_6O	1502.7	953.128	1.14905	–
9	Acetic acid M	C64197	$C_2H_4O_2$	1483.5	911.458	1.05683	Monomers
10	Acetic acid D	C64197	$C_2H_4O_2$	1474.5	892.517	1.16891	Dimers
11	2-Furaldehyde D	C98011	$C_5H_4O_2$	1,469	881.152	1.33063	Dimers
12	2-Furaldehyde M	C98011	$C_5H_4O_2$	1464.4	871.682	1.08095	Monomers
13	3-Ethylpyridine	C536787	C_7H_9N	1388.6	730.572	1.11642	–
14	1-Hexanol M	C111273	$C_6H_{14}O$	1377.4	711.631	1.33063	Monomers
15	2-Butanone, 3-hydroxy D	C513860	$C_4H_8O_2$	1300.6	595.075	1.32292	Dimers
16	2-Butanone, 3-hydroxy M	C513860	$C_4H_8O_2$	1298.4	592.065	1.08668	Monomers
17	1-Butanol D	C71363	$C_4H_{10}O$	1156.1	365.866	1.39434	Dimers
18	1-Butanol M	C71363	$C_4H_{10}O$	1156.4	366.296	1.18007	Monomers
19	Isobutanol M	C78831	$C_4H_{10}O$	1109.6	311.744	1.17231	Monomers
20	Isobutanol D	C78831	$C_4H_{10}O$	1110.3	312.534	1.36949	Dimers
21	n-Pentanal	C110623	$C_5H_{10}O$	994	219.538	1.42151	–
22	Ethyl propanoate	C105373	$C_5H_{10}O_2$	944.9	190.384	1.1563	–
23	2-Butanone	C78933	C_4H_8O	925	179.682	1.25147	–
24	2-Methylpyrazine D	C109080	$C_5H_6N_2$	1274.1	547.149	1.39146	Dimers
25	2-Methylpyrazine M	C109080	$C_5H_6N_2$	1,276	550.571	1.09067	Monomers
26	Amyl acetate M	C628637	$C_7H_{14}O_2$	1,193	415.396	1.31099	Monomers
27	Amyl acetate D	C628637	$C_7H_{14}O_2$	1192.3	414.54	1.74781	Dimers
28	2-Octanone	C111137	$C_8H_{16}O$	1297.1	590.208	1.75051	–
29	Acetone	C67641	C_3H_6O	864.8	150.836	1.11503	–
30	2-Butanol	C78922	$C_4H_{10}O$	1044.8	255.417	1.16148	–
31	2-Hexenal	C505577	$C_6H_{10}O$	1229.7	470.587	1.18911	–
32	Butyl acetate	C123864	$C_6H_{12}O_2$	1024.3	240.282	1.23439	–
33	(Z)-4-Heptenal M	C6728310	$C_7H_{12}O$	1204.8	432.369	1.13614	Monomers
34	(Z)-4-Heptenal D	C6728310	$C_7H_{12}O$	1192.9	415.279	1.62404	Dimers
35	Ethyl acetate D	C141786	$C_4H_8O_2$	893.7	164.095	1.3305	Dimers
36	Ethyl acetate M	C141786	$C_4H_8O_2$	911.2	172.623	1.10347	Monomers
37	Isopentyl acetate	C123922	$C_7H_{14}O_2$	1121.9	325.264	1.30052	–
38	3-Pentanone D	C96220	$C_5H_{10}O$	989.7	216.833	1.36179	Dimers
39	3-Pentanone M	C96220	$C_5H_{10}O$	980	210.783	1.10587	Monomers
40	γ-pentalactone M	C108292	$C_5H_8O_2$	1561.1	1091.954	1.13706	Monomers
41	γ-pentalactone D	C108292	$C_5H_8O_2$	1,557	1081.744	1.41232	Dimers
42	2,3-Butandiol	C513859	$C_4H_{10}O_2$	1544.3	1050.075	1.3642	–
43	Linalool	C78706	$C_{10}H_{18}O$	1559.6	1088.162	1.22272	–
44	1-Octen-3-ol	C3391864	$C_8H_{16}O$	1508.7	966.427	1.58577	–

(Continued)

TABLE 1 (Continued)

Count	Compound	CAS	Molecular formula	RI	Rt (sec)	Dt (a.u.)	Comment
45	(E)-2-Hexen-1-ol	C928950	$C_6H_{12}O$	1402.3	754.262	1.49336	–
46	2-Ethyl-3-methylpyrazine	C15707230	$C_7H_{10}N_2$	1408.5	765.195	1.1697	–
47	1-Hexanol D	C111273	$C_6H_{14}O$	1375.2	708.067	1.65737	Dimers
48	1-Hexanol P	C111273	$C_6H_{14}O$	1375.6	708.658	1.98876	–
49	(E)-2-Heptenal D	C18829555	$C_7H_{12}O$	1340.9	653.667	1.66735	Dimers
50	(E)-2-Heptenal M	C18829555	$C_7H_{12}O$	1342.1	655.441	1.25211	Monomers
51	1-Pentanol D	C71410	$C_5H_{12}O$	1262.8	526.538	1.53559	Dimers
52	1-Pentanol M	C71410	$C_5H_{12}O$	1263.4	527.625	1.25637	Monomers
53	2-Pentyl furan	C3777693	$C_9H_{14}O$	1238.6	485.078	1.25023	–
54	3-Octanone M	C106683	$C_8H_{16}O$	1228.9	469.345	1.30575	Monomers
55	3-Octanone D	C106683	$C_8H_{16}O$	1229.9	470.82	1.70414	Dimers
56	3-Methyl-but-3-en-1-ol	C763326	$C_5H_{10}O$	1199.8	425.097	1.4331	–
57	Heptaldehyde	C111717	$C_7H_{14}O$	1192.9	415.264	1.68781	–
58	Isopentyl alcohol D	C123513	$C_5H_{12}O$	1218.2	452.629	1.50494	Dimers
59	Isopentyl alcohol M	C123513	$C_5H_{12}O$	1,216	449.188	1.24207	Monomers
60	2,6-Dimethylpyrazine D	C108509	$C_6H_8N_2$	1345.3	660.334	1.52233	Dimers
61	2,6-Dimethylpyrazine M	C108509	$C_6H_8N_2$	1345.3	660.334	1.14674	Monomers
62	Hexan-2-one M	C591786	$C_6H_{12}O$	1138.5	344.359	1.19866	Monomers
63	1-Hydroxy-2-propanone	C116096	$C_3H_6O_2$	1322.6	626.444	1.23317	–
64	2,5-Dimethylpyrazine	C123320	$C_6H_8N_2$	1321.3	624.475	1.10184	–
65	Cyclohexanone	C108941	$C_6H_{10}O$	1303.5	599.035	1.16139	–
66	Ethyl hexanoate	C123660	$C_8H_{16}O_2$	1245.7	496.842	1.33927	–
67	Hexan-2-one D	C591786	$C_6H_{12}O$	1141.3	347.658	1.50162	Dimers

RI, retention index; Rt, retention time; Dt, drift time.

3.3 Fingerprint spectrum analysis of Fritillaria samples from six different species

Figure 5 shows the fingerprints of the VOCs in six samples of Fritillaria. Each row in the figure represents all the signal peaks selected in one sample, and each column represents the signal peaks of the same VOCs in different samples.

Comparative analysis of VOCs in samples CBM-01, CBM-02, ZBM-01, PBM-01, YBM-01, and HBBM-01 showed that, as shown in the red box, 2,5-dimethylpyrazine, 2-methylpyrazine, cyclohexane, 2-ethyl-3-methylpyrazine, butyl acetate, and 2,6-dimethylpyrazine were present in sample CBM-01 in higher levels. As shown in the white box, unknown peak 1, unknown peak 7, and 1-octen-3-ol were higher in the CBM-2 sample. As shown in the orange box, 2-methylpropanol, 2-butanol, unknown peak 2, hexan-2-one, isoamyl acetate, 3-methyl-but-3-en-1-ol, unknown peak 3, and benzaldehyde were higher in ZBM-1. As shown in the blue box, amyl acetate, 2-butanone, and unknown peak 6 were higher in the PBM-01 sample. As shown in the green box, unknown peak 4, 3-ethylpyridine, 2-methylpropionic acid, γ-pentalactone, 2-butanone,3-hydroxy, 2,3-butanedione, methyl 2-furoate, (Z)-4-heptenal, linalool, 1-octen-3-ol, hexanol, 2-octanone, ethyl caproate, 3-methylbutanol, and unknown peak 5 were higher in the YBM-01 sample. As shown in the purple box, butyric acid, propionic acid, furfural, acetic acid,

1-hydroxy-2-propanone, heptanal, butanol, glutaraldehyde, ethyl acetate, ethyl propionate, and (E)-2-hexenol were higher in the HBBM-01 sample. As shown in the yellow box, 2-hexenal, 3-pentanone, (E)-2-heptenal, pentanol, 2-pentylfuran, and 3-octanone were higher in both the ZBM-01 and YBM-01 samples.

This shows that GC-IMS can form a unique fingerprint, visualize the differences of VOCs in different varieties of Fritillaria, and quickly distinguish and identify different varieties of Fritillaria.

3.4 Chemometric analysis

Chemometrics is an emerging branch of chemistry formed by the intersection of chemistry and mathematics, computer science, etc. It is of great significance in the quality control and research and evaluation of traditional Chinese medicine by establishing a link between the measured values of a chemical system and the state of the system through statistical or mathematical methods (29). The chemometric analysis of VOCs in different varieties of Fritillaria is helpful for finding the differential components to identify their varieties.

3.4.1 Principal component analysis

Principal component analysis (PCA) is a commonly used unsupervised analysis method which reduces the dimensionality of
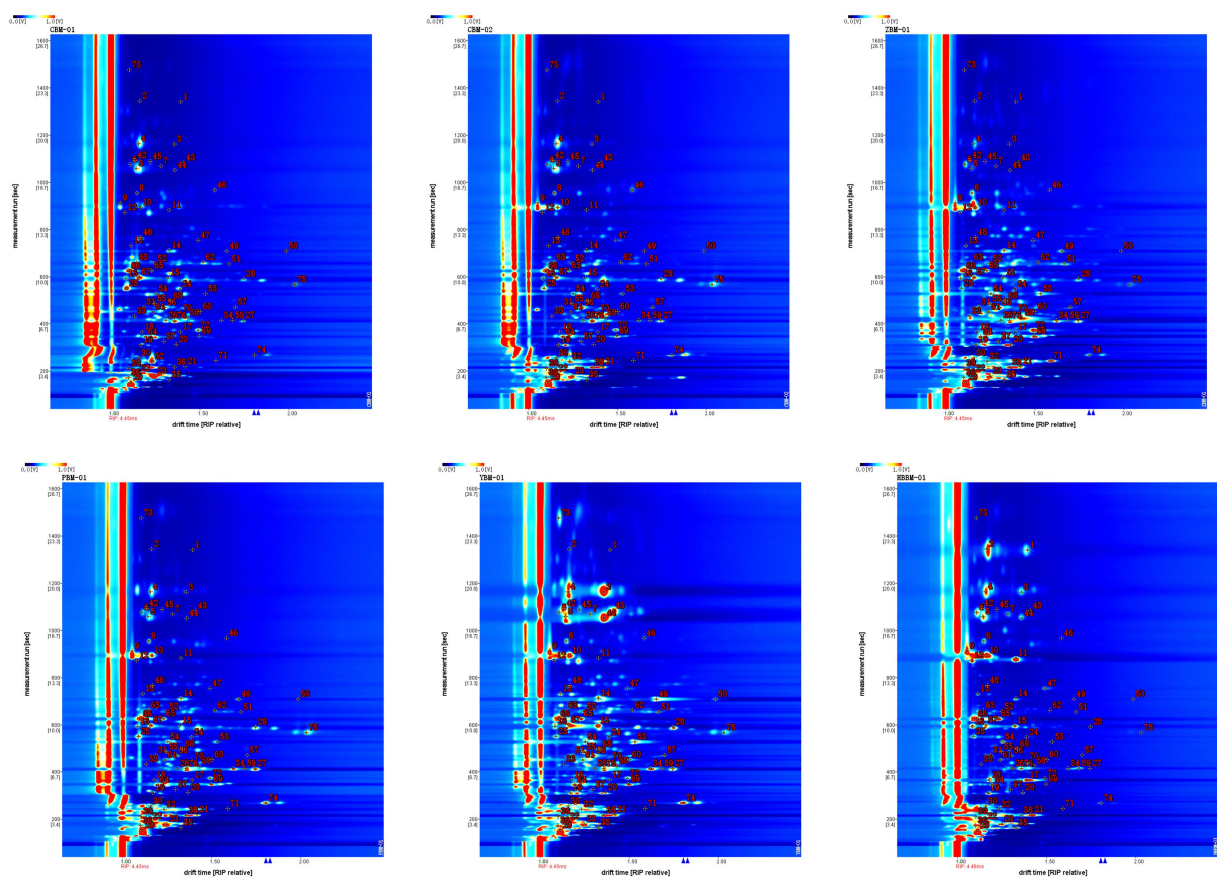
FIGURE 4
Characteristic peak position plot of volatile components of six species of Fritillaria.
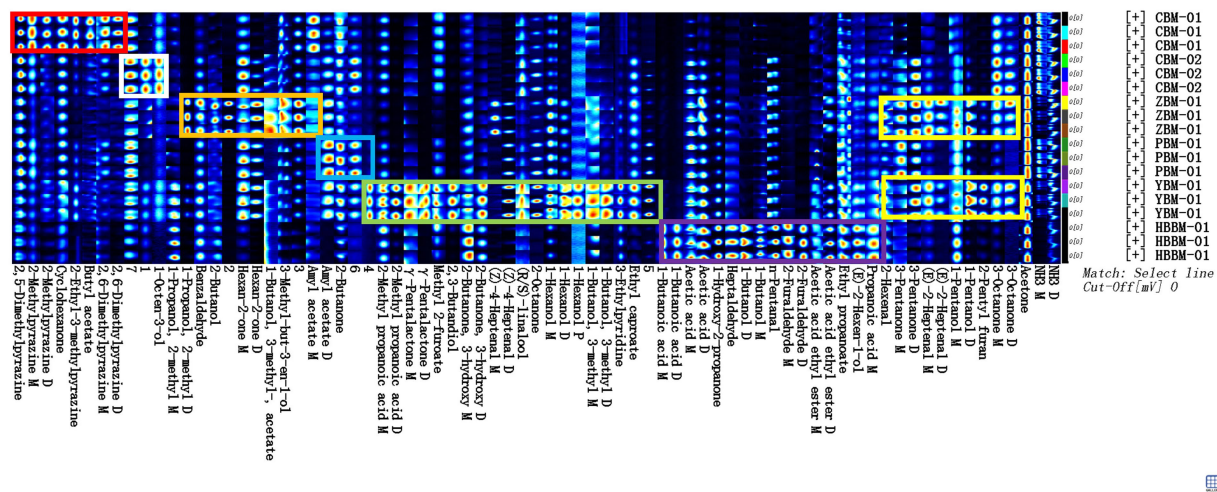
FIGURE 5
Gallery plot of different varieties of Fritillaria via GC-IMS.

the data while retaining as much original information as possible and can respond to the overall situation of the chemical measurement data for complex traditional Chinese medicine systems (30). As shown in the Figure 6, the PCA of the VOCs in the six varieties of Fritillaria was performed, and the results are shown in Figure 6, which shows that

the six groups of samples were well separated. When the samples are close to each other, it indicates that the difference in VOCs between the samples is relatively small, and on the contrary, it indicates that there is a significant difference in the VOCs between them. The distance between CBM-01 and the other Fritillaria was relatively large,

which indicates that PCA can distinguish Fritillariae cirrhosae bulbus from the other varieties of Fritillaria very well. The distance between CBM-02 and PBM-01 was closer, which indicates that the difference in the VOCs between the two kinds of samples is small, similar to a previous study. These results indicated significant differences in VOCs among the six varieties and showed that the PCA could effectively distinguish the four other species of Fritillaria from Fritillariae cirrhosae bulbus.

3.4.2 Cluster analysis

Heat maps can be used to reflect data via color changes, which can visually represent the differences between data using color shades (31). As shown in the Figure 7, the 67 VOCs identified with GC-IMS were clustered and analyzed, and the differences in the VOCs of the six varieties of Fritillaria were clearer and more explicit, as shown in Figure 7. The clustering heat map shows that there are obvious differences in the VOCs in different varieties of Fritillaria (32). Among them, the contents of acetic acid and ethyl propanoate substances in CBM-01 were significantly less than those in other Fritillaria. The contents of (Z)-4-heptenal, 1-propanol, 2-methyl, 3-methyl-but-3-en-1-ol, and hexan-2-one substances were higher in ZBM-01 than in the other Fritillaria, while the contents of 1-hexanol, 2,3-butandiol, and 2-methyl propanoic acid substances were higher in YBM-01 than in the other Fritillaria. The contents of, 1-butanol, 2-furaldehyde, and 1-butanoic acid substances were higher in HBBM-01 than in the other Fritillaria.

3.4.3 Partial least-squares discriminant analysis

Partial least-squares discriminant analysis (PLS-DA) is a supervised pattern statistical analysis method that enables the visualization of complex data and is often used to deal with classification and discrimination problems (33). As shown in the Figure 8, to further explore the volatiles in different varieties of Fritillaria, PLS-DA modeling was performed with 69 VOCs identified as dependent variables and different varieties as independent variables. The results are shown in Figure 8. In this model, the six groups of samples were well separated from each other. The long distance between CBM-01 and other samples indicated that the VOCs of CBM-01 and other samples were significantly different. Meanwhile, a close distance between CBM-02 and PBM-01 samples can be observed, which is consistent with the results of PCA analysis.

The variable importance projection (VIP) indicates the strength of influence and explanatory ability of the differential components on the classification discrimination of various samples, which is an important index for screening differential compounds. The larger the VIP value of the sample, the more significant the variable is in distinguishing the sample. As shown in Figure 9, 1-Octen-3-ol, 3-Octanone, and 2,5-Dimethylpyrazine are the most important components that affect the difference of six varieties of Fritillaria (Figure 9).

4 Discussion

In this study, a total of 76 substances, including 67 VOCs were detected. Firstly, based on the GC-IMS odor fingerprint data, it was preliminarily found that the types of VOCs in different varieties of Fritillaria are similar, but there are significant differences in content. So, we further utilize chemometrics to analyze all the obtained data. The results of PCA and PLS-DA indicate that the distribution of VOCs in samples of different varieties is relatively independent, which also confirms Fritillariae ussuriensis bulbus is often used as a substitute for
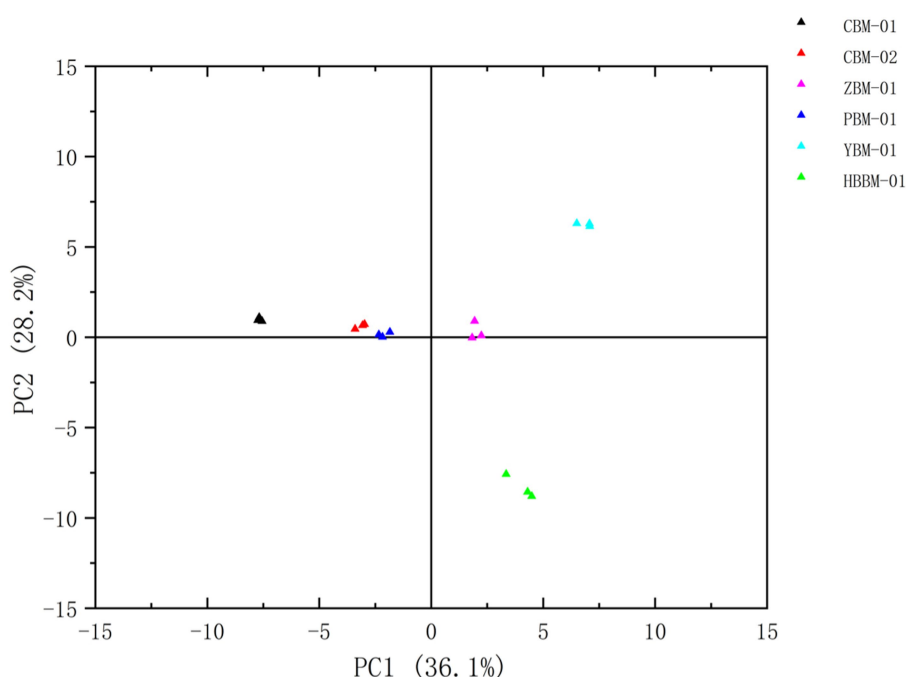
FIGURE 6
Plot of the PCA scores of VOCs in six species of Fritillaria.

FIGURE 7
Cluster heat map of VOCs in six species of Fritillaria.
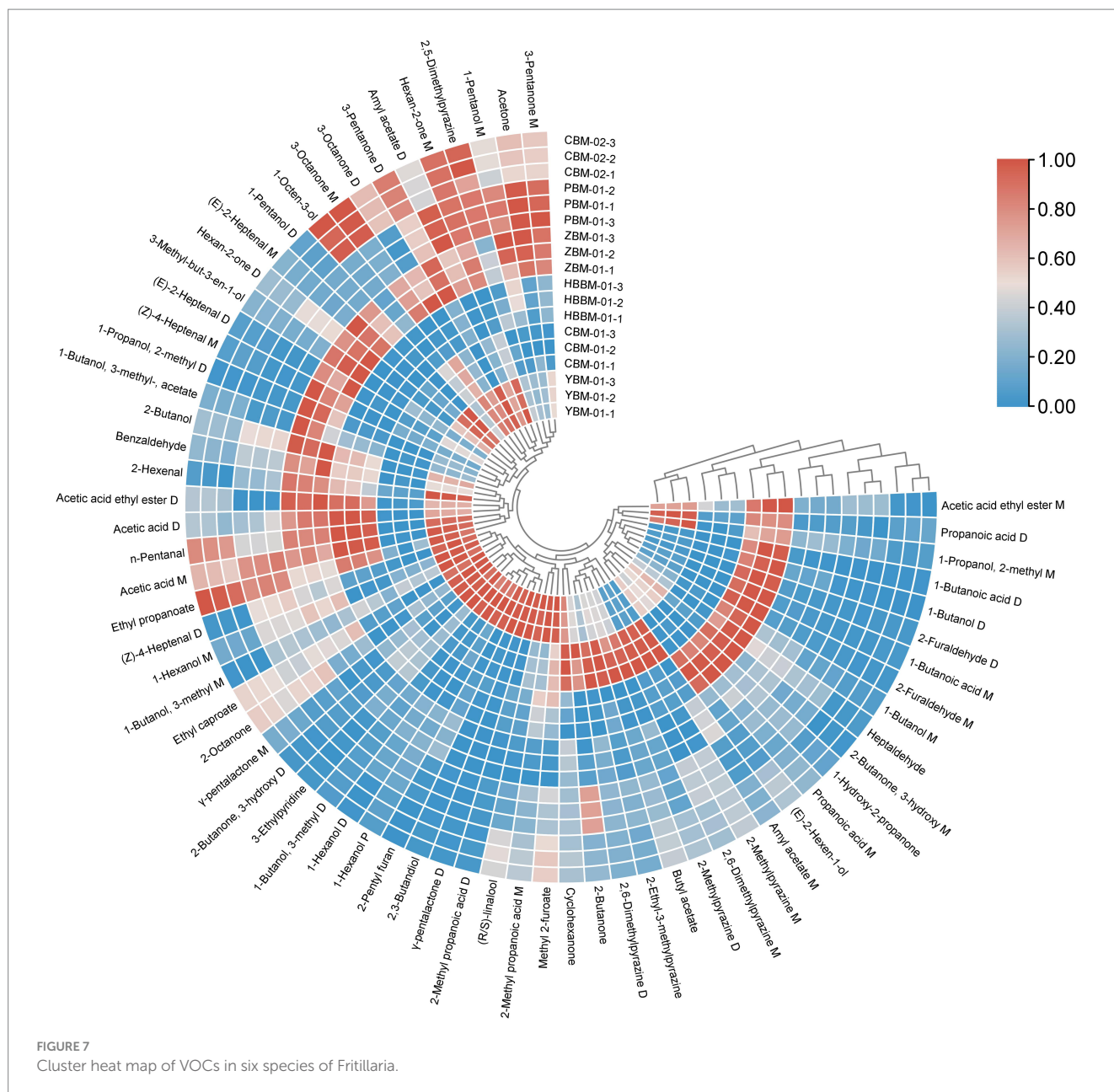
Fritillariae cirrhosae bulbus because of its high similarity to Fritillariae cirrhosae bulbus. Although its clinical effect is not as good as that of Fritillariae cirrhosae bulbus, it is of great significance to alleviate the shortage of resources of Fritillariae cirrhosae bulbus. Through the results of the heat map, it can be seen that there are components with higher content in different varieties of Fritillaria, such as CBM-01 contains a lot of pyrazine compounds, 1-Octan-3-ol having the highest content in CBM-02, and 3-Methyl-but-3-en-1-ol, 1-Butanol-3-Methyl acetate and other substances having the highest content in ZBM-01. The results of the heat map also mutually confirm the conclusions of the odor fingerprint spectrum. That's also why Fritillariae thunbergh bulbus has better efficacy in relieving coughs and resolving phlegm than Fritillariae cirrhosae bulbus, Fritillariae pallidiflorae bulbus, and Fritillariae ussuriensis bulbus, which is related to the fact that it contains more bemacropodin A and bemacropodin B (34).

Compared with the traditional methods such as DNA barcoding technique and high-performance liquid chromatography (HPLC), the determination of VOCs in different Fritillaria samples via GC-IMS to differentiate between species has greatly improved the identification method and efficiency, and the pretreatment of samples is more efficient and convenient. It is very helpful for quickly identifying different varieties of Fritillaria.

5 Conclusion

In this study, the VOCs of six species of Fritillaria were analyzed and systematically compared using GC-IMS. A total of 79 peaks were detected, with 67 VOCs identified, mainly including acids, ketones, esters, alcohols, aldehydes, furans, and pyrazine. Among them,
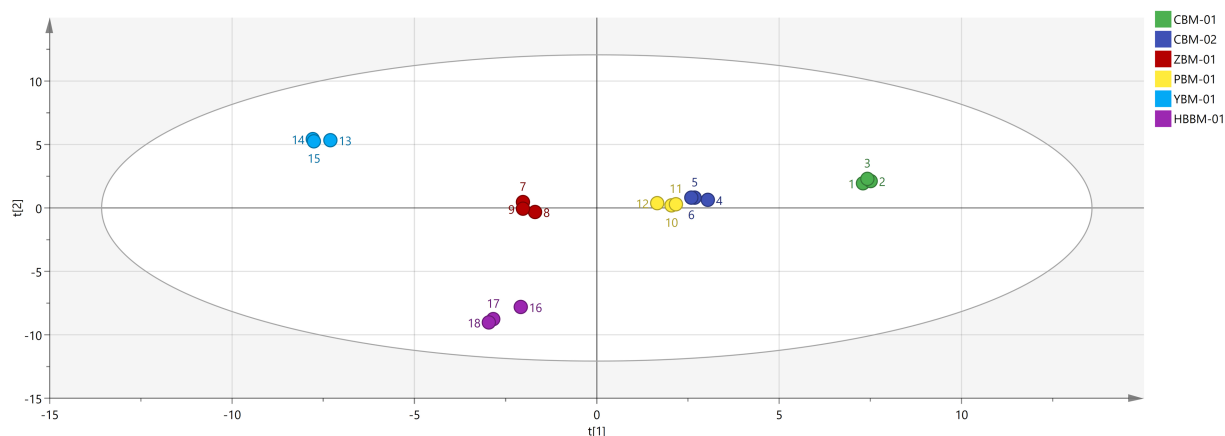
FIGURE 8
PLS-DA analysis of VOCs in 6 species of Fritillaria.
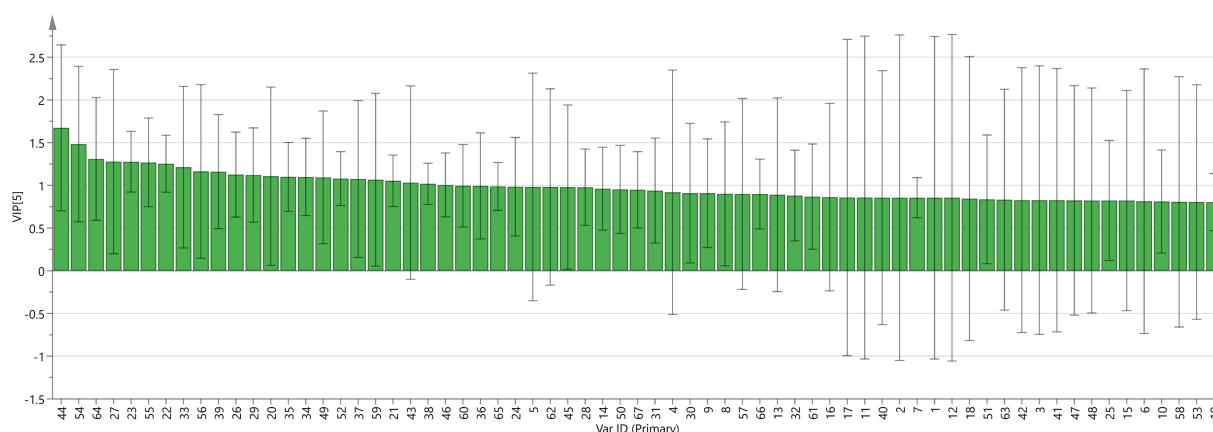
FIGURE 9
VIP values of the characteristic variables.

CBM-01 contains a lot of pyrazine compounds, with 1-Octan-3-ol having the highest content in CBM-02, and 3-Methyl-but-3-en-1-ol, 1-Butanol-3-Methyl acetate and other substances having the highest content in ZBM-01.

Based on statistical analysis with chemometrics, it was found that there were some differences in the ion migration spectra of different Fritillaria varieties. Fingerprints were established based on the characteristic components fitted by the graph plug-in software, and after principal component analysis (PCA), cluster analysis (CA), and partial least-squares discriminant analysis (PLS-DA), we could effectively and quickly distinguish Fritillariae cirrhosae bulbus and its common other Fritillaria species. This provides a new method for the quality control and identification of quality relationships of Fritillariae cirrhosae bulbus. This study demonstrates that GC-IMS provides an important reference value for the identification and authenticity assessment of different varieties of Fritillaria, which is conducive to ensuring the quality of Fritillaria in the market, thus guaranteeing the safety and effectiveness of medication.

Data availability statement

The original contributions presented in the study are included in the article/supplementary material, further inquiries can be directed to the corresponding authors.

Author contributions

YD: Conceptualization, Data curation, Formal analysis, Investigation, Methodology, Software, Supervision, Writing – original draft. ShaL: Conceptualization, Data curation, Formal analysis, Investigation, Methodology, Software, Supervision, Writing – original draft. LY: Conceptualization, Data curation, Formal analysis, Funding acquisition, Writing – original draft. YH: Conceptualization, Data curation, Writing – original draft. XG: Formal analysis, Resources, Validation, Writing – original draft. YM: Methodology, Supervision, Validation, Writing – original draft. ShuL: Funding acquisition, Project administration, Writing – original draft, Writing – review &

editing. DH: Formal analysis, Funding acquisition, Resources, Software, Supervision, Writing – original draft, Writing – review & editing.

investigation, data curation, formal analysis, and writing – original draft and editing.

Conflict of interest

LY was employed by Chongqing Healn Drug Sales Co., Ltd. YD was employed by Hunan Fenghuang Lanke Traditional Chinese Medicine Co., Ltd.

The remaining authors declare that the research was conducted in the absence of any commercial or financial relationships that could be construed as a potential conflict of interest.

Publisher's note

All claims expressed in this article are solely those of the authors and do not necessarily represent those of their affiliated organizations, or those of the publisher, the editors and the reviewers. Any product that may be evaluated in this article, or claim that may be made by its manufacturer, is not guaranteed or endorsed by the publisher.

References

1. Kardan M, Yazdani Z, Morsaljahan Z, Ebrahimzadeh MA, Rafiei A. Cytotoxic effect of methanolic extracts of *Fritillaria imperialis* bulbs and Eryngium caucasicum leaves on hepatoma and colon cancer cells. *Asian Pac J Trop Biomed*. (2019) 9:353–8. doi: 10.4103/2221-1691.262084

2. Liu FJ, Chen XY, Yang J, Zhao Z, Wang QL, Li P, et al. Revealing active components and action mechanism of Fritillariae Bulbus against non-small cell lung cancer through spectrum-effect relationship and proteomics. *Phytomedicine*. (2023) 110:154635. doi: 10.1016/j.phymed.2022.154635

3. Pan F, Su T, Liu Y, Hou K, Chen C, Wu W. Extraction, purification and antioxidation of a polysaccharide from Fritillaria unibracteata var. wabuensis. *Int J Biol Macromol*. (2018) 112:1073–83. doi: 10.1016/j.ijbiomac.2018.02.070

4. Liu S, Yang T, Ming TW, Gaun TKW, Zhou T, Wang S, et al. Isosteroid alkaloids from Fritillaria cirrhosa bulbus as inhibitors of cigarette smoke-induced oxidative stress. *Fitoterapia*. (2020) 140:104434. doi: 10.1016/j.fitote.2019.104434

5. Gong Q, Li YW, He M, Guo WJ, Kan XC, Xu DW, et al. Peiminine protects against lipopolysaccharide-induced mastitis by inhibiting the AKT/NF-κB, ERK1/2 and p38 signaling pathways. *Int J Mol Sci*. (2018) 19:2637. doi: 10.3390/ijms19092637

6. Zhu Y, Le P, Hu J, Chen Y, Chen FX. Current anti-Alzheimer's disease effect of natural products and their principal targets. *J Integr Neurosci*. (2019) 18:327–39. doi: 10.31083/j.jin.2019.03.1105

7. National Pharmacopoeia Commission. *Pharmacopoeia of the People's Republic of China*. Beijing: China Medical Science and Technology Press (2020).

8. Hou CL, Lu XF, Lei XT, Tang YY, Zhao RY, Li B. Effect of Fritillaria cirrhosae bulbus on ovalbumin sensitized mouse asthma and its mechanism. *Med J Chin People's Lib Army*. (2022) 47:789–94. doi: 10.11855/j.issn.0577-7402.2022.08.0789

9. Xu Y, Ming TW, Gaun TKW, Wang S, Ye B. A comparative assessment of acute oral toxicity and traditional pharmacological activities between extracts of Fritillaria cirrhosae Bulbus and Fritillaria pallidiflora Bulbus. *J Ethnopharmacol*. (2019) 238:111853. doi: 10.1016/j.jep.2019.111853

10. Wu F, Tian M, Sun YF, Wu CH. Efficacy, chemical composition, and pharmacological effects of herbal drugs derived from Fritillaria cirrhosa D. Don and Fritillaria thunbergii Miq. *Front Pharmacol*. (2022) 13:985935. doi: 10.3389/FPHAR.2022.985935

11. Xu W, Chen SY, Ma J, Li P, Shao BC, Ge L. Investigation of association of chemical profiles with the tracheobronchial relaxant activity of Chinese medicinal herb Beimu derived from various Fritillaria species. *J Ethnopharmacol*. (2017) 210:39–46. doi: 10.1016/j.jep.2017.08.027.2018

12. Rashid I, Yaqoob U. Traditional uses, phytochemistry and pharmacology of genus Fritillaria—a review. *Bull Natl Res Cent*. (2021) 45:124. doi: 10.1186/S42269-021-00577-Z

13. Chen B, Tong JL, Zhou AZ, Ruan HS, Wang XL, Peng X. Quality markers screening of phlegm-eliminating effect of Fritillaria thunbergii and their content differences by UPLC-Q-TOF-MS spectrum-effect analysis technology. *Chin Pharm J*. (2021) 56:462–71. doi: 10.11669/cpj.2021.06.006

14. Jiao HY, Lou Y, Xue X, Tang QF. Isosteroidal alkaloids from Fritillariae pallidiflorae Bulbum inhibit airway inflammation and remodeling by modulating Wnt/β-catenin signal pathway in asthma rats. *Mod Tradit Chin Med Mater Med World Sci Technol*. (2020) 22:1871–6. doi: 10.11842/wst.20191206001

15. Chen HZ, Zhang SY, Huang YB, Li SM, Chen JF, Ao H. Comparative study on the content determination and the anti-tussive and anti-inflammatory effects of the total alkaloids of Pingbeimu and Chuanbeimu. *Sci Technol Food Ind*. (2017) 38:63–7. doi: 10.13386/j.issn1002-0306.2017.15.014

16. Lu Q, Xue SJ, Yang D, Li L. Comparison of ingredient composition and physicochemical properties between Fritillaria hupehensis and Fritillaria thunbergii. *Sci Technol Food Ind*. (2023) 44:49–55. doi: 10.13386/j.issn1002-0306.2022040052

17. Liu CL, Zuo ZT, Xu FR, Wang YZ. Authentication of herbal medicines based on modern analytical technology combined with chemometrics approach: a review. *Crit Rev Anal Chem*. (2023) 53:1393–418. doi: 10.1080/10408347.2021.2023460

18. Zhang XY, Li LY, Pu JZ, Zhang YZ. Traditional identification of Fritillaria cirrhosa and its common and easily confused products in the market. *Anhui Univ Chin Med*. (2023) 42:92–6. doi: 10.3969/j.issn-2095-7246.2023.06.019

19. Zhang FL, Liu W, Mao JF, Yin Q, Lan QK, Liu Q, et al. Nucleosides-based identification model for Fritillariae Cirrhosae Bulbus. *China J Chin Mater Med*. (2021) 46:3337–48. doi: 10.19540/j.cnki.cjcmm.20210316.101

20. Deng JK, Zhao HB, Qi B, Wang D, Wu YB, Dai SX, et al. Volatile characterization of crude and refined walnut oils from aqueous enzymatic extraction by GC-IMS and GC-MS. *Arab J Chem*. (2023) 17:105404. doi: 10.1016/j.arabjc.2023.105404

21. Yan Y, Lu W, Tian T, Shu N, Yang Y, Fan S, et al. Analysis of volatile components in dried fruits and branch exudates of Schisandra chinensis with different fruit colors using GC-IMS technology. *Molecules*. (2023) 28:6865. doi: 10.3390/molecules28196865

22. Xiang Y, Lei C, Hu G, Zhou W, Li Y, Huang D. Investigation of 60Co irradiation on the volatile organic compounds from finger citron (Citri Sarcodactylis Fructus) using GC-IMS. *Food Secur*. (2023) 12:3543. doi: 10.3390/foods12193543

23. Wu Y, Li Z, Zou S, Dong L, Lin X, Chen Y, et al. Chemical composition and flavor characteristics of cider fermented with Saccharomyces cerevisiae and non-*Saccharomyces cerevisiae*. *Food Secur*. (2023) 12:3565. doi: 10.3390/foods12193565

24. Zhang L, Li XY, Chen HX, Wu ZJ, Hu M, Yao MS. Haze air pollution health impacts of breath-borne VOCs. *Environ Sci Technol*. (2022) 56:8541–51. doi: 10.1021/acs.est.2c01778

25. Song YJ, Guo T, Liu SJ, Gao YL, Wang Y. Identification of Polygonati Rhizoma in three species and from different producing areas of each species using HS-GC-IMS. *LWT*. (2022) 172:114142. doi: 10.1016/j.lwt.2022.114142

26. Li HY, Wang YL, Yue YS, Li H, Hou FG, Fan XH, et al. Rapid identification of Bletilla striata and its counterfeit Polygonatum odoratum decoction pieces based on gas chromatography-ion mobility spectroscopy. *Chin Tradit Herb Drug*. (2023) 54:1–10. doi: 10.7501/j.issn.0253-2670.2024.02.026

27. Zhou S, Feng D, Zhou Y, Duan H, He Y, Jiang Y, et al. Characteristic volatile organic compound analysis of different Cistanches based on HS-GC-IMS. *Molecules*. (2022) 27:6789. doi: 10.3390/molecules27206789

28. Li C, Wan H, Wu X, Yin J, Zhu L, Chen H, et al. Discrimination and characterization of the volatile organic compounds in Schizonepetae Spica from six regions of China using HS-GC-IMS and HS-SPME-GC-MS. *Molecules*. (2022) 27:4393. doi: 10.3390/molecules27144393

29. Sun LL, Wang M, Ren XL. Application progress on chemical pattern recognition in quality control of Chinese materia medica. *Chin Tradit Herb Drug*. (2017) 48:4339–45. doi: 10.7501/j.issn.0253-2670.2017.20.03130

30. Yu BC, Li Z, Wu JY, Ying JM, Tang YQ, Wu BC, et al. Quality control of Gastrodia elata by high-performance liquid chromatography with fluorescence detection (HPLC–FLD) and principal component analysis (PCA) and hierarchical cluster analysis (HCA). *Anal Lett*. (2020) 53:746–59. doi: 10.1080/00032719.2019.1674867

31. Kuang LX, Wang ZQ, Zhang JY, Li HF, Xu GF, Li J. Factor analysis and cluster analysis of mineral elements contents in different blueberry cultivars. *J Food Compos Anal*. (2022) 109:104507. doi: 10.1016/j.jfca.2022.104507

32. Zhao MY, Gou JB, Zhang KX, Ruan JJ. Principal components and cluster analysis of trace elements in buckwheat flour. *Food Secur*. (2023) 12:225. doi: 10.3390/foods12010225

33. Li T, Chen S. Authenticity identification and classification of Rhodiola species in traditional Tibetan medicine based on Fourier transform near-infrared spectroscopy and chemometrics analysis. *Spectrochim Acta A Mol Biomol Spectrosc*. (2018) 204:131–40. doi: 10.1016/j.saa.2018.06.004

34. Xu LX, Fan LZ, Jiang S, Yang XR, Wang XT, Yang CJ. Recent progress of chemical constituents and pharmacological effects of Fritillaria. *Chin J Med Chem*. (2022) 32:61–73. doi: 10.14142/j.cnki.cn21-1313/r.2022.01.010

Traditional method of rhubarb processing optimized by combining flavor analysis with anthraquinone content determination

Taotao Liu[†], Miao Yu, Yue Dai, Yongqing Xiao and Li Li*

Institute of Chinese Materia Medica, China Academy of Chinese Medical Sciences, Beijing, China

Introduction: Rhubarb is a popular food that relieves constipation and aids with weight loss. The traditional method of preparation, includes steaming and sun-drying rhubarb nine times (SDR-9) to reduce its toxicity and increase efficacy.

Methods: Flavor analysis includes odor analysis by gas chromatography−ion mobility spectrometry and taste characterization using an electronic tongue.

Results: Odor analysis of the samples prepared through SDR-9 identified 61 volatile compounds, including aldehydes, esters, alcohols, ketones, acids, alkenes, and furans. Of these, 13 volatile components were the key substances associated with odor. This enabled the process to be divided into two stages: 1−5 times of steaming and sun-drying and 6−9 times. In the second stage, SDR-6 and SDR-9 were grouped together in terms of odor. Analysis using electronic tongue revealed that the most prominent taste was bitterness. A radar map indicated that the bitterness response was the highest for raw rhubarb, whereas that for processed (steamed and sun-dried) rhubarb decreased. Orthogonal partial least squares discriminant analysis (OPLS-DA) clustering results for SDR-6 and SDR-9 samples indicated that their tastes were similar. Anthraquinones were analyzed via high-performance liquid chromatography; moreover, analysis of the taste and components of the SDR samples revealed a significant correlation.

Discussion: These results indicate that there are similarities between SDR-6 and SDR-9 in terms of smell, taste, and composition, indicating that the steaming and sun-drying cycles can be conducted six times instead of nine.

KEYWORDS

electronic tongue, gas chromatography-ion mobility spectrometry, rhubarb, taste flavor, high-performance liquid chromatography

1 Introduction

Rhubarb (Rhei Radix et Rhizoma), including *Rheum palmatum* L., *Rheum tanguticum* Maxim. ex Balf, and *Rheum officinale* Baill., has a long history of use as a conventional Chinese medicine worldwide (1). It has a variety of pharmacological properties, including antibacterial, anti-inflammatory, antitumor, hepatoprotective, renoprotective, immunoregulatory, free radical scavenging, purgative, and cardiovascular protective properties (2). Rhubarb can be used clinically to treat obesity as it inhibits proinflammatory signaling pathways and modulates glucose−lipid homeostasis (3). Rhein, a crucial component of rhubarb, can inhibit obesity caused by a high-fat diet, decrease fat mass, and reduce the size of white and brown adipocytes. It can also lower the levels of serum cholesterol, low-density lipoprotein cholesterol, and fasting blood

glucose in mice (4). Aloe-emodin, emodin, chrysophanol, and physcion in rhubarb are other important chemicals that promote weight loss (5). Europeans and Americans have regarded edible rhubarb as a palatable food since the 19th century (6); however, long-term consumption of raw and processed rhubarb increases the risk of melanosis coli and liver and kidney damage, which are primarily attributed to anthraquinones (7, 8). Compared with raw rhubarb, the processed version has relatively fewer side effects and rarely causes diarrhea (9).

In China, rhubarb is commonly used after processing. Four processes have been recorded in the Chinese Pharmacopeia, which include cleaning, roasting with wine, steaming, and charcoal frying to obtain raw rhubarb, roasted rhubarb with wine, steamed rhubarb with wine, and carbonized rhubarb, respectively (10). Different methods are used throughout the world for various purposes (11). Steaming and sun-drying nine times is one characteristic method of processing Chinese Materia Medica and is commonly used to increase the activity of most traditional Chinese medicines and reduce or avoid side effects. The long-term consumption of raw rhubarb can damage renal function in rats; however, processed rhubarb reduces the risk of renal injury (9). Forty-three traditional Chinese medicines, including rhubarb, are steamed and dried several times, as described in the ancient medical literature (12). Overall, the process of steaming and sun-drying nine times yields good clinical effects and is worthy of further study. However, the pharmacological activities and primary active ingredients of rhubarb have been the main focus of most studies (6). There are few studies on the odor and taste of rhubarb processed by steaming and sun-drying nine times. Moreover, the processing period is long and tedious, this traditional Chinese medicine is subject to rot and mildew during exposure to the climate. Therefore, it is necessary to devise a method to simplify the preparation process.

Based on the above findings, after steaming and sun-drying nine times, the odor and taste of rhubarb change to varying degrees, which is a vital indicator for process control and quality evaluation. However, as traditional evaluation methods primarily rely on sensory identification by humans and other subjective analyses, the results are inevitably affected by sensory differences and the detection environment. As a result, ensuring the objectivity and accuracy of the evaluation is an important issue for the quality evaluation of traditional Chinese medicines. Artificial intelligence is rapidly developing, and electronic tongues and noses have become widely available in recent years. As a modern, intelligent, sensory, qualitative analysis, and testing tool, the electronic tongue consists of an interactive and sensitive sensor array and a signal acquisition circuit that is combined with a data processing method based on pattern recognition. An artificial lipid bilayer membrane with unique and wide selectivity of an area can be used to directly output taste values, including sour, sweet, bitter, astringent, fresh, salty, bitter aftertaste, and richness from a sample solution (13). It may be applied to studies of food (14), beverages (15), tea (16), alcohol discrimination (17), and environmental analysis (18). It can detect overall taste, but not the specific compounds involved (19).

In addition to the electronic tongue, gas chromatography–ion mobility spectrometry (GC–IMS) is a novel technique that can be used to identify ions based on differences in the migration rates of various gas-phase ions in an electric field. In the ionization region, gas molecules are converted into charged ions, which then enter a drift tube. Identification and analysis are performed based on the different migration velocities of gaseous ions in the electric field. GC–IMS is a powerful analytical method that combines the simplicity and rapidity of GC with the high-resolution and accurate analysis of IMS. The advantages of this method are its low detection limit, short analysis time, and ease of operation (20). GC–IMS is increasingly being used for analyzing food flavors (21), discriminating traditional medicines (22, 23), and classifying white wines (24).

The flavor index is a traditional method of evaluating the quality of rhubarb. The effective component is not only the common index of rhubarb quality but also the standard component of quality control in Chinese Pharmacopeia. Thus, it can be used as the standard of evaluation. To simplify the process and improve efficiency, the flavor and components of rhubarb prepared by steaming and sun-drying nine times were analyzed using GC–IMS, the electronic tongue, and high-performance liquid chromatography (HPLC).

2 Materials and methods

2.1 Rhubarb processing and sample preparation

Fresh *Rheum palmatum* L. was cleaned and prepared based on the Chinese Pharmacopeia (2020 edition) (The State Pharmacopeia Committee of the People's Republic of China, 2020) to obtain raw rhubarb samples (Shengpian in Chinese). Initially, 2.5 kg of Huangjiu was added to 5.0 kg of Shengpian and mixed well until fully absorbed. Using an induction cooker (1800 w), the raw rhubarb was steamed for 4 h, followed by natural sun-drying. A 0.5-kg sample was used in one cycle of steaming and sun-drying (hereinafter referred to as SDR-1); the remaining sample was repeatedly subjected to the same process, with 0.5-kg sample removed after each cycle. A total of nine samples (SDR-1–9) were obtained and each sample was prepared in triplicate. Finally, the samples were powdered using 40-mesh sieve and a grinder.

2.2 GC–IMS analysis

The FlavourSpec flavor analyzer (G.A.S., Dortmund, Germany) uses GC–IMS technology to measure the volatile headspace components. Rhubarb samples (3.0 g) were incubated in a 20-mL headspace vial for 20 min at 60°C. A 200-μL sample was then injected into an MXT-WAX metal capillary GC column (30 m × 0.53 mm; Restek Corporation, the United States) at 85°C with nitrogen (99.99%) as the carrier gas. Flow rates started at 2 mL/min for 2 min and increased to 10 mL/min for 8 min, then to 100 mL/min for 10 min, and finally to 100 mL/min for 20 min. The sample then entered the ion transfer tube. After the molecules were ionized in the ionization region, they migrated to the Faraday disk for detection by an electric field and reverse drift gas to achieve separation. Nitrogen (99.99%) was used as the drift gas with a flow rate of 150 mL/min. The GC–IMS instrument with software (G.A.S.) was used to obtain the three- and two-dimensional spectra, fingerprints, and principal component analysis (PCA) graph.

2.3 Quantitative analysis of anthraquinones

2.3.1 Reagents and materials

The nine reference components are chrysophanol-8-O-β-D-glucoside, emodin-8-O-β-D-glucoside, aloe-emodin-3-

(hydroxymethyl)-O-β-D-glucoside, physcion-8-O-β-D-glucoside, aloe-emodin, rhein, emodin, chrysophanol, and physcion (designated A–I), which were purchased from the National Institutes for Food and Drug Control. The purity of all components was greater than 98%. HPLC-grade solutions, methanol, and reagents were purchased from Thermo Fisher Scientific (United States).

2.3.2 Chromatographic conditions

The HPLC system (Waters, United States) consisted of a Waters 2695 Separations Module and Waters 2998 PDA detector. The output signal of the detector was recorded using an Empower 3 workstation. For the separation of the sample, a Roc C18 column (4.6 mm × 250 mm, 5 μm) was used and the UV detection wavelength was set to 280 and 430 nm. The mobile phase consisted of methanol (A) and 0.1% glacial acetic acid (B) with gradient elution (0–5 min, A 54%; 5–15 min, A 54–64%; 15–20 min, A 64–73%; 20–23 min, A 73–83%; 23–26 min, A 83–90%; 26–27 min, A 90–100%; and 27–33 min, A 100%) at a flow rate of 1.0 mL/min. The injection volume was 10 μL and the column temperature was maintained at 35°C.

2.3.3 Preparation of rhubarb test solution

Raw rhubarb (0.5 g) was placed in a cone bottle with a plug and 25 mL of methanol was added. Ultrasonic extraction lasted for 10 min. After cooling, the solution was filtered through a paper filter prior to HPLC analysis. The sample solution was filtered through a 0.22-μm filter.

2.3.4 Preparation of standard solution

Each standard stock solution comprised nine components, including chrysophanol-8-O-β-D-glucoside (0.0164 mg/mL), emodin-8-O-β-D-glucoside (0.0201 mg/mL), aloe-emodin-3-(hydroxymethyl)-O-β-D-glucoside (0.0097 mg/mL), emodin-8-O-β-D-glucoside (0.0142 mg/mL), aloe-emodin (0.0200 mg/mL), rhein (0.0270 mg/mL), emodin (0.0780 mg/mL), chrysophanol (0.0344 mg/mL), and physcion (0.0222 mg/mL), and was prepared by dissolving in methanol. Six different volumes (1, 5, 10, 15, 20, and 25 μL) of the standard solution were used to establish a calibration curve. A working solution was prepared for each standard. The stock solutions were stored at 4°C.

2.4 Electronic tongue analysis

A TS-5000Z electronic tongue (INSET Inc., Japan) was used to analyze the taste characteristics of rhubarb. An artificial lipid membrane sensor in the electronic tongue simulates the taste perception mechanism of living organisms and evaluates taste by detecting changes in membrane potential generated by the interaction between substances and artificial lipid membranes. The five detective sensors include AAE, CT0, CA0, C00, and AE1, which represent umami (richness), saltiness, sourness, bitterness (aftertaste-A), and astringency (aftertaste-B). The first taste and aftertaste corresponding to each sensor and the specific ingredients that impart these tastes are listed in Table 1. Briefly, 100 mL of pure water was added to 1 g of rhubarb and placed in an ultrasonic cleaning machine for 30 min, followed by centrifugation at 3,000 rpm for 5 min. The supernatant was filtered through filter paper, and the filtrate was tested. Each sample was processed three times. Finally, the detection data were transformed into taste values using the electronic tongue software (the Taste Sensing System and Taste Analyzed System applications).

2.5 Statistical analysis

The VOCal software and three plug-ins supported by GC–IMS were used to analyze the rhubarb samples. The spectrum of qualitative and quantitative analyses and data may be viewed using VOCal software. The three-dimensional spectrum, two-dimensional top view, and difference spectrum were used to directly compare the spectral differences among samples using the Reporter plug-in. The differences in volatile headspace components were compared using the Gallery Plot plug-in visually and quantitatively using fingerprint. GC–IMS was used to detect the peak intensity response value and the Dynamic PCA plug-in was used to analyze the data. A one-way ANOVA for multiple comparisons was performed using GraphPad Prism software (v.6.02, GraphPad Software, San Diego, CA, United States). To determine the correlation of volatile compounds in rhubarb samples for different steaming and sun-drying times, a correction heatmap was generated using the OriginPro 2021 software (v.9.8.0, OriginLab, Northampton, MA, United States). IBM SPSS Statistics software (R26.0.0.0, IBM, United States) was used for Pearson's correlation analysis. The data obtained from the electronic tongue was analyzed using the Taste Sensing System (v.2.0.0.0, Insent, Japan) and Taste Analyzed System (v.1.0.0.5, Insent) application. Orthogonal partial least squares discriminant analysis (OPLS-DA) of the electronic tongue data was viewed using SIMCA (v.14.1, Umetrics, Sweden).

TABLE 1 First taste and aftertaste corresponding to each sensor and the specific ingredients that impart these tastes.

Sensor	Corresponding sense of taste	
	First taste	Aftertaste
AAE	Umami (caused by amino acids and nucleic acids)	Richness (sustainable perception)
CT0	Saltiness (caused by inorganic salts such as table salt)	——
CA0	Sourness (caused by acetic acid, citric acid, and tartaric acid)	——
C00	Bitterness (caused by bitter substances that are perceived as rich at low concentrations)	Aftertaste-B (caused by drinks such as beer and coffee)
AE1	Astringency (caused by astringent substances, perceived as an irritating aftertaste at low concentrations)	Aftertaste-A (caused by drinks such as tea and red wine)
AN0	——	B-bitterness2 (caused by bitter medicine)
BT0		H-bitterness (caused by hydrochloride compounds)

3 Results

3.1 Odor analysis using GC–IMS

3.1.1 Visual topographic plots of rhubarb samples subjected to different steaming and sun-drying times

The three-dimensional spectrum in Figure 1A presents the differences in the volatile headspace components of the rhubarb samples. The two-dimensional spectrum is presented in Figure 1B. The normalized reaction ion peak occurs at abscissa 1.0, and each point on both sides represents a volatile organic compound. Obvious differences were observed in the volatile organic compounds at different steaming and sun-drying times. SDR-1 was used as the reference sample, and the spectra of the other samples were subtracted from the reference. As indicated in Figure 1C, the background after deduction is white when the two volatile organic compounds (VOCs) are consistent, whereas red and blue backgrounds indicate that the concentrations are higher and lower than those of the reference, respectively. Figure 1C indicates an increase in the content of some volatile components as the number of processing cycles increases. Decreases in the levels of these compounds were also observed.

3.1.2 Volatile compounds in rhubarb samples subjected to different steaming and sun-drying times

A total of 61 VOCs were identified in the rhubarb samples, including aldehydes, alcohols, ketones, esters, and furans, as previously described (25). Among them, 14 aldehydes, 12 alcohols, 12 ketones, and nine esters were the main VOCs. The details of these VOCs are listed in Table 2.

This Maillard reaction, also known as a carbonyl–amino compound reaction, refers to the formation of a dark brown substance because of the rearrangement, dehydration, condensation, and polymerization of carbonyl and amino compounds. Rhubarb contains sugars, amino acids, and polyphenols, which provide conditions for enzymatic browning and facilitate the Maillard reaction during processing (26).

3.2 Complete spectral analysis of rhubarb samples

Complete data on VOCs and their differences among the rhubarb samples are shown in Figure 2. The contents in the areas denoted with yellow, red, and green rectangles significantly increased during steaming and sun-drying. Furfural, 2-acetyl furan, 2-methyl tetrahydrofuran-3-one, 3-hydroxy butan-2-one, and propanal contents in the yellow rectangle were higher in SDR-6–9 than in SDR-1–5, whereas it gradually increased in SDR-6–9. In the red rectangle, tetrahydrofuran, ethyl lactate, and benzaldehyde contents were higher in SDR-6–9 than in SDR-1–5, whereas those in SDR-6–9 were stable. The contents of 2-cyclohexen-1-one, gamma-butyrolactone, isobutyric acid, 1-hydroxy propan-2-one, 3-methyl butanal, and 2-methyl propanal in the green rectangle gradually increased during processing. However, the contents of pentanal, 1-penten-3-one, methyl acetate, heptan-2-one, and cyclopentanone in the orange rectangle significantly decreased during processing.

Furthermore, the relative contents of other compounds fluctuated during processing without any significant differences.

3.3 Cluster analysis of characteristic volatile flavoring compounds in rhubarb samples

The differences in volatile compounds were analyzed using PCA. As shown in Figure 3A, the cumulative variance contribution rate of PC1 (14%) and PC2 (59%) was 73%, indicating that the PCA separation model was effective. The PCA plot indicated that the distance between SDR-1–5 and SDR-6–9 was relatively large, as evidenced by two distinct stages. The distance among SDR-1–5 was relatively close, except for SDR-1, and the differences between the groups were small. The distance interval among SDR-6–9 was similar, and they clustered with one another, indicating little difference in composition; however, each sample could be distinguished from the others.

To further assess the changes in the characteristic volatile components of rhubarb after different steaming and sun-drying times, cluster heat maps were generated based on the peak intensities of 61 characteristic markers (Figure 3B). The response value of the compound increased with increasing red intensity and decreased with increasing blue intensity. As shown in the figure, rhubarb processing can be divided into two stages: odor fluctuation and odor stability. In Figure 3B, these odor substances are divided into four categories according to the clustering results, namely, ①, ②, ③, and ④. The composition of the odor substances varied at different stages; among these, ① compounds played a crucial role in distinguishing the different stages. The odor fluctuation stage included SDR-1–5. At this stage, the response value of the ① compounds was low, indicating that no changes occurred in these odor substances during the first to fifth cycles of steaming and sun-drying. The odor-stable stage included SDR-6–9, which formed a clear boundary with the fifth cycle. The response value of ① compounds was significantly increased ($p < 0.05$) and reached the maximum value, reaching a stable stage of rhubarb odor. A total of 26 volatile odor substances, including the eight aldehydes propanal (M), propanal (D), benzaldehyde (M), benzaldehyde (D), furfural (M), furfural (D), 3-methyl butanal, and 2-methyl propanal (D) were present in the ① compounds. These usually have a low odor threshold and contribute significantly to odor. Furans, such as 2-acetyl furan, tetrahydrofuran (M), tetrahydrofuran (D), 2-methyl tetrahydrofuran-3-one (M), and 2-methyl tetrahydrofuran-3-one (D), are products of the Maillard reaction that occurs during the heat processing of rhubarb. They also have a low threshold and significantly contribute to odor. The Maillard reaction, also known as a carbonyl–amino compound reaction, refers to the formation of a dark brown substance through rearrangement, dehydration, condensation, and polymerization of carbonyl and amino compounds. Rhubarb contains sugars, amino acids, and polyphenols, which provide conditions for enzymatic browning and facilitate the Maillard reaction during processing (26). The proportion of these two types of compounds and their respective high response values are responsible for the primary odor of the SDR-9 samples. As a result, these eight aldehydes and five furans are key odor substances after nine cycles of steaming and sun-drying. Contrary to the ① compounds, ②, ③, and ④ compounds were present in high quantities in SDR-1–5. They exhibited a different pattern from the sixth round of steaming and sun-drying. The volatile components in the ② compounds, such as nonanal, heptanal, hexanal (M,

FIGURE 1
Volatile compounds in rhubarb samples at different steaming and sun-drying times. **(A)** Three-dimensional topography. **(B)** Topographic plot of GC–IMS spectra. **(C)** Comparison of the results from the spectral diagram (SDR-1) with one sample selected as the reference.
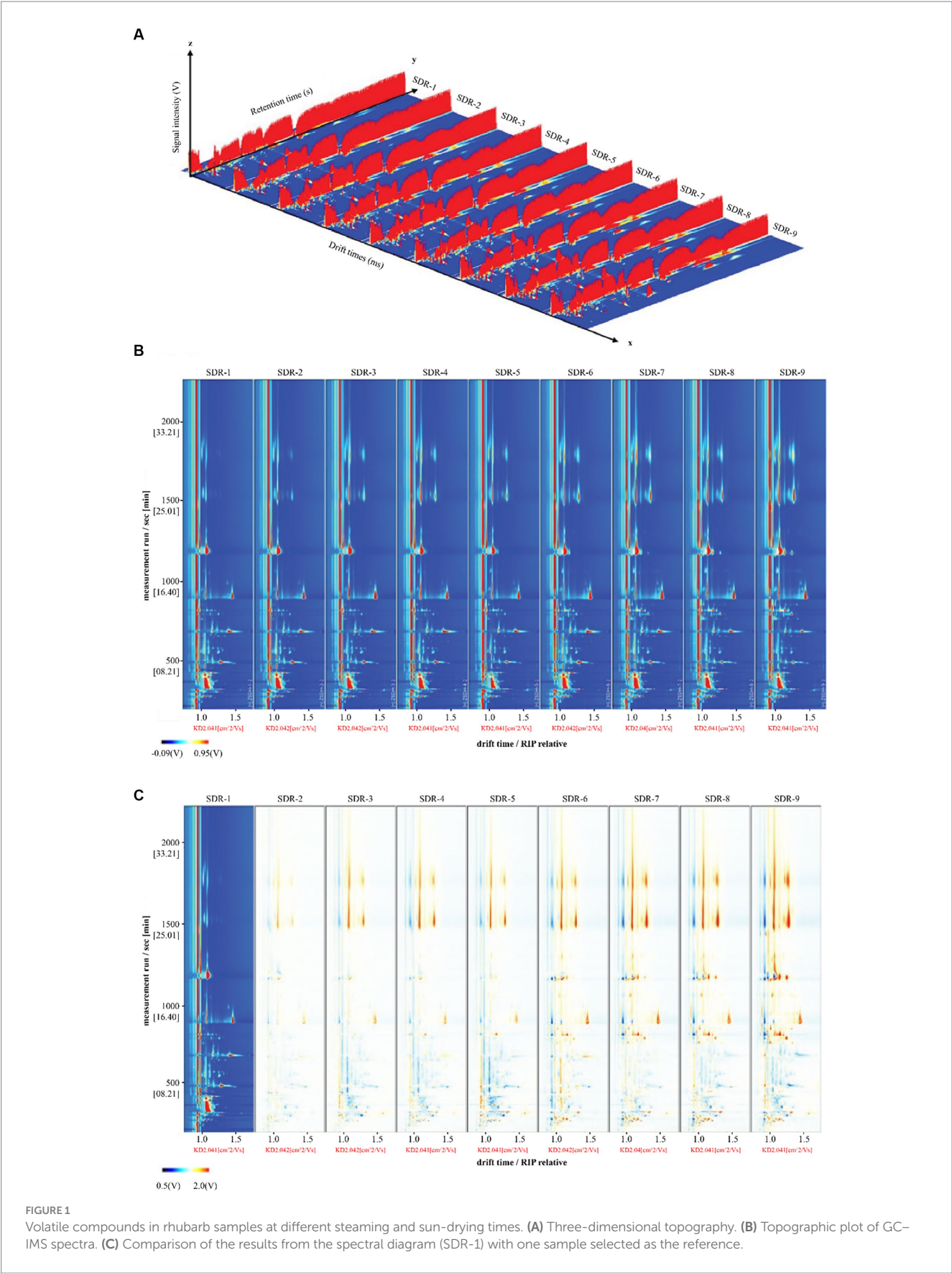
TABLE 2 Gas chromatography—ion mobility spectrometry global area set integration parameters obtained from the rhubarb samples after different cycles of steaming and sun-drying.

Count	Compound	CAS#	Formula	MW	RI	Rt [s]	Dt [a.u.]
1	Dimethyl sulfide	C75183	C_2H_6S	62.1	789.3	238.388	0.964
2	Propanal (D)	C123386	C_3H_6O	58.1	833.3	261.118	1.148
3	Propanal (M)	C123386	C_3H_6O	58.1	834.0	261.519	1.046
4	2-Methyl propanal (M)	C78842	C_4H_8O	72.1	843.4	266.672	1.099
5	2-Methyl propanal (D)	C78842	C_4H_8O	72.1	845.3	267.734	1.282
6	Propan-2-one	C67641	C_3H_6O	58.1	847.2	268.736	1.117
7	Methyl acetate	C79209	$C_3H_6O_2$	74.1	859.3	275.563	1.031
8	Tetrahydrofuran (D)	C109999	C_4H_8O	72.1	861.4	276.755	1.231
9	Tetrahydrofuran (M)	C109999	C_4H_8O	72.1	863.7	278.108	1.064
10	Ethyl acetate (M)	C141786	$C_4H_8O_2$	88.1	900.8	300.318	1.099
11	Ethyl acetate (D)	C141786	$C_4H_8O_2$	88.1	903.2	301.799	1.342
12	Butan-2-one	C78933	C_4H_8O	72.1	916.0	309.905	1.250
13	Methanol	C67561	CH_4O	32.0	920.8	312.969	0.982
14	3-Methyl butanal	C590863	$C_5H_{10}O$	86.1	930.3	319.243	1.403
15	Ethanol	C64175	C_2H_6O	46.1	940.1	325.777	1.146
16	Pentanal	C110623	$C_5H_{10}O$	86.1	979.2	353.205	1.430
17	1-Penten-3-one	C1629589	C_5H_8O	84.1	1009.6	379.249	1.323
18	1-Propanol (D)	C71238	C_3H_8O	60.1	1050.5	423.267	1.255
19	1-Propanol (M)	C71238	C_3H_8O	60.1	1051.8	424.736	1.110
20	Camphene	C79925	$C_{10}H_{16}$	136.2	1076.7	453.960	1.218
21	Hexanal (M)	C66251	$C_6H_{12}O$	100.2	1097.2	479.693	1.257
22	Hexanal (D)	C66251	$C_6H_{12}O$	100.2	1098.7	481.988	1.567
23	2-Methyl-1-propanol (D)	C78831	$C_4H_{10}O$	74.1	1102.7	488.251	1.364
24	2-Methyl-1-propanol (M)	C78831	$C_4H_{10}O$	74.1	1106.3	493.883	1.167
25	Butan-1-ol (D)	C71363	$C_4H_{10}O$	74.1	1155.7	578.603	1.376
26	Butan-1-ol (M)	C71363	$C_4H_{10}O$	74.1	1156.1	579.398	1.186
27	1-Penten-3-ol	C616251	$C_5H_{10}O$	86.1	1168.5	602.797	0.945
28	Alpha-terpinene	C99865	$C_{10}H_{16}$	136.2	1173.5	612.495	1.218
29	Ethyl crotonate (D)	C623701	$C_6H_{10}O_2$	114.1	1177.3	620.106	1.555
30	Ethyl crotonate (M)	C623701	$C_6H_{10}O_2$	114.1	1178.7	622.787	1.181
31	Heptan-2-one	C110430	$C_7H_{14}O$	114.2	1186.0	637.530	1.265
32	Cyclopentanone	C120923	C_5H_8O	84.1	1191.4	648.753	1.106
33	Heptanal	C111717	$C_7H_{14}O$	114.2	1193.6	651.975	1.331
34	Limonene (M)	C138863	$C_{10}H_{16}$	136.2	1202.8	663.613	1.224
35	Limonene (D)	C138863	$C_{10}H_{16}$	136.2	1203.1	664.031	1.294
36	3-Methyl-1-butanol (M)	C123513	$C_5H_{12}O$	88.1	1216.8	681.825	1.246
37	3-Methyl-1-butanol (D)	C123513	$C_5H_{12}O$	88.1	1217.0	682.067	1.490
38	(E)-2-hexenal	C6728263	$C_6H_{10}O$	98.1	1226.2	694.257	1.183
39	Gamma-terpinene	C99854	$C_{10}H_{16}$	136.2	1250.1	727.017	1.220
40	1-Pentanol	C71410	$C_5H_{12}O$	88.1	1259.8	740.707	1.256
41	2-Methyl tetrahydrofuran-3-one (M)	C3188009	$C_5H_8O_2$	100.1	1274.2	761.668	1.075
42	2-Methyl tetrahydrofuran-3-one (D)	C3188009	$C_5H_8O_2$	100.1	1274.5	762.062	1.427
43	3-Hydroxybutan-2-one (M)	C513860	$C_4H_8O_2$	88.1	1295.0	792.784	1.052
44	3-Hydroxybutan-2-one (D)	C513860	$C_4H_8O_2$	88.1	1296.4	794.982	1.333

(Continued)

TABLE 2 (Continued)

Count	Compound	CAS#	Formula	MW	RI	Rt [s]	Dt [a.u.]
45	1-Hydroxypropan-2-one (M)	C116096	$C_3H_6O_2$	74.1	1308.8	814.758	1.032
46	1-Hydroxypropan-2-one (D)	C116096	$C_3H_6O_2$	74.1	1310.1	816.955	1.236
47	Ethyl lactate (D)	C97643	$C_5H_{10}O_3$	118.1	1356.1	895.115	1.543
48	Ethyl lactate (M)	C97643	$C_5H_{10}O_3$	118.1	1356.4	895.637	1.139
49	Nonanal	C124196	$C_9H_{18}O$	142.2	1405.1	986.519	1.474
50	2-Cyclohexen-1-one	C930687	C_6H_8O	96.1	1441.7	1060.988	1.110
51	Furfural (M)	C98011	$C_5H_4O_2$	96.1	1486.9	1160.527	1.086
52	Furfural (D)	C98011	$C_5H_4O_2$	96.1	1493.1	1174.958	1.345
53	Acetic acid	C64197	$C_2H_4O_2$	60.1	1496.2	1182.140	1.159
54	2-Acetyl furan	C1192627	$C_6H_6O_2$	110.1	1537.9	1284.113	1.112
55	Benzaldehyde (D)	C100527	C_7H_6O	106.1	1548.3	1310.942	1.474
56	Benzaldehyde (M)	C100527	C_7H_6O	106.1	1549.1	1313.162	1.152
57	Propanoic acid	C79094	$C_3H_6O_2$	74.1	1631.7	1547.304	1.102
58	Isobutyric acid (D)	C79312	$C_4H_8O_2$	88.1	1700.0	1771.927	1.368
59	Isobutyric acid (M)	C79312	$C_4H_8O_2$	88.1	1701.7	1777.724	1.154
60	Gamma-butyrolactone (D)	C96480	$C_4H_6O_2$	86.1	1703.8	1785.192	1.306
61	Gamma-butyrolactone (M)	C96480	$C_4H_6O_2$	86.1	1707.6	1798.815	1.084

[a]RI represents the retention index calculated using an MXT-WAX metal capillary chromatographic column.
[b]Rt represents the retention time in the capillary GC column.
[c]Dt represents the drift time in the drift tube.
[d]D, dimer; M, monomer.

FIGURE 2
Gallery Plot maps (fingerprints) of the volatile organic compounds in rhubarb samples at different steaming and sun-drying times.
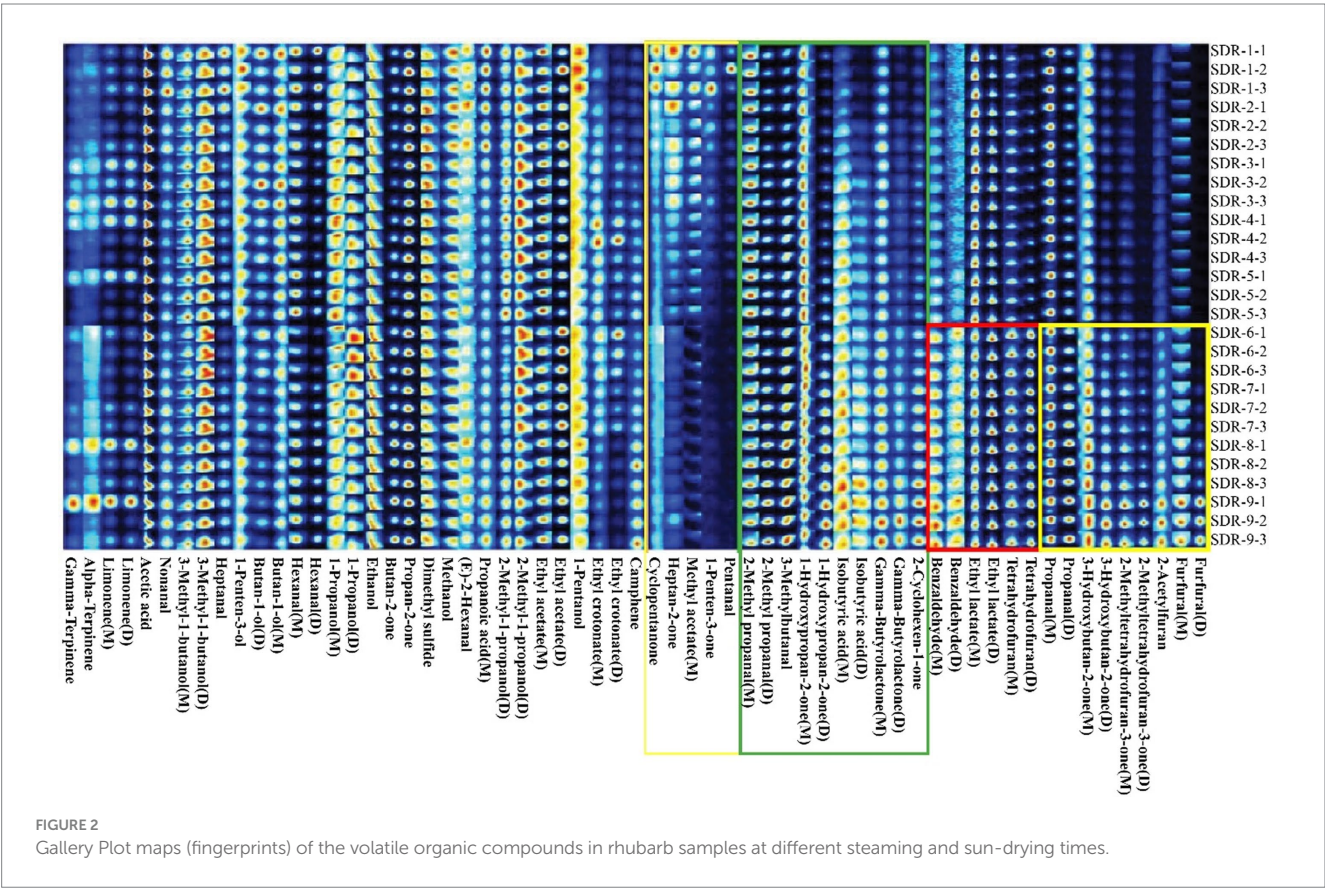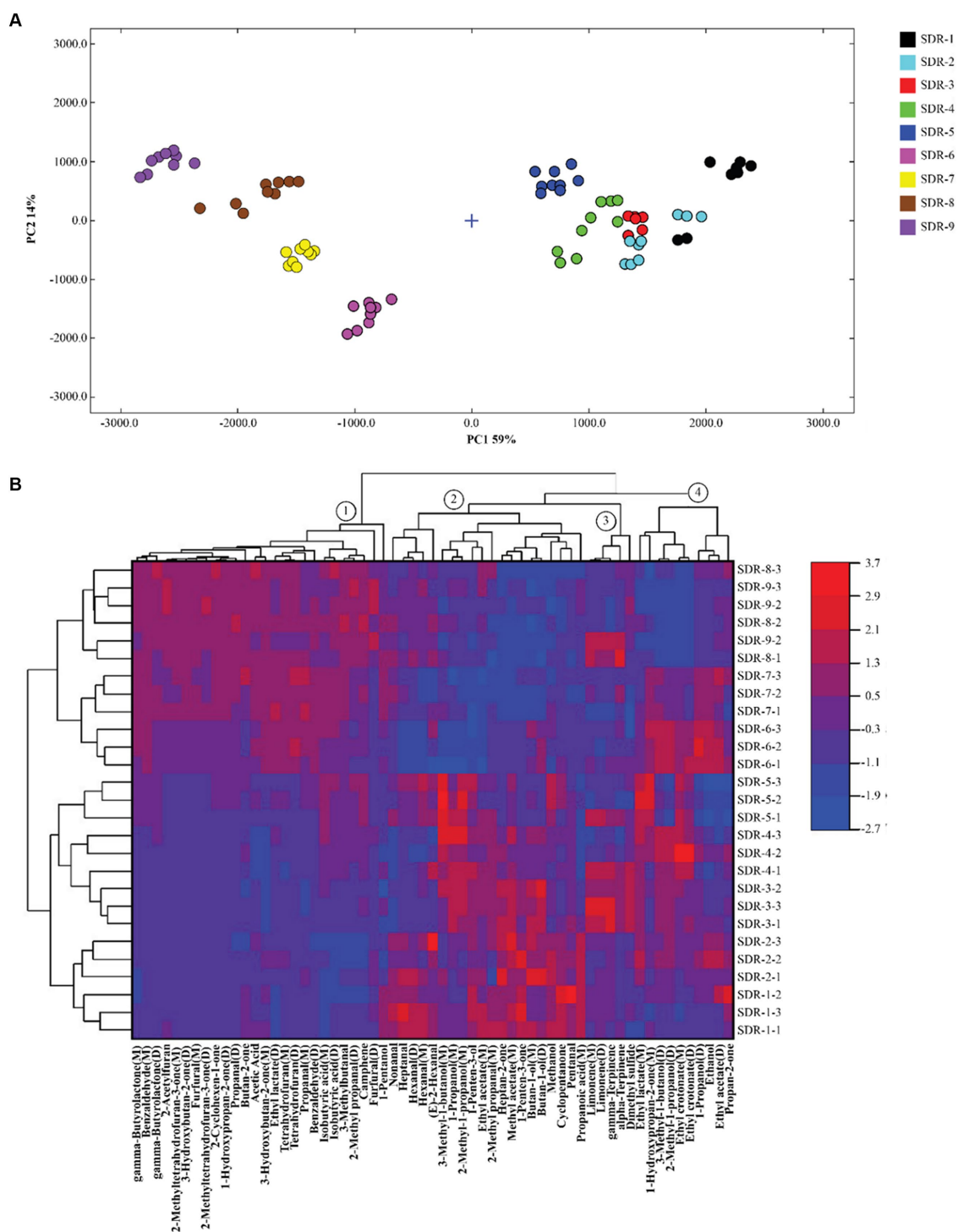
FIGURE 3
Principal component analysis (A) and cluster heat mapping (B) of the characteristic volatile components in rhubarb samples at different steaming and sun-drying times.

D), 2-methyl propanol (M), (E)-2-hexanal, 3-methyl-1-butanol (M), 1-propanol, 2-methyl-1-propanol (M), 1-penten-3-ol, and ethyl acetate, significantly decreased ($p < 0.05$) after six to seven cycles of steaming and sun-drying. The other volatile substances in the ② compounds continued to decrease from the sixth to the ninth cycle. The ③ compounds primarily comprised four olefins and one sulfide, which fluctuated during the

process. The ④ compounds were mainly alcohols, esters, and ketones, which reached their highest values during the sixth and seventh cycles drying, followed by a decrease in the eighth and ninth cycles.

Taken together, six steaming and sun-drying cycles may be considered a key process point. After six rounds, the rhubarb composition tends to be stable, and there is no significant difference

in composition between SDR-6 and SDR-9. Therefore, replacing SDR-9 with SDR-6 is an effective method to streamline the process.

3.4 Quantitative analysis of anthraquinones using HPLC

3.4.1 Separation of nine standard components using HPLC

The standard solution was separated by HPLC. The retention times of chrysophanol-8-O-β-D-glucoside, physcion-8-O-β-D-glucoside, aloe-emodin-3-(hydroxymethyl)-O-β-D-glucoside, emodin-8-O-β-D-glucoside, aloe-emodin, rhein, emodin, chrysophanol, and physcion were 13.60, 13.85, 14.27, 18.14, 21.07, 24.73, 28.86, 30.70, and 31.87 min, respectively (Figures 4A,B). This method was also applied to the prepared rhubarb samples (Figure 4C).

3.4.2 Linearity, limit of detection, and limit of quantification

Linearity was defined using a calibration curve. Six different volumes (1, 5, 10, 15, 20, and 25 μL) of the standard solution were used to establish a calibration curve. The following linear regression equation was obtained from the calibration curve: $Y = a\,x + b$, where a is the slope and b is the intercept of the calibration curve, x is the infection volume of the standard components, and Y is the peak area. The correlation coefficients for all marker components exhibited excellent linearity ($R^2 > 0.9992$). The linear relationship of components A–I was good at 0.0164–0.4100, 0.0201–0.5025, 0.0097–0.2425, 0.0142–0.3550, 0.0200–0.5000, 0.0270–0.6750, 0.0780–1.9500, 0.0344–0.8600, and 0.0222–0.5550 μg, respectively. The limit of detection (LOD) and limit of quantification (LOQ) were calculated based on the standard deviation (SD) and the slope (S) of the calibration curve using the equations: $LOD = (3.3 \times SD)/S$ and $LOQ = (10 \times SD)/S$. From the calibration curve of the peak area versus concentration, the SD was the SD of the response. It was estimated by the SD of the intercepts of the regression line in the calibration curve. S was the slope of the calibration curve. Table 3 lists the specific results.

3.4.3 Precision

The raw rhubarb solution was injected continuously six times based on the chromatographic conditions described in Section 2.2, with an injection volume of 10 μL. The repeatability of the analytical method was considered reliable according to the RSD (1.98 < 2%). The anthraquinone content in the raw rhubarb is listed in Table 4.

3.4.4 Robustness

The rhubarb sample solution was injected at 0, 2, 4, 8, 12, and 24 h after preparation. Table 5 lists the robustness of the contents. An RSD value of less than 2% indicated that the sample composition was not changed significantly within 24 h; therefore, the method was considered robust.

3.4.5 Accuracy

The accuracy of the method was verified by a recovery test. The recovery test was done by adding a standard solution to a known quantity of rhubarb sample. The assay was repeated six times. The recovery values of the nine components varied between 97.48 and 104.99% and the RSD values were between 0.50 and 1.76% (Table 6).

3.4.6 Analysis of anthraquinone components in different rhubarb samples

The SDR-9 samples were analyzed by HPLC. The amount of the anthraquinone components was calculated from the calibration curve of the standards. Table 7 lists the content of the nine components in the nine samples.

3.5 Taste analysis with an electronic tongue

For the electronic tongue analysis, artificial saliva (also called reference solution) was used as the standard output. The state of the artificial saliva tested using the electronic tongue simulates the state of saliva in humans. The tasteless point is the output value of the reference solution. The acid tasteless point of the reference solution (reference) is negative 13, whereas the salty tasteless point is negative 6. When the taste value of the sample is lower than that of the tasteless point, the sample does not have taste, and vice versa. The richness in Table 2 represents the aftertaste of umami and reflects the persistence of the freshness of the sample. A bitter aftertaste (aftertaste-B) reflects the residual degree of bitterness, whereas an astringent aftertaste (aftertaste-A) reflects the residual degree of astringency. The prominent taste characteristics of the rhubarb samples included bitterness, aftertaste-B, B-bitterness2, richness, umami, and aftertaste-A (Figure 5A). The other taste response values were close to or below the tasteless point, and the differences between samples were primarily reflected in richness. Of these, bitterness had the highest response value and contributed the most to the taste of the rhubarb samples.

Orthogonal partial least squares discriminant analysis was used to analyze the data obtained from the electronic tongue. The score plot of the OPLS-DA model is shown in Figure 5B, in which R^2X, R^2Y, and Q^2 were 0.956, 0.951, and 0.908, respectively. The values were all >0.5 and close to 1, indicating that the model had a high goodness-of-fit and prediction ability. The clustering results of SDR-6 and SDR-9 in the figure were close, indicating that their tastes were similar to one another. Rhubarb samples were distributed in different quadrants in Figure 5B, which was divided into two parts: SDR-1–5 and SDR-6–9. This indicates that their respective tastes are similar. The results were similar to those of the GC–IMS analysis. The variable influence on the projection (VIP) value chart (Figure 5C) reflects the contribution of the tastes to model classification, and VIP > 1 was considered the standard for screening the different tastes. Figure 5C shows that the tastes contributing mostly to the model classification were richness, bitterness, aftertaste-B, and sourness. In addition, the OPLS-DA model was verified using permutation tests (Figure 5D), which revealed that R^2 and Q^2 ($n = 200$) were 0.225 and -0.851, respectively, indicating no over-fitting phenomenon in the reliability of the model.

3.6 Correlation analysis between the taste of rhubarb samples and content of nine anthraquinone components

Pearson correlation analysis was conducted using SPSS software (R26.0.0.0, IBM, United States) and the resulting data were imported into OriginPro 2021 software (v.9.8.0, OriginLab, Northampton, MA, United States) to generate a heatmap (Figure 6). The flavors with a significant positive correlation with anthraquinones was richness, aftertaste-B, bitterness, sourness, and astringency, which is similar to

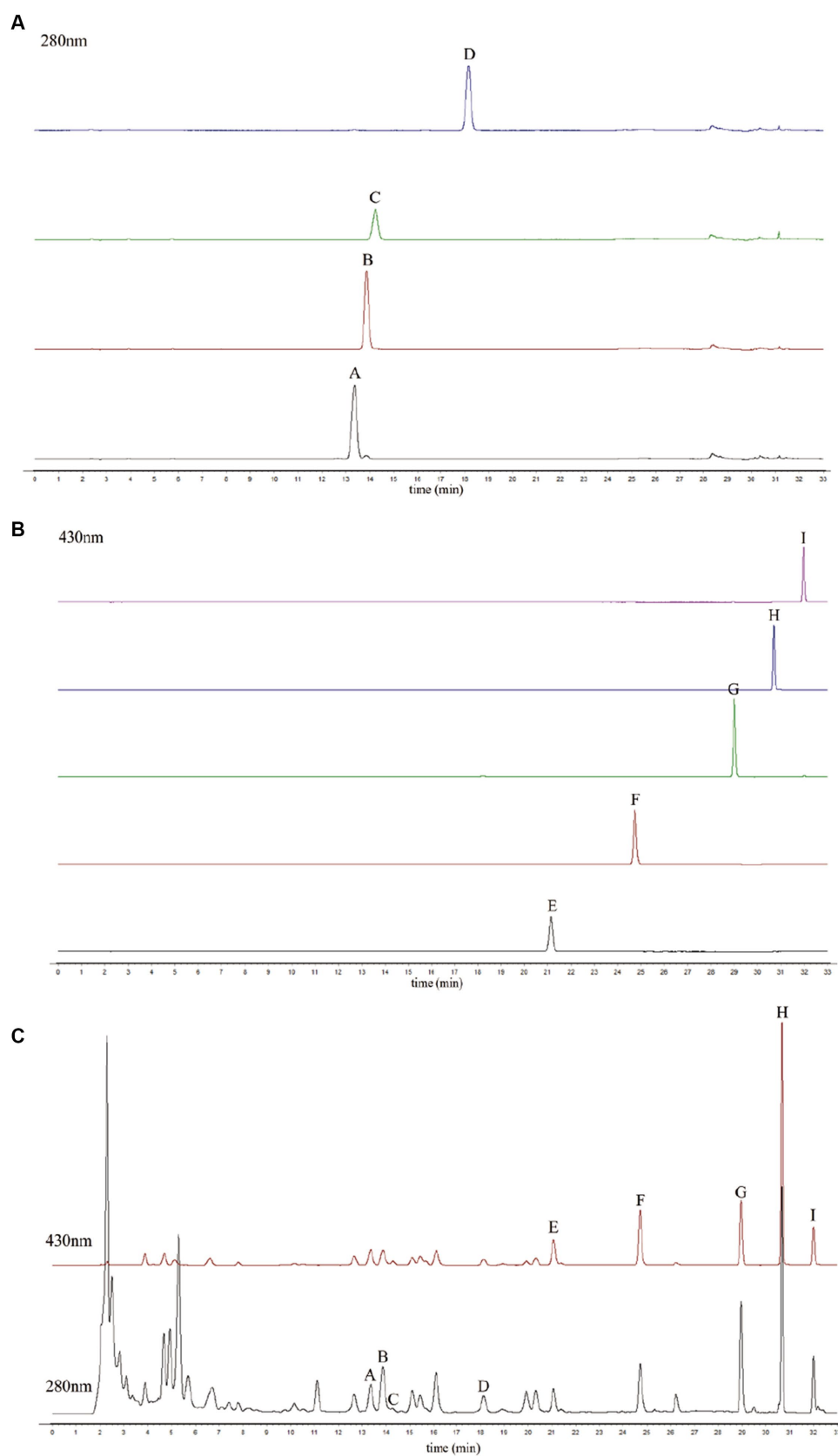FIGURE 4

High-performance liquid chromatography (HPLC) chromatogram of the standard components at 280 nm **(A)**, at 430 nm **(B)**, and the raw rhubarb samples **(C)**. (A) Chrysophanol-8-O-β-D-glucoside, (B) emodin-8-O-β-D-glucoside, (C) aloe-emodin-3-(hydroxymethyl)-O-β-D-glucoside, (D) physcion-8-O-β-D-glucoside, (E) aloe-emodin,(F) rhein, (G) emodin, (H) chrysophanol, and **(I)** physcion.

TABLE 3 Linearity, correlation coefficient (R2), limit of detection (LOD), and limit of quantification (LOQ) of the study compounds.

Components	Regression equation	R^2 ($n = 6$)	LOD (µg/mL)	LOQ (µg/mL)
Chrysophanol-8-O-β-D-glucoside	$Y = 1129835.5134\, x - 4143.8306$	0.9997	0.107	0.324
Emodin-8-O-β-D-glucoside	$Y = 1166589.5924\, x - 4843.5435$	0.9999	0.051	0.153
Aloe-emodin-3-(hydroxymethyl)-O-β-D-glucoside	$Y = 1566373.4619\, x - 1584.9194$	0.9999	0.014	0.043
Physcion-8-O-β-D-glucoside	$Y = 646464.1072\, x - 1080.1774$	0.9999	0.068	0.207
Aloe-emodin	$Y = 2655755.6048\, x - 3898.7532$	1.0000	0.032	0.098
Rhein	$Y = 2383813.2019\, x - 31300.4484$	0.9998	0.001	0.003
Emodin	$Y = 2411001.4165\, x - 108200.5661$	0.9995	0.069	0.208
Chrysophanol	$Y = 1263925.5673\, x - 25731.3339$	0.9992	0.059	0.180
Physcion	$Y = 1958043.5193\, x - 9490.6710$	0.9999	0.037	0.112

TABLE 4 Analytical results of the precision tests.

Components	Reference concentration (µg/mL)	Mean ± SD (%)	RSD (%)
Chrysophanol-8-O-β-D-glucoside	16.40	0.1304 ± 0.0007	0.52
Emodin-8-O-β-D-glucoside	20.10	0.1095 ± 0.0005	0.44
Aloe-emodin-3-(hydroxymethyl)-O-β-D-glucoside	9.70	0.0422 ± 0.0002	0.39
Physcion-8-O-β-D-glucoside	14.20	0.0449 ± 0.0006	1.24
Aloe-emodin	20.00	0.0707 ± 0.0013	1.90
Rhein	27.00	0.1419 ± 0.0028	1.98
Emodin	78.00	0.1681 ± 0.0028	1.65
Chrysophanol	34.40	0.3208 ± 0.0054	1.67
Physcion	22.20	0.1143 ± 0.0017	1.44

TABLE 5 Analytical results of the robustness of the method.

Components	Mean ± SD of peak area	RSD (%)
Chrysophanol-8-O-β-D-glucoside	586,544 ± 3,944	0.67
Emodin-8-O-β-D-glucoside	975,405 ± 3,021	0.31
Aloe-emodin-3-(hydroxymethyl)-O-β-D-glucoside	76,240 ± 568	0.75
Physcion-8-O-β-D-glucoside	376,999 ± 1,105	0.29
Aloe-emodin	429,562 ± 8,048	1.87
Rhein	760,992 ± 11,225	1.48
Emodin	712,528 ± 8,988	1.26
Chrysophanol	1,886,078 ± 29,245	1.55
Physcion	364,090 ± 5,181	1.42

the results of the VIP value chart. Umami and H-bitterness were negatively correlated with the anthraquinone glycoside components.

4 Conclusion

Flavor analysis includes odor determination using GC–IMS and taste characterization using an electronic tongue. During the odor analysis of SDR-9, 61 volatile compounds, including aldehydes, esters, alcohols, ketones, acids, alkenes, and furans, were identified. Among these, 13 volatile components were the predominant substances for

odor, which divided the process into two stages: 1–5 cycles of steaming and sun-drying and 6–9 times. In the second stage, SDR-6 and SDR-9 were grouped in terms of odor. The electronic tongue analysis revealed that the most prominent taste was bitterness. The OPLS-DA clustering results of SDR-6 and SDR-9 were close, indicating that their tastes are similar to one another. Moreover, anthraquinones were determined by HPLC and there was a significant correlation between taste and the components of the SDR samples. Based on the above results, there are similarities in smell, taste, and composition between SDR-6 and SDR-9; thus, the traditional process of steaming and sun-drying nine times can be reduced to six.

TABLE 6 Analytical results of the recovery of the method.

Components	Theoretical yield (mg)	Actual yield (mg)	Recovery (%)	RSD (%)
Chrysophanol-8-O-β-D-glucoside	0.6041	0.6023	99.37	1.25
	0.6030	0.6019	99.61	
	0.6056	0.5986	97.48	
	0.6036	0.6072	101.29	
	0.6008	0.5974	98.77	
	0.5991	0.5969	99.19	
Emodin-8-O-β-D-glucoside	0.4750	0.4839	104.44	0.71
	0.4752	0.4852	104.97	
	0.4756	0.4817	103.05	
	0.4751	0.4832	104.05	
	0.4752	0.4847	104.73	
	0.4753	0.4853	104.99	
Aloe-emodin-3-(hydroxymethyl)-O-β-D-glucoside	0.2021	0.2043	102.28	1.76
	0.202	0.2029	100.91	
	0.2019	0.2037	101.86	
	0.202	0.2017	99.67	
	0.2021	0.2038	101.71	
	0.2024	0.2001	97.59	
Physcion-8-O-β-D-glucoside	0.3075	0.3101	101.83	1.40
	0.3074	0.3126	103.63	
	0.308	0.3141	104.30	
	0.3074	0.3086	100.86	
	0.3081	0.3144	104.44	
	0.3076	0.3111	102.46	
Aloe-emodin	0.3624	0.3652	101.93	0.69
	0.363	0.3660	102.11	
	0.3627	0.3673	103.23	
	0.3622	0.3650	101.96	
	0.3628	0.3676	103.31	
	0.3624	0.3648	101.68	
Rhein	0.7172	0.7212	101.48	0.98
	0.7161	0.7201	101.47	
	0.717	0.7243	102.69	
	0.7161	0.7271	104.09	
	0.7179	0.7229	101.85	
	0.7176	0.7227	101.87	
Emodin	0.7063	0.7182	104.06	0.51
	0.7065	0.7184	104.07	
	0.7058	0.7189	104.49	
	0.7061	0.7194	104.53	
	0.7065	0.7164	103.37	
	0.7075	0.7172	103.31	
Chrysophanol	1.4813	1.4985	102.53	0.80
	1.4743	1.4994	103.70	
	1.4756	1.5003	103.63	
	1.4759	1.4957	102.91	
	1.4305	1.4611	104.82	
	1.4305	1.4568	104.14	

(Continued)

TABLE 6 (Continued)

Components	Theoretical yield (mg)	Actual yield (mg)	Recovery (%)	RSD (%)
Physcion	0.5074	0.5161	103.93	0.50
	0.5074	0.5146	103.24	
	0.5089	0.5146	102.56	
	0.5077	0.5142	102.93	
	0.5080	0.5141	102.77	
	0.5078	0.5135	102.59	

TABLE 7 Components of nine anthraquinone components in the SDR samples.

	Content (mg/g, %)								
	A	B	C	D	E	F	G	H	I
SDR-1	96.4±2.1	69.2±2.4	51.1±1.0	37.5±2.7	86.1±5.0	168.6±10.8	184.6±6.7	394.8±25.2	140.6±35.9
SDR-2	123.1±5.4	99.6±3.5	37.4±1.7	50.2±3.1	63.2±3.1	121.7±6.6	132.5±4.7	282.0±9.8	99.4±22.9
SDR-3	128.8±1.8	84.6±1.7	47.7±1.5	51.7±2.8	67.3±3.4	131.6±5.2	142.9±5.3	295.0±10.8	127.8±21.7
SDR-4	113.0±8.0	74.4±5.2	39.7±3.6	46.0±4.7	65.9±5.7	111.6±18.8	136.6±10.0	267.2±17.0	115.1±23.7
SDR-5	90.8±4.3	56.5±2.5	38.8±1.7	37.3±2.2	62.2±2.6	107.3±6.8	125.5±2.2	294.5±10.7	122.4±21.0
SDR-6	96.2±1.0	58.6±1.0	36.4±1.2	35.1±1.6	55.7±1.5	107.7±1.2	121.0±2.5	241.7±5.6	97.7±15.8
SDR-7	69.4±8.3	53.7±6.2	33.5±3.9	29.3±2.3	54.9±5.8	102.2±12.4	119.4±13.0	231.1±20.3	97.6±7.3
SDR-8	61.6±7.8	39.6±4.8	32.0±3.7	25.4±2.5	56.2±5.7	100.4±12.7	119.5±12.5	231.5±19.3	103.1±12.3
SDR-9	71.1±7.9	39.9±4.4	33.5±3.7	28.6±3.1	56.9±5.0	94.8±10.5	112.5±10.5	246.5±17.5	104.3±20.2
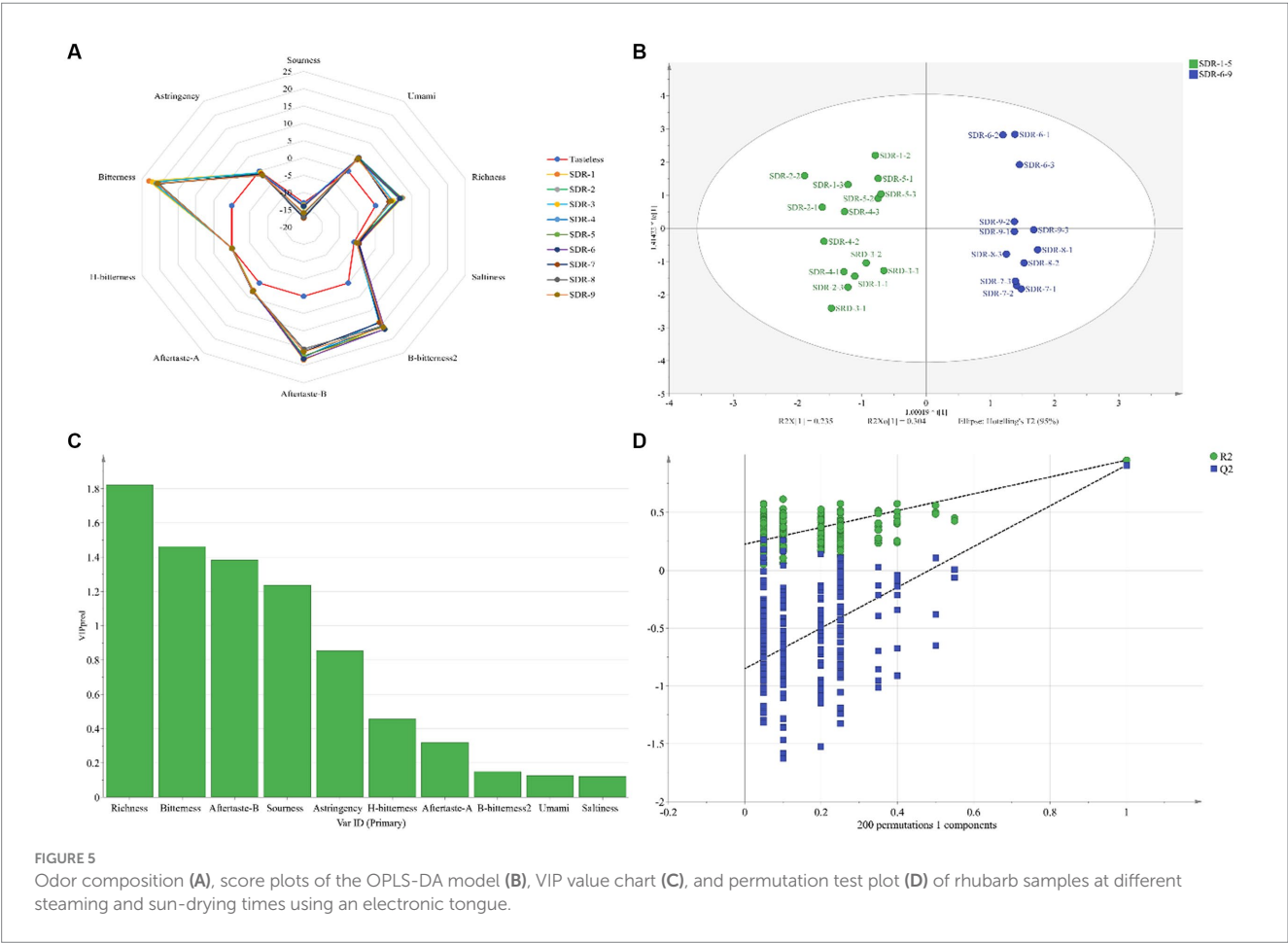
FIGURE 5
Odor composition (A), score plots of the OPLS-DA model (B), VIP value chart (C), and permutation test plot (D) of rhubarb samples at different steaming and sun-drying times using an electronic tongue.
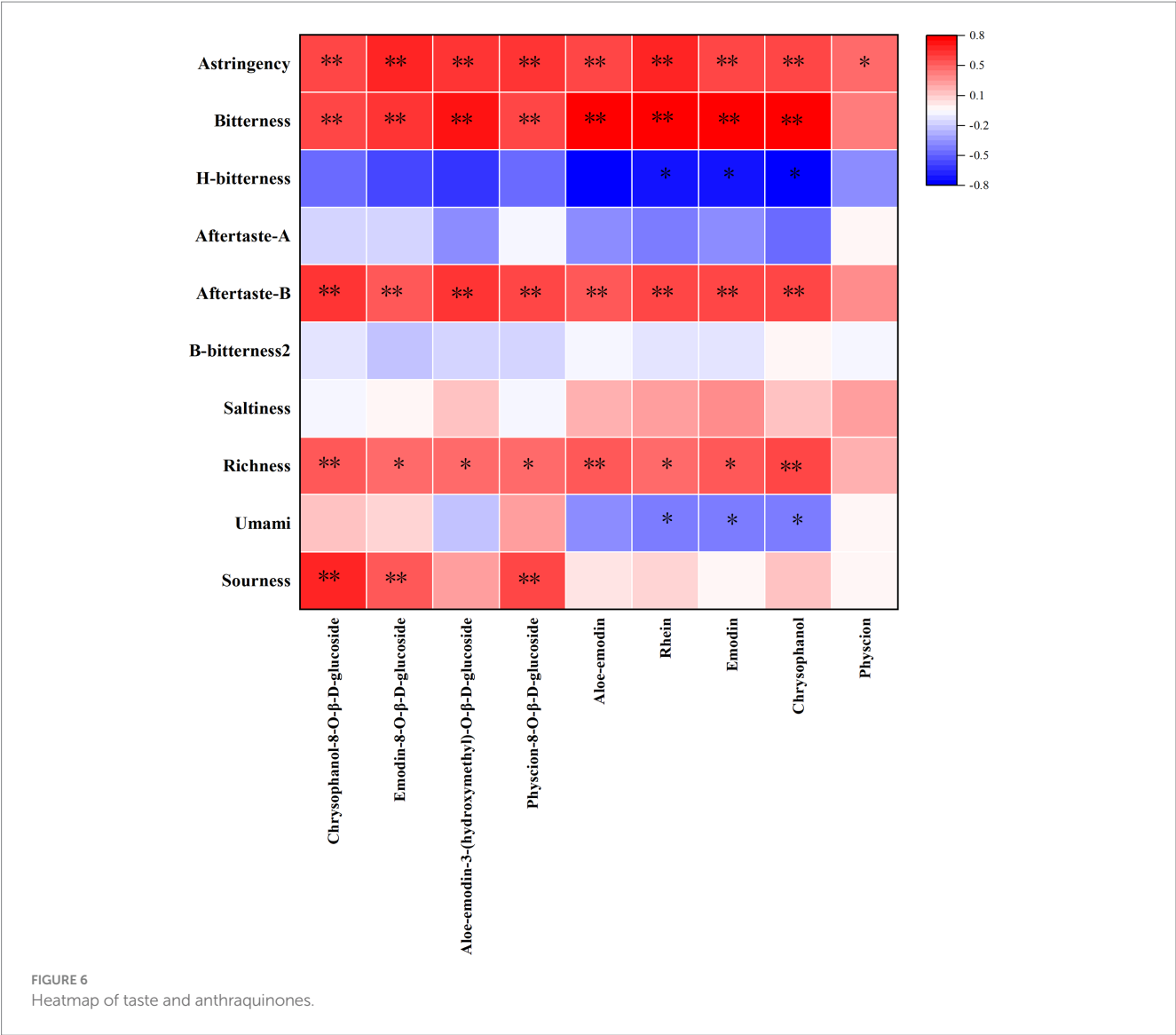
FIGURE 6
Heatmap of taste and anthraquinones.

Data availability statement

The original contributions presented in the study are included in the article; further inquiries can be directed to the corresponding author.

Ethics statement

The animal study was approved by Experimental Animal Ethics Committee, Institute of Traditional Chinese Medicine, Chinese Academy of Traditional Chinese Medicine; Approval number 2023B109. The study was conducted in accordance with the local legislation and institutional requirements.

Author contributions

TL: Data curation, Writing – original draft, Writing – review & editing. MY: Data curation, Formal analysis, Methodology, Writing – review & editing. YD: Conceptualization, Validation, Writing – review & editing. YX: Project administration, Supervision, Writing – review

& editing. LL: Writing – review & editing, Data curation, Funding acquisition, Resources, Software.

Funding

Conflict of interest

TL was employed by Chongqing Taiji Industry (Group) Co., Ltd.

The remaining authors declare that the research was conducted in the absence of any commercial or financial relationships that could be construed as a potential conflict of interest.

Publisher's note

All claims expressed in this article are solely those of the authors and do not necessarily represent those of their affiliated organizations, or those of the publisher, the editors and the reviewers. Any product that may be evaluated in this article, or claim that may be made by its manufacturer, is not guaranteed or endorsed by the publisher.

References

1. Huang Q, Lu G, Shen HM, Chung MCM, Ong CN. Anti-cancer properties of anthraquinones from rhubarb. *Med Res Rev*. (2007) 27:609–30. doi: 10.1002/med.20094

2. Cao YJ, Pu ZJ, Tang YP, Shen J, Chen YY, Kang A, et al. Advances in bio-active constituents, pharmacology and clinical applications of rhubarb. *Chin Med*. (2017) 12:36. doi: 10.1186/s13020-017-0158-5

3. Liudvytska O, Kolodziejczyk-Czepas J. A review on rhubarb-derived substances as modulators of cardiovascular risk factors—a special emphasis on anti-obesity action. *Nutrients*. (2022) 14:2053. doi: 10.3390/nu14102053

4. Zhang Y, Fan S, Hu N, Gu M, Chu C, Li Y, et al. Rhein reduces fat weight in db/db mouse and prevents diet-induced obesity in C57BL/6 mouse through the inhibition of PPAR γ signaling. *PPAR Res*. (2012) 2012:1–9. doi: 10.1155/2012/374936

5. Shi Y, Zhong Y, Sun A, Gao B, Sun C, Xiong J. Validation of a rapid and simple high-performance liquid chromatography-electrospray ionization-mass spectrometry method for simultaneous analysis of 15 key chemicals in slimming foods and herbal products. *J Chromatogr Sci*. (2018) 56:912–9. doi: 10.1093/chromsci/bmy068

6. Yang L, Yang L, Pei W, Dong L, Chen J. Color-reflected chemical regulations of the scorched rhubarb (Rhei Radix et rhizoma) revealed by the integration analysis of visible spectrophotometry, Fourier transform infrared spectroscopy and high performance liquid chromatography. *Food Chem*. (2022) 367:130730. doi: 10.1016/j.foodchem.2021.130730

7. Wang JB, Qin Y, Kong WJ, Wang ZW, Zeng LN, Fang F, et al. Identification of the antidiarrhoeal components in official rhubarb using liquid chromatography–tandem mass spectrometry. *Food Chem*. (2011) 129:1737–43. doi: 10.1016/j.foodchem.2011.06.041

8. Zhuang T, Gu X, Zhou N, Ding L, Yang L, Zhou M. Hepatoprotection and hepatotoxicity of Chinese herb rhubarb (Dahuang): how to properly control the 'general (Jiang Jun)' in Chinese medical herb. *Biomed Pharmacother*. (2020) 127:110224. doi: 10.1016/j.biopha.2020.110224

9. Zhao L, Hu CJ, Pan X, Geng YY, Cheng ZM, Xiong R. Comparative study on influences of long-term use of raw rhubarb and stewed rhubarb on functions of liver and kidney in rats. *Chin J Hosp Pharm*. (2015) 35:1384–7. doi: 10.13286/j.cnki.chinhosppharmacyj.2015.15.11

10. Zhang Q, Chen YY, Yue SJ, Wang WX, Zhang L, Tang YP. Research progress on processing history evolution as well as effect on chemical compositions and traditional pharmacological effects of Rhei Radix et Rhizoma. *Zhongguo Zhong Yao Za Zhi*. (2021) 46:539–51. doi: 10.19540/j.cnki.cjcmm.20201105.601

11. Liu Y, Li L, Xiao YQ, Yao JQ, Li PY, Yu DR, et al. Global metabolite profiling and diagnostic ion filtering strategy by LC–QTOF ms for rapid identification of raw and processed pieces of *Rheum palmatum* L. *Food Chem*. (2016) 192:531–40. doi: 10.1016/j.foodchem.2015.07.013

12. Teng SS, Sun Z, Qiu Y, Yuan B, Wang N. Investigation, optimization and evaluation of the traditional processing technology of nine-time repeatedly steaming and sun-drying. *J Changchun Univ Chin Med*. (2022) 38:109–13. doi: 10.13463/j.cnki.cczyy.2022.01.026

13. Xie YN, Shen SH, Chen GY, Xie MZ, Qu HY, He Q. Research on taste masking of five-juice decoction based on technology combined intelligent sensory evaluation of electronic-tongue with artificial sensory evaluation. *Chin J Mod Appl Pharm*. (2022) 39:772–6. doi: 10.13748/j.cnki.issn1007-7693.2022.06.009

14. Yin X, Lv Y, Wen R, Wang Y, Chen Q, Kong B. Characterization of selected Harbin red sausages on the basis of their flavour profiles using HS-SPME-GC/MS combined with electronic nose and electronic tongue. *Meat Sci*. (2021) 172:108345. doi: 10.1016/j.meatsci.2020.108345

15. Immohr LI, Hedfeld C, Lang A, Pein-Hackelbusch M. Suitability of E-tongue sensors to assess taste-masking of pediatric liquids by different beverages considering their physico-chemical properties. *AAPS PharmSciTech*. (2017) 18:330–40. doi: 10.1208/s12249-016-0526-y

16. Xu M, Wang J, Zhu L. The qualitative and quantitative assessment of tea quality based on E-nose, E-tongue and E-eye combined with chemometrics. *Food Chem*. (2019) 289:482–9. doi: 10.1016/j.foodchem.2019.03.080

17. Rodriguez-Mendez ML, Apetrei C, Gay M, Medina-Plaza C, De Saja JA, Vidal S, et al. Evaluation of oxygen exposure levels and polyphenolic content of red wines using an electronic panel formed by an electronic nose and an electronic tongue. *Food Chem*. (2014) 155:91–7. doi: 10.1016/j.foodchem.2014.01.021

18. Facure MH, Schneider R, Dos Santos DM, Correa DS. Impedimetric electronic tongue based on molybdenum disulfide and graphene oxide for monitoring antibiotics in liquid media. *Talanta*. (2020) 217:121039. doi: 10.1016/j.talanta.2020.121039

19. Duan Z, Dong S, Dong Y, Gao Q. Geographical origin identification of two salmonid species via flavor compound analysis using headspace-gas chromatography-ion mobility spectrometry combined with electronic nose and tongue. *Food Res Int*. (2021) 145:110385. doi: 10.1016/j.foodres.2021.110385

20. Wang S, Chen H, Sun B. Recent progress in food flavor analysis using gas chromatography–ion mobility spectrometry (GC–IMS). *Food Chem*. (2020) 315:126158. doi: 10.1016/j.foodchem.2019.126158

21. Huang Q, Dong K, Wang Q, Huang X, Wang G, An F, et al. Changes in volatile flavor of yak meat during oxidation based on multi-omics. *Food Chem*. (2022) 371:131103. doi: 10.1016/j.foodchem.2021.131103

22. He J, Ye L, Li J, Huang W, Huo Y, Gao J, et al. Identification of ophiopogonis radix from different producing areas by headspace-gas chromatography-ion mobility spectrometry analysis. *J Food Biochem*. (2022) 46:e13850. doi: 10.1111/jfbc.13850

23. Lv W, Lin T, Ren Z, Jiang Y, Zhang J, Bi F, et al. Rapid discrimination of *citrus reticulata* 'chachi' by headspace-gas chromatography-ion mobility spectrometry fingerprints combined with principal component analysis. *Food Res Int*. (2020) 131:108985. doi: 10.1016/j.foodres.2020.108985

24. Garrido-Delgado R, Arce L, Guamán AV, Pardo A, Marco S, Valcárcel M. Direct coupling of a gas–liquid separator to an ion mobility spectrometer for the classification of different white wines using chemometrics tools. *Talanta*. (2011) 84:471–9. doi: 10.1016/j.talanta.2011.01.044

25. Yang BB, Rong R, Lyu QT, Jiang HQ, Gong LL, Yang Y. Analysis of the volatile components in rhubarb with different extraction methods by GC-MS. *Chem Anal Meter*. (2013) 22:14–6. doi: 10.3969/j.issn.1008–6145.2013.06.004

26. Li DH, Wu HW, Yang XR, Li GF, Li XW, Song QJ, et al. Study on the browning mechanism of fresh rhubarb during processing. *Lishizhen Med Mater Med Res*. (2022) 33:1127–31.

Characterization of flavor profile of Steamed beef with rice flour using gas chromatography-ion mobility spectrometry combined with intelligent sensory (Electronic nose and tongue)

Tianyang Wang[1,2], Lian Yang[1], Yiling Xiong[1,2], Baozhu Wu[1,2], Yang Liu[1], Mingfeng Qiao[1], Chenglin Zhu[3], Huachang Wu[1,2], Jing Deng[1,2]* and Ju Guan[1]*

[1]Cuisine Science Key Laboratory of Sichuan Province, Sichuan Tourism University, Chengdu, Sichuan, China, [2]College of Food and Biological Engineering, Chengdu University, Chengdu, Sichuan, China, [3]College of Food Science and Technology, Southwest Minzu University, Chengdu, Sichuan, China

The intelligent senses (Electronic nose and tongue), were combined with headspace gas chromatography-ion mobility spectrometry (HS-GC-IMS) and free amino acid were used in combination to determine the aroma and taste components during the processing of Chinese traditional dish Steamed beef with rice flour (SBD). The findings revealed that E-nose and E-tongue, could clearly distinguish and identify the aroma and taste of SBD. A total of 66 volatile substances and 19 free amino acids were identified by HS-GC-IMS and amino acid analyzer, respectively. The highest contribution to aroma in the production of SBD was alcohols, esters and aldehydes. Further analysis of relative odor activity showed that 3-Methylbutanol-D, 3-Methylbutanol-M and 3-Methylthio propanal is the marinating stage (T2) main aroma components. Ethyl 3-methylbutanoate-M and Ethyl 3-methylbutanoate-D were the main aroma components in the seasoning stage (T3). Additionally, the calculation of the taste activity value showed that Glutamic contributed significantly to the umami of SBD. Alanine was a representative taste component in the marinating stage (T2), while Proline, Aspartic, Lysine, Glutamic, Valine, Arginine, and Histidine were characteristic amino acids of the seasoning stage (T3). Consequently, this study offers valuable insights into the industrial-scale production and flavor regulation of SBD products.

KEYWORDS

Steamed beef with rice flour, intelligent senses, GC-IMS, free amino acid, chemometrics

1 Introduction

With the rapid pace of modern life, the demand for prepared dishes in the food market has been growing steadily (1, 2). The production of classic folk dishes using industrial technology is an important way to develop newly prepared dishes and improve production efficiency. However, there is no specific standard for the aroma characteristics of folk classic

dishes, which mainly depends on the chef's experience, and it is challenging to maintain the uniqueness of the aroma characteristics of the dishes in industrial production (3, 4). Therefore, exploring the characteristic flavor of classic dishes, which can provide a specific, quantifiable description of the flavor, is a necessary means of standard industrial production (5, 6).

Steamed beef with rice flour dish (SBD) is a classic dish of Sichuan cuisine, the first of China's eight major cuisines, and its origins can be traced back to the Qing Guangxu Dynasty (1862 AD). The unique and complicated process involved in the production of SBD is the result of a long history. The recipe for this dish includes beef and cooked rice flour, which, together with its specific cooking methods, endow SBD with its superb flavor and taste. Its critical processing consists of two main stages: marinating and steaming (Figure 1). In particular, adding rice flour makes the beef taste even smoother and adds layers of texture to the meat. On the other hand, SBD has long been well-known by many domestic consumers and is widely recognized in overseas Chinese communities and internationally. However, there are no studies on the characteristics and changes of aroma formation and taste characteristics of SBD during the cooking process. This limitation hinders the effective monitoring and further improvement of the industrialized SBD product quality.

Food flavor is one of the most essential characteristics of overall palatability and quality and is an important driver of consumer preference (7). In addition to the complexity of the dish's make a profile, dishes' aroma and taste profiles could not be obtained by a single assay (4). Together, GC-IMS, E-nose, and E-tongue were applied effectively to analyze the aroma and taste substances of food matrices such as meat products, aquatic products, tea, and fruit wine (8–11). Compared to gas chromatography-mass spectrometer (GC–MS), gas chromatography-ion mobility spectrometry (GC-IMS) can provide a more intuitive representation of the characteristics and differences in volatile compounds among samples (12). Meanwhile, HS-GC-IMS can directly detect SBD through headspace vials without the need for enrichment and concentration, greatly enhancing the efficiency of detecting aroma components in SBD. To date, the use of intelligent sensory techniques in combination with advanced instrumentation for the study of flavor profiles of food products has become a meaningful way to produce classic folk dishes by industrial means and to develop new pre-prepared dishes and food products

(13). It provides more comprehensive, robust, and objective scientific information (14). Previous studies have successfully used intelligent sensory techniques to explore the flavor characteristics of classic folk dishes during the cooking process, such as Dongpo pork, Tomato sour soup beef, and Dezhou braised chicken (5, 8, 15).

This study investigated the labeling and formation of characteristic aroma and taste substances in the SBD during processing using intelligent sensory combined with HS-GC-IMS and amino acid analysis techniques and combined relative odor activity value (ROAV) and taste activity value (TAV) calculations. This study will help provide data on the formation of aroma and flavor at different stages of the production process of this classic dish and provide a theoretical basis for the industrial production and development of SBD.

2 Materials and methods

2.1 SBD cooking model and sample preparation

The SBD cooking model of this study was prepared according to the local standard "Technical Specification for Chinese Sichuan classic dishes (DB51/T 1728-2014)." According to the request, the fresh tenderloin from the adult yellow beef is selected for preparation (Food Technology Company, Chengdu, China). Fresh raw beef (T1) was first cut into slices (10×1×5 cm) and marinated with ginger, cooking wine and salt for 10 min (T2). Then add cooked rice noodles, Pixian pea sauce (JuanCheng, Chengdu, China) and condiments for seasoning (T3) in a steam pot for 20 min (T4), 40 min (T5), and 60 min (T6). This cooking model was repeated three times (Figure 1).

2.2 E-nose analysis

The electronic nose (FOX 4000, A MOS, France) is equipped with 18 sensor chambers that can identify classes of volatile compounds. The sensor's performance in recognizing aromas is shown as follows: PA/2, P30/1, P30/2, TA/2, and LY2/AA were sensitive to organic compounds, LY2/LG, P40/1, P40/2, T40/2 and T40/1 were sensitive to gases with high oxidizing power, LY2/G and LY2/gCTI were
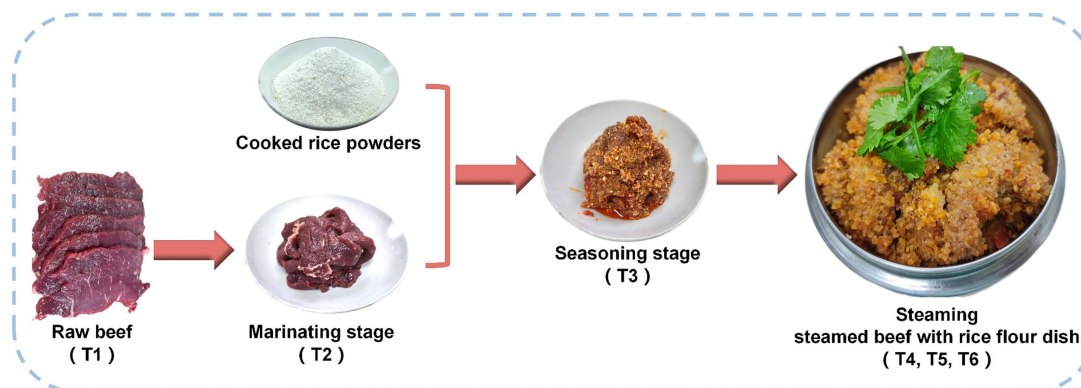

FIGURE 1
Schematic diagram of the different processing of Steamed beef with rice flour dish (SBD).

sensitive to amines; LY2/Gh is selective for anilines, LY2/gCT is sensitive to alkanes and aromatic components, T30/1 is sensitive to polar compounds, P10/1 is sensitive to non-polar compounds; P10/2 is sensitive to alkanes, T70/2 is sensitive to aromatic compounds (16, 17).

Accurately weighed 2 g of crushed sample, capped with polyethene sealing cap membrane and placed into a 10 mL headspace vial for electronic nose, and incubated and equilibrated for 5 min at an incubation temperature of 40°C before injecting 1.5 mL of headspace vials into the detector of the electronic nose via a manual injection. A sample was measured 10 times, and data from 5 of these stable measurements were recorded for multivariate analysis (18).

2.3 E-tongue analysis

All samples were analyzed by an α-Astree electronic tongue (Alpha MOS, France) equipped with seven potentiometric sensors and an automatic sampler (19). The sensors were specifically sensitive to sweetness (ANS), saltiness (CTS), umami (NMS), sourness (AHS), bitterness (SCS) and two reference electrodes (PKS and CPS), respectively (20).

The crushed samples were diluted at a ratio of 1:10, followed by the addition of pure water for ultrasonic extraction lasting 10 min. Subsequently, the mixture was filtered. 80 mL of the sample was transferred into a 150 mL specific electronic tongue beaker for analysis. The signal acquisition time, stirring rate, and analysis duration were established at 120 s, 60 revolutions per min, and 3 min, correspondingly. Additionally, the metal probe attached to the sensor underwent thorough cleaning with deionized water for 1 min following each analysis prior to measurement. Response values were gathered within the time frame of 100–120 s based on the recommendations provided by Zhang et al. (11). The mean value of each sample served as the foundational data for robust principal component analysis (rPCA) in multivariate research.

2.4 HS-GC-IMS analysis

The HS-GC-IMS analysis was performed following the method of Wu et al. (17). The VOCs of SBD samples were characterized through a HS-GC-IMS system (Flavorspec®, G.A.S. Instrument, Munich, Germany) with a MXT-WAX capillary column (30 m × 0.53 mm × 1 μm) (Restek, Mount Ayr, United States). The crushed SBD sample, weighing precisely 2 g, was transferred to a 20 mL headspace vial equipped with a magnetic screw seal cover. Subsequently, the vial was incubated at 60°C for a duration of 10 min. An automated injection system injected exactly 1.5 mL of the headspace sample into the injector (without employing split mode), utilizing a heated syringe maintained at a temperature of 85°C. Drift gas flow rate was set at 150 mL/min. A high-purity N2 (99.99% purity) was utilized, and the GC column flow rate was programmed as follows: 2 mL/min for 5 min, 10 mL/min for 10 min, 15 mL/min for 5 min, 50 mL/min for 10 min, and 100 mL/min for 10 min. As reported in previous studies, it was determined that the retention index (RI) of volatile compounds was calculated using n-ketone C4–C9 as an external reference, compounds were identified by comparing the RI and ion drift time of the volatile compounds to the retention indices

and drift times of the standards in the HS-GC-IMS library (8, 11). Additionally, GC-IMS allowed for the accurate detection and identification of some volatile monomers and dimers, which was impossible with GC–MS (21).

2.5 Free amino acid analysis (FAAs)

The determination of free amino acid levels in the SBD sample was carried out according to the method with slight adjustments as outlined by Xu et al. (22). The SBD sample weighing 3 g was accurately mixed with a measure of 20 mL sulfosalicylic acid (7 g/100 mL). The mixture was subjected to extraction for 30 min under ultrasonic vibration (KQ-300VDV, Kunshan Instrument, China) and subsequently centrifuged at 10,000×g for 15 min using the centrifuge (CR21N, Hitachi Koki Co., Ltd., Ibaraki, Japan). The supernatant was collected and later using a 0.22 μm filtered membrane. The determination of free amino acids was performed utilizing an Amino Acid Automatic (S-433D, SYKAM, Germany) Analyzer, Separation by sulfonic acid based strongly acidic cation exchange resin column (LCA K07/Li 150 mm × 4.6 mm), with identification and quantification achieved by comparing the retention times and peak areas of individual amino acid standards (Sigma-Aldrich, St. Louis, MO, USA) (23).

2.6 Relative odor activity value (ROAV)

The food contains numerous volatile organic compounds, but only a few significantly contribute to its flavor. These specific compounds, known as significant flavor compounds, are considered crucial for determining the overall flavor of the food (ROAV) (24). Based on the peak intensity characterization of HS-GC-IMS, the threshold value for each aroma compound in the sample was determined by referring to Xu et al.'s research methodology (25). Then, the relative odor activity value (ROAV) of each aroma compound was calculated as follows:

$$\text{ROAV} = 100 \times \frac{C_i}{C_{\max}} \times \frac{T_{\max}}{T_i}$$

In the formula, C_i is the relative content of the aroma compound in samples (%); T_i is the aroma threshold of the compound in food (μg/kg), $C_{\max}$ and $T_{\max}$ represent the relative content and aroma threshold of the compound that contributes the most to the overall flavor of the sample. For all compounds, ROAV ≤ 100, A higher ROAV value indicates a more significant contribution of the component to the overall flavor profile of the model (26, 27).

2.7 Taste activity value (TAV)

The TAV has emerged as a widely accepted and effective method for evaluating taste in recent years (22). It involves calculating the ratio between the concentration of a taste substance and its taste threshold, allowing us to determine the contribution of compounds with free amino acid taste characteristics to the overall taste perception (28). TAV is calculated as follows:
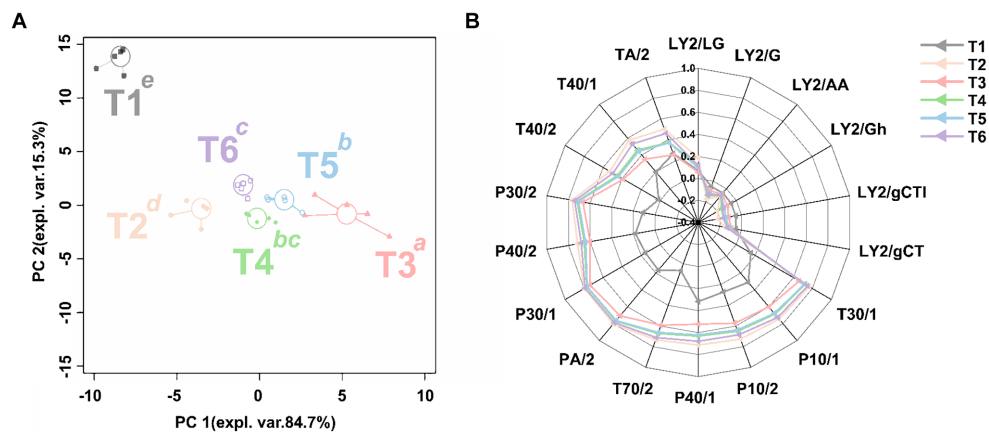
FIGURE 2
The rPCA model based on the response value of E-nose sensor. The score plot **(A)** illustrates the overall trend of the samples. Lowercase superscript letters indicate significant differences ($p < 0.05$) between samples on PC1. The radar chart **(B)** illustrates the response value of the sensor on PC1.

$$TAV = \frac{w_1}{w_2}$$

In the formula, w_1 is the compound content in the sample/ (mg/100 g), and w_2 is the compound/(mg/100 g) taste threshold. A $TAV \geq 1$ for an amino acid indicates that it is a significant contributor to the overall taste experience, while an amino acid with $0.1 \leq TAV \leq 1$ is considered to have an essential modifying effect on taste (13).

2.8 Statistical analysis

The statistical analysis was performed using the R language. Before conducting univariate analyses, the data distribution was transformed by the Box and Cox method to achieve normality (29). ANOVA was performed to find significant differences in the E-nose and E-tongue sensor's response to aroma and taste from different groups, respectively, followed by the Tukey HSD post-hoc test ($p < 0.05$) (30). For each rPCA model, we computed a score plot and a Pearson correlation plot based on the loadings (31). The three-dimensional (3D) topographic plots, two-dimensional (2D) difference plots, and gallery plots were generated using the Laboratory Analytical Viewer, Reporter and Gallery Plot provided by the HS-GC-IMS instrument. Using online tools.[1] Through making a heat map to determine the vital components of the SBD.

3 Results

3.1 Intelligent senses analysis of Steamed beef with rice flour

3.1.1 E-nose analysis of SBD

In this study, the rPCA model is established to describe the aroma characteristics of the SBD. The proportion of PC 1 in the entire model,

as depicted in Figure 2A, amounts to 84.7%, exhibiting significant variations among samples at different stages ($p < 0.05$). Based on the intensity of the 18 sensors' responses to a specific characteristic gas, the main characteristic gas in each stage was tentatively speculated. As shown in Figure 2B, the response of each sensor was lower in the raw meat sample (T1), while the organic compounds (PA/2, P30/1, P30/2) and gases with high oxidizing power (P40/1, P40/2, T40/2, T40/1), polar compounds (T30/1); non-polar compounds (P10/1), alkanes (P10/2), aromatic compounds (T70/2) increased during the seasoning stage (T3). In contrast, gases with high oxidizing power (T40/1, T40/2, LY2/LG) and while the organic compounds were the main contributors in the steaming stage (T2), followed by organic compounds (TA/2). Furthermore, as the steaming process progresses, the sensor response values of the electronic nose gradually increase, reaching their highest point at the end of the steaming process (T6). Steaming for 20 min (T4) and 40 min (T5) resulted in the predominant gases being organic compounds, high oxidizing power gases, aromatic compounds, and alkanes (TA/2, T40/1, T40/2, P40/1, P40/2, T70/2, P10/1, P10/2), with these compounds peaking at the end of the steaming process (T6). These results indicate that the odor of SBD underwent significant changes during the marinating, seasoning stage, and steaming process.

3.1.2 E-tongue analysis of SBD

To gain a comprehensive understanding of the taste characteristics of SBD during the production process, an rPCA model was established based on the response values obtained from the seven sensors of the electronic tongue, as illustrated in Figure 3. PC1 accounts for 73.2% of the sample, better summarizing the sample differences. Based on the intensity of the seven sensors' responses to a specific characteristic, the main taste characteristics in each stage was tentatively speculated. As shown in Figure 3A, the electronic tongue sensor response values of samples at different stages in the SBD have significant differences on PC1 ($p < 0.05$). As shown in Figure 3B, in the raw meat sample (T1), the response value of each sensor was low, but with the progress of cooking, the response value of the electronic tongue sensor increases. After removing the reference electrode (CPS, PKS), the bitter, sweet, umami, and salty sensors (SCS, ANS, CTS) become the
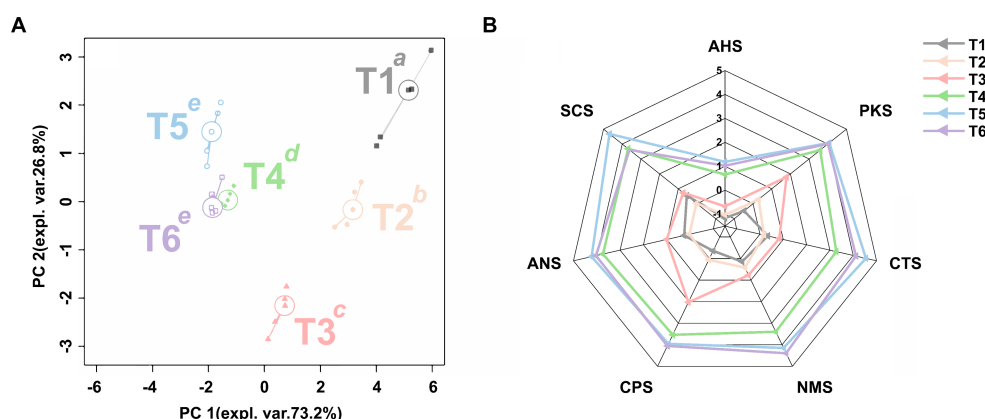
---

1 https://www.omicstudio.cn

FIGURE 3
The rPCA model based on the response value of electronic tongue sensor. The score plot **(A)** illustrates the overall trend of the samples. Lowercase superscript letters indicate significant differences ($p < 0.05$) between samples on PC1. The radar chart **(B)** illustrates the response value of the sensor on PC1.

main feature during the marinating stage (T2). And the electronic tongue sensor responses further increase during the seasoning stage (T3). It is worth noting that at 20 min (T4), into the steaming process, all the taste components began to gradually increase, and at 40 min (T5) into the steaming process, the bitterness (SCS) and saltiness (CTS) of SBD were the most intense. Then, at the end of cooking (T6), the umami (NMS) is the most intense in the SBD.

3.2 Volatile compounds were analyzed by HS-GC-IMS

3.2.1 HS-GC-IMS topographic map of SBD

The processing's pipeline of HS-GC-IMS information on the VOCs in the SBD by during the stages is summarized in Figure 4. The 3D topographic map conveniently and intuitively shows the difference of GC-IMS spectrum of SBD in the production process (Figure 4A). In the SBD, the levels of VOCs in stages T2–T6 were significantly elevated compared to the control group T1. To visually highlight the variations in VOCs among the samples, choosing the difference map illustrates 2D representation (Figure 4B) for comparison. Specifically, compared with T1, the red area in the SBD after processing has increased, among which T4–T6 have a similar red area. The peak intensity of VOCs was the highest when SBD was produced in the T3 stage. In the gallery plot (Figure 4C), it can be seen that VOCs in SBD samples at different processing stages mainly include esters and alcohols. VOCs of the SBD were qualitatively analyzed according to gas chromatography retention time and ion migration time, and the results were shown in Table 1, 66 volatile organic compounds (mono-polymers and di-polymers) were characterized in the six samples, including esters (15), alcohols (14), olefins (9), aldehydes (8), ketones (7), heterocyclic (7), acids (2), and others (4).

3.2.2 Types of volatile compounds in SBD

In order to clearly show the differences of VOCs categories in the process of SBD, the peak intensity of the qualitative compounds was normalized to obtain a 3D histogram of relative proportion (Figure 5). The SBD VOCs consist of alcohols, esters, aldehydes, heterocyclics,

ketones, acids, alkenes and other compounds. In the process of SBD processing, the VOCs with a large change in peak intensity are alcohols, esters and aldehydes. The peak of alcohols in the marinating stage (T2) was 39.09%, significantly higher than that in the control group (T1) (13.56%). However, the content of alcohols was only 30.74% at the end of steaming (T6). Compared with the control group, the peak intensity of esters in the marinating stage (T2) increased to 23.05%, and the peak intensity in the seasoning stage (T3) reached the highest, which was 26.42%, but in the subsequent steaming, it gradually decreased to 24.37%. The content of aldehydes gradually increased from the marinating stage (T2), and reached the highest value of 16.43% at the end of steaming.

3.3 ROAV calculations for volatile compounds in SBD

In this study, a total of 11 key aroma compounds, were successfully identified (Table 2) including 3-Methylbutanol-D, 3-Methylbutanol-M, Butyraldehyde, 3-Methylthio propanal, Nonanal-M, Nonanal-D, Ethyl hexanoate-M, Ethyl 3-methylbutanoate-M, Ethyl 3-methylbutanoate-D, Methyl butyrate and 2-Pentylfuran were successfully identified. To highlight the overall trend of VOCs above, an rPCA model and class heat map were built based on their peak intensity, as shown in Figure 6. In the rPCA model, PC1 accounted for 87% of the variation across the sample set, summarizing the differences between the groups (Figure 6A). In the SBD, the VOCs of the control group (T1) and steam for 60 min (T6) had the most significant difference. The content of 3-Methylbutanol-M, Methyl butyrate, Ethyl hexanoate-M and 3-Methylbutanol-D in T1 are the highest. In contrast, 3-Methylthio propanal, Ethyl 3-methyl butanoate-M, Butyraldehyde, 2-Pentylfuran, Nonanal-D, Nonanal-M and Ethyl 3-methyl butanoate-D were detected in T6 group (Figure 6B). Heat map analysis further shows that the peak intensity of esters of compounds with key aroma compounds in SBD samples was the highest, followed by alcohols and aldehydes (Figure 6C). Moreover, the peak intensity of aldehyde compounds Nonanal-M and Nonanal-D in raw meat (T1) was higher, the peak intensity of alcohol compounds
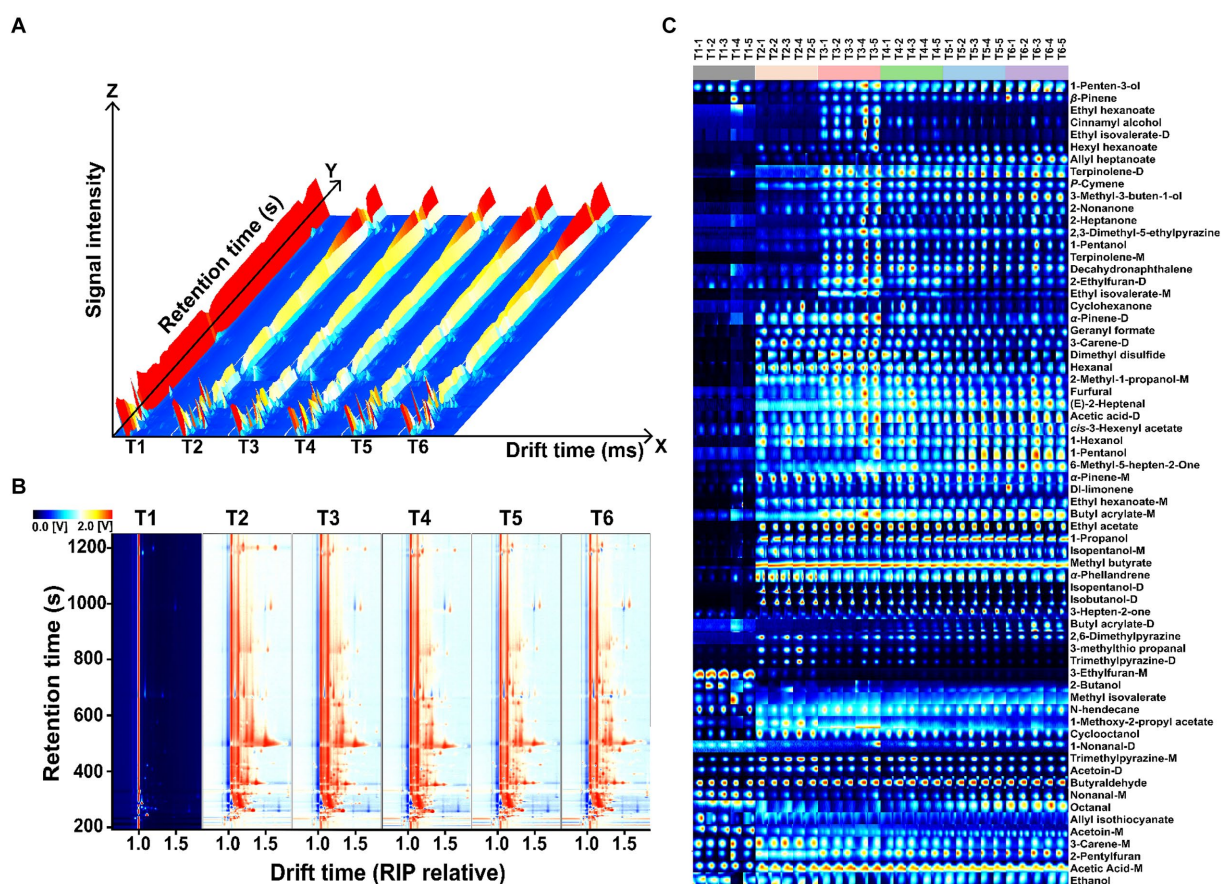
FIGURE 4
Presents the GC-IMS diagram of SBD at various processing stages. **(A)** 3D topographic maps, **(B)** gallery plot indicating changes in VOCs concentration across different stages, and **(C)** 2D difference map illustrating the variation from the control sample T1 by subtracting spectra of T2-T6. The color scheme employs red and blue to represent high or low compound concentrations, respectively.

3-Methylbutanol-D, 3-Methylbutanol-M and aldehyde compound 3-Methylthio propanal were relatively higher in marinating stage (T2), and the peak intensity of ester compounds Ethyl 3-methylbutanoate-M, Ethyl 3-methyl butanoate-D were the highest in seasoning stage (T3). Additionally, as the cooking process progressed, the level of Butyraldehyde, Nonanal-M, Nonanal-D, 2-Pentylfuran showed an increasing trend, with the peak intensity of these compounds being highest at the end (T6) of the steaming process.

3.4 Analysis of free amino acids in taste (FAAs) of SBD

Free amino acids are an essential part that often contributes to taste. In this study, 19 important free amino acids in the SBD at different processing stages were characterized, and their TAV were further calculated to evaluate their contribution to the overall taste characteristics of the SBD. In all stages of SBD (T1–T6), only Glu has a TAV value greater than 1 in T3–T6, indicating that Glu has a core contribution to the overall taste after SBD marinating. The TAV values for other free amino acids were between 0.1 and 1, indicating that they contributed to SBD overall taste (Supplementary Table S1). In order to show the

differences and overall trends of free amino acids in each stage of the SBD, an rPCA model and a class heat map were established according to the content of free amino acids, as shown in Figure 7. In the entire rPCA model, PC1 accounts for 97.6% of the total samples and explains most of the difference. Among them, the differences were most significant in the marinating stage (T2) and the seasoning stage (T3) ($p < 0.05$). In detail, the content of Ala was higher in the T2 stage, while Pro, Asp, Lys, Glu, Val, Arg, and His were higher in the T3 stage (Figures 7A,B).

Moreover, the free amino acids were further divided into umami, sweet, bitter, acerbic and tasteless amino acids for analysis. The results shown in Figure 7C showed that the umami, sweet and bitter amino acids significantly increased during the T2–T3 stages of the SBD production ($p < 0.05$). The content of tasteless amino acid changed little in each stage, while the content of acerbic amino acid remained at a low level all the time. The results of the heat map of different stages of SBD showed that the content of sweet amino acids Ala was higher in the T1 and the T2 stages (Figure 7D). In the seasoning stage (T3), the contents of umami amino acids Asp and Glu, sweet amino acid Pro and bitter amino acids His, Arg, Val, and Lys are higher. As the steaming process progresses, during the steaming (T4–T6) stages, the content of some amino acids begins to rise and gradually increases to the highest level at the end of the steaming process. Including Asp, Pro, His, and Val taste amino acids.

TABLE 1 The peak intensity (mean±sd) of volatile organic compounds in different SBD stages was characterized by GC-IMS.

Count	Compounds	CAS	Formula	RI#	DT[ms]	Peak intensity					
						T1	T2	T3	T4	T5	T6
Esters	Ethyl Acetate	141-78-6	$C_4H_8O_2$	904.9	1.32917	$2.53 \times 10^2 \pm 1.30 \times 10^2$ c *	$5.22 \times 10^3 \pm 7.24 \times 10^2$ b	$7.22 \times 10^3 \pm 1.38 \times 10^2$ a	$6.25 \times 10^3 \pm 5.57 \times 10^2$ ab	$5.38 \times 10^3 \pm 3.67 \times 10^2$ b	$5.13 \times 10^3 \pm 9.29 \times 10^2$ b
	Ethyl hexanoate-M	123-66-0	$C_8H_{16}O_2$	1,213.6	1.32158	$9.62 \times 10^2 \pm 8.53 \times 10^2$ c	$9.04 \times 10^3 \pm 5.87 \times 10^2$ a	$9.48 \times 10^3 \pm 4.17 \times 10^2$ a	$8.04 \times 10^3 \pm 5.41 \times 10^2$ ab	$7.84 \times 10^3 \pm 3.39 \times 10^2$ ab	$7.30 \times 10^3 \pm 6.61 \times 10^2$ b
	Ethyl 3-methylbutanoate-M	108-64-5	$C_7H_{14}O_2$	1,064.6	1.26613	$1.23 \times 10^2 \pm 4.73 \times 10^1$ d	$2.39 \times 10^2 \pm 2.49 \times 10^1$ c	$1.32 \times 10^3 \pm 8.13 \times 10^1$ a	$6.39 \times 10^2 \pm 1.92 \times 10^2$ b	$4.44 \times 10^2 \pm 3.76 \times 10^1$ b	$4.78 \times 10^2 \pm 6.84 \times 10^1$ b
	Ethyl 3-methylbutanoate-D	108-64-5	$C_7H_{14}O_2$	1,065.0	1.65372	$1.72 \times 10^2 \pm 4.68 \times 10^1$ b	$1.13 \times 10^2 \pm 2.10 \times 10^1$ c	$5.54 \times 10^2 \pm 9.83 \times 10^1$ a	$1.70 \times 10^2 \pm 4.54 \times 10^1$ b	$1.11 \times 10^2 \pm 6.52 \times 10^0$ bc	$1.31 \times 10^2 \pm 1.45 \times 10^1$ bc
	Butyl 2-propenoate-M	141-32-2	$C_7H_{12}O_2$	1,186.9	1.26163	$1.25 \times 10^2 \pm 2.91 \times 10^1$ d	$2.07 \times 10^2 \pm 3.08 \times 10^1$ c	$2.73 \times 10^2 \pm 2.71 \times 10^1$ bc	$2.57 \times 10^2 \pm 4.93 \times 10^1$ bc	$3.08 \times 10^2 \pm 2.10 \times 10^1$ ab	$3.54 \times 10^2 \pm 3.29 \times 10^1$ a
	Butyl 2-propenoate-D	141-32-2	$C_7H_{12}O_2$	1,186.0	1.6939	$1.42 \times 10^2 \pm 7.30 \times 10^1$ bc	$8.96 \times 10^1 \pm 9.39 \times 10^0$ d	$1.12 \times 10^2 \pm 2.07 \times 10^1$ cd	$1.36 \times 10^2 \pm 3.10 \times 10^1$ bc	$1.83 \times 10^2 \pm 1.00 \times 10^1$ ab	$3.06 \times 10^2 \pm 7.88 \times 10^1$ a
	Geranyl formate	105-86-2	$C_{11}H_{18}O_2$	1,292.9	1.21058	$1.02 \times 10^3 \pm 1.09 \times 10^2$ d	$4.83 \times 10^3 \pm 5.40 \times 10^2$ ab	$5.01 \times 10^3 \pm 4.78 \times 10^2$ a	$4.16 \times 10^3 \pm 5.06 \times 10^2$ bc	$4.04 \times 10^3 \pm 1.81 \times 10^2$ bc	$3.77 \times 10^3 \pm 2.85 \times 10^2$ c
	(Z)-3-Hexenyl acetate	3681-71-8	$C_8H_{14}O_2$	1,362.8	1.32946	$1.47 \times 10^2 \pm 1.83 \times 10^1$ b	$2.83 \times 10^2 \pm 4.18 \times 10^1$ a	$3.28 \times 10^2 \pm 1.70 \times 10^1$ a	$2.64 \times 10^2 \pm 3.88 \times 10^1$ a	$2.92 \times 10^2 \pm 2.42 \times 10^1$ a	$3.12 \times 10^2 \pm 3.94 \times 10^1$ a
	Methyl butyrate	623-42-7	$C_5H_{10}O_2$	990.5	1.12459	$6.99 \times 10^2 \pm 8.54 \times 10^1$ c	$7.32 \times 10^3 \pm 1.43 \times 10^2$ a	$7.20 \times 10^3 \pm 7.01 \times 10^1$ a	$6.99 \times 10^3 \pm 2.26 \times 10^2$ ab	$6.82 \times 10^3 \pm 2.49 \times 10^2$ b	$6.63 \times 10^3 \pm 2.43 \times 10^2$ b
	Isovaleric acid, methyl	556-24-1	$C_6H_{12}O_2$	1,017.1	1.19216	$2.54 \times 10^2 \pm 1.40 \times 10^2$ a	$8.42 \times 10^1 \pm 1.97 \times 10^1$ c	$1.13 \times 10^2 \pm 3.92$ bc	$1.07 \times 10^2 \pm 1.09 \times 10^1$ bc	$1.58 \times 10^2 \pm 2.13 \times 10^1$ ab	$1.39 \times 10^2 \pm 1.07 \times 10^1$ b
	1-Methoxy-2-propanol acetate	108-65-6	$C_6H_{12}O_3$	1,234.1	1.17298	$1.35 \times 10^2 \pm 2.67 \times 10^1$ c	$2.23 \times 10^2 \pm 4.11 \times 10^1$ a	$2.14 \times 10^2 \pm 4.38 \times 10^1$ ab	$1.46 \times 10^2 \pm 2.57 \times 10^1$ bc	$1.08 \times 10^2 \pm 2.05 \times 10^1$ cd	$9.66 \times 10^1 \pm 2.42 \times 10^1$ d
	Allyl heptanoate	142-19-8	$C_{10}H_{18}O_2$	1,188.5	1.4365	$1.06 \times 10^2 \pm 5.24 \times 10^1$ d	$3.90 \times 10^2 \pm 8.92 \times 10^1$ c	$5.17 \times 10^2 \pm 1.39 \times 10^2$ c	$9.02 \times 10^2 \pm 1.89 \times 10^2$ b	$1.26 \times 10^3 \pm 1.61 \times 10^2$ a	$1.42 \times 10^3 \pm 2.00 \times 10^2$ a
	Hexyl hexanoate	6378-65-0	$C_{12}H_{24}O_2$	1,395.4	1.57128	$3.60 \times 10^2 \pm 5.69 \times 10^1$ b	$1.24 \times 10^3 \pm 4.13 \times 10^2$ a	$2.00 \times 10^3 \pm 1.04 \times 10^3$ a	$1.64 \times 10^3 \pm 4.21 \times 10^2$ a	$1.81 \times 10^3 \pm 3.34 \times 10^2$ a	$1.81 \times 10^3 \pm 2.39 \times 10^2$ a
	Ethyl hexanoate-D	123-66-0	$C_8H_{16}O_2$	1,227.1	1.78994	$1.48 \times 10^2 \pm 1.47 \times 10^2$ b	$9.75 \times 10^1 \pm 2.65 \times 10^1$ b	$3.70 \times 10^2 \pm 1.07 \times 10^2$ a	$7.13 \times 10^1 \pm 1.23 \times 10^1$ b	$7.66 \times 10^1 \pm 6.84$ b	$8.38 \times 10^1 \pm 9.49$ b
	Allyl Isothiocyanate	57-06-7	C_4H_5NS	930.0	1.0915	$1.06 \times 10^3 \pm 3.73 \times 10^2$ a	$8.68 \times 10^2 \pm 7.42 \times 10^1$ ab	$7.50 \times 10^2 \pm 3.26 \times 10^1$ ab	$6.25 \times 10^2 \pm 5.36 \times 10^1$ bc	$6.14 \times 10^2 \pm 2.71 \times 10^1$ bc	$5.22 \times 10^2 \pm 2.01 \times 10^1$ c
Alcohols	2-Methyl-1-propanol-D	78-83-1	$C_4H_{10}O$	1,095.7	1.37398	$3.63 \times 10^2 \pm 1.05 \times 10^2$ d	$6.89 \times 10^3 \pm 5.28 \times 10^2$ a	$5.20 \times 10^3 \pm 9.09 \times 10^1$ b	$4.80 \times 10^3 \pm 3.77 \times 10^2$ bc	$4.47 \times 10^3 \pm 2.37 \times 10^2$ c	$4.09 \times 10^3 \pm 5.22 \times 10^2$ c
	3-Methylbutanol-D	123-51-3	$C_5H_{12}O$	1,204.7	1.51194	$2.95 \times 10^3 \pm 3.65 \times 10^2$ e	$2.16 \times 10^4 \pm 1.93 \times 10^3$ a	$1.50 \times 10^4 \pm 7.57 \times 10^2$ b	$1.20 \times 10^4 \pm 1.37 \times 10^3$ c	$1.06 \times 10^4 \pm 9.82 \times 10^2$ cd	$9.66 \times 10^3 \pm 1.02 \times 10^3$ d
	3-Methylbutanol-M	123-51-3	$C_5H_{12}O$	1,203.5	1.25161	$7.11 \times 10^2 \pm 3.15 \times 10^2$ c	$6.35 \times 10^3 \pm 3.73 \times 10^2$ a	$4.30 \times 10^3 \pm 4.94 \times 10^2$ b	$4.46 \times 10^3 \pm 1.11 \times 10^2$ b	$4.51 \times 10^3 \pm 9.26 \times 10^1$ b	$4.57 \times 10^3 \pm 1.64 \times 10^2$ b
	Pentanol-M	71-41-0	$C_5H_{12}O$	1,296.1	1.50898	$1.05 \times 10^2 \pm 1.24 \times 10^1$ d	$1.81 \times 10^2 \pm 9.09 \times 10^1$ cd	$2.24 \times 10^2 \pm 1.15 \times 10^2$ c	$2.68 \times 10^2 \pm 5.25 \times 10^1$ bc	$4.00 \times 10^2 \pm 6.13 \times 10^1$ ab	$4.76 \times 10^2 \pm 8.23 \times 10^1$ a
	Pentanol-D	71-41-0	$C_5H_{12}O$	1,250.3	1.51605	$1.05 \times 10^2 \pm 1.77 \times 10^1$ c	$1.89 \times 10^2 \pm 4.09 \times 10^1$ b	$4.21 \times 10^2 \pm 6.01 \times 10^1$ a	$3.03 \times 10^2 \pm 7.89 \times 10^1$ a	$3.49 \times 10^2 \pm 4.56 \times 10^1$ a	$3.39 \times 10^2 \pm 8.80 \times 10^1$ a
	3-Methyl-3-buten-1-ol	763-32-6	$C_5H_{10}O$	1,311.2	1.16675	$1.36 \times 10^2 \pm 1.75 \times 10^1$ d	$4.06 \times 10^2 \pm 7.18 \times 10^1$ c	$1.70 \times 10^3 \pm 1.91 \times 10^2$ ab	$1.48 \times 10^3 \pm 1.45 \times 10^2$ b	$1.50 \times 10^3 \pm 6.37 \times 10^1$ b	$1.88 \times 10^3 \pm 2.63 \times 10^2$ a
	1-Penten-3-ol	616-25-1	$C_5H_{10}O$	1,181.2	1.35689	$4.27 \times 10^2 \pm 9.54 \times 10^1$ b	$2.16 \times 10^2 \pm 4.83 \times 10^1$ c	$7.19 \times 10^2 \pm 1.21 \times 10^2$ a	$6.39 \times 10^2 \pm 1.25 \times 10^2$ a	$6.19 \times 10^2 \pm 2.51 \times 10^1$ a	$7.69 \times 10^2 \pm 1.33 \times 10^2$ a
	1-Hexanol	111-27-3	$C_6H_{14}O$	1,349.2	1.30244	$1.46 \times 10^2 \pm 2.71 \times 10^1$ b	$7.84 \times 10^2 \pm 2.37 \times 10^2$ a	$7.86 \times 10^2 \pm 9.88 \times 10^1$ a	$7.97 \times 10^2 \pm 1.63 \times 10^2$ a	$7.88 \times 10^2 \pm 6.73 \times 10^1$ a	$7.86 \times 10^2 \pm 1.02 \times 10^2$ a
	2-butanol	78-92-2	$C_4H_{10}O$	1,024.6	1.29733	$1.45 \times 10^2 \pm 6.23 \times 10^1$ a	$8.51 \times 10^1 \pm 3.57 \times 10^1$ ab	$7.96 \times 10^1 \pm 2.93 \times 10^1$ b	$6.94 \times 10^1 \pm 5.96 \times 10^0$ b	$9.57 \times 10^1 \pm 1.44 \times 10^1$ ab	$1.00 \times 10^2 \pm 1.15 \times 10^1$ ab
	Propanol	71-23-8	C_3H_8O	1,031.8	1.11502	$6.01 \times 10^2 \pm 6.09 \times 10^1$ c	$7.95 \times 10^3 \pm 8.75 \times 10^2$ b	$7.96 \times 10^3 \pm 8.52 \times 10^2$ b	$8.38 \times 10^3 \pm 9.31 \times 10^2$ b	$1.09 \times 10^4 \pm 5.55 \times 10^2$ a	$9.40 \times 10^3 \pm 8.97 \times 10^2$ ab
	Ethanol	64-17-5	C_2H_6O	913.9	1.06125	$3.32 \times 10^2 \pm 1.62 \times 10^2$ a	$3.35 \times 10^2 \pm 5.26 \times 10^1$ a	$2.77 \times 10^2 \pm 7.46 \times 10^1$ a	$2.89 \times 10^2 \pm 6.50 \times 10^1$ a	$3.31 \times 10^2 \pm 5.61 \times 10^1$ a	$3.47 \times 10^2 \pm 4.90 \times 10^1$ a
	2-Methyl-1-propanol-M	78-83-1	$C_4H_{10}O$	1,107	1.17449	$4.31 \times 10^1 \pm 7.06 \times 10^0$ e	$5.52 \times 10^2 \pm 4.14 \times 10^1$ bc	$7.00 \times 10^2 \pm 2.19 \times 10^1$ a	$5.67 \times 10^2 \pm 3.54 \times 10^1$ b	$4.05 \times 10^2 \pm 3.80 \times 10^1$ d	$4.65 \times 10^2 \pm 8.84 \times 10^1$ cd
	Cinnamyl alcohol	104-54-1	$C_9H_{10}O$	1,274.5	1.56659	$5.10 \times 10^1 \pm 8.00$ c	$5.04 \times 10^1 \pm 4.91$ c	$2.82 \times 10^2 \pm 6.41 \times 10^1$ a	$1.42 \times 10^2 \pm 3.99 \times 10^1$ b	$9.76 \times 10^1 \pm 1.70 \times 10^1$ b	$1.09 \times 10^2 \pm 4.47 \times 10^1$ b
	Cyclooctanol	696-71-9	$C_8H_{16}O$	1,148.8	1.12058	$1.23 \times 10^3 \pm 3.68 \times 10^2$ b	$3.69 \times 10^3 \pm 4.46 \times 10^2$ a	$3.29 \times 10^3 \pm 2.62 \times 10^2$ a	$3.44 \times 10^3 \pm 2.44 \times 10^2$ a	$3.04 \times 10^3 \pm 2.95 \times 10^2$ a	$2.94 \times 10^3 \pm 2.51 \times 10^2$ a

TABLE 1 (Continued)

Count	Compounds	CAS	Formula	RI#	DT[ms]	Peak intensity					
						T1	T2	T3	T4	T5	T6
Alkenes	Limonene	138-86-3	$C_{10}H_{16}$	1,206.8	1.21404	$4.14 \times 10^2 \pm 4.51 \times 10^{2\,b}$	$6.71 \times 10^2 \pm 2.20 \times 10^{2\,ab}$	$6.21 \times 10^2 \pm 2.22 \times 10^{1\,ab}$	$9.94 \times 10^2 \pm 2.71 \times 10^{2\,a}$	$1.03 \times 10^3 \pm 7.90 \times 10^{1\,a}$	$1.14 \times 10^3 \pm 4.53 \times 10^{2\,a}$
	α-pinene-M	80-56-8	$C_{10}H_{16}$	1,033.7	1.20957	$2.29 \times 10^2 \pm 1.17 \times 10^{2\,d}$	$1.49 \times 10^3 \pm 1.67 \times 10^{2\,ab}$	$1.60 \times 10^3 \pm 4.15 \times 10^{1\,a}$	$1.42 \times 10^3 \pm 1.70 \times 10^{2\,ab}$	$1.06 \times 10^3 \pm 1.10 \times 10^{2\,c}$	$1.17 \times 10^3 \pm 1.57 \times 10^{2\,bc}$
	α-pinene-D	80-56-8	$C_{10}H_{16}$	1,033.7	1.31662	$2.23 \times 10^1 \pm 4.44^{\,d}$	$1.50 \times 10^2 \pm 2.68 \times 10^{1\,ab}$	$1.82 \times 10^2 \pm 1.33 \times 10^{1\,a}$	$1.22 \times 10^2 \pm 3.01 \times 10^{1\,b}$	$7.93 \times 10^1 \pm 7.03^{\,c}$	$8.23 \times 10^1 \pm 2.49 \times 10^{1\,c}$
	3-Carene-D	13466-78-9	$C_{10}H_{16}$	1,139.2	1.26709	$6.20 \times 10^1 \pm 9.71 \times 10^{1\,d}$	$9.33 \times 10^2 \pm 1.17 \times 10^{2\,a}$	$9.20 \times 10^2 \pm 9.53 \times 10^{1\,a}$	$6.91 \times 10^2 \pm 1.13 \times 10^{2\,b}$	$5.31 \times 10^2 \pm 5.33 \times 10^{1\,bc}$	$4.81 \times 10^2 \pm 8.49 \times 10^{1\,c}$
	3-Carene-M	13466-78-9	$C_{10}H_{16}$	1,140.1	1.1892	$3.55 \times 10^2 \pm 4.13 \times 10^{1\,ab}$	$4.44 \times 10^2 \pm 3.50 \times 10^{1\,a}$	$3.51 \times 10^2 \pm 7.95 \times 10^{0\,ab}$	$3.11 \times 10^2 \pm 4.03 \times 10^{1\,bc}$	$2.53 \times 10^2 \pm 1.86 \times 10^{1\,d}$	$2.64 \times 10^2 \pm 3.59 \times 10^{1\,cd}$
	Terpinolene-D	586-62-9	$C_{10}H_{16}$	1,279.4	1.28723	$1.37 \times 10^2 \pm 4.14 \times 10^{1\,b}$	$1.21 \times 10^2 \pm 5.04^{\,b}$	$3.59 \times 10^2 \pm 3.79 \times 10^{1\,a}$	$3.34 \times 10^2 \pm 5.64 \times 10^{1\,a}$	$4.11 \times 10^2 \pm 2.46 \times 10^{1\,a}$	$4.07 \times 10^2 \pm 5.42 \times 10^{1\,a}$
	Terpinolene-M	586-62-9	$C_{10}H_{16}$	1,279.9	1.21944	$8.83 \times 10^1 \pm 1.31 \times 10^{1\,d}$	$1.64 \times 10^2 \pm 1.56 \times 10^{1\,c}$	$1.36 \times 10^3 \pm 7.73 \times 10^{1\,a}$	$9.67 \times 10^2 \pm 1.97 \times 10^{2\,b}$	$9.25 \times 10^2 \pm 1.16 \times 10^{2\,b}$	$8.41 \times 10^2 \pm 2.01 \times 10^{2\,b}$
	β-pinene	127-91-3	$C_{10}H_{16}$	1,116.6	1.21818	$4.82 \times 10^2 \pm 6.17 \times 10^{2\,bc}$	$2.73 \times 10^2 \pm 5.88 \times 10^{1\,c}$	$9.95 \times 10^2 \pm 9.42 \times 10^{1\,a}$	$7.55 \times 10^2 \pm 1.42 \times 10^{2\,ab}$	$8.31 \times 10^2 \pm 6.00 \times 10^{1\,ab}$	$1.14 \times 10^3 \pm 3.04 \times 10^{2\,a}$
	α-phellandrene	99-83-2	$C_{10}H_{16}$	1,161	1.21523	$5.28 \times 10^2 \pm 5.41 \times 10^{2\,a}$	$3.65 \times 10^2 \pm 9.28 \times 10^{1\,a}$	$3.27 \times 10^2 \pm 3.50 \times 10^{1\,a}$	$3.44 \times 10^2 \pm 1.36 \times 10^{2\,a}$	$3.44 \times 10^2 \pm 2.87 \times 10^{1\,a}$	$3.61 \times 10^2 \pm 1.09 \times 10^{2\,a}$
Aldehydes	Nonanal-M	124-19-6	$C_9H_{18}O$	1,395.2	1.49576	$1.85 \times 10^3 \pm 7.25 \times 10^{1\,a}$	$9.19 \times 10^2 \pm 2.99 \times 10^{2\,c}$	$9.78 \times 10^2 \pm 3.80 \times 10^{2\,bc}$	$1.04 \times 10^3 \pm 2.63 \times 10^{2\,bc}$	$1.44 \times 10^3 \pm 1.99 \times 10^{2\,ab}$	$1.62 \times 10^3 \pm 7.58 \times 10^{1\,a}$
	3-Methylthio propanal	3268-49-3	C_4H_8OS	1,449.1	1.39672	$2.37 \times 10^2 \pm 3.61 \times 10^{1\,c}$	$1.20 \times 10^3 \pm 4.93 \times 10^{2\,a}$	$6.04 \times 10^2 \pm 1.63 \times 10^{2\,b}$	$6.21 \times 10^2 \pm 2.56 \times 10^{2\,b}$	$3.86 \times 10^2 \pm 5.14 \times 10^{1\,bc}$	$3.03 \times 10^2 \pm 4.01 \times 10^{1\,c}$
	Octanal	124-13-0	$C_8H_{16}O$	1,295.5	1.41812	$2.76 \times 10^2 \pm 4.10 \times 10^{1\,a}$	$1.75 \times 10^2 \pm 3.56 \times 10^{1\,b}$	$1.29 \times 10^2 \pm 2.57 \times 10^{1\,b}$	$1.68 \times 10^2 \pm 2.70 \times 10^{1\,b}$	$3.26 \times 10^2 \pm 2.84 \times 10^{1\,a}$	$3.67 \times 10^2 \pm 4.24 \times 10^{1\,a}$
	(E)-2-Heptenal	18829-55-5	$C_7H_{12}O$	1,333.4	1.25527	$8.51 \times 10^1 \pm 1.48 \times 10^{1\,d}$	$2.69 \times 10^2 \pm 1.26 \times 10^{1\,c}$	$2.93 \times 10^2 \pm 1.15 \times 10^{1\,bc}$	$2.99 \times 10^2 \pm 3.08 \times 10^{1\,bc}$	$3.44 \times 10^2 \pm 3.63 \times 10^{1\,ab}$	$3.58 \times 10^2 \pm 3.00 \times 10^{1\,a}$
	Furfural	98-01-1	$C_5H_4O_2$	1,445.7	1.08713	$3.50 \times 10^2 \pm 1.35 \times 10^{1\,b}$	$3.54 \times 10^2 \pm 2.66 \times 10^{1\,b}$	$6.14 \times 10^2 \pm 8.08 \times 10^{1\,a}$	$6.31 \times 10^2 \pm 1.32 \times 10^{2\,a}$	$6.08 \times 10^2 \pm 4.09 \times 10^{1\,a}$	$6.85 \times 10^2 \pm 6.16 \times 10^{1\,a}$
	Nonanal-D	124-19-6	$C_9H_{18}O$	1,395.9	1.93198	$2.68 \times 10^2 \pm 3.96 \times 10^{1\,ab}$	$1.92 \times 10^2 \pm 2.90 \times 10^{1\,b}$	$2.49 \times 10^2 \pm 1.28 \times 10^{2\,ab}$	$2.31 \times 10^2 \pm 6.32 \times 10^{1\,ab}$	$2.92 \times 10^2 \pm 5.28 \times 10^{1\,a}$	$3.39 \times 10^2 \pm 6.24 \times 10^{1\,a}$
	Hexanal	66-25-1	$C_6H_{12}O$	1,088.8	1.25499	$3.15 \times 10^2 \pm 4.01 \times 10^{1\,e}$	$3.45 \times 10^3 \pm 1.42 \times 10^{2\,a}$	$3.41 \times 10^3 \pm 8.85 \times 10^{1\,a}$	$2.84 \times 10^3 \pm 1.50 \times 10^{2\,b}$	$2.56 \times 10^3 \pm 8.60 \times 10^{1\,c}$	$2.30 \times 10^3 \pm 1.61 \times 10^{2\,d}$
	Butyraldehyde	123-72-8	C_4H_8O	854.3	1.11424	$8.37 \times 10^3 \pm 8.94 \times 10^{2\,c}$	$9.94 \times 10^3 \pm 6.75 \times 10^{2\,b}$	$1.22 \times 10^4 \pm 4.24 \times 10^{2\,a}$	$1.33 \times 10^4 \pm 6.53 \times 10^{2\,a}$	$1.31 \times 10^4 \pm 4.37 \times 10^{2\,a}$	$1.28 \times 10^4 \pm 3.99 \times 10^{2\,a}$
Ketones	3-Hydroxy-2-butanone-D	513-86-0	$C_4H_8O_2$	1,293.6	1.33027	$1.56 \times 10^3 \pm 2.64 \times 10^{2\,b}$	$2.35 \times 10^3 \pm 3.55 \times 10^{2\,a}$	$1.69 \times 10^3 \pm 1.61 \times 10^{2\,ab}$	$1.62 \times 10^3 \pm 3.83 \times 10^{2\,b}$	$1.92 \times 10^3 \pm 1.32 \times 10^{2\,ab}$	$1.82 \times 10^3 \pm 9.65 \times 10^{1\,ab}$
	3-Hydroxy-2-butanone-M	513-86-0	$C_4H_8O_2$	1,297.9	1.08651	$5.55 \times 10^3 \pm 4.70 \times 10^{2\,a}$	$2.60 \times 10^3 \pm 1.19 \times 10^{2\,bc}$	$2.27 \times 10^3 \pm 1.58 \times 10^{2\,cd}$	$2.22 \times 10^3 \pm 2.11 \times 10^{2\,d}$	$2.66 \times 10^3 \pm 1.00 \times 10^{2\,b}$	$2.84 \times 10^3 \pm 1.79 \times 10^{2\,b}$
	6-Methyl-5-hepten-2-one	110-93-0	$C_8H_{14}O$	1,343.5	1.17549	$8.54 \times 10^1 \pm 1.12 \times 10^{1\,c}$	$2.06 \times 10^2 \pm 4.35 \times 10^{1\,b}$	$3.15 \times 10^2 \pm 7.95 \times 10^{1\,a}$	$3.45 \times 10^2 \pm 5.88 \times 10^{1\,a}$	$3.56 \times 10^2 \pm 5.20 \times 10^{1\,a}$	$4.19 \times 10^2 \pm 4.32 \times 10^{1\,a}$
	Cyclohexanone	108-94-1	$C_6H_{10}O$	1,289.7	1.46084	$8.52 \times 10^1 \pm 1.45 \times 10^{1\,b}$	$2.16 \times 10^2 \pm 7.44 \times 10^{1\,a}$	$1.35 \times 10^2 \pm 2.37 \times 10^{1\,ab}$	$1.83 \times 10^2 \pm 7.18 \times 10^{1\,a}$	$1.38 \times 10^2 \pm 2.07 \times 10^{1\,a}$	$1.41 \times 10^2 \pm 2.06 \times 10^{1\,a}$
	2-Nonanone	821-55-6	$C_9H_{18}O$	1,363.7	1.4139	$1.04 \times 10^2 \pm 1.36 \times 10^{1\,c}$	$2.02 \times 10^2 \pm 3.80 \times 10^{1\,b}$	$3.82 \times 10^2 \pm 5.38 \times 10^{1\,a}$	$2.65 \times 10^2 \pm 4.54 \times 10^{1\,b}$	$2.74 \times 10^2 \pm 2.67 \times 10^{1\,b}$	$2.81 \times 10^2 \pm 6.00 \times 10^{1\,b}$
	2-Heptanone	110-43-0	$C_7H_{14}O$	1,176.2	1.63167	$1.14 \times 10^2 \pm 3.77 \times 10^{1\,b}$	$1.00 \times 10^2 \pm 7.55 \times 10^{0\,b}$	$3.41 \times 10^2 \pm 1.44 \times 10^{2\,a}$	$2.30 \times 10^2 \pm 4.61 \times 10^{1\,a}$	$2.32 \times 10^2 \pm 2.10 \times 10^{1\,a}$	$2.78 \times 10^2 \pm 7.05 \times 10^{1\,a}$
	3-Hepten-2-one	1119-44-4	$C_7H_{12}O$	917.4	1.22565	$1.38 \times 10^3 \pm 1.14 \times 10^{2\,d}$	$2.36 \times 10^3 \pm 1.78 \times 10^{2\,c}$	$3.01 \times 10^3 \pm 2.09 \times 10^{2\,b}$	$3.59 \times 10^3 \pm 3.12 \times 10^{2\,a}$	$3.85 \times 10^3 \pm 3.28 \times 10^{2\,a}$	$3.51 \times 10^3 \pm 1.73 \times 10^{2\,a}$

(Continued)

TABLE 1 (Continued)

Count	Compounds	CAS	Formula	RI#	DT[ms]	Peak intensity					
						T1	T2	T3	T4	T5	T6
Heterocycles	2,3,5-Trimethylpyrazine-D	14667-55-1	$C_7H_{10}N_2$	1,448.6	1.63356	$6.36\times10^2\pm8.14\times10^1$ [c]	$2.91\times10^3\pm1.13\times10^3$ [a]	$1.52\times10^3\pm3.74\times10^2$ [b]	$1.57\times10^3\pm6.56\times10^2$ [b]	$9.96\times10^2\pm1.35\times10^2$ [bc]	$7.95\times10^2\pm6.08\times10^1$ [c]
	2,3,5-Trimethylpyrazine-M	14667-55-1	$C_7H_{10}N_2$	1,447.9	1.18318	$2.32\times10^3\pm3.99\times10^2$ [c]	$5.46\times10^3\pm8.83\times10^2$ [a]	$4.02\times10^3\pm3.50\times10^2$ [ab]	$4.24\times10^3\pm8.87\times10^2$ [ab]	$3.58\times10^3\pm3.78\times10^2$ [b]	$3.15\times10^3\pm2.81\times10^2$ [b]
	2,6-Dimethylpyrazine	108-50-9	$C_6H_8N_2$	1,351.2	1.53163	$2.55\times10^2\pm1.46\times10^1$ [b]	$7.51\times10^2\pm2.17\times10^2$ [a]	$5.93\times10^2\pm9.90\times10^1$ [a]	$6.56\times10^2\pm1.68\times10^2$ [a]	$6.61\times10^2\pm5.82\times10^1$ [a]	$7.32\times10^2\pm8.75\times10^1$ [a]
	2-Pentylfuran	3777-69-3	$C_9H_{14}O$	1,243.3	1.25673	$4.29\times10^2\pm9.25\times10^1$ [b]	$6.22\times10^2\pm2.29\times10^1$ [a]	$6.84\times10^2\pm4.17\times10^1$ [a]	$6.78\times10^2\pm4.17\times10^1$ [a]	$6.22\times10^2\pm5.63\times10^1$ [a]	$6.95\times10^2\pm6.83\times10^1$ [a]
	2-Ethylfuran-D	3208-16-0	C_6H_8O	971.1	1.3158	$1.26\times10^2\pm3.75\times10^1$ [d]	$2.08\times10^2\pm5.67\times10^1$ [c]	$5.56\times10^2\pm3.57\times10^1$ [a]	$4.18\times10^2\pm9.01\times10^1$ [ab]	$2.54\times10^2\pm3.07\times10^1$ [c]	$2.83\times10^2\pm6.36\times10^1$ [bc]
	2-Ethylfuran-M	3208-16-0	C_6H_8O	976.3	1.04775	$8.26\times10^3\pm1.21\times10^3$ [a]	$1.07\times10^3\pm2.23\times10^2$ [b]	$4.27\times10^2\pm2.45\times10^1$ [c]	$4.48\times10^2\pm4.59\times10^1$ [c]	$4.43\times10^2\pm3.11\times10^1$ [c]	$4.16\times10^2\pm4.59\times10^1$ [c]
	2,3-Dimethyl-5-ethylpyrazine	15707-34-3	$C_8H_{12}N_2$	1,499.2	1.22599	$2.08\times10^2\pm2.66\times10^1$ [b]	$2.32\times10^2\pm1.75\times10^1$ [b]	$6.36\times10^2\pm1.52\times10^2$ [a]	$5.75\times10^2\pm9.65\times10^1$ [a]	$6.25\times10^2\pm5.96\times10^1$ [a]	$6.31\times10^2\pm5.97\times10^1$ [a]
Acids	Acetic acid-D	64-19-7	$C_2H_4O_2$	1,445.2	1.15187	$1.26\times10^2\pm2.03\times10^1$ [c]	$4.57\times10^2\pm6.17\times10^1$ [b]	$6.30\times10^2\pm7.15\times10^1$ [a]	$6.32\times10^2\pm1.16\times10^2$ [a]	$5.55\times10^2\pm2.80\times10^1$ [ab]	$6.05\times10^2\pm9.32\times10^1$ [ab]
	Acetic acid-M	64-19-7	$C_2H_4O_2$	1,443.6	1.05353	$3.94\times10^3\pm1.21\times10^2$ [c]	$6.30\times10^3\pm1.63\times10^2$ [b]	$6.92\times10^3\pm3.30\times10^2$ [a]	$6.58\times10^3\pm9.46\times10^1$ [ab]	$6.95\times10^3\pm1.38\times10^2$ [a]	$6.73\times10^3\pm1.29\times10^2$ [a]
Others	Decalin	91-17-8	$C_{10}H_{18}$	1,156	1.34461	$7.15\times10^1\pm1.63\times10^1$ [b]	$6.71\times10^1\pm9.91$ [b]	$1.75\times10^2\pm1.51\times10^1$ [a]	$1.50\times10^2\pm3.01\times10^1$ [a]	$1.45\times10^2\pm1.46\times10^1$ [a]	$1.44\times10^2\pm2.39\times10^1$ [a]
	P-cymene	99-87-6	$C_{10}H_{14}$	1,249.9	1.32991	$1.32\times10^2\pm1.72\times10^1$ [c]	$1.29\times10^3\pm2.29\times10^2$ [b]	$2.04\times10^3\pm1.83\times10^2$ [b]	$1.50\times10^3\pm2.44\times10^2$ [b]	$1.40\times10^3\pm1.34\times10^2$ [b]	$1.30\times10^3\pm2.44\times10^2$ [b]
	Dimethyl disulfide	624-92-0	$C_2H_6S_2$	1,066.6	1.13349	$2.01\times10^2\pm3.72\times10^1$ [c]	$1.92\times10^3\pm3.90\times10^2$ [b]	$3.46\times10^3\pm4.07\times10^2$ [a]	$2.83\times10^3\pm5.95\times10^2$ [a]	$1.67\times10^3\pm2.72\times10^2$ [b]	$1.50\times10^3\pm4.27\times10^2$ [b]
	Undecane	1120-21-4	$C_{11}H_{24}$	1,111	1.08945	$8.54\times10^2\pm2.34\times10^2$ [a]	$5.65\times10^2\pm6.09\times10^1$ [ab]	$5.14\times10^2\pm3.70\times10^1$ [b]	$5.16\times10^2\pm4.45\times10^1$ [b]	$6.64\times10^2\pm5.44\times10^1$ [ab]	$6.75\times10^2\pm6.21\times10^1$ [ab]

*For each volatile compound, the same superscript after the sd value indicates a significant difference ($p < 0.05$).

#RI, RT and Dt represent retention index, retention time and drift time, respectively.

FIGURE 5
3D histogram based on the peak intensity of VOCs detected by GC-IMS in the T1–T6 processing stage of the SBD model.
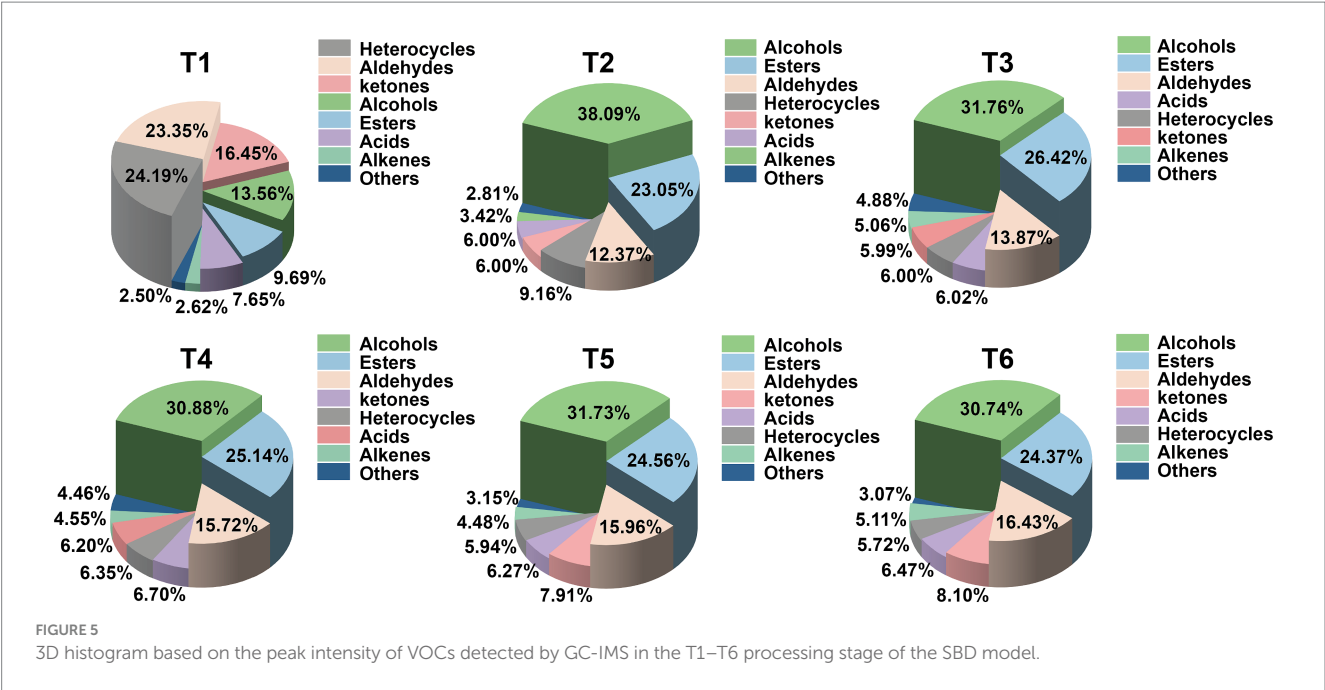
TABLE 2 The relative odor activity values of T1–T6 samples in SBD models.

Compounds	CAS	Threshold (μg/kg)	ROAV						Aroma description*
			T1	T2	T3	T4	T5	T6	
3-Methylbutanol-D#	123-51-3	6.10	11.67	15.93	12.90	18.86	28.03	23.31	Alcohol, bananas
3-Methylbutanol-M	123-51-3	6.10	2.21	4.35	4.15	7.54	11.85	11.79	Alcohol, bananas
Nonanal-M	124-19-6	3.10	15.51	1.46	1.35	3.05	7.94	8.22	Citrus, cucumber
2-Pentylfuran	3777-69-3	5.80	1.74	0.45	0.62	1.16	1.68	1.87	Butter, flowers
3-Methylthio propanal	3268-49-3	0.06	100.00	100.00	41.89	73.45	95.00	68.94	Cooked potatoes
Ethyl hexanoate-M	123-66-0	20.00	0.73	1.96	2.50	3.95	6.38	5.37	Fennel, apple peel
Ethyl 3-methylbutanoate-M	108-64-5	0.07	37.49	14.54	100.00	100.00	100.00	100.00	Fennel, apple
Ethyl 3-methylbutanoate-D	108-64-5	0.07	51.95	6.77	38.52	28.60	26.48	29.24	Fennel, apple
Nonanal-D	124-19-6	3.10	2.06	0.28	0.32	0.64	1.61	1.72	Citrus, cucumber
Methyl butyrate	623-42-7	59.00	0.30	0.53	0.67	1.24	1.83	1.77	Apple, banana
Butyraldehyde	123-72-8	100.00	2.29	0.41	0.65	1.33	2.13	1.95	Banana, pungent

#M represents a monomer, D represents a dimer.
*Volatile Substance description from Vcf-online system (Accessed on 18 March 2024 at 22:00, www.vcf-online.nl/VcfHome.cfm).

4 Discussion

The flavor profile of SBD is extremely complex. Therefore, combining different techniques should be considered as necessary to obtain SBD's characteristic flavor profiles. In recent years, the integration of diverse methodologies has gained extensive application in the field of culinary science. Wu et al. found that the combination of electronic nose and HS-GC-IMS could comprehensively obtain the flavor characteristics of beef cooked in tomato sour soup (8). Xu successfully used gas chromatography and an automated amino acid analyzer to evaluate the contribution of the processing stages to the nonvolatile components of roasted lamb (22). To our knowledge, this

study represents the inaugural endeavor to thoroughly investigate the flavor attributes of SBD throughout its preparation process, employing an array of analytical tools including the E-nose, E-tongue, GC-IMS, and automated amino acid analyzer.

In this investigation, it was discovered that E-noses and E-tongues possess significant capabilities in discerning and differentiating the flavor profiles of SBD, with promising prospects for their future utilization in real-time industrial monitoring of SBD quality. However, the E-nose and E-tongues has some limitations, such as the failure to identify the composition of the aroma and taste (11, 14). To address this issue, we further adopted HS-GC-IMS and amino acid analyzer technology. The HS-GC-IMS is used for trace gas analysis, while
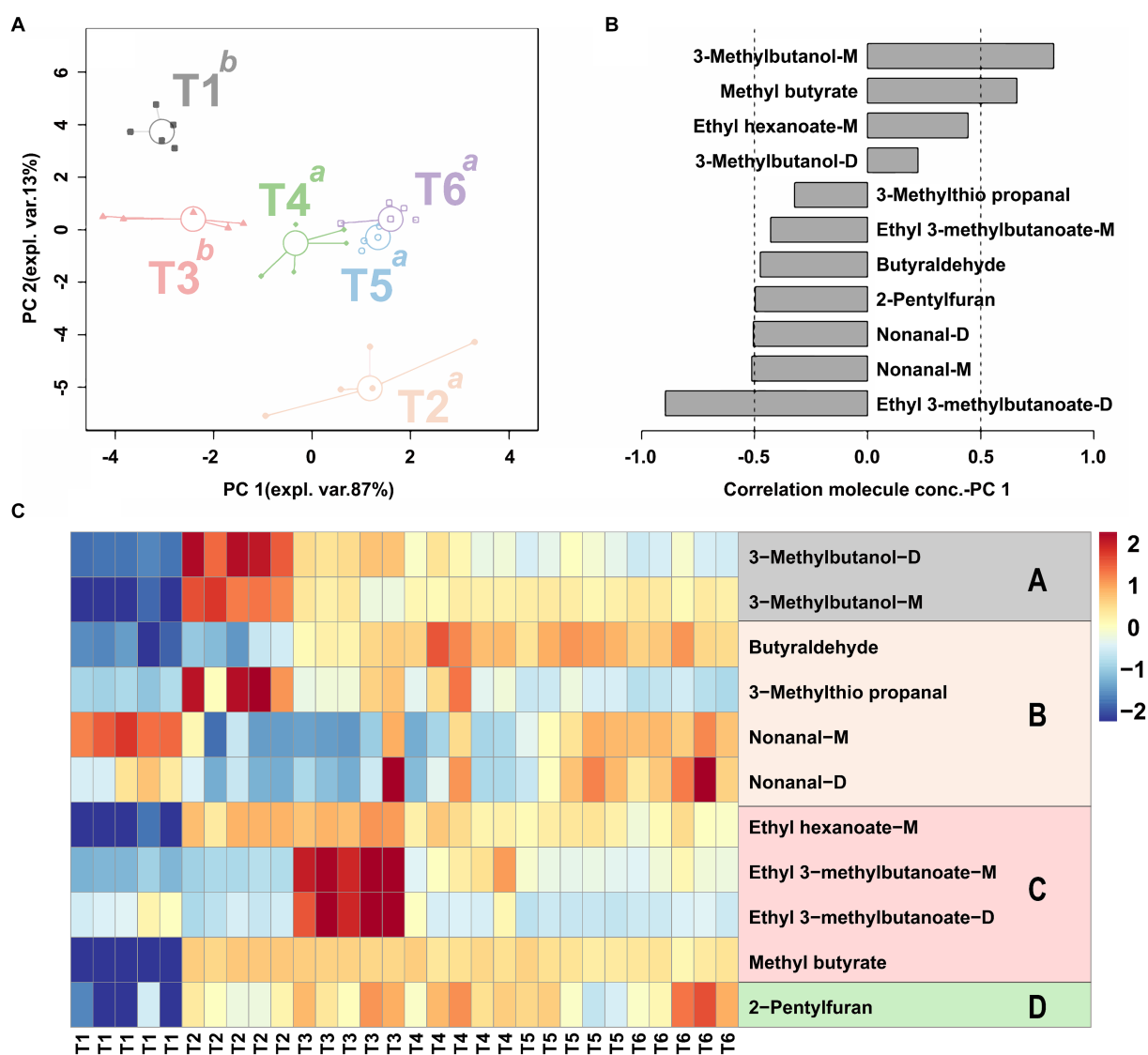
FIGURE 6

The rPCA model calculated based on the peak intensity has relative odor activity aroma compounds show significant differences in the peak intensity. The score plot **(A)** shows the overall trend of the sample in six stages of SBD. Superscript lowercase letters indicate significant differences between samples on PC 1. The loading plot **(B)** evidences significant correlations ($p < 0.05$) between the peak intensity of each VOCs and its importance over PC 1. The heat maps **(C)** depict aroma compounds' relative odor activity in the SBD model at different stages, with letters A−D representing alcohols, aldehydes, esters, and heterocycles, respectively.

amino acid analyzer is the most common method for detecting taste components of meat products (12, 32, 33).

A total of 66 volatiles and 19 free amino acids, including alcohols, esters, aldehydes, heterocycles, ketones, acids and alkenes compounds, were successfully identified during the of processing SBD. To further clarify the contribution of aroma compounds to the odor activity of SBD, the characteristic aroma markers of SBD were screened by calculating ROAV value. A sum of 11 volatile compounds were obtained as characteristic markers (ROAV > 1). 3-Methylbutanol-D, 3-Methylbutanol-M, and 3-Methylthio propanal are the main aroma contributors during the marinating stage. Ethyl 3-methyl butanoate-M and Ethyl 3-methyl butanoate-D are the main aroma contributors in the seasoning stage. However, it is worthy to note that the ROAV values of 11 characteristic aroma marker compounds are the highest when the steaming time is 40 min (T5), indicating that the steaming

further promotes the formation of SBD aroma. This is due to thermal degradation and the Maillard reaction that occur during the steaming process (34). This is also consistent with the research results of Gruffat which showed that the thermal degradation of lipids and Maillard reaction further promote the formation of meat aroma (35).

Alcohols mainly from polyunsaturated fatty acids and lipids degradation, which help to form the ideal aroma. Although alcohols exert a less pronounced influence on meat aroma compared to aldehydes, they play an important role in the overall aroma formation of SBD. The alcohols substance found in this investigation was 3-Methylbutanol. It rises gradually during the steaming process and reaches its highest level at the end of the steaming. Which provides the alcohol and bananas flavor for SBD and was also found in beef aged by Yu et al. (36). During the steaming process, the key factor in producing flavor was by promoting thermal oxidation reactions (37,
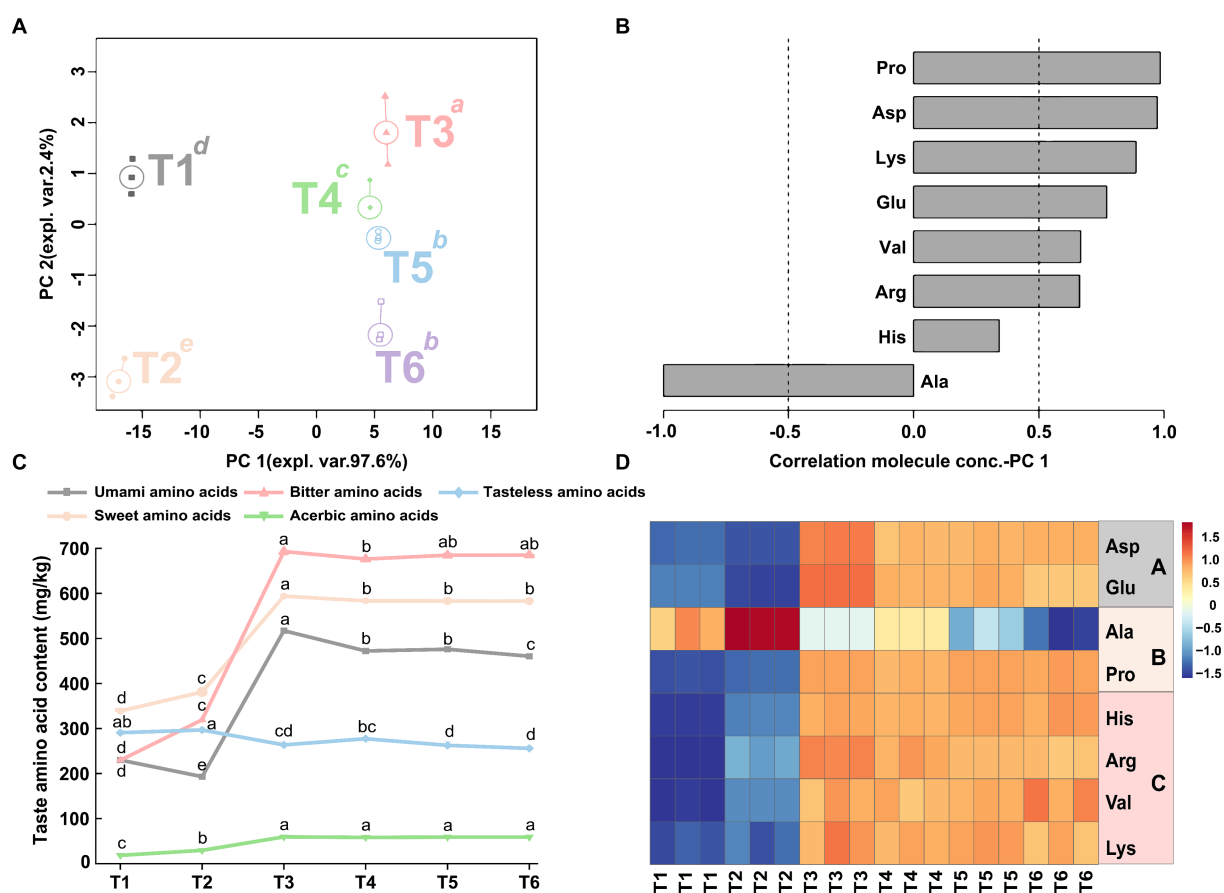
FIGURE 7
The rPCA model was established based on the content of amino acids with taste characteristics in SBD samples. The score plot **(A)** illustrates the overall trend of the samples. Lowercase superscript letters indicate significant differences ($p < 0.05$) between samples on PC1. Each sample group is depicted by a circle indicating its median value. The load plots **(B)** showcase the correlation between the taste activity value of each free amino acid and their significance on PC 1. The line graph **(C)** shows the variation trend of taste of T1–T6. The heat map **(D)** shows the ingredients with taste modifications in taste activity value of T1–T6, with the letters A–C representing umami, sweet, and bitter amino acids, respectively.

38). This can also partially explain why the contribution of 3-Methylbutanol aroma to SBD increases with the prolonged steaming time. In addition, the formation pathways of characteristic flavor of meat also include Maillard reaction and Strecker degradation reaction, lipid and Maillard interaction, including esters and aldehydes (39–41).

Esters, such as Ethyl hexanoate, Ethyl 3-methylbutanoate, and Methyl butyrate, are commonly present in fermented foods like fermented soybeans and jams (2, 42). These esters have a low odor threshold which enables them to contribute to the distinctive aroma of fennel and fruity in SBD (43). Some of the Ethyl 3-methylbutanoate in SBD may come from the flavoring added during the seasoning stage, which may contribute to a superior fruity flavor and fennel aroma.

Aldehydes are secondary by-products of lipid oxidation and are important volatiles in all meat products, affected by processing techniques, temperature and duration (18, 44). In this study, the aldehyde compounds of SBD were mainly formed during the steaming process. Although they have a low threshold, they play a crucial role in the overall odor profile of SBD. As the stewing time increases, the trend of aldehyde compounds increasing gradually can be observed, and the aromatic aldehydes observed during this process are mainly straight-chain aldehydes, like Nonanal and Butyraldehyde. These aldehydes have citrus, cucumber, banana, and spicy odor

characteristics resulting from the oxidative thermal degradation of linoleic acid (45). 3-Methylthio propanal, a branched aldehyde obtained by the Sterck degradation of branched amino acids, will provide the characteristic aroma of cooked potato for SBD (46).

In terms of free amino acid analysis, there were significant differences in the 19 free amino acids of SBD, and the total amino acid content was the highest in the seasoning stage (Supplementary Table S1). Further calculation of taste activity value showed that the TAV value of a taste compound Glu was greater than 1, indicating that the taste of SBD can be detected online by labeling Glu, while Asp, Ala, His, Arg, Val, Lys can be used as potential taste markers for online detection of SBD taste. Glu serves as the hallmark amino acid for umami, the fifth primary taste sensation alongside sweet, sour, salty, and bitter (47). This distinctive taste perception primarily arises from the recognition of protein-coupled receptors specific to glutamate, such as mGluR4 and the heteromeric T1R1 + T1R3 receptor (48), while the combination of Ala and Glu can enhance the freshness of SBD, which is consistent with Jiang et al.'s research results (28). In addition, the study also found that the content of umami, sweet and bitter amino acids was the highest in the seasoning stage. As the steaming time increases, the flavor amino acids showed varying degrees of reduction, which may be due to the heat treatment under high heat conditions through the

Maillard reaction to convert into small molecule aroma compounds including aldehydes, ketones, esters and alcohols (32, 49).

5 Conclusion

In this study, the E-nose and E-tongue in intelligent sensory technology were combined with an amino acid analyzer and HS-GC-IMS to track the aroma and taste changes of the SBD throughout the manufacturing process. The results showed that the intelligent sensory system can effectively recognize SBD's aroma and taste characteristics. By HS-GC-IMS, 66 volatile organic compounds (VOCs) were successfully identified and further using the results of relative odor activity value (ROAV) assessment, it was shown that nine of these VOCs were essential for aroma contribution, namely. 3-Methylbutanol, 2-Pentylfuran, 3-Methylthio propanal, Ethyl hexanoate, Ethyl 3-methylbutanoate, Nonanal, Methyl butyrate and Butyraldehyde. Nineteen free amino acids were detected, and the subsequent taste activity value (TAV) revealed that Glu significantly contributed to the umami taste of SBD. Additionally, it was found that the Seasoning stage (T3) and Steaming (T5) played a crucial role in developing the SBD flavor. This study analyses the aroma and taste dynamics during the production of SBD to provide theoretical guidance and insights into the quality qualities of SBD during industrial processing to a certain extent.

Data availability statement

The datasets presented in this study can be found in online repositories. The names of the repository/repositories and accession number(s) can be found in the article/Supplementary material.

Author contributions

TW: Writing – original draft, Writing – review & editing. LY: Writing – review & editing. YX: Writing – review & editing. BW: Writing – review & editing. YL: Writing – review & editing. MQ: Writing – review & editing. CZ: Writing – review & editing. HW: Writing – review & editing. JD: Funding acquisition, Resources, Writing – review & editing. JG: Writing – review & editing, Formal analysis, Methodology.

Conflict of interest

The authors declare that the research was conducted in the absence of any commercial or financial relationships that could be construed as a potential conflict of interest.

Publisher's note

All claims expressed in this article are solely those of the authors and do not necessarily represent those of their affiliated organizations, or those of the publisher, the editors and the reviewers. Any product that may be evaluated in this article, or claim that may be made by its manufacturer, is not guaranteed or endorsed by the publisher.

Supplementary material

The Supplementary material for this article can be found online at: https://www.frontiersin.org/articles/10.3389/fnut.2024.1435364/full#supplementary-material

References

1. Ahn H-J, Kim J-H, Jo C, Lee J-W, Yook H-S, Byun M-W. Effects of gamma irradiation on residual nitrite, residual ascorbate, color, and N-nitrosamines of cooked sausage during storage. *Food Control*. (2004) 15:197–203. doi: 10.1016/S0956-7135(03)00047-1

2. Xia A-N, Tang X-J, Dong G-Z, Lei S-M, Liu Y-G, Tian X-M. Quality assessment of fermented rose jams based on physicochemical properties, HS-GC-MS and HS-GC-IMS. *LWT*. (2021) 151:112153. doi: 10.1016/j.lwt.2021.112153

3. Wang Z, Cai R, Yang X, Gao Z, Yuan Y, Yue T. Changes in aroma components and potential Maillard reaction products during the stir-frying of pork slices. *Food Control*. (2021) 123:107855. doi: 10.1016/j.foodcont.2020.107855

4. Bai S, Wang Y, Luo R, Shen F, Bai H, Ding D. Formation of flavor volatile compounds at different processing stages of household stir-frying mutton sao zi in the northwest of China. *LWT*. (2021) 139:110735. doi: 10.1016/j.lwt.2020.110735

5. Li W, Zheng L, Xiao Y, Li L, Wang N, Che Z, et al. Insight into the aroma dynamics of Dongpo pork dish throughout the production process using electronic nose and GC×GC-MS. *LWT*. (2022) 169:113970. doi: 10.1016/j.lwt.2022.113970

6. Chen J, Cai X, Liu J, Yuan C, Yi Y, Qiao M. Investigation of different ingredients affected the flavor changes of Yu-Shiang shredded pork by using GC-IMS and GC-MS combined with E-nose and E-tongue. *Heliyon*. (2024) 10:e31486. doi: 10.1016/j.heliyon.2024.e31486

7. Zhu C, Yang Z, Lu X, Yi Y, Tian Q, Deng J, et al. Effects of *Saccharomyces cerevisiae* strains on the metabolomic profiles of Guangan honey pear cider. *LWT*. (2023) 182:114816. doi: 10.1016/j.lwt.2023.114816

8. Wu W, Wang X, Hu P, Zhang Y, Li J, Jiang J, et al. Research on flavor characteristics of beef cooked in tomato sour soup by gas chromatography-ion mobility spectrometry and electronic nose. *LWT*. (2023) 179:114646. doi: 10.1016/j.lwt.2023.114646

9. Nie S, Li L, Wang Y, Wu Y, Li C, Chen S, et al. Discrimination and characterization of volatile organic compound fingerprints during sea bass (Lateolabrax japonicas) fermentation by combining GC-IMS and GC-MS. *Food Biosci*. (2022) 50:102048. doi: 10.1016/j.fbio.2022.102048

10. Lu W, Chen J, Li X, Qi Y, Jiang R. Flavor components detection and discrimination of isomers in Huaguo tea using headspace-gas chromatography-ion mobility

spectrometry and multivariate statistical analysis. *Anal Chim Acta*. (2023) 1243:340842. doi: 10.1016/j.aca.2023.340842

11. Zhang Q, Ma J, Yang Y, Deng J, Zhu K, Yi Y, et al. Effects of *S. cerevisiae* strains on the sensory characteristics and flavor profile of kiwi wine based on E-tongue, GC-IMS and 1H-NMR. *LWT*. (2023) 185:115193. doi: 10.1016/j.lwt.2023.115193

12. Wang S, Chen H, Sun B. Recent progress in food flavor analysis using gas chromatography–ion mobility spectrometry (GC–IMS). *Food Chem*. (2020) 315:126158. doi: 10.1016/j.foodchem.2019.126158

13. Lin R, Yuan H, Wang C, Yang Q, Guo Z. Study on the flavor compounds of Fo Tiao Qiang under different thawing methods based on GC–IMS and electronic tongue technology. *Food Secur*. (2022) 11:1330. doi: 10.3390/foods11091330

14. Lu L, Hu Z, Hu X, Li D, Tian S. Electronic tongue and electronic nose for food quality and safety. *Food Res Int*. (2022) 162:112214. doi: 10.1016/j. foodres.2022.112214

15. Yao W, Cai Y, Liu D, Chen Y, Li J, Zhang M, et al. Analysis of flavor formation during production of Dezhou braised chicken using headspace-gas chromatography-ion mobility spectrometry (HS-GC-IMS). *Food Chem*. (2022) 370:130989. doi: 10.1016/j. foodchem.2021.130989

16. Xiong Y, Guan J, Wu B, Wang T, Yi Y, Tang W, et al. Exploring the profile contributions in Meyerozyma guilliermondii YB4 under different NaCl concentrations using GC-MS combined with GC-IMS and an electronic nose. *Molecules*. (2023) 28:6979. doi: 10.3390/molecules28196979

17. Wu B, Zhu C, Deng J, Dong P, Xiong Y, Wu H. Effect of Sichuan pepper (zanthoxylum genus) addition on flavor profile in fermented ciba chili (capsicum genus) using GC-IMS combined with E-nose and E-tongue. *Molecules*. (2023) 28:5884. doi: 10.3390/molecules28155884

18. Chen J, Tao L, Zhang T, Zhang J, Wu T, Luan D, et al. Effect of four types of thermal processing methods on the aroma profiles of acidity regulator-treated tilapia muscles using E-nose, HS-SPME-GC-MS, and HS-GC-IMS. *LWT*. (2021) 147:111585. doi: 10.1016/j.lwt.2021.111585

19. Wang Y, Wang D, Lv Z, Zeng Q, Fu X, Chen Q, et al. Analysis of the volatile profiles of kiwifruits experiencing soft rot using E-nose and HS-SPME/GC–MS. *LWT*. (2023) 173:114405. doi: 10.1016/j.lwt.2022.114405

20. Deng Y, Wang R, Zhang Y, Li X, Gooneratne R, Li J. Comparative analysis of flavor, taste, and volatile organic compounds in opossum shrimp paste during long-term natural fermentation using E-nose, E-tongue, and HS-SPME-GC-MS. *Food Secur*. (2022) 11:1938. doi: 10.3390/foods11131938

21. Liu N, Shen S, Huang L, Deng G, Wei Y, Ning J, et al. Revelation of volatile contributions in green teas with different aroma types by GC–MS and GC–IMS. *Food Res Int*. (2023) 169:112845. doi: 10.1016/j.foodres.2023.112845

22. Xu Y, Zhang D, Liu H, Wang Z, Hui T, Sun J. Comprehensive evaluation of volatile and nonvolatile compounds in oyster cuts of roasted lamb at different processing stages using traditional Nang roasting. *Food Secur*. (2021) 10:1508. doi: 10.3390/foods10071508

23. Cai X, Zhu K, Li W, Peng Y, Yi Y, Qiao M, et al. Characterization of flavor and taste profile of different radish (*Raphanus Sativus* L.) varieties by headspace-gas chromatography-ion mobility spectrometry (GC/IMS) and E-nose/tongue. *Food Chem X*. (2024) 22:101419. doi: 10.1016/j.fochx.2024.101419

24. Lu Y, Wang Y, Zhao G, Yao Y. Identification of aroma compounds in Zhuhoujiang, a fermented soybean paste in Guangdong China. *LWT*. (2021) 142:111057. doi: 10.1016/j.lwt.2021.111057

25. Xu J, Zhang Y, Yan F, Tang Y, Yu B, Chen B, et al. Monitoring changes in the volatile compounds of tea made from summer tea leaves by GC-IMS and HS-SPME-GC-MS. *Food Secur*. (2022) 12:146. doi: 10.3390/foods12010146

26. Gao L, Zhang L, Liu J, Zhang X, Lu Y. Analysis of the volatile flavor compounds of pomegranate seeds at different processing temperatures by GC-IMS. *Molecules*. (2023) 28:2717. doi: 10.3390/molecules28062717

27. Fang X, Xu W, Jiang G, Sui M, Xiao J, Ning Y, et al. Monitoring the dynamic changes in aroma during the whole processing of Qingzhuan tea at an industrial scale: from fresh leaves to finished tea. *Food Chem*. (2024) 439:137810. doi: 10.1016/j. foodchem.2023.137810

28. Jiang S, Zhu Y, Peng J, Zhang Y, Zhang W, Liu Y. Characterization of stewed beef by sensory evaluation and multiple intelligent sensory technologies combined with chemometrics methods. *Food Chem*. (2023) 408:135193. doi: 10.1016/j. foodchem.2022.135193

29. Box GEP, Cox DR. An analysis of transformations. *J Roy Stat Soc Ser B*. (2018) 26:211–43. doi: 10.1111/j.2517-6161.1964.tb00553.x

30. Zhou B, Liu X, Lan Q, Wan F, Yang Z, Nie X, et al. Comparison of aroma and taste profiles of kiwi wine fermented with/without peel by combining intelligent sensory, gas chromatography-mass spectrometry, and proton nuclear magnetic resonance. *Food Secur*. (2024) 13:1729. doi: 10.3390/foods13111729

31. Hubert M, Rousseeuw PJ. ROBPCA: a new approach to robust principal component analysis. *Technometrics*. (2005) 47:64–79. doi: 10.1198/004017004000000563

32. Chu Y, Ding Z, Wang J, Xie J. Exploration of the evolution and production of volatile compounds in grouper (*Epinephelus coioides*) during cold storage. *Food Biosci*. (2023) 52:102496. doi: 10.1016/j.fbio.2023.102496

33. Zhang Z, Sun H, Liu J, Zhang H, Huang F. Changes in eating quality of Chinese braised beef produced from three different muscles. *Int J Gastron Food Sci*. (2022) 29:100584. doi: 10.1016/j.ijgfs.2022.100584

34. Zhang M, Chen M, Fang F, Fu C, Xing S, Qian C, et al. Effect of sous vide cooking treatment on the quality, structural properties and flavor profile of duck meat. *Int J Gastron Food Sci*. (2022) 29:100565. doi: 10.1016/j.ijgfs.2022.100565

35. Gruffat D, Bauchart D, Thomas A, Parafita E, Durand D. Fatty acid composition and oxidation in beef muscles as affected by ageing times and cooking methods. *Food Chem*. (2021) 343:128476. doi: 10.1016/j.foodchem.2020.128476

36. Yu H, Zhang S, Liu X, Lei Y, Wei M, Liu Y, et al. Comparison of physiochemical attributes, microbial community, and flavor profile of beef aged at different temperatures. *Front Microbiol*. (2022) 13:1091486. doi: 10.3389/fmicb.2022.1091486

37. Wojtasik-Kalinowska I, Szpicer A, Binkowska W, Hanula M, Marcinkowska-Lesiak M, Poltorak A. Effect of processing on volatile organic compounds formation of meat—review. *Appl Sci*. (2023) 13:705. doi: 10.3390/app13020705

38. Li J, Han D, Huang F, Zhang C. Effect of reheating methods on eating quality, oxidation and flavor characteristics of braised beef with potatoes dish. *Int J Gastron Food Sci*. (2023) 31:100659. doi: 10.1016/j.ijgfs.2023.100659

39. Rao J, Meng F, Li Y, Chen W, Liu D, Zhang J. Effect of cooking methods on the edible, nutritive qualities and volatile flavor compounds of rabbit meat. *J Sci Food Agric*. (2022) 102:4218–28. doi: 10.1002/jsfa.11773

40. Cheng L, Li X, Tian Y, Wang Q, Li X, An F, et al. Mechanisms of cooking methods on flavor formation of Tibetan pork. *Food Chem X*. (2023) 19:100873. doi: 10.1016/j. fochx.2023.100873

41. Liu Z, Huang Y, Kong S, Miao J, Lai K. Selection and quantification of volatile indicators for quality deterioration of reheated pork based on simultaneously extracting volatiles and reheating precooked pork. *Food Chem*. (2023) 419:135962. doi: 10.1016/j. foodchem.2023.135962

42. Chen Y, Li P, Liao L, Qin Y, Jiang L, Liu Y. Characteristic fingerprints and volatile flavor compound variations in Liuyang Douchi during fermentation via HS-GC-IMS and HS-SPME-GC-MS. *Food Chem*. (2021) 361:130055. doi: 10.1016/j. foodchem.2021.130055

43. Xie B, Xu Y, Yao Z, Zhu B, Li X, Sun Y. Effects of different thermal treatment temperatures on volatile flavour compounds of water-boiled salted duck after packaging. *LWT*. (2022) 154:112625. doi: 10.1016/j.lwt.2021.112625

44. Yang Y, Zhang X, Wang Y, Pan D, Sun Y, Cao J. Study on the volatile compounds generated from lipid oxidation of Chinese bacon (unsmoked) during processing. *Euro J Lipid Sci Tech*. (2017) 119:1600512. doi: 10.1002/ejlt.201600512

45. Zeng Z, Zhang H, Chen JY, Zhang T, Matsunaga R. Direct extraction of volatiles of Rice during cooking using solid-phase microextraction. *Cereal Chem*. (2007) 84:423–7. doi: 10.1094/CCHEM-84-5-0423

46. Martínez-Onandi N, Rivas-Cañedo A, Nuñez M, Picon A. Effect of chemical composition and high pressure processing on the volatile fraction of serrano dry-cured ham. *Meat Sci*. (2016) 111:130–8. doi: 10.1016/j.meatsci.2015.09.004

47. Kondoh T, Torii K. MSG intake suppresses weight gain, fat deposition, and plasma leptin levels in male Sprague–Dawley rats. *Physiol Behav*. (2008) 95:135–44. doi: 10.1016/j.physbeh.2008.05.010

48. Kong Y, Yang X, Ding Q, Zhang Y-Y, Sun B-G, Chen H-T, et al. Comparison of non-volatile umami components in chicken soup and chicken enzymatic hydrolysate. *Food Res Int*. (2017) 102:559–66. doi: 10.1016/j.foodres.2017.09.038

49. Khan MI, Jo C, Tariq MR. Meat flavor precursors and factors influencing flavor precursors—a systematic review. *Meat Sci*. (2015) 110:278–84. doi: 10.1016/j. meatsci.2015.08.002

Development of an ic-CLEIA for precise detection of 3-CQA in herbs and patent medicines: ensuring quality control and therapeutic efficacy

Longjiang Wu[1], Mei Dang[1,2], Rao Wu[1], Murtala Bindawa Isah[1,3,4] and Xiaoying Zhang[1,5,6]*

[1]Chinese-German Joint Institute for Natural Product Research, Shaanxi International Cooperation Demonstration Base, Shaanxi University of Technology, Hanzhong, China, [2]Department of Biological Sciences, Faculty of Science, National University of Singapore, Singapore, Singapore, [3]Department of Biochemistry, Faculty of Natural and Applied Sciences, Umaru Musa Yar'adua University Katsina, Katsina, Nigeria, [4]Biomedical Research and Training Centre, Yobe State University, Damaturu, Nigeria, [5]Centre of Molecular and Environmental Biology, Department of Biology, University of Minho, Braga, Portugal, [6]Department of Biomedical Sciences, Ontario Veterinary College, University of Guelph, Guelph, ON, Canada

Background: 3-caffeoylquinic acid (3-CQA), a member of the chlorogenic acid family, possesses diverse pharmacological properties, such as scavenging, antioxidant, and antiapoptotic activity, rendering substantial value to alimentary consumables and therapeutic substances. However, the pervasiveness of non-standard practices, notably the misuse and abuse of indigenous botanicals, coupled with the inherent susceptibility of 3-CQA to degradation under light and heat exposure, engenders discernible disparateness in the quality profiles of the same kinds of herbs. Consequently, precise quantification of 3-CQA becomes imperative.

Methods: In this context, an artificial antigen was synthesized as a specific conjugate of 3-CQA and bovine serum albumin (3-CQA-BSA), followed by the generation of a monoclonal antibody (mAb) against the conjugate. Through optimization, a mAb-based indirect competitive chemiluminescence enzyme immunoassay (ic-CLEIA) was developed.

Results: It demonstrated an IC_{50} and the calibration range of 2.97 ng/mL and 0.64–13.75 ng/mL, respectively, outperforming the conventional enzyme-linked immunosorbent assay (ELISA). Notably, the ic-CLEIA displayed 10.71% cross-reactivity with 3,5-dicaffeoylquinic acid, alongside minimal cross-reactivity toward other isomeric counterparts and analogs. Validation experiments on herbs and Chinese patent medicines using ic-CLEIA, confirmed by high-performance liquid chromatography (HPLC) analysis, revealed a robust correlation coefficient of 0.9667 between the two modalities.

Conclusion: These findings unequivocally demonstrated that the proposed ic-CLEIA represents a viable and reliable analytical method for 3-CQA determination. This method holds significant potential for ensuring the quality control and therapeutic efficacy germane to herbs and patent medicines, spanning diverse therapeutic milieus and applications.

1 Introduction

Phenolic compounds, as secondary metabolites of plants, have garnered significant attention in recent years due to their remarkable bioactivity (1–3). Among these compounds, chlorogenic acids (CGAs), a class of phenolic acids, have particularly attracted interest owing to their antioxidative and free radical-scavenging properties (4, 5). CGAs comprise a family of esters derived from quinic acid and specific trans-cinnamic acids, predominantly caffeic, p-coumaric, and ferulic acid. Within the CGA family, although the quantification of 5-caffeoylquinic acid (5-CQA) has been extensively reported (6, 7), limited research exists on its structural isomers like 3-caffeoylquinic acid (3-CQA) and 4-caffeoylquinic acid (4-CQA).

Considering this, this study focuses on 3-CQA, an ester of caffeic acid and (−)-quinic acid. On the one hand, 3-CQA displays intriguing biological effects, low toxicity, and promising commercial value. Notably, it acts as the primary active ingredient in *Honeysuckle* and *Euphorbia*, demonstrating antibacterial, antiviral, antioxidant, anti-inflammatory, hypolipidemic, and neuroprotective effects (Figure 1) (8–11). Recently, it has been reported to alleviate and prevent diabetes mellitus and associated complications such as diabetic nephropathy and diabetic retinopathy (12). In addition, 3-CQA has shown promise in countering high-fat diet (HFD)-induced activation of the TLR4 signaling pathway and the expression of *TNF-α* and *IL-6* in the liver, thus ameliorating non-alcoholic fatty liver disease (NAFLD) (13). On the other hand, beyond its presence in *Honeysuckle* and *Euphorbia*, 3-CQA is widely distributed in other plants of the *Euphorbiaceae*, *Lonicerae*, and *Soniaceae*
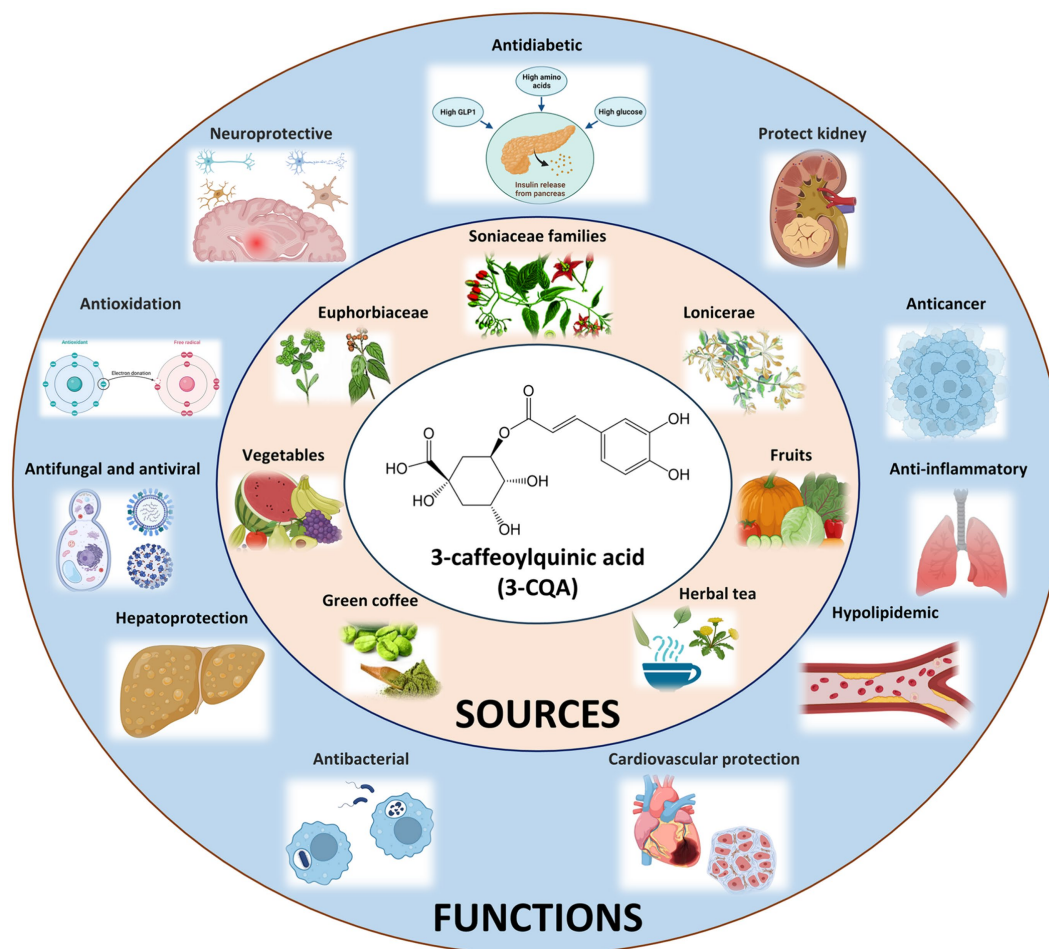

FIGURE 1
Origins and Bioactive Impacts of 3-CQA. The chemical structure of 3-CQA is represented within the white circle, sources of 3-CQA are delineated within the pink circle, and the bioactive effects of 3-CQA are elucidated within the blue circle.

families, as well as in various vegetables and fruits (Figure 1) (14–17). However, the prevalence of non-standard practices, along with the vulnerability of the compound *per se* to degradation from light and heat, often leads to considerable variations and challenges in quality control.

Given the impressive pharmacological activities and the scarcity of quantification studies, there is an imperative demand for the development of analytical methods for 3-CQA-containing herbs and associated products. In this context, we capitalized on the intrinsic advantages of canonical chemiluminescence enzyme-linked immunosorbent assay (CLEIA) over other instrumental techniques and traditional immunoassays, particularly in terms of high sensitivity, time-saving, ease of operation, and high-throughput evaluation. Specifically, we generated an artificial antigen by chemically conjugating 3-CQA with bovine serum albumin (BSA) and produced a monoclonal antibody (mAb). Following the optimization of the reaction system, a mAb-based indirect competitive CLEIA (ic-CLEIA) was developed, with a half-maximum inhibitory concentration (IC$_{50}$ value) of 2.97 ng/mL and a calibration range of 0.64–13.75 ng/mL, surpassing those of the conventional enzyme-linked immunosorbent assay (ELISA). Further cross-reactivity (CR) tests revealed that the established ic-CLEIA offered favorable specificity to 3-CQA. Moreover, we determined 3-CQA content in six herbs and seven patient medicine samples, with the results showing a strong correlation coefficient of 0.9667 between the ic-CLEIA and high-performance liquid chromatography (HPLC).

These findings indicate that the proposed ic-CLEIA enables rapid, simple, and environmentally friendly detection of 3-CQA. More importantly, to our knowledge, this study represents the first incorporation of ic-CLEIA into the quantification of 3-CQA, holding significant potential for ensuring the quality control of herbal products and patent medicines across various applications. Our study thus

serves as an instructive example for 3-CQA determination and opens avenues for extending the application of this method to the quantification of other molecules within the CGA family.

2 Materials and methods

2.1 Preparation of artificial antigens

The 3-CQA artificial antigen was synthesized through the carbodiimide method (Figure 2) (18). All chemicals utilized were of analytical grade and purchased from Sigma (St Louis, MO, United States). Initially, 30 mg of either BSA or ovalbumin (OVA), 6 mg of 6-aminohexanoic acid, and 25 mg of 1-ethyl-3 (3-dimethylaminopropyl) carbodiimide (EDAC) were precisely weighted and dissolved in an 8 mL solution of 2-(N-morpholino) ethanesulfonic acid. The mixture was stirred at room temperature for 12 h. Upon reaction completion, the mixture was transferred to a dialysis bag and subjected to dialysis in phosphate-buffered saline (PBS) at 4°C for 72 h, yielding a solution of aminated carrier protein. Subsequently, 7.09 mg of 3-CQA, along with 4.38 mg of N-hydroxysuccinimide (NHS) and 3.3 mg of EDAC were weighed and dissolved in 500 μL N, N-dimethylformamide (DMF). The reaction was conducted at 17°C, 130 rpm for 16 h to generate the activated intermediate of 3-CQA. This activated intermediate was then added dropwise to the aminated carrier protein solution. Followed by stirring overnight, the mixture was dialyzed against 10 mM PBS, (pH 7.4) at 4°C for 2 days, with the dialysis solution changed four times, ensuring the removal of any unreacted 3-CQA. The resulting 3-CQA-BSA and 3-CQA-OVA bio-conjugates were finally stored at −20°C until use. Spectroscopic analysis was conducted using a Specord 50 UV–VIS
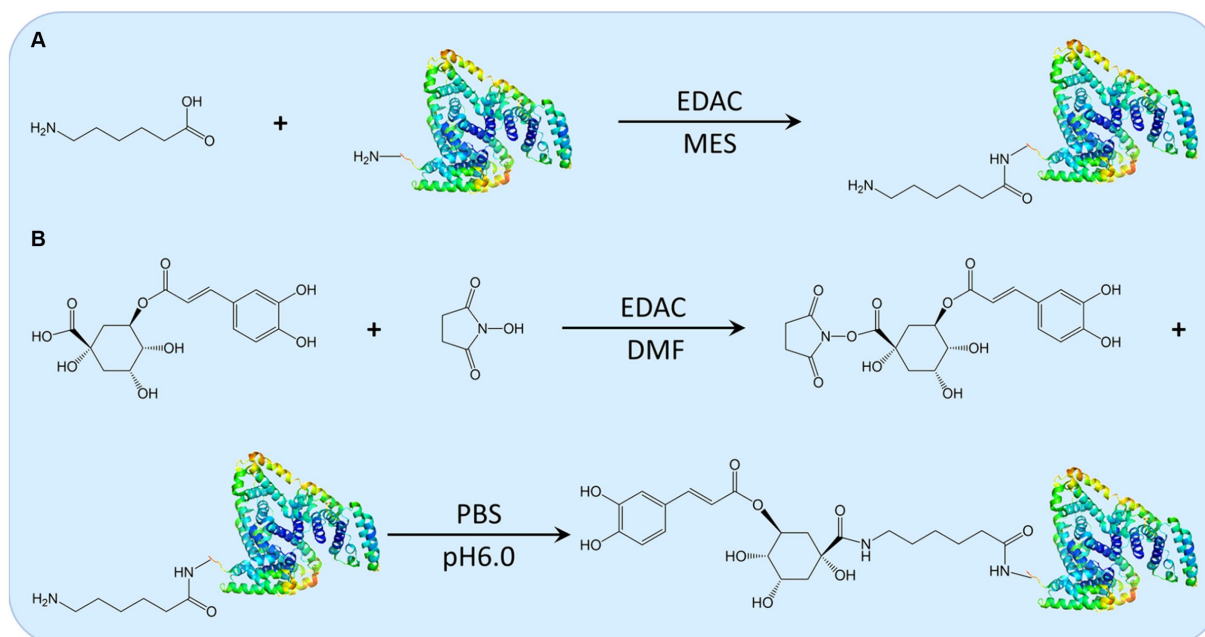

FIGURE 2
The schematic illustration of the synthesis route for 3-CQA-BSA Conjugate. Depiction of the synthesis routes for the aminated carrier protein **(A)** and the activated intermediate 3-CQA, along with the 3-CQA-BSA bio-conjugate **(B)**.

spectrophotometer (Analytik AG, Jena, Germany) to confirm the successful coupling of 3-CQA to the carrier protein.

2.2 Generation of monoclonal antibody

The hybridoma technique was employed to produce the monoclonal antibody as follows. Six female BALB/c mice (6 to 10 weeks old) were obtained from Beijing HFK Bio-technology (Beijing, China). Following 2 weeks of adaptive feeding, the mice were immunized with equal amounts of 3-CQA-BSA (1 mg/mL, dissolved in PBS) and Freund's complete adjuvant (Sigma, St Louis, MO, United States). Subsequently, four booster injections were administered at two-week intervals, each containing 3-CQA-BSA solution emulsified with Freund's incomplete adjuvant (Sigma, St Louis, MO, United States). After the fifth injection, blood samples were collected from each mouse and centrifuged. The specificity of the obtained serum was determined using an indirect competitive ELISA (ic-ELISA). The positive mice were then identified, and splenocytes from these mice were fused with sp2/0 mouse myeloma cells (ATCC, Manassas, VA, United States) using PEG4000 at 37°C. Hybridomas were sequentially cultivated in HAT medium (containing hypoxanthine, aminopterin, and thymidine) and HT medium (lacking amino purine) at 37°C in a CO_2 incubator (Thermo, Franklin, MA, United States) after fusion. After 10 days, subclone culture of surviving hybridoma cells was performed using a limited dilution method, and positive clones were detected by ic-ELISA. The identified clones were further amplified to produce ascites, which were then purified using the ammonium sulfate precipitation method [19]. Following dialysis against H_2O for 48 h, the mAb was lyophilized. The purity and concentration of purified mAb were determined by sodium dodecyl sulfate polyacrylamide gel electrophoresis (SDS-PAGE) and a BCA Protein Assay Kit (Sangon biotech, Shanghai, China), respectively. The isotype of mAb was identified using a mouse monoclonal antibody isotyping kit (Sino Biological, Beijing, China).

All the procedures described above complied with the Chinese Regulations of Laboratory Animals and were approved by the institutional experimental animal ethics committee (Chinese-German Joint Institute for Natural Product Research, Shaanxi University of Technology, and Approval Number 2021–01).

2.3 Optimization of working buffer and establishment of the standard curve for ic-CLEIA

To establish the optimal conditions for the ic-CLEIA, a checkerboard titration was employed. The protocols of the ic-CLEIA were performed as previously [20]. A gradient concentration of 3-CQA-OVA (0.125, 0.5, 2.0, and 8.0 μg/mL; 100 μL/well) was diluted in PBS and added to a 96-well white microliter plate (Costar Inc., Cambridge, MA, United States), followed by incubation at 4°C overnight. After washing each well three times with PBST (PBS solution containing 0.05% Tween-20, pH 7.4), the plates were blocked with 5% skimmed milk powder (SMP) (Sigma, St Louis, MO, United States) in PBS (200 μL/well) at 37°C for 2 h. Subsequently, different concentrations of mAb (1:2000, 1:4000, 1:8000, 1:16000, 1:32000, 1:64000, and 1:128000; 100 μL/well) were

added to different wells, followed by incubation at 4°C for 50 min. For ic-CLEIA standard curve, 3-CQA standard solutions in PBS (0.01, 0.025, 0.05, 0.1, 0.25, 0.5, 1, 2.5, 5, 10, 25, 50, and 100 ng/mL; 50 μL) and the diluted antibody in PBS (50 μL) were added to each well and incubated at 4°C for 50 min. After a washing step, goat anti-mouse IgG-horse radish peroxidase (HRP) (SinoBiological, Beijing, China) dissolved in PBS supplemented with 2% SMP was added at a 1:5000 dilution (100 μL/well), and the plates were incubated at 37°C for 50 min. Afterward, 100 μL of chemiluminescent substrate solution (Heliosense Biotechnology, Xiamen, China) was pipetted into each well, and the emitted photons were immediately read at 595 nm using a Tecan Infinite F200 reader (Mannedorf, Switzerland). To investigate the effects of different factors on the overall reaction system, different pH (6.5, 7.0, 7.4, and 8.0), methanol aqueous solution (5, 10, 30, and 50%; v/v), Tween-20 (0.01, 0.02, 0.04, 0.06, and 0.08%, v/v), sodium chloride solution (0.1 M, 0.2 M, and 0.4 M) were prepared and tested.

All incubation steps were performed in the dark throughout the procedure. The competitive inhibition curves for 3-CQA were plotted using GraphPad Prism 8.0 (GraphPad Inc., San Diego, CA).

2.4 Establishment of the standard curve for ic-ELISA

The protocols of ic-ELISA are similar to the ic-CLEIA, 3-CQA-OVA antigen, anti-3-CQA mAb, and goat anti-mouse IgG-HRP were successively incubated under optimized conditions. 3-CQA standard solutions in PBS (1, 2, 4, 8, 16, 32, 64, 128, 256, and 512 ng/mL; 50 μL) and the diluted antibody in PBS (50 μL) were added to each well and incubated at 4°C for 50 min. Subsequent to four washes, 3, 3′, 5, 5′-tetramethylbenzidine (TMB, 100 μL/well) solution was added and incubated at 37°C for 10 min. The reaction was then terminated by adding 2 M H_2SO_4 (50 μL/well), and the absorbance was measured at the wavelength of 450 nm (OD_{450}). The competitive inhibition curve was plotted using $Lg[10*C_{3\text{-CQA}}$ (ng/mL)] as the abscissa and B/B_0 (B_0 is the OD_{450} value without standard, and B is the OD_{450} value with standard present) as the ordinate.

2.5 Cross-reactivity assay

To evaluate CR, the structural analogs of 3-CQA including 4-CQA, 5-CQA, 3,5-dicaffeoylquinic acid, 4,5-dicaffeoylquinic acid, 3,4-dicaffeoylquinic acid, and tea polyphenols (DESITE Biotech, Chengdu, China) were used in place of 3-CQA within the ic-CLEIA assay. The respective CR values of these analogs were determined using the following equation:

$$CR(\%) = IC_{50}(3-CQA) / IC_{50}(3-CQA\ analogues) \times 100\%.$$

2.6 HPLC analysis

HPLC determination of 3-CQA was performed using a Dionex Ultimate 3,000 UHPLC system (Thermo Fisher Scientific,

Waltham, MA, United States). The method was established with reference to the Chinese Pharmacopeia (21). Briefly, 3-CQA solutions were prepared by dissolving in 50% methanol at different concentrations (25, 50, 100, 200, 400, and 800 μg/mL). Subsequently, the 3-CQA solutions were separated using a Shimadzu Intersil ODS3-C18 column (reversed-phase, 150 × 4.6 mm, 4.0 μm) with a mobile phase system consisting of acetonitrile and 0.4% (v/v) phosphoric acid aqueous. The remaining parameters were set as follows: column temperature = 30°C, injection volume = 10 μL, and detection wavelength = 327 nm (Supplementary Table S1), and the retention time of 3-CQA was 11.2 min. The standard curve of 3-CQA-HPLC was plotted based on the retention time of the 3-CQA reference. It was then used to extrapolate the amount of 3-CQA in the herbs and patent medicines.

2.7 Sample preparation and extraction of 3-CQA

Samples of six herbs (*Honeysuckle*, *Eucommia*, *Dandelion*, *Houttuynia*, *Virgate wormwood*, and *Lonicera* stem), seven Chinese patent medicines (*Shuang-Huang-Lian* capsule, Vitamin C *Yin-Qiao* tablet, *Yin-Zhi-Huang* granule, *Yin-Huang* granule, *Kou-Yan-Qing* granule, compound *Jin-Yin-Hua* granule, and *Jin-Sang-Zi* lozenge) were purchased from local pharmacies and supermarkets in Hanzhong, Shaanxi, China. The extraction of 3-CQA was conducted following the procedure prescribed in the Chinese Pharmacopeia (21). Each herb (0.1 g) and patent medicine (0.5 g) were ground into powder and dissolved in 50% methanol (5 mL). The resulting solutions were then subjected to sonication for 30 min at 250 W. After sonication, the extracts were weighed, and the lost weight was replenished with 50% methanol, followed by centrifugation at 4000 rpm for 5 min. The whole process was carried out under protected conditions to avoid exposure to light. The obtained supernatant was directly employed for immunoassay analysis after dilution. For HPLC analysis, the supernatant was further filtered through a 0.22 μm cellulose membrane prior to analysis.

2.8 Recovery analysis

A total of six samples, comprising three herbs and three patent medicines, were prepared in triplicate. For each sample, 0.5 mg and 1.0 mg of 3-CQA were added, leaving one sample remaining without the addition of 3-CQA as a control. The 3-CQA in the resulting mixture was extracted, followed by appropriate dilution for subsequent HPLC and ic-CLEIA analyses. Each spiked sample was measured four times in parallel. The spiked recoveries were calculated using the following formula:

$$\text{Recovery}\,(\%) = \left(C_{\text{Measured}}\,(mg/g) - C3 - CAQ_{\text{in unspiked samples}}\,(mg/g)\right) / C_{\text{Spike}}\,(mg/g) \times 100\%.$$

3 Results

3.1 Characterization of the artificial antigen and antibody

The characteristic peaks of BSA and 3-CQA were observed at 280 nm and 326 nm, respectively. In contrast, the characteristic absorption peaks of the 3-CQA-BSA bio-conjugate were identified between 280 and 326 nm (Figure 3A), demonstrating the successful synthesis of the complete artificial antigen. Likewise, the absorption peak of 3-CQA-OVA was shifted compared to that of 3-CQA and OVA (data not shown), indicating that the conjugated antigen 3-CQA-OVA was also successfully synthesized.
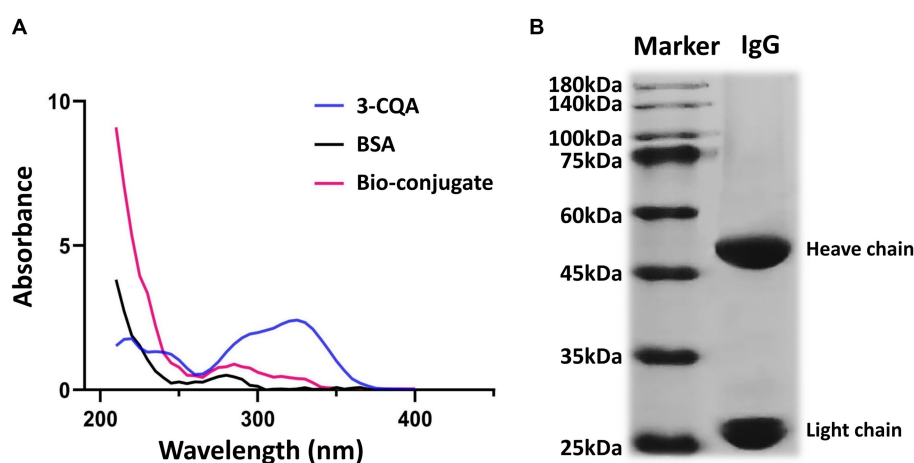
FIGURE 3
Characterization of the hapten and anti-3-CQA mAb. **(A)** Ultraviolet spectrometry analysis of 3-CQA, BSA, and 3-CQA-BSA bio-conjugate. **(B)** SDS-PAGE analysis of the mAb.

Regarding the antibody against the 3-CQA-BSA, the antiserum titer of the immunized mice was determined to be 1: 160000 using the ic-ELISA (Supplementary Figure S1). Subsequent purification of mouse ascites yielded two distinct bands corresponding to the heavy (50 kDa) and light chains (25 kDa) on SDS-PAGE (Figure 3B), affirming the high purity of the obtained antibodies. The purified mAb was then concentrated to 3.12 mg/mL and was classified as an IgG1 isotype with a kappa light chain.

3.2 Optimization of ic-CLEIA condition

The relative light unit (RLU) value decreased sharply with the antibody titer from 1:2000 to 1:8000, and the trend gradually flattened as the titer reached 1:16000 (Supplementary Figure S2). Additionally, when the coating concentration of 3-CQA-OVA was below 2 μg/mL, the RLU exhibited a sharp decline (Supplementary Figure S2). Consequently, an antibody dilution of 1:8000 (0.39 μg/mL) and a coating concentration of 2 μg/mL were deemed appropriate conditions for ic-CLEIA. Regarding the pH conditions, both slightly acidic and slightly alkaline environments resulted in an increase in the IC_{50}. Conversely, a neutral pH led to minimum IC_{50} while the RLU_0/IC_{50} ratio reached the maximum (Figure 4A). Therefore, pH = 7.0 was selected as the optimal pH value. The impact of surfactants (Tween-20) and organic solvents (methanol) on the reaction system was also investigated. The IC_{50}

values displayed a continuous increasing trend with higher concentration of methanol and Tween-20 added (Figures 4B,C). As such, deionized water in the absence of surfactants and organic reagents was chosen as the optimal reaction condition. Moreover, the effect of salt concentration on ic-CLEIA was explored. As shown in Figure 4D, the IC_{50} value progressively decreases with the increase of salt ion concentration in the range of 0.1–0.4 M, and reached the minimum value at 0.4 M. In case of the absence of salt ions, the IC_{50} value was distinctly lower than the case of the added salt ions, with a maximum value of RLU_0/IC_{50} value. With comprehensive consideration, deionized water without Na^+, surfactant, and organic reagent was selected as the working buffer, and the pH value was adjusted to 7.0.

3.3 Establishment of enzyme-linked immunoassay method

Under the optimized conditions, representative competitive inhibition curve revealed an IC_{50} value of 2.97 ng/mL and the limit of detection (LOD, IC_{10}) value of 0.39 ng/mL (Figure 5A). The linear range was from 0.64 ng/mL (IC_{20}) to 13.75 ng/mL (IC_{80}). An ic-ELISA method for detecting 3-CQA was established under the same conditions as ic-CLEIA, with a linear range of 10.21–127.36 ng/mL, an IC_{50} value of 36.06 ng/mL, and a LOD value of 6.71 ng/mL (Figure 5B).
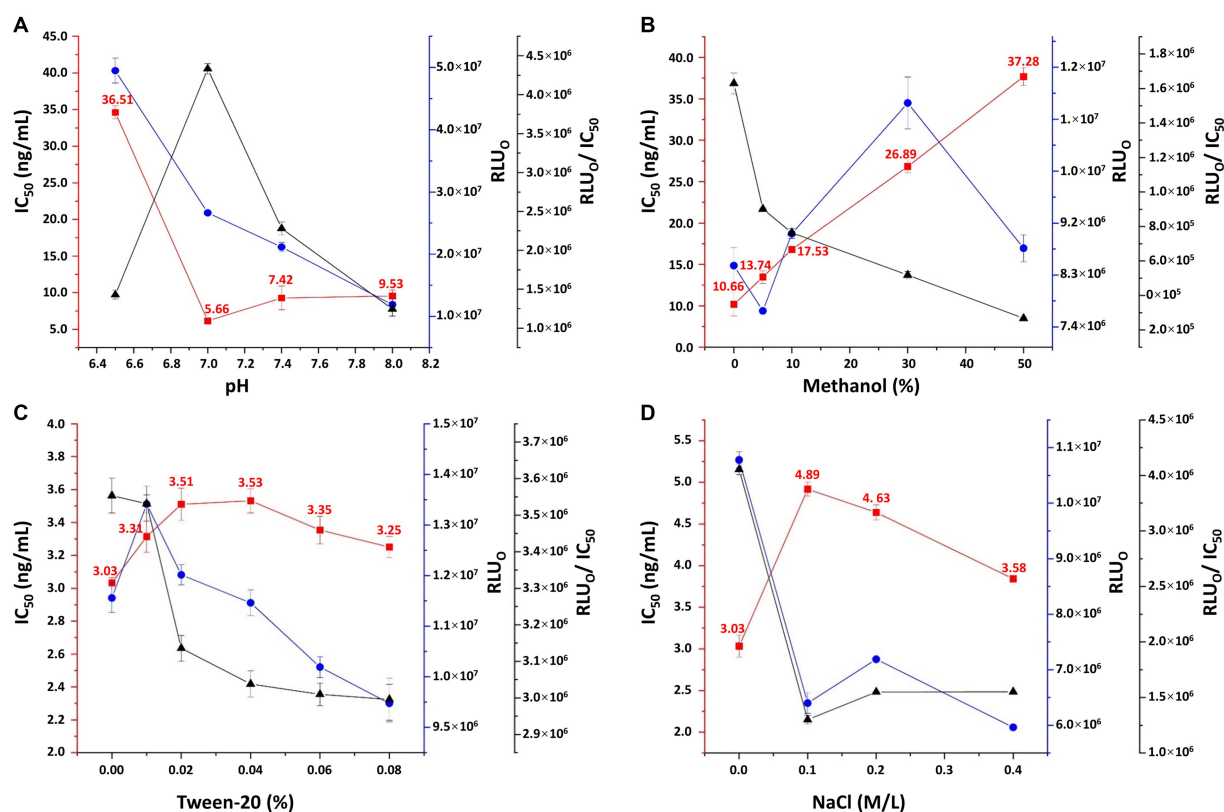

FIGURE 4
Optimization of pH (A), methanol concentration (B), Tween-20 concentration (C), and sodium chloride concentration (D) in working buffer. RLU_0: relative light unit without competing reagents. Each value represents the average of four replicates.
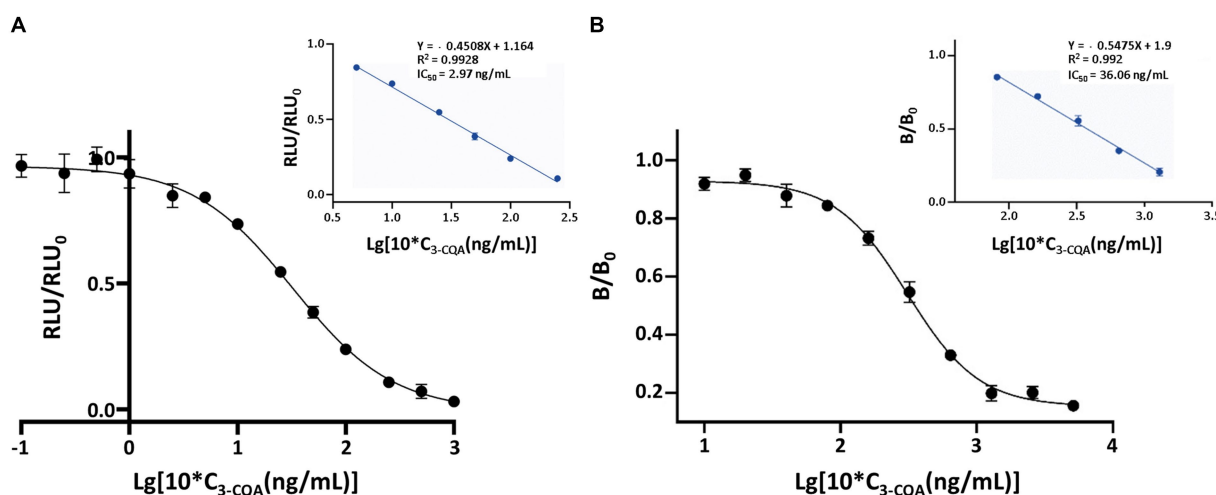
FIGURE 5
Standard curves of the ic-CLEIA **(A)** and ic-ELISA **(B)** for 3-CQA. RLU and RLU_0 mean the relative light unit with and without competing reagents, respectively. B and B_0 mean the absorbance value with and without competing reagents, respectively. Each value represents the average of four replicates.

3.4 Cross-reactivity

4-CQA, 5-CQA, 3,5-dicaffeoylquinic acid, 4,5-dicaffeoylquinic acid, and 3,4-dicaffeoylquinic acid were subjected to ic-CLEIA and their IC_{50} values were determined sequentially. The CR was 0.62, 1.81, 10.71, 0.31, and 2.10%, respectively (Table 1).

3.5 High-performance liquid chromatography analysis of 3-CQA

A reversed-phase HPLC was developed for 3-CQA determination, and the retention time was 11.2 min (Supplementary Figure S3). The regression curve equation was $Y = 0.5494X + 4.744$ ($R^2 = 0.9999$, $n = 4$; Supplementary Figure S4).

3.6 Real and spiked samples detection

3-CQA was extracted from herbs, and patent medicines samples, and the 3-CQA content was determined using the established ic-CLEIA method. The 3-CQA contents of *Honeysuckle* and *Eucommia* were significantly higher than that of other herbs. *Shuang-huang-lian* capsules contain about 1.5% (w/w) 3-CQA, the highest content among the patent medicines (Table 2).

3-CQA standard was added to herb and patent medicines to obtain specific concentration (5 or 10 mg/g). The recovery of 3-CQA after extraction was determined by the ic-CLEIA or HPLC. The ic-CLEIA showed recoveries ranging from 75.87 to 121.70%, and the relative standard deviation was 0.09 to 12.39% (Table 2).

3.7 Comparison of ic-CLEIA and HPLC for detection of 3-CQA

The results of the ic-CLEIA method showed good correlation with those of HPLC ($R^2 = 0.9667$), indicating that the method developed could achieve reliable and accurate determination of 3-CQA in samples (Supplementary Figure S5).

4 Discussion
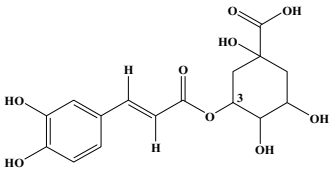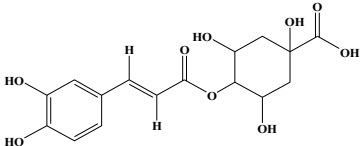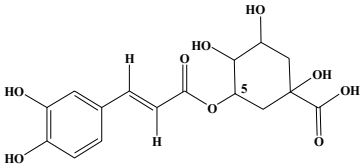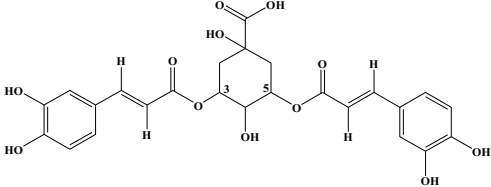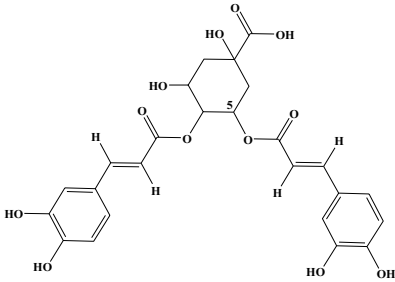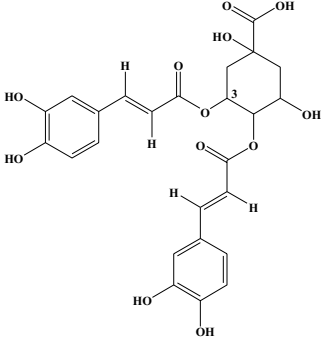
3-CQA, a prominent member of the CGA family, exhibits a broad spectrum of bioactive and therapeutic functions (8, 22, 23). Its widespread distribution in edible foods and herbs (24, 25), coupled with the prevalence of non-standard practices in its determination, underscores the pressing need for the development of a robust quantification method. In this pursuit, we sought to establish a highly sensitive and specific ic-CLEIA method for 3-CQA analysis, as reports have yet to explore the application of ic-CLEIA for determining 3-CQA levels prior to this study.

The inherent small molecule nature of 3-CQA renders it devoid of immunogenicity. We devised a method wherein 3-CQA was chemically conjugated with BSA or OVA to generate an artificial antigen capable of eliciting an immune response in mice. Leveraging the mAb specifically targeting the conjugate, we developed an ic-CLEIA with remarkable efficacy. It demonstrated an IC_{50} of 2.97 ng/mL, displaying linear absorbance values across a concentration range of 0.64–13.75 ng/mL. Impressively, the LOD of the ic-CLEIA was 0.39 ng/mL, comparable to the reported LOD (0.1 ng/mL) using ELISA (26), while significantly outperforming the ic-ELISA (6.71 ng/mL) in our parallel investigations. In addition, in comparison to previously reported instrumental methods for 3-CQA analysis (Table 3), including HPLC, reverse-phase rapid resolution liquid chromatography, capillary zone electrophoresis technique, and near-infrared spectroscopy, our ic-CLEIA emerged as a superior alternative reflected in the aspects such as high sensitivity and avoidance of expensive equipment and specialized operations. While Zhang's ic-ELISA demonstrated a detection range of 0.10–1.51 ng/mL, which is narrower than our ic-CLEIA range of 0.64–13.75 ng/mL, our ic-CLEIA method provides a broader detection range to accommodate a wider variety of sample concentrations.

Moreover, in terms of specificity, the established ic-CLEIA revealed relatively low cross-reactivity (<5%) with most 3-CQA structural analogs, with only 3, 5-dicaffeoylquinic acid exhibiting

TABLE 1 Cross-reactivity for 3-CQA and its structural analogs.

Compound	Structure	IC$_{50}$ (ng/mL)	CR (%)
3-CQA		2.97	100.00
4-CQA		480.62	0.62
5-CQA		164.44	1.81
3,5-dicaffeoylquinic acid		27.74	10.71
4,5-dicaffeoylquinic acid		971.56	0.31
3,4-dicaffeoylquinic acid		141.73	2.10

slightly higher cross-reactivity (10.71%) (Table 1). This occurrence implies the active role of the substitution of hydroxyl moiety in position 3 of the quinic acid in influencing cross-reactivity patterns. These results suggest the relatively high specificity of the ic-CLEIA method in determining 3-CQA. Moreover, the spiked recoveries, a critical index for evaluating the reliability of immunoassays (35), ranged from 75.87 to 121.70%, with relative standard deviations varying from 0.09 to 12.39%, thereby affirming the capability of the ic-CLEIA for detecting 3-CQA in herbs and patent medicines.

One thing worth highlighting is the eco-friendliness and user-friendly attributes of our detection process. Through optimization, we uncovered that the deionized water in the absence of ions, surfactants, and organic reagents serves as an optimal buffer for ic-CLEIA. The exclusion of organic solvents and the elimination of complex sample pre-treatment present clear advantages over HPLC and other instrumental techniques. Meanwhile, in this study, we set the interaction time at 50 min; considering the vulnerability of 3-CQA and other CGA family compounds, further optimization of reaction time may enable

TABLE 2 Content of 3-CQA in real and spiked samples (*n* = 4).

Samples	Spiked (mg/g)	ic-CLEIA			HPLC		
		Measured (mg/g)	Recovery (%)	RSD[a] (%)	Measured (mg/g)	Recovery (%)	RSD[a] (%)
Lonicera stem	/	2.28	/	0.21	2.78	/	0.06
Virgate wormwood	/	0.74	/	0.05	1.05	/	<0.01
Houttuynia	/	0.62	/	0.02	0.89	/	0.03
Kou-Yan-Qing granule	/	5.20	/	0.32	3.68	/	0.03
Compound *Jin-Yin-Hua* granule	/	1.52	/	0.13	1.64	/	<0.01
Yin-Zhi-Huang granule	/	1.80	/	0.03	1.06	/	0.01
Jin-Sang-Zi Lozenge	/	0.27	/	0.03	0.29	/	0.01
Dandelion	0	1.33	/	/	1.04	/	/
	5	7.17	115.57	0.33	5.77	94.56	0.76
	10	9.64	83.06	1.90	9.64	85.99	0.87
Honeysuckle	0	18.37	/	/	21.31	/	/
	5	23.60	104.60	12.39	26.43	102.35	0.24
	10	29.76	113.90	0.09	30.61	92.97	0.37
Eucommia	0	11.91	/	/	12.44	/	/
	5	17.36	105.77	3.10	16.91	89.34	0.59
	10	22.36	112.53	6.60	21.09	86.49	0.08
Shuang-Huang-Lian capsule	0	12.80	/	/	12.74	/	/
	5	18.59	115.85	5.29	18.09	106.99	0.47
	10	20.39	75.87	0.41	21.75	90.10	2.47
Vitamin C *Yin-Qiao* tablet	0	8.50	/	/	4.44	/	/
	5	14.80	121.70	0.93	9.58	102.83	0.38
	10	19.64	111.44	3.64	13.99	95.45	0.06
Yin-Huang granule	0	1.96	/	/	2.45	/	/
	5	5.76	75.99	10.90	7.06	92.06	0.43
	10	10.50	92.45	2.97	12.60	101.43	0.21

[a]Relative standard deviation.

even greater efficiency in simultaneous detection of 3-CQA, realizing the rapid high-throughput quantification.

Furthermore, the established ic-CLEIA was applied for the analysis of 3-CQA contents in 13 herb or patent medicine samples, revealing varying levels of 3-CQA across different samples (Supplementary Table S2), with higher contents observed in *Honeysuckle* and *Eucommia*. According to the Chinese Pharmacopeia, the minimum effective contents of 3-CQA in *Honeysuckle*, *Eucommia*, and *Lonicera* stem are 1.5% (15 mg/g), 0.08% (0.8 mg/g), and 0.1% (1 mg/g), respectively (21). Consequently, the herbs in this study met the criteria for qualified 3-CQA content. In addition, these herbs with therapeutic effects as individual components are essential raw materials in patient medicines, such as *Lianhua Qingwen* capsule, renowned for their antipyretic, antibacterial, and anti-inflammatory effects (36). We tested a total of 7 patent medicines, five of which adhere to clear 3-CQA content regulations in pharmacopeia: *Shuang-huang-lian* capsules (≥ 3 mg/

capsule), *Yin-huang* granules (≥ 5 mg/bag), *Yin-Zhi-huang* granules (≥ 1.8 mg/bag), *Kou-yan-qing* granules (≥ 4 mg/bag), and Vitamin C *Yin-qiao* tablets (≥ 1.5 mg/tablet) (21). Detailed information on these medicines (Supplementary Table S2) confirms their compliance with the minimum 3-CQA content requirements. Additionally, good linearity was observed between the ic-CLEIA and HPLC analysis in detecting 3-CQA ($R^2 = 0.9667$, Supplementary Figure S5), further attesting to the reliability and efficiency of our developed ic-CLEIA for 3-CQA analysis.

Of course, although herbal medicine quality control mandates active ingredient detection, it is equally essential to achieve real-time and rapid detection of toxic and harmful substances generated or retained during herbal growth and processing. Our study serves as a compelling paradigm for 3-CQA determination, opening avenues for extending the application of this method to quantify other members within the CGA family, like 4-CQA, contributing to advancements in herbal medicine analysis and quality assurance.

TABLE 3 Methods developed in chlorogenic acid analysis.

Methods	Characteristics	Samples	Detection range	Reference
High-performance liquid chromatography (HPLC)	Precise; sample needs to be derivatized	Brazilian green propolis	3.75–22.5 µg/mL	(27)
Reverse-phase rapid resolution liquid chromatography	High sensitivity, precise	Green coffee samples	12.33–143.50 µg/mL	(28)
Gas chromatography–mass spectrometry	Wide range of applications, efficient	Coffee samples	Not mentioned	(29)
Spectrophotometric assays	Simple equipment, relatively large error	*Chamerionangustifolium L.*	Not mentioned	(30)
Capillary zone electrophoresis technique	Convenient, fast, economical and reliable	Tobacco residues	3–500 µg/mL	(31)
Near-infrared spectroscopy	Fast, easy operation, efficient	*Flos Mume*	20.51–1312.94 µg/mL	(32)
Flow injection chemiluminescent	High sensitivity, fast	Fruits (apple, grape, hawthorn)	50 ng/mL–50 µg/mL	(33)
Colloidal gold-based immunochromatographic assay	Fast, easy operation, visual	*Flos Lonicerae Japonicae*	>100 ng/mL	(34)
ic-ELISA	Fast, feasible, high sensitivity and specific	*Flos Lonicerae Japonicae*	0.10–1.51 ng/mL	(26)
ic-CLEIA	Fast, feasible, high sensitivity and specific	Herbs and patent medicines	0.64–13.75 ng/mL	Current study

5 Conclusion

Collectively, we established an ic-CLEIA with a lower IC_{50} value (2.97 ng/mL) and a wider detection range (0.64–13.75 ng/mL) compared to the ic-ELISA (IC_{50}: 36.06 ng/mL; detection range: 10.21–127.36 ng/mL). Without complex sample pre-treatment steps, this novel approach was validated under different sample conditions, including herbs and patent medicines. The recoveries were satisfactory (75.87–121.70%) with RSD of 0.09 to 12.39%. The results were strongly correlated with HPLC analysis ($R^2 = 0.9667$). In conclusion, the established method was simple, time-saving, sensitive and efficient for rapid detection of 3-CQA.

Data availability statement

The original contributions presented in the study are included in the article/Supplementary material, further inquiries can be directed to the corresponding author/s.

Ethics statement

The animal study was approved by Chinese-German Joint Institute for Natural Product Research, Shaanxi University of Technology, and approval no. 2021–01. The study was conducted in accordance with the local legislation and institutional requirements.

Author contributions

LW: Conceptualization, Data curation, Investigation, Methodology, Validation, Writing – original draft. MD: Conceptualization, Funding acquisition, Methodology, Writing – review & editing. RW: Data curation, Validation, Writing – review & editing. MI: Writing – review & editing. XZ: Conceptualization, Funding acquisition, Supervision, Writing – review & editing.

Funding

Conflict of interest

The authors declare that the research was conducted in the absence of any commercial or financial relationships that could be construed as a potential conflict of interest.

The author(s) declared that they were an editorial board member of Frontiers, at the time of submission. This had no impact on the peer review process and the final decision.

Publisher's note

All claims expressed in this article are solely those of the authors and do not necessarily represent those of their affiliated organizations, or those of the publisher, the editors and the reviewers. Any product that may be evaluated in this article, or claim that may be made by its manufacturer, is not guaranteed or endorsed by the publisher.

Supplementary material

The Supplementary material for this article can be found online at: https://www.frontiersin.org/articles/10.3389/fnut.2024.1439287/full#supplementary-material

References

1. Soto-Hernandez M, Palma Tenango M, García-Mateos M. *Phenolic compounds-biological activity*. (2017).

2. Zhang Y, Cai P, Cheng G, Zhang Y. A brief review of phenolic compounds identified from plants: their extraction, analysis, and biological activity. *Nat Prod Commun*. (2022) 17:10697. doi: 10.1177/1934578X211069721

3. Lou Z, Zheng X, Bede D, Dai W, Wan C, Wang H, et al. New perspectives for mechanisms, ingredients, and their preparation for promoting the formation of beneficial bacterial biofilm. *J Food Meas Charact*. (2023) 17:2386–403. doi: 10.1007/s11694-022-01777-5

4. Liang N, Kitts D. Role of Chlorogenic acids in controlling oxidative and inflammatory stress conditions. *Nutrients*. (2015) 8:16. doi: 10.3390/nu8010016

5. Liang N, Dupuis J, Yada R, Kitts D. Chlorogenic acid isomers directly interact with Keap 1-Nrf2 signaling in Caco-2 cells. *Mol Cell Biochem*. (2019) 457:105–18. doi: 10.1007/s11010-019-03516-9

6. Nevena GL, Branislava R, Emilia S, Dusica R, Ivan N, Nebojsa K, et al. Determination of 5-Caffeoylquinic acid (5-Cqa) as one of the major classes of Chlorogenic acid in commercial tea and coffee samples. *Vojnosanit Pregl*. (2015) 72:1018–23. doi: 10.2298/VSP130915096G

7. Wianowska D, Gil M. Recent advances in extraction and analysis procedures of natural Chlorogenic acids. *Phytochem Rev*. (2019) 18:273–302. doi: 10.1007/s11101-018-9592-y

8. Liu W, Li J, Zhang X, Zu Y, Yang Y, Liu W, et al. Current advances in naturally occurring Caffeoylquinic acids: structure, bioactivity, and synthesis. *J Agric Food Chem*. (2020) 68:10489–516. doi: 10.1021/acs.jafc.0c03804

9. Anggreani E, Lee CY. Neuroprotective effect of Chlorogenic acids against Alzheimer's disease. International journal of food science. *Nutr Diet*. (2017) 6:330–7. doi: 10.19070/2326-3350-1700059

10. Adeosun W, More G, Steenkamp P, Prinsloo G, Moco S, Levanova A, et al. Influence of seasonal and geographic variation on the anti-Hsv-1 properties and Chlorogenic acids content of Helichrysum Aureonitens Sch. Bip. *Front Mol Biosci*. (2022) 9:961859. doi: 10.3389/fmolb.2022.961859

11. Singdam P, Naowaboot J, Senggunprai L, Boonloh K, Hipkaeo W, Pannangpetch P. The mechanisms of Neochlorogenic acid (3-Caffeoylquinic acid) in improving glucose and lipid metabolism in rats with insulin resistance induced by a high fat-high fructose diet. *Trends Sci*. (2023) 20:6455–5. doi: 10.48048/tis.2023.6455

12. Yan Y, Zhou X, Guo K, Zhou F, Yang H. Use of Chlorogenic acid against diabetes mellitus and its complications. *J Immunol Res*. (2020) 2020:1–6. doi: 10.1155/2020/9680508

13. Shi A, Li T, Zheng Y, Song Y, Wang H, Wang N, et al. Chlorogenic acid improves Nafld by regulating gut microbiota and Glp-1. *Front Pharmacol*. (2021) 12:693048. doi: 10.3389/fphar.2021.693048

14. Lu H, Tian Z, Cui Y, Liu Z, Ma X. Chlorogenic acid: a comprehensive review of the dietary sources, processing effects, bioavailability, beneficial properties, mechanisms of action, and future directions. *Compr Rev Food Sci Food Saf*. (2020) 19:3130–58. doi: 10.1111/1541-4337.12620

15. Meinhart AD, Damin FM, Caldeirão L, de Jesus FM, da Silva LC, da Silva CL, et al. Study of new sources of six Chlorogenic acids and Caffeic acid. *J Food Compos Anal*. (2019) 82:103244. doi: 10.1016/j.jfca.2019.103244

16. Gamiotea-Turro D, Camaforte NAP, Valerino-Diaz AB, Ortiz Nuñez Y, Rinaldo D, Dokkedal AL, et al. Qualitative and quantitative analysis of Ethanolic extract and phenolic fraction of Jatropha Aethiopica (Euphorbiaceae) leaves and their hypoglycemic potential. *J Agric Food Chem*. (2018) 66:1419–27. doi: 10.1021/acs.jafc.7b05648

17. Yu HC, Huang SM, Lin WM, Kuo CH, Shieh CJ. Comparison of artificial neural networks and response surface methodology towards an efficient ultrasound-assisted extraction of Chlorogenic acid from *Lonicera Japonica*. *Molecules (Basel, Switzerland)*. (2019) 24:2304. doi: 10.3390/molecules24122304

18. Song J, Wang R-M, Wang Y-Q, Tang Y-R, Deng A-P. Hapten design, modification and preparation of artificial antigens. *Chin J Anal Chem*. (2010) 38:1211–8. doi: 10.1016/S1872-2040(09)60063-3

19. Liu J, Zhang H, Zhang D, Gao F, Wang J. Production of the monoclonal antibody against Sudan 2 for immunoassay of Sudan dyes in egg. *Anal Biochem*. (2012) 423:246–52. Epub 2012/02/14. doi: 10.1016/j.ab.2012.02.001

20. Xu L, Suo XY, Zhang Q, Li XP, Chen C, Zhang XY. Elisa and Chemiluminescent enzyme immunoassay for sensitive and specific determination of Lead (ii) in water, food and feed samples. *Foods (Basel, Switzerland)*. (2020) 9:305. doi: 10.3390/foods9030305

21. Commission CP. *The pharmacopoeia of the People's republic of China*. China Medical Science Press Beijing (2020).

22. Ud Din SR, Saeed S, Khan SU, Kiani FA, Alsuhaibani AM, Zhong M. Bioactive compounds (bacs): a novel approach to treat and prevent cardiovascular diseases. *Curr Probl Cardiol*. (2023) 48:101664. doi: 10.1016/j.cpcardiol.2023.101664

23. Gupta A, Atanasov AG, Li Y, Kumar N, Bishayee A. Chlorogenic acid for Cancer prevention and therapy: current status on efficacy and mechanisms of action. *Pharmacol Res*. (2022) 186:106505. doi: 10.1016/j.phrs.2022.106505

24. Li Z, Zhang J, Meng Q, Yang L, Qiu M, Li Y, et al. The content and distribution of 18 phenolic compounds in 462 batches of edible flowers from 73 species commercially available in China. *Food Res Int*. (2023) 166:112590. doi: 10.1016/j.foodres.2023.112590

25. Woźniak D, Nawrot-Hadzik I, Kozłowska W, Ślusarczyk S, Matkowski A. Handbook of Dietary Phytochemicals. Berlin: Springer, pp. 1065–1104. (2021).

26. Zhang B, Nan TG, Zhan ZL, Kang LP, Yang J, Lai CJ, et al. A monoclonal antibody-based enzyme-linked immunosorbent assay for the determination of Chlorogenic acid in honeysuckle. *J Pharm Biomed Anal*. (2018) 148:1–5. doi: 10.1016/j.jpba.2017.09.023

27. Sun S, Liu M, He J, Li K, Zhang X, Yin G. Identification and determination of seven phenolic acids in Brazilian green Propolis by Uplc-Esi-Qtof-Ms and Hplc. *Molecules (Basel, Switzerland)*. (2019) 24:1791. doi: 10.3390/molecules24091791

28. Velkoska-Markovska L, Jankulovska MS, Petanovska-Ilievska B, Hristovski K. Development and validation of Rrlc–Uv method for determination of Chlorogenic acid in green coffee. *Acta Chromatogr*. (2020) 32:34–8. doi: 10.1556/1326.2019.00547

29. Heo J, Adhikari K, Choi KS, Lee J. Analysis of caffeine, Chlorogenic acid, Trigonelline, and volatile compounds in cold brew coffee using high-performance liquid chromatography and solid-phase microextraction-gas chromatography-mass spectrometry. *Foods (Basel, Switzerland)*. (2020) 9:1746. doi: 10.3390/foods9121746

30. Kaškonienė V, Stankevičius M, Drevinskas T, Akuneca I, Kaškonas P, Bimbiraitė-Survilienė K, et al. Evaluation of phytochemical composition of fresh and dried raw material of introduced *Chamerion Angustifolium* L. using chromatographic, spectrophotometric and chemometric techniques. *Phytochemistry*. (2015) 115:184–93. doi: 10.1016/j.phytochem.2015.02.005

31. Li Z, Huang D, Tang Z, Deng C, Zhang X. Fast determination of Chlorogenic acid in tobacco residues using microwave-assisted extraction and capillary zone electrophoresis technique. *Talanta*. (2010) 82:1181–5. doi: 10.1016/j.talanta.2010.06.037

32. Yan H, Pu Z, Wang Y, Guo S, Wang T, Li S, et al. Rapid qualitative identification and quantitative analysis of Flos Mume based on Fourier transform near infrared spectroscopy. *Spectrochim Acta A Mol Biomol Spectrosc*. (2021) 249:119344. doi: 10.1016/j.saa.2020.119344

33. Wang X, Wang J, Yang N. Chemiluminescent determination of Chlorogenic acid in fruits. *Food Chem*. (2007) 102:422–6. doi: 10.1016/j.foodchem.2006.03.002

34. Zhang B, Nan TG, Xin J, Zhan ZL, Kang LP, Yuan Y, et al. Development of a colloidal gold-based lateral flow dipstick immunoassay for rapid detection of Chlorogenic acid and Luteoloside in Flos Lonicerae Japonicae. *J Pharm Biomed Anal*. (2019) 170:83–8. doi: 10.1016/j.jpba.2019.03.035

35. Xu J, Zhu LY, Shen H, Zhang HM, Jia XB, Yan R, et al. A critical view on spike recovery for accuracy evaluation of analytical method for medicinal herbs. *J Pharm Biomed Anal*. (2012) 62:210–5. doi: 10.1016/j.jpba.2011.12.034

36. Fu S, Cheng R, Deng Z, Liu T. Qualitative analysis of chemical components in Lianhua Qingwen capsule by Hplc-Q Exactive-Orbitrap-Ms coupled with Gc-Ms. *J Pharm Anal*. (2021) 11:709–16. doi: 10.1016/j.jpha.2021.01.004

Widely targeted metabolomics and SPME-GC-MS analysis revealed the quality characteristics of non-volatile/ volatile compounds in Zheng'an Bai tea

Li Liu[1†], Dahe Qiao[2†], Xiaozeng Mi[2], Shirui Yu[1], Tingting Jing[3]* and Yanlin An[1]*

[1]Department of Food Science and Engineering, Moutai Institute, Renhuai, China, [2]Guizhou Tea Research Institute, Guizhou Academy of Agricultural Sciences, Guiyang, China, [3]State Key Laboratory of Tea Plant Biology and Utilization, Anhui Agricultural University, Hefei, China

Background: As albino tea under the geographical protection of agricultural products, Zheng'an Bai tea is not only rich in amino acids, polyphenols and other beneficial components for the human body, but also its leaf color will turn green as the temperature gradually rises, thus causing changes in the quality characteristics of tea leaves. However, these changing characteristics have not yet been revealed.

Methods: In-depth quality analysis was carried out on the fresh leaves of Zheng'an Bai tea at four different developmental stages and four samples from the processing stage through extensive targeted metabolomics and SPME-GC-MS analysis.

Results: In this study, a total of 573 non-volatile metabolites were detected from the fresh leaves and processing samples of Zheng'an Bai tea, mainly including 96 flavonoids, 75 amino acids, 56 sugars and alcohols, 48 terpenoids, 46 organic acids, 44 alkaloids, and 39 polyphenols and their derivatives. In fresh leaves, the most significant differential metabolites (VIP > 1, p < 0.05) among different samples mainly include substances such as ethyl gallate, theaflavin, isovitexin and linalool, while the main differential metabolites of samples in the processing stage include alkaloids, polyphenols and flavonoids such as zarzissine, methyl L-Pyroglutamate, theaflavin 3,3'-digallate, euscaphic acid and ethyl gallate. Overall, substances such as sugars and alcohols, alkaloids and polyphenols show the greatest differences between fresh leaves and the processing process. Meanwhile, 97 kinds of volatile metabolites were detected in these samples, most of which had a higher content in the fresh leaves. Moderate spreading is conducive to the release of the aroma of tea leaves, but fixation causes a sharp decrease in the content of most volatile metabolites. Ultimately, 9 volatile substances including geraniol, linalool, nerolidol, jasmone, octanal, 1-Nonanal, heptaldehyde, methyl salicylate and 1-Octen-3-ol were identified as the key aroma components (OAV >1) of Zheng'an Bai tea.

Conclusion: In conclusion, this study has for the first time comprehensively revealed the quality change characteristics of fresh leaves at different developmental stages and during the processing of Zheng'an Bai tea, and provided a foundation for further process improvement.

KEYWORDS

Zheng'an Bai tea, widely targeted metabolomics, non-volatile/volatiles, fresh leaves, tea processing, SPME-GC-MS

1 Introduction

The unique taste, pleasant aroma, and abundant nutrients have made tea one of the most popular non-alcoholic beverages (1). The widespread cultivation of tea plants [*Camellia sinensis* (L.) O. Kuntze] worldwide has made them one of the most important cash crops for many countries to increase farmers' income. China is the origin country of tea and has abundant tea tree resources, hundreds or even thousands of tea varieties are made into six traditional tea types such as green tea and black tea with different flavors according to their quality characteristics and different processing procedures (2, 3). Meanwhile, in recent years, some naturally mutated tea plant resources have attracted increasing attention from researchers due to their characteristics such as low caffeine or high anthocyanins (4, 5). "Zheng'an Bai tea" is a famous green tea produced in Zheng'an County, Guizhou Province, made from the tender buds and leaves of the naturally mutated tea cultivar "Baiye 1." Due to its high amino acid content and other characteristics, it has been listed as a Chinese National Geographical Indication Product since 2011 (6). Unlike other yellowing or purpling tea plant varieties, "Zheng'an Bai tea" belongs to the temperature-sensitive variety, whose leaves appear white at lower temperatures and gradually turn green as the temperature rises. Although many reports have conducted in-depth studies on the molecular regulatory basis of albino tea plants, the quality of tea is influenced by many factors such as climate, water and fertilizer, and processing (7–9). At present, there are no reports on the metabolic profiles of different leaf positions and the quality change characteristics of fresh leaves during processing.

Compared with common tea varieties, naturally mutated tea varieties often have unique quality characteristics. For example, 22 anthocyanins were identified in purple tea varieties such as "Zijuan" or "Ziyan," and their contents reached more than 1 μg/g (dry weight) (10); while in the yellow-leaf tea variety, the theanine content of "Zhonghuang 2 (yellow-leaf tea)" was significantly higher than that of "Longjing 43 (normal tea)" (11). For tea varieties with albino leaves, both light-sensitive and temperature-sensitive varieties have the characteristics of low polyphenol content and high amino acid content, which gives the tea soup a higher freshness (12). Many studies have shown that with the development of tea leaves, the secondary metabolite profiles such as catechins, caffeine, theanine, and anthocyanins will undergo significant changes (13). For "Zheng'an Bai tea," the amino acid content gradually decreases with the development of the leaves, the contents of catechin (EGC), epicatechin gallate (ECG), epicatechin (EC), catechin (C), epigallocatechin gallate (EGCG), and gallocatechin (GC) in albino or yellowing variegated leaves were significantly lower than those in normal leaves (14). But due to factors such as altitude and unique climate, the metabolic profile characteristics of different leaf positions still need to be revealed.

Although volatile components account for only 0.01% of the dry weight of tea, they contribute to the main aroma quality of tea (15, 16). Many studies have conducted in-depth analysis of the volatile metabolites and aroma changing characteristics in tea. For example, Xia et al. (17) analyzed the influence of three fixation methods on the aroma quality of "Anji Bai tea" (albino tea), identified 9 key components that caused the aroma changes of Anji Bai tea, and proved that linalool and geraniol contribute to the formation of floral, fruity and honey aromas of tea; the analysis of harvest seasons and etiolated varieties revealed that the relative content of volatile

compounds in steamed green tea was significantly negatively correlated with the season ($p < 0.05$). The contents of volatile compounds such as (+)-δ-cadinene, farnesyl acetone, carvone, trans-β-ionone and nerolidol were higher in spring tea. However, the differences in the total volatile compounds among the three albino varieties of steamed green tea were not significant ($p > 0.05$) (18). Compared with "Yinghong 9," the "Huangyu" variety contains higher levels of α-farnesene, β-cyclocitral, nerolidol and trans-geranylacetone, which have been confirmed to be related to the flower and fruit aroma in the fermented leaves (19). It was found in the study of purple tea that anaerobic treatment facilitated the accumulation of 2-heptanol, (E)-2-hexenal, ethyl salicylate, phenylethyl alcohol and (E, E)-2, 4-decadienal, but inhibited the formation of (Z)-3-hexenyl acetate and methyl jasmonate (20). Furthermore, Gao et al. also detected and analyzed the volatile substances in the flowers of three albino tea plants and one normal tea plant, and discovered that acetophenone and (R)-1-phenylethanol were positively correlated with the sweet flavor, while methyl salicylate, 2-heptanol, (E)-2-hexenal, nonanal and 2-pentanol were positively correlated with the green smell (21). The above studies mainly focused on the change characteristics of volatile metabolites in specific process conditions or tissues, and there were no studies on the change trend of volatile metabolites/aroma in tea leaves at different development stages and during the whole processing process. Therefore, the revelation of aroma changes of "Zheng'an Bai tea" still needs to be strengthened (22–24).

In this study, we focused on exploring the dynamic changes of non-volatile/volatile metabolites throughout the entire process from the fresh leaves, the processing, to the finished tea of "Zheng'an Bai tea." A total of eight stages of samples, including buds (BUD), the first leaf (FL), the second leaf (SL), the first bud and the first leaf (FBFL), spreading for 3 h (TF3h), spreading for 6 h (TF6h), fixation (SQ) and drying (DRY), were detected and analyzed by widely targeted metabolomics and GC–MS techniques to comprehensively reveal the metabolic profile and key aroma components of "Zheng'an Bai tea." This will help us recognize and understand the formation basis of the quality of "Zheng'an Bai tea" and the influence brought by the processing techniques.

2 Materials and methods

2.1 Plant materials and reagents

The samples of buds (BUD), the first leaf (FL), the second leaf (SL), the first bud and the first leaf (FBFL) of "Baiye 1" and samples at different processing stages (spreading for 3 h, TF3h; spreading for 6 h, TF6h; fixation, SQ; drying, DRY) were collected. All these samples were collected from the tea garden of Zhongguan Town, Zheng'an County, Guizhou Province (28°43′ N, 107°61′ E). Some of the collected fresh samples were transported to the laboratory in dry ice and stored in a −80°C refrigerator for later use, while the other portion was processed into dry tea according to the following process: The first buds and first leaf collected was placed in a well-ventilated room at room temperature for 6 h of spreading. The tea was turned over 2–3 times during spreading to maintain a humidity level between 75 and 85%. After spreading, the tea was quickly straightened in a tea straightening machine and then fixed at 230°C for 4–5 min. Finally, it

was dried at 110°C for 1.5 h in a dryer. Deionized water was produced using a Milli-Q water purification system (Millipore, Billerica, Massachusetts). Methanol, acetonitrile, and ammonium acetate (LC–MS grade) were obtained from Merck (Darmstadt, Germany), and formic acid was obtained from TCI (TCI America). All the samples were stored in a − 80°C refrigerator until they were detected.

2.2 Sample preparation and extraction

Before the samples were formally prepared, all the tea leaves were freeze—dried for 24 h first to ensure the consistency of water content. Then, weigh 50 mg of the freeze-dried sample and add 1 ml of the extraction solution (methanol:acetonitrile:water volume ratio = 2:2:1). Vortex the centrifuge tube containing the sample for 30 s to ensure sufficient mixing. Then, add steel balls, perform ultrasonic treatment at 45 Hz for 10 min, followed by low temperature ultrasonic treatment for 10 min, and then stand at −20°C for 1 h (25, 26). After standing, the sample was centrifuged at 12,000 rpm for 15 min at 4°C, and 500 μl of the supernatant was taken and dried in a vacuum concentrator. Add 160 μl of extraction solution (acetonitrile:water volume ratio 1:1) to dissolve the metabolites; vortex for 30 s, and ultrasonicate for 10 min in an ice-water bath; centrifuge the sample at 12,000 rpm for 15 min at 4°C; carefully remove 120 μl of the supernatant into a 2 ml injection bottles for testing. All samples included three replicates.

2.3 UPLC-ESI-MS/MS analysis

A Waters UPLC Acquity I-Class PLUS ultra-high performance liquid chromatography was coupled to an AB Sciex Qtrap 6,500+ mass spectrometer system for the detection of metabolites (UPLC-ESI-MS/MS). The specific UPLC conditions are as follows: C18 column (1.8 μm, 2.1 mm × 100 mm, Acquity UPLC HSS T3), mobile phase A is a mixture of 0.1% formic acid and 5 mM ammonium acetate aqueous solution, and mobile phase B is 0.1% formic acid acetonitrile. The flow rate is 350 μl/min. The gradient elution conditions are: 98:2 v/v at 0 min, hold for 1.5 min, 50:50 v/v at 5 min, 2:98 v/v at 9 min, hold for 1 min; 98:2 v/v at 11 min, hold for 3 min, and the injection volume is 2 μl. The temperature of the electrospray ionization (ESI) source was set at 550°C, and the ion source gases I (GSI), gas II (GSII), and curtain gas (CUR) were set at 50, 55, and 35 psi, respectively. The collision-induced ionization parameters were set to medium. For more detailed methods, please refer to the research of Shi et al. (27). Based on the GB-PLANT commercial database, qualitative/quantitative mass spectrometry analysis was performed on the metabolites of the samples. The characteristic ions of each substance were screened out by triple quadrupole, and the signal intensity of the characteristic ions was obtained in the detector. After obtaining the metabolite mass spectrometry analysis data of different samples, the peak area integration was performed on all the mass spectrometry peaks, and the integration correction was performed on the mass spectrometry peaks of the same metabolite in different samples. Based on KEGG databases, the identified metabolites were classified and pathway analyzed.[1]

2.4 Extraction of volatile compounds

The volatile substances in tea were enriched by the method of automatic solid-phase microextraction (SPME) (28). After freeze-drying the tea samples, use a ball mill to grind the freeze-dried tea samples into powder, take 0.100 g and place it in a 15 ml gas chromatography–mass spectrometry glass bottle, and add 5 μl of ethyl decanoate at 1 μg/ml as an internal standard. Adsorption was conducted using the SPME Arrow of model 36SP05T3 (C-WR/PDMS 80/10-P3) from Thermo Scientific, and its adsorption phase was mainly PDMS (Polydimethylsiloxane). Place the sample bottle at 60°C, adsorb for 50 min, and then use GC–MS to detect volatile substances. GC conditions: Inlet temperature of 250°C, thermal desorption of volatile components for 10 min, separation using a fused silica chromatographic column (DB-5, 30 m × 0.25 mm × 0.25 μm, Folsom, USA). Carrier gas: Helium at a flow rate of 1 ml/min; the starting temperature of the column oven is 50°C, maintained for 2 min, raised to 80°C at a rate of 2°C/min, maintained for 1 min; raised to 100°C at a rate of 3°C/min, maintained for 4 min; raised to 130°C at a rate of 3°C/min, maintained for 4 min; raised to 150°C at a rate of 5°C/min, maintained for 0 min; raised to 200°C at a rate of 10°C/min, maintained for 0 min; raised to 240°C at a rate of 20°C/min, maintained for 3 min. Mass spectrometry conditions: Ion source EI, electron energy 80 eV, full ion scan mode, mass scan range 41–350 m/z. Finally, the volatile metabolites were identified based on the National Institute of Standards and Technology (NIST) mass spectrometry database and retention index (RI) (24, 29, 30).

2.5 Semi-quantitation and calculation of odor activity values

The concentration of volatile compounds was calculated based on their peak areas and the peak area of the internal standard compound. The odor activity value (OAV) of the volatiles was obtained by dividing the concentration by their odor threshold (15, 31–37). Furthermore, some flavor thresholds were obtained through the online data of VCF (Volatile Compounds in Food; https://www.vcf-online.nl/VcfHome.cfm). In addition, it should be noted that all metabolite detections were entrusted to Biomarker Technologies Co., Ltd.

2.6 Statistics analysis

The original peak area information of each substance is normalized according to the total peak area of the sample (38). And PCA analysis and Spearman correlation analysis were performed to verify the reproducibility of the intra-group samples and control samples. Based on the grouping information, the fold change of metabolites between different groups was calculated and compared, and the significance p-value of each compound was calculated using the T-test. At the same time, the (O)PLS-DA model was constructed based on the online analysis toolbox BMKCloud.[2] The screening

---

1 https://www.genome.jp/kegg/

2 https://international.biocloud.net/zh/software/agriculture/list

criteria for different metabolites were $p < 0.05$, and VIP > 1 (39). In all (O)PLS-DA analyses, the values of R2Y and Q2 of the model are both greater than 0.9.

3 Results and discussion

3.1 Overall view of non-volatile metabolites in Zheng'an Bai tea

A total of 573 non-volatile metabolites were detected in fresh leaves at different development stages and samples at different processing stages of "Zheng'an Bai tea," including 96 flavonoids and their derivatives, 75 amino acids and their derivatives, 56 saccharides and alcohols, 48 terpenoids and their derivatives, 46 organic acids, 44 alkaloids and their derivatives, 39 polyphenols and their derivatives, 13 phenylpropanoids and 12 lignans and coumarins (Figure 1A). While Wang et al. (40) identified a total of 527 non-volatile metabolites in green tea, including 109 flavonoids, 89 phenolic acids, 81 lipids, 64 amino acids and their derivatives, 37 organic acids, 25 alkaloids, and 12 sugars and alcohols. In comparison, Zheng'an Bai tea contains fewer flavonoids and a greater variety of amino acids. Meanwhile, Spearman Rank Correlation analysis showed that there was good biological reproducibility among the samples within each group, which indicated that the data in this study had good reproducibility and reliability (Supplementary Figure S1).

Metabolites interact with each other in organisms to form different pathways. By annotating all identified metabolites through the KEGG database, the top 20 annotation information indicates that a large number of secondary metabolites such as amino acids and flavonoids are enriched, reflecting the abundant content of these substances in "Zheng'an Bai tea" (Figures 1B,C). Based on the metabolomics data of 573 non-volatile metabolites (Supplementary Table S1), PCA analysis was performed using an unsupervised pattern. The results showed that these samples were clearly classified into 9 different groups, suggesting that there may be significant differences in non-volatile metabolism between different groups (Figure 1D). The first principal component and the second principal component explained 32.9 and 16.5% of the variation results, respectively. Compared with other samples, the fixing and drying samples were closely clustered together, indicating that the metabolic differences between these samples were relatively small.

3.2 The content changes of non-volatile metabolites in different tissues

Polyphenols are one of the most important components of tea tree leaves (41). Overall, the buds of "Zhengan Bai tea" contain a relatively large amount of polyphenols and terpenoids, and ultimately show a lower content in the dried samples (Figure 2). The
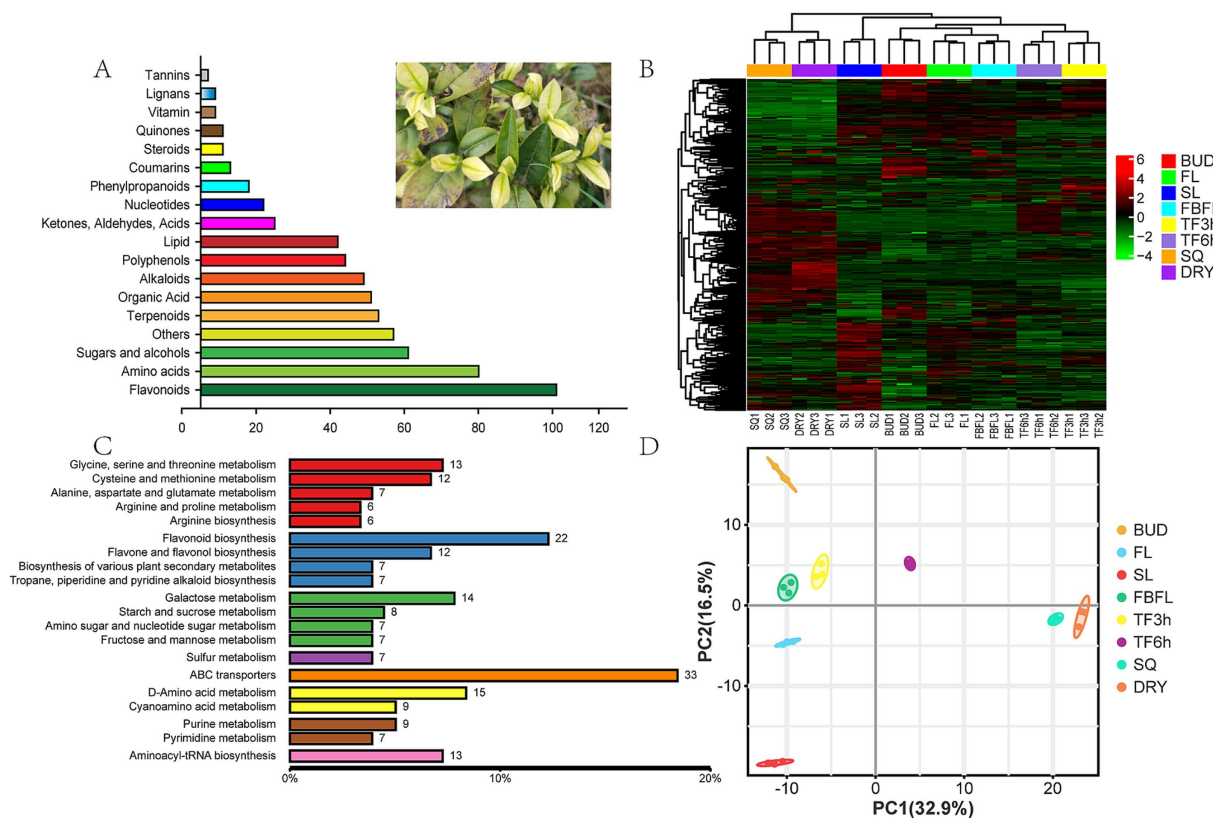
FIGURE 1
Overview of non-volatile metabolites. **(A)** Classification of non-volatile metabolites, **(B)** heatmap analysis of non-volatile metabolites, **(C)** the main enrichment pathway for non-volatile metabolites, **(D)** PCA analysis based on non-volatile metabolites.
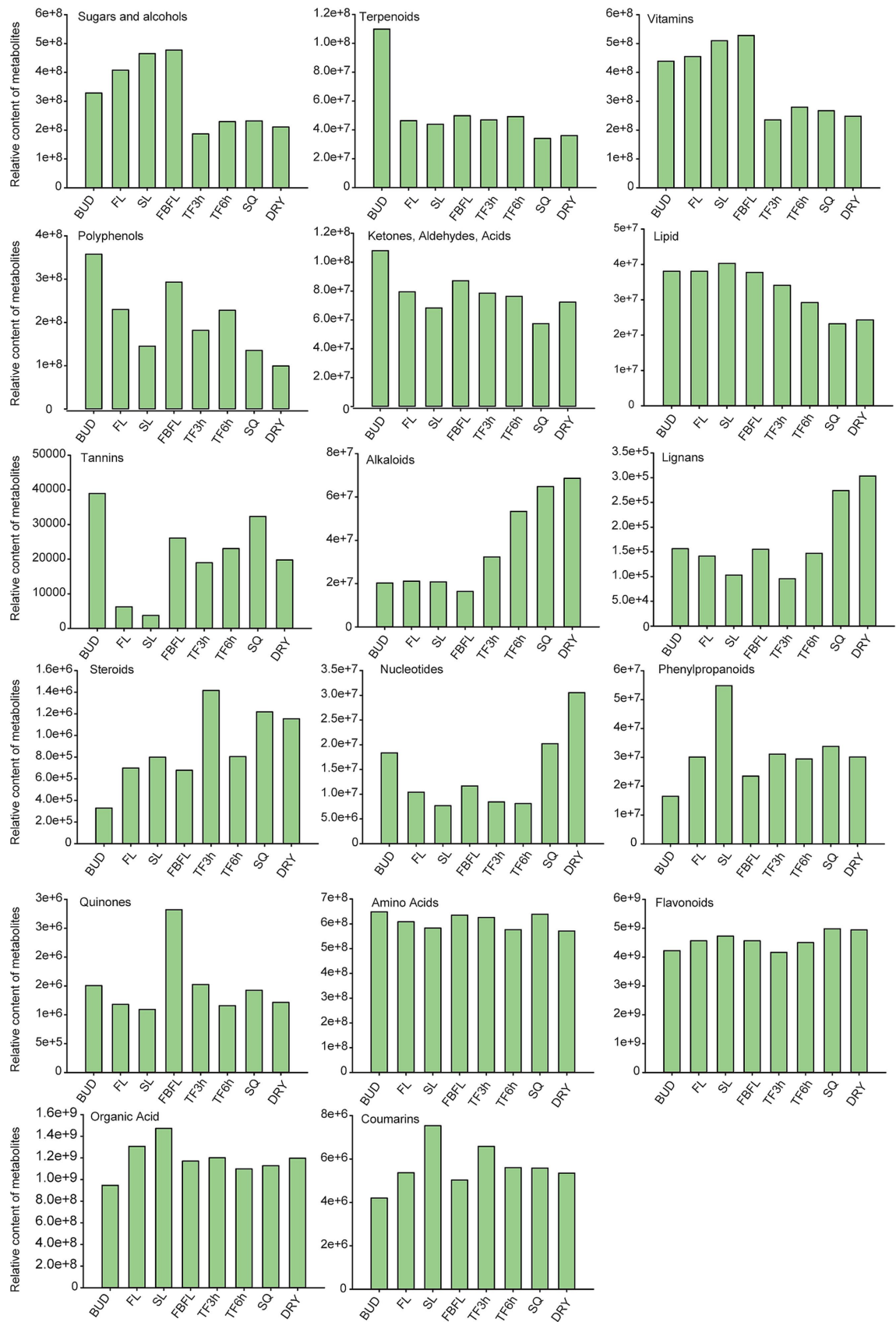
FIGURE 2
The changing trends of different types of non-volatile metabolites in eight tissues (the relative contents were calculated based on the peak areas of metabolites in the widely targeted metabolomics).

contents of sugars, alcohols and vitamins in tea leaves after spreading are all lower than those in fresh leaves. In addition, the lipid content gradually decreases during the processing process, which is similar to the research results of Li et al. (42). While substances such as alkaloids, lignins and nucleotides generally showed an increasing trend during the processing. Amino acids, organic acids and flavonoids are important taste substances and beneficial components in tea (27, 43). Their contents change slightly in fresh leaves at different stages and during the processing. Furthermore, Figure 2 also shows the dynamic change characteristics of substances such as tannins, ketones, aldehydes, acids and coumarins in different tissues. Compared with other stages, the high temperature in the fixation stage leads to the most drastic changes in metabolites, which is consistent with the previous research results (17, 40).

3.3 The non-volatile differential metabolites among the fresh leaves

Many studies have shown that the quality characteristics of different leaf positions of tea plants are significantly different (1, 44, 45). For Zheng'an Bai tea, 133,165,114 differential metabolites were detected in the FL (first leaf), SL (second leaf) and FBFL (first bud and first leaf) compared to the bud, respectively (Figures 3A–C). A total of 88 and 99 differential metabolites were identified between the first and second leaves and first buds and first leaf, respectively. At the same time, a total of 114 differential metabolites were found between the FBFL and the SL (Figures 3D–F). For fresh leaves at different stages of development, the metabolites with top 20 fold changes values contain a large number of sugars, alcohols, organic acids, amino acids, polyphenols, flavonoids and alkaloids (Figures 3G–L; Supplementary Figures S2A–F). In addition, many terpenes, alkaloids and polyphenols also showed diverse variation characteristics at different leaf positions. Further KEGG enrichment analysis showed that flavonoids and flavonoid biosynthesis pathways were enriched in fresh leaves of tea plants at different developmental stages (Supplementary Figures S2G–L). Among the top 20 metabolites with the largest fold changes, ethyl gallate, theaflavic acid, isovitexin, linalool and vincetoxicoside B were the most common. All the differential metabolites and OPLS—DA model information are presented in Supplementary Table S2 and Supplementary Figure S3, respectively.

3.4 Characteristics of the quality change of non-volatiles in the processing process

The quality of tea beverages is not only related to fresh leaves, but also the processing technology can also significantly affect the quality of dry tea (31, 46). At different stages of processing, the content of many non-volatile metabolites in Zheng'an Bai tea changed significantly. Compared with the TF3h, 117, 192, and 207 different metabolites were identified in the TF6h, SQ, and DRY stages, respectively (Figures 4A–C; Supplementary Figures S3A–C). Compared with TF6h stage, SQ and DRY identified 142 and 168

different metabolites, respectively. However, after fixation, enzymatic reactions in tea decreased significantly, and only 77 different metabolites were identified compared to the DRY tea (Figures 4D–F; Supplementary Figures S4D–F) (47). The above results indicate that the fixation and drying processes are very important for the formation of tea quality (9, 38). Among these different metabolites, there are a large number of flavonoids, polyphenols, terpenoids, sugar alcohols, and organic acids (Supplementary Figures S3G–L). Similar to the research results of Chen et al. in large-leaf black tea (30), during specific processing stages, some alkaloids such as zarzissine, methyl L-Pyroglutamate, piperidine, flavonoids such as theaflavin 3,3′-digallate, terpenoids such as euscaphic acid, and polyphenols such as ethyl gallate changed significantly. KEGG enrichment analysis showed that during different spreading stages, many plant hormones such as salicylic acid and a large amount of amino acids such as arginine were enriched. The different metabolites between the spreading samples (including TF3h and TF6h) and the SQ and DRY samples are all significantly enriched in the flavonoid metabolic pathway. Previous studies have shown that the spreading process can promote the hydrolysis of some proteins to increase the content of amino acids, accompanied by a decrease in the content of tea polyphenols, soluble sugars, and others (40, 48). While the different metabolites between the SQ and DRY samples are mainly enriched in the amino sugar and amino acid pathways (Figures 4G–L).

3.5 Total volatiles metabolites in Zheng'an Bai tea

A total of 97 volatiles components were detected in the samples of different developing tissues and processing stages of Zheng'an Bai tea (Supplementary Table S3). This number is more than the 47 in Longjing tea and the 91 in Fudingdabai tea (35, 49). However, this may be because leaves at different developmental stages are included in this study. Among them, the number of aroma components detected in the samples of BUD and TF6h was the highest, both of which were 72, while the number of aroma components in the samples of TF3h and SQ was the least, which was 58 (Figure 5A). This once again proves that moderate spreading is beneficial for the release of tea aroma (35). Among the 97 volatile components in these samples, benzyl alcohol, geraniol, nonanal, methyl salicylate, cis-jasmone, hexanal, nonanal and linalool oxide are common characteristic volatile substances in tea (30, 50). All volatiles substances are classified into 7 categories, among which alcohols and esters have the largest number, both being 27, followed by alkanes and aldehydes, with 21 and 12, respectively, (Figure 5B). This result is slightly different from the study of black tea by Yin et al. (51). Similar to the results of the widely-target metabolome analysis, all samples were well divided into eight groups by PCA analysis based on volatiles substances, and the interpretation rates of the first principal component and the second principal component reached 40.1 and 15.2%, respectively (Figure 5C). Meanwhile, similar to the research results of Wang et al. (40), most of the volatiles substances decreased sharply in the fixing stage (Figure 5D).

3.6 Key aroma compounds identified using OAVs in the Zheng'an Bai tea

Aroma is one of the important flavor characteristics of tea, which is not only related to the quality of fresh leaves, but also affected by processing technology (2). The odor activity value (OAV) is an important index for objectively evaluating the contribution of volatile substances to aroma and is widely used in many studies (52, 53). Volatile components with an OAV value greater than 1 are usually considered to have an important contribution to the aroma (47). For example, Qin et al. (29) identified 11 OAV > 1 key aroma compounds in steamed green tea

through OAV analysis. In this study, we conducted OAV analysis on all volatile components based on the odor threshold values (Supplementary Table S4). As shown in Table 1, the volatile metabolites with an OAV value greater than 1 in at least one tissue are presented in detail. The results indicate that the contents of most volatile metabolites are relatively high in fresh leaves and during the spreading stage, but they decrease sharply or are difficult to be detected after fixation. Nine key aroma components of OAV >1 were identified in the dried tea samples, including 1-Octen-3-ol, nerolidol, linalool, methyl salicylate, jasmone, geraniol, heptaldehyde, 1-Nonanal, and octanal. Among them, 1-octen-3-ol, linalool, methyl salicylate, nonanal and geraniol have odors such as
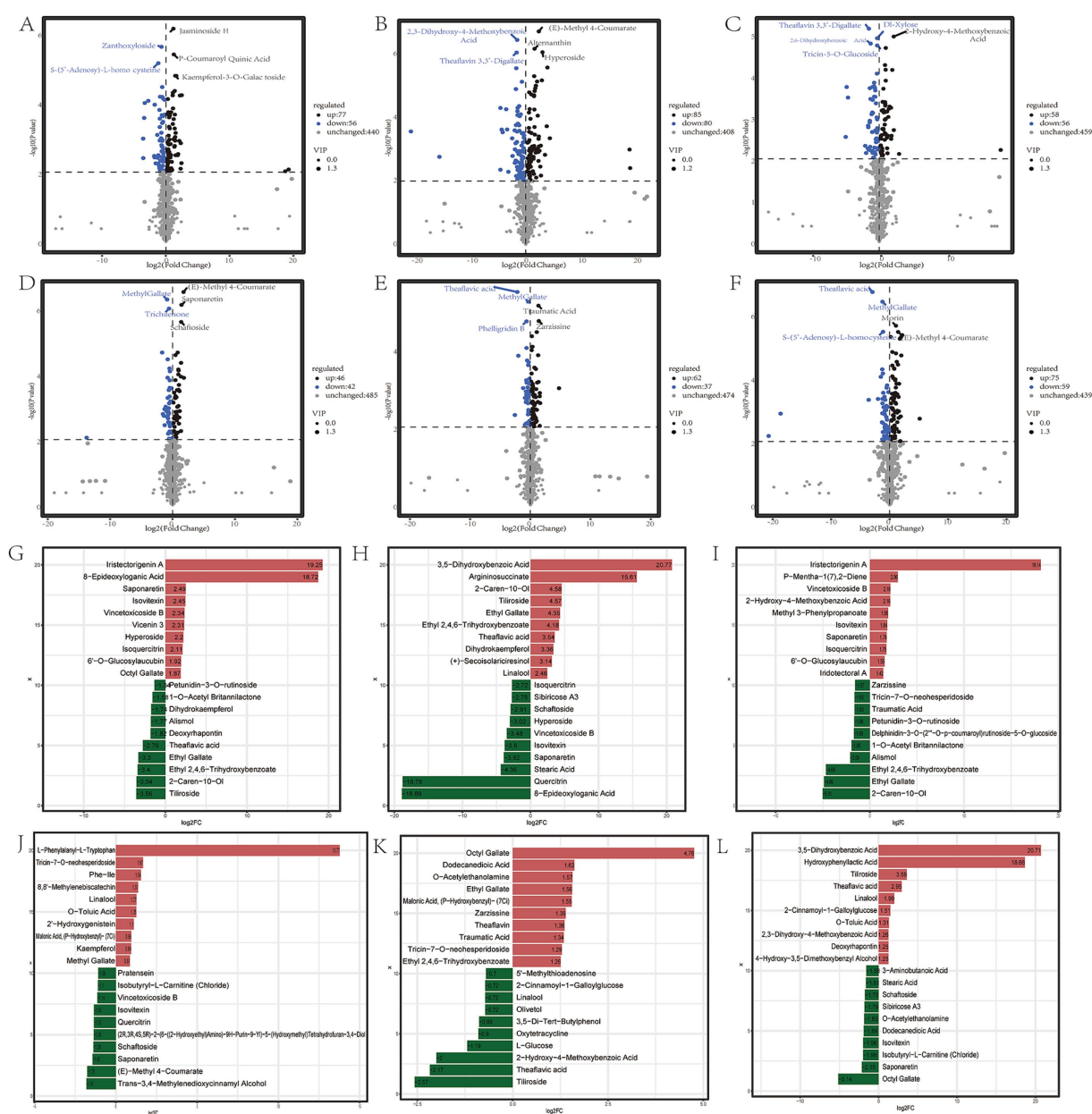
FIGURE 3
Differential metabolites of different fresh leaf samples. **(A–F)** Represent the number of differential metabolites in BUD vs. FL; BUD vs. SL; BUD vs. FBFL; FL vs. SL; FL vs. FBFL, and SL vs. FBFL, respectively; **(G–L)**, respectively, represent the top 20 metabolites with the largest fold change in the comparison groups of BUD vs. FL; BUD vs. SL; BUD vs. FBFL; FL vs. SL; FL vs. FBFL, and SL vs. FBFL.
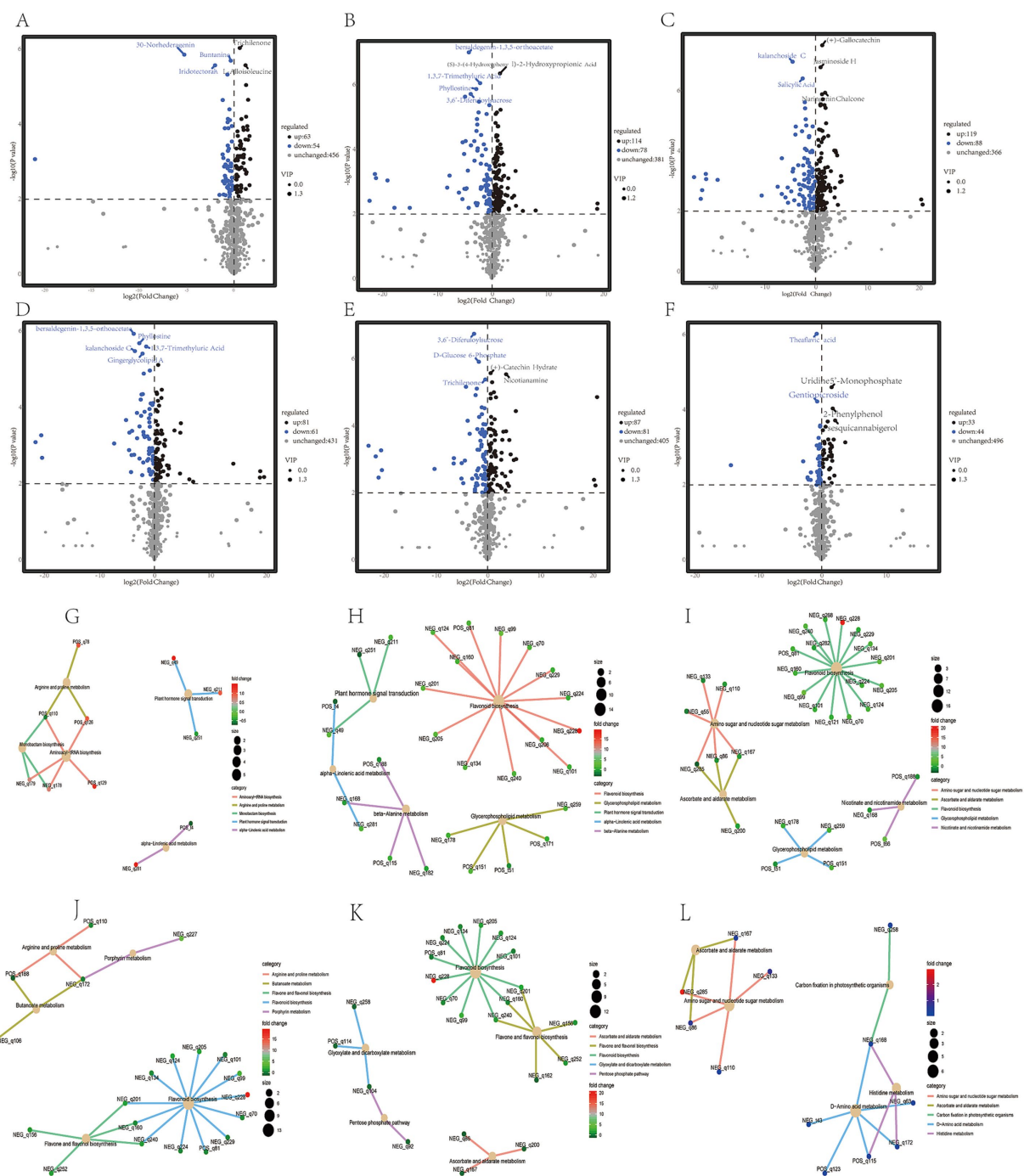
FIGURE 4
Differential metabolite heat map analysis and KEGG enrichment analysis of different samples during processing. **(A–F)** Represent the number of differential metabolites in TF3h vs. TF6h; TF3h vs. SQ; TF3h vs. DRY; TF6h vs. SQ; TF6h vs. DRY, and SQ vs. DRY, respectively. **(G–L)** Represent the KEGG enrichment analysis of the differential metabolites in TF3h vs. TF6h; TF3h vs. SQ; TF3h vs. DRY; TF6h vs. SQ; TF6h vs. DRY, and SQ vs. DRY, respectively.

fresh, floral and sweet scents, and they have also been identified as the key aroma substances of Longjing tea (49, 53). While jasmone and octanal are, respectively, one of the key aroma components of Lu'an Guapian tea and Xinyang Maojian tea (28, 29). Meanwhile, heptaldehyde is regarded as one of the contributing components of the chestnut-like aroma in tea (47).

It is worth noting that due to the lack of standard substances for related metabolites, relative quantification or semi-quantification is carried out by the internal standard method, which may cause a certain deviation in the accurate detection of substance content. And due to the different characteristics of compounds, this deviation effect may be different for each metabolite. Therefore,
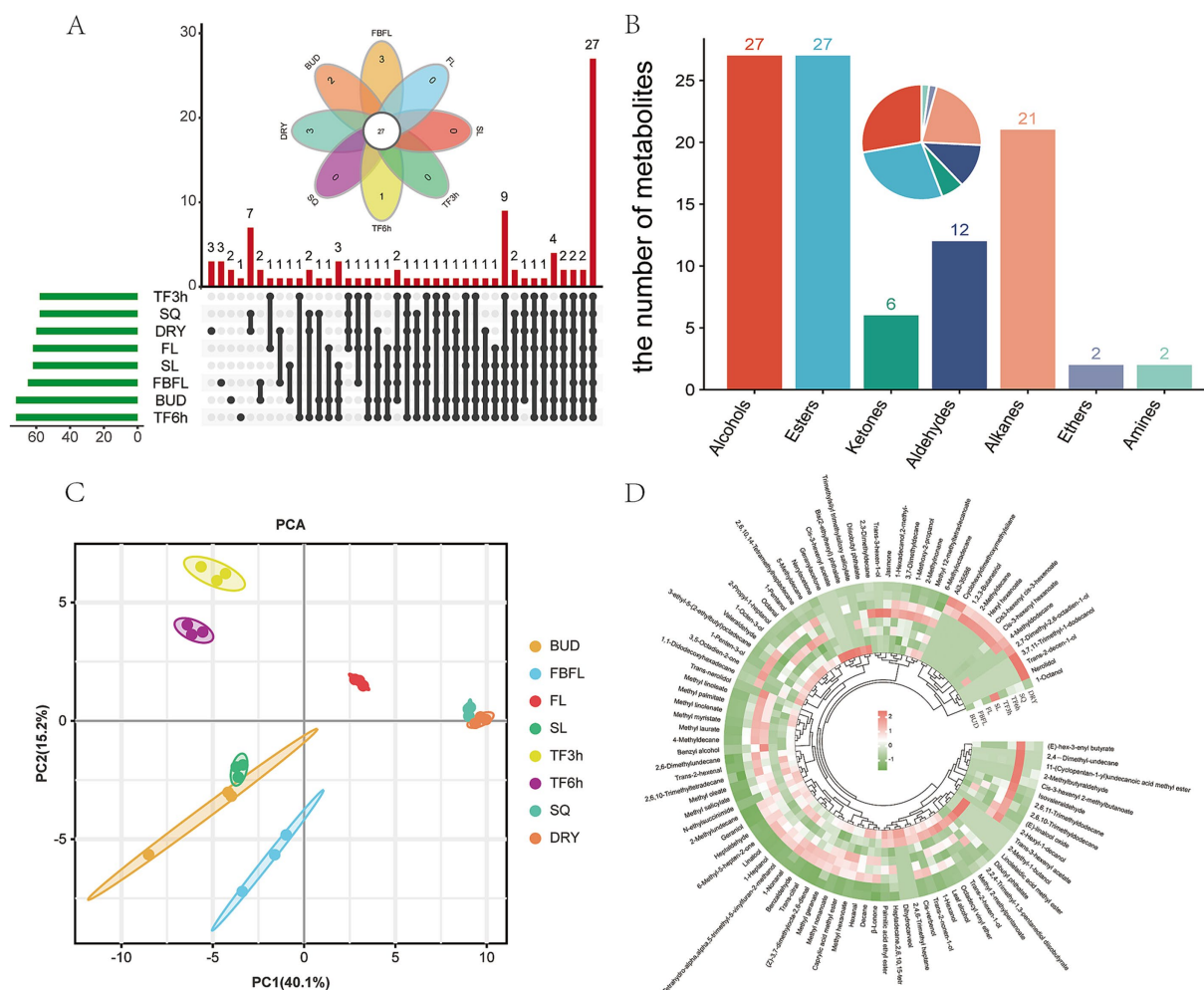
FIGURE 5
Overview of volatile metabolites. **(A)** Venn diagram analysis of volatile metabolites in different samples, **(B)** Classification statistics of volatile metabolites, **(C)** PCA analysis of volatile metabolites, **(D)** heatmap analysis of volatile metabolites.

although the OAV values of many other volatile metabolites such as 2-Methylbutyraldehyde, trans-2-decen-1-ol and cis-3-hexenyl cis-3-hexenoate are less than 1, they may also contribute to the aroma of Zheng'an Bai tea (24, 50, 54, 55). However, since SPME-GC-MS/MS is a highly selective method that is very effective for aldehydes and ketones but not so effective for critical sulfur-containing compounds, we will further analyze its aroma characteristics by combining sensory evaluation methods in future studies. Meantime, when identifying differential metabolites, relatively loose standards may lead to the identification of more differential metabolites.

4 Conclusion

In this study, a total of 573 non-volatile metabolites were identified in total, including 96 flavonoids and their derivatives, 75 amino acids and their derivatives, 56 sugars and alcohols, 48 terpenoids and their derivatives, 46 organic acids, 44 alkaloids and their derivatives, and 39 polyphenols and their derivatives. Among the top 20 differential metabolites of fresh leaves, ethyl gallate, theaflavin, isovitexin, linalool and vincetoxicoside B are the most common. However, the differential metabolites among the samples at the processing stage change abundantly. Overall, sugars and alcohols, alkaloids and polyphenols show the greatest differences between fresh leaves and samples at the processing stage. Meanwhile, we identified 97 volatile metabolites including alcohols, aldehydes and esters. The results showed that the fixation process led to a sharp decrease in the content of most volatile substances, while 9 volatiles substances with an OAV > 1, such as geraniol, octanal, linalool, jasmone and nerolidol, were identified as the key aroma components of Zheng'an Bai tea. Due to the lack of accurate quantitative data, this study may have certain limitations. However, we not only comprehensively revealed the quality characteristics of Zheng'an Bai tea, but also revealed for the first time the dynamic change trend of tea quality at different stages from fresh leaves, processing to dry tea.

TABLE 1 The OAV value of volatile metabolites (OAV value is greater than 1 in at least one tissues, more detailed information has been shown in Supplementary Table S4).

CAS	Name	Odor description	Threshold (mg/kg)	OAV							
				BUD	FBFL	FL	SL	TF3h	TF6h	SQ	DRY
106-26-3	Neral	Green, grassy, fresh	0.053	13.0	8.6	8.6	10.3	17.1	15.8	0.0	0.0
141-27-5	Trans-citral	Citrus, lemon-like	0.04	2.2	1.5	1.8	1.3	3.1	3.0	0.0	0.0
39028-58-5	(E)-linalool oxide	Floral, honey-like	3	1.0	1.6	0.9	0.2	3.3	3.9	0.2	0.2
3391-86-4	1-Octen-3-ol	Green, vegetative-like	0.007	9.6	6.2	0.0	9.5	0.0	6.6	1.8	1.4
96-17-3	2-Methylbutyraldehyde	Almond, chocolate	0.04	0.0	0.0	0.0	0.0	0.0	3.8	0.2	0.9
30086-02-3	3,5-Octadien-2-one	Creamy and fruity smell	0.0005	725.9	0.0	376.7	0.0	0.0	1026.4	0.0	0.0
544-12-7	Trans-3-hexen-1-ol	Green, leafy, grassy	0.07	0.0	0.0	0.5	0.0	3.9	0.0	0.0	0.0
79-77-6	β-ionone	Floral, sweet	0.09	1.9	1.3	1.1	2.2	1.4	2.3	0.6	0.3
100-51-6	Benzyl alcohol	Floral, rose-like, phenolic	0.1	47.4	0.7	12.8	108.6	44.5	17.0	0.2	0.3
6728-26-3	Trans-2-hexenal	Green, fruity	0.04	3.3	5.1	1.6	2.6	4.9	1.9	0.0	0.0
34995-77-2	Tetrahydro-alpha,alpha,5-trimethyl-5-vinylfuran-2-methanol	Floral	6	2.5	4.8	0.4	2.8	3.4	4.3	0.0	0.0
7212-44-4	Nerolidol	Floral, green, citrus	0.00025	0.0	0.0	0.0	0.0	0.0	0.0	0.0	51.2
40716-66-3	Trans-nerolidol	Slight neroli-like	0.25	0.6	0.4	0.2	1.1	1.9	0.0	0.0	0.0
78-70-6	Linalool	Floral, sweet	0.005	4227.6	7196.1	2803.1	3508.8	5112.0	7535.1	73.2	107.6
106-70-7	Methyl hexanoate	Sweet, balsamic, creamy	0.075	1.6	1.2	0.2	3.0	2.4	2.1	0.1	0.1
110-93-0	6-Methyl-5-hepten-2-one	Green, grassy, fresh	0.1	5.5	5.1	1.5	3.0	5.7	7.2	0.0	0.0
119-36-8	Methyl salicylate	Fresh, sweet	0.06	119.7	91.3	41.0	107.4	82.8	73.9	2.3	1.6
488-10-8	Jasmone	Floral	0.007	36.2	33.3	11.4	72.8	227.7	79.1	45.0	31.8
106–24–1	Geraniol	Rose-like, sweet	0.0075	14860.0	16259.5	6189.3	10919.7	13427.5	14939.0	278.3	206.7
3796-70-1	Geranylacetone	Floral, green, fruity	0.1	1.7	0.0	0.0	0.0	0.0	0.0	0.0	0.0
928-96-1	Leaf alcohol	Grass, green, fruit	0.4	1.0	1.4	0.0	0.9	0.0	1.0	0.0	0.0
590-86-3	3-methylbutanal	Malt	0.1	0.3	0.4	0.0	0.6	0.7	1.9	0.2	0.3
111-70-6	1-Heptanol	Green, sweet	0.2	0.7	1.4	0.3	1.1	1.3	1.4	0.0	0.0
111-71-7	Heptaldehyde	Green, oily, grassy	0.01	18.5	13.6	4.3	12.3	18.9	18.8	1.6	2.4
124-19-6	1-Nonanal	Floral, fatty, green	0.04	13.9	22.8	6.9	14.7	29.3	31.7	6.9	3.2
111-87-5	1-Octanol	Green, citrus, fatty	0.1	0.0	2.4	0.0	6.8	0.0	1.7	2.2	0.3
124-13-0	Octanal	Citrus, fruit, green	0.0007	96.3	49.4	0.0	79.1	0.0	73.1	6.6	14.8

Data availability statement

The datasets presented in this study can be found in online repositories. The names of the repository/repositories and accession number(s) can be found in the article/Supplementary material.

Author contributions

LL: Writing – original draft, Writing – review & editing. DQ: Writing – original draft, Writing – review & editing. XM: Data curation, Methodology, Software, Writing – review & editing. SY: Investigation, Methodology, Writing – review & editing. TJ: Conceptualization, Data curation, Formal analysis, Funding acquisition, Investigation, Methodology, Project administration, Resources, Software, Supervision, Validation, Visualization, Writing – original draft, Writing – review & editing. YA: Conceptualization, Data curation, Formal analysis, Funding acquisition, Investigation, Methodology, Project administration, Resources, Software, Supervision, Validation, Visualization, Writing – original draft, Writing – review & editing.

Funding

Conflict of interest

The authors declare that they have no known competing financial interests or personal relationships that could have appeared to influence the work reported in this paper.

Publisher's note

All claims expressed in this article are solely those of the authors and do not necessarily represent those of their affiliated organizations, or those of the publisher, the editors and the reviewers. Any product that may be evaluated in this article, or claim that may be made by its manufacturer, is not guaranteed or endorsed by the publisher.

Supplementary material

The Supplementary material for this article can be found online at: https://www.frontiersin.org/articles/10.3389/fnut.2024.1484257/full#supplementary-material

References

1. Qiu Z, Liao J, Chen J, Li A, Lin M, Liu H, et al. Comprehensive analysis of fresh tea (*Camellia Sinensis* cv. Lingtou Dancong) leaf quality under different nitrogen fertilization regimes. *Food Chem*. (2024) 439:138127. doi: 10.1016/j.foodchem.2023.138127

2. Xu Y, Liu Y, Yang J, Wang H, Zhou H, Lei P. Manufacturing process differences give Keemun black teas their distinctive aromas. *Food Chem*. (2023) 19:19. doi: 10.1016/j.fochx.2023.100865

3. Xia E, Tong W, Hou Y, An Y, Chen L, Wu Q, et al. The reference genome of tea plant and resequencing of 81 diverse accessions provide insights into genome evolution and adaptation of tea plants. *Mol Plant*. (2020) 13:1013–26. doi: 10.1016/j.molp.2020.04.010

4. Xu W, Wang X, Jia W, Wen B, Liao S, Zhao Y, et al. Dynamic changes in the major chemical and volatile components during the "Ziyan" tea wine processing. *LWT*. (2023) 186:115273. doi: 10.1016/j.lwt.2023.115273

5. Chen Y, Yang J, Meng Q, Tong H. Non-volatile metabolites profiling analysis reveals the tea flavor of "Zijuan" in different tea plantations. *Food Chem*. (2023) 412:412. doi: 10.1016/j.foodchem.2023.135534

6. Teng R, Ao C, Huang H, Shi D, Mao Y, Zheng X, et al. Research of processing Technology of Longjing tea with 'Baiye 1' based on non-targeted aroma metabolomics. *Food Secur*. (2024) 13:1338. doi: 10.3390/foods13091338

7. Huang W, Fang S, Su Y, Xia D, Wu Y, Liu Q, et al. Insights into the mechanism of different withering methods on flavor formation of black tea based on target metabolomics and transcriptomics. *LWT*. (2023) 189:115537. doi: 10.1016/j.lwt.2023.115537

8. Ran W, Li Q, Hu X, Zhang D, Yu Z, Chen Y, et al. Comprehensive analysis of environmental factors on the quality of tea (*Camellia Sinensis Var. sinensis*) fresh leaves. *Sci Hortic*. (2023) 319:112177. doi: 10.1016/j.scienta.2023.112177

9. Shan X, Deng Y, Niu L, Chen L, Zhang S, Jiang Y, et al. The influence of fixation temperature on Longjing tea taste profile and the underlying non-volatile metabolites changes unraveled by combined analyses of metabolomics and E-tongue. *LWT*. (2024) 191:115560. doi: 10.1016/j.lwt.2023.115560

10. Tan L, Zhang P, Cui D, Yang X, Zhang D, Yang Y, et al. Multi-omics analysis revealed anthocyanin accumulation differences in purple tea plants 'Ziyan', 'Zijuan' and their dark-purple hybrid. *Sci Hortic*. (2023) 321:112275. doi: 10.1016/j.scienta.2023.112275

11. Wang L, Yue C, Cao H, Zhou Y, Zeng J, Yang Y, et al. Biochemical and transcriptome analyses of a novel chlorophyll-deficient Chlorina tea plant cultivar. *BMC Plant Biol*. (2014) 14:352. doi: 10.1186/s12870-014-0352-x

12. Li N, Yang Y, Ye J, Lu J, Zheng X, Liang Y. Effects of sunlight on gene expression and chemical composition of light-sensitive albino tea plant. *Plant Growth Regul*. (2015) 78:253–62. doi: 10.1007/s10725-015-0090-6

13. Zhang Y, Wei K, Li H, Wang L, Ruan L, Pang D, et al. Identification of key genes involved in Catechin metabolism in tea seedlings based on transcriptomic and Hplc analysis. *Plant Physiol Biochem*. (2018) 133:107–15. doi: 10.1016/j.plaphy.2018.10.029

14. Lu M, Li Y, Jia H, Xi Z, Gao Q, Zhang Z-Z, et al. Integrated proteomics and transcriptome analysis reveal a decreased Catechins metabolism in variegated tea leaves. *Sci Hortic*. (2022) 295:110824. doi: 10.1016/j.scienta.2021.110824

15. Guo X, Ho C-T, Schwab W, Wan X. Aroma profiles of green tea made with fresh tea leaves plucked in summer. *Food Chem*. (2021) 363:363. doi: 10.1016/j.foodchem.2021.130328

16. Yue C, Cao H, Zhang S, Hao Z, Wu Z, Luo L, et al. Aroma characteristics of Wuyi rock tea prepared from 16 different tea plant varieties. *Food Chem*. (2023) 17:17. doi: 10.1016/j.fochx.2023.100586

17. Xia D, Zhang J, Xiong Z, Huang W, Wei Y, Feng W, et al. Effects of different fixation methods on the aroma quality of Anjibai tea. *LWT*. (2024) 204:116430. doi: 10.1016/j.lwt.2024.116430

18. Mi S, Han S, Wang M, Han B. Comprehensive analysis of the effect of etiolated tea cultivars and harvest seasons on volatile compounds and in vitro antioxidant capacity in steamed green teas. *Food Chem*. (2024) 22:22. doi: 10.1016/j.fochx.2024.101279

19. Mei X, Lin C, Wan S, Chen B, Wu H, Zhang L. A comparative metabolomic analysis reveals difference manufacture suitability in "Yinghong 9" and "Huangyu" teas (*Camellia Sinensis*). *Front Plant Sci*. (2021) 12:12. doi: 10.3389/fpls.2021.767724

20. Yang G, Zhou M, Shi J, Peng Q, Lin Z, Lv H, et al. How anaerobic treatment is controlling the volatile components and key odorants of purple-colored leaf tea. *J Food Compos Anal*. (2023) 122:105451. doi: 10.1016/j.jfca.2023.105451

21. Gao Y, Chen Y, Wang F, Chen J, Chen G, Xu Y, et al. Volatile composition and aroma description of tea (*Camellia Sinensis*) flowers from albino cultivars. *Horticulturae*. (2023) 9:610. doi: 10.3390/horticulturae9050610

22. Li J, Xiao Y, Zhou X, Liao X, Wu S, Chen J, et al. Characterizing the cultivar-specific mechanisms underlying the accumulation of quality-related metabolites in specific Chinese tea (*Camellia Sinensis*) germplasms to diversify tea products. *Food Res Int*. (2022) 161:161. doi: 10.1016/j.foodres.2022.111824

23. Yamashita H, Kambe Y, Ohshio M, Kunihiro A, Tanaka Y, Suzuki T, et al. Integrated metabolome and transcriptome analyses reveal etiolation-induced metabolic changes leading to high amino acid contents in a light-sensitive Japanese albino tea cultivar. *Front Plant Sci*. (2021) 11:11. doi: 10.3389/fpls.2020.611140

24. Yu Q, Huang C, Zhu R, Lu D, Liu L, Lai J, et al. Chemometrics-based investigation of non-volatiles/volatiles flavor of Tencha (*Camellia Sinensis* cv. Yabukita, Longjing 43 and Baiye 1). *Food Res Int*. (2023) 173:173. doi: 10.1016/j.foodres.2023.113461

25. Chen R, Lai X, Wen S, Li Q, Cao J, Lai Z, et al. Analysis of tea quality of large-leaf black tea with different harvesting tenderness based on metabolomics. *Food Control*. (2024) 163:110474. doi: 10.1016/j.foodcont.2024.110474

26. Li CF, Xu YX, Ma JQ, Jin JQ, Huang DJ, Yao MZ, et al. Biochemical and transcriptomic analyses reveal different metabolite biosynthesis profiles among three color and developmental stages in 'Anji Baicha' (*Camellia Sinensis*). *BMC Plant Biol*. (2016) 16:195. doi: 10.1186/s12870-016-0885-2

27. Shi J, Simal-Gandara J, Mei J, Ma W, Peng Q, Shi Y, et al. Insight into the pigmented Anthocyanins and the major potential co-pigmented flavonoids in purple-Coloured leaf teas. *Food Chem*. (2021) 363:363. doi: 10.1016/j.foodchem.2021.130278

28. Zhang J, Xia D, Li T, Wei Y, Feng W, Xiong Z, et al. Effects of different over-fired drying methods on the aroma of Lu'an Guapian tea. *Food Res Int*. (2023) 173:173. doi: 10.1016/j.foodres.2023.113224

29. Qin M, Zhou J, Luo Q, Zhu J, Yu Z, Zhang D, et al. The key aroma components of steamed green tea decoded by Sensomics and their changes under different withering degree. *Food Chem*. (2024) 439:439. doi: 10.1016/j.foodchem.2023.138176

30. Zhang S, Sun L, Wen S, Chen R, Sun S, Lai X, et al. Analysis of aroma quality changes of large-leaf black tea in different storage years based on Hs-Spme and Gc–Ms. *Food Chem*. (2023) 20:991. doi: 10.1016/j.fochx.2023.100991

31. Fang X, Liu Y, Xiao J, Ma C, Huang Y. Gc–Ms and Lc-Ms/Ms metabolomics revealed dynamic changes of volatile and non-volatile compounds during withering process of black tea. *Food Chem*. (2023) 410:410. doi: 10.1016/j.foodchem.2023.135396

32. Zhu Y, Lv H-P, Shao C-Y, Kang S, Zhang Y, Guo L, et al. Identification of key odorants responsible for chestnut-like aroma quality of green teas. *Food Res Int*. (2018) 108:74–82. doi: 10.1016/j.foodres.2018.03.026

33. Yan, Tian Y, Zhao F, Wang R, Zhou H, Zhang N, et al. Analysis of the key aroma components of Pu'er tea by synergistic fermentation with three beneficial microorganisms. *Food Chem*. (2024) 21:21. doi: 10.1016/j.fochx.2023.101048

34. Hao Z, Feng J, Chen Q, Lin H, Zhou X, Zhuang J, et al. Comparative volatiles profiling in Milk-flavored white tea and traditional white tea Shoumei via HS-SPME-GC-TOFMS and OAV analyses. *Food Chem*. (2023) 18:100710. doi: 10.1016/j.fochx.2023.100710

35. He Y, Li J, Mei H, Zhuang J, Zhao Z, Jeyaraj A, et al. Effects of leaf-spreading on the volatile aroma components of green tea under red light of different intensities. *Food Res Int*. (2023) 168:168. doi: 10.1016/j.foodres.2023.112759

36. Qin D, Wang Q, Jiang X, Ni E, Fang K, Li H, et al. Identification of key volatile and odor-active compounds in 10 Main fragrance types of Fenghuang Dancong tea using Hs-Spme/Gc-Ms combined with multivariate analysis. *Food Res Int*. (2023) 173:173. doi: 10.1016/j.foodres.2023.113356

37. Gemert LJV. (2003). Compilations of odour threshold values in air, water and other media. The Netherlands: Oliemans Punter & Partners BV.

38. Zhou J, Zhang X, Liu W, Zhang Q, Wu Y, Wu L. Widely targeted metabolomics analysis of the Main bioactive compounds of Ganpu tea processing through different drying methods. *LWT*. (2023) 189:115501. doi: 10.1016/j.lwt.2023.115501

39. Chen H, Zhang X, Jiang R, Ouyang J, Liu Q, Li J, et al. Characterization of aroma differences on three drying treatments in Rucheng Baimao (Camellia Pubescens) white tea. *LWT*. (2023) 179:114659. doi: 10.1016/j.lwt.2023.114659

40. Wang H, Hua J, Yu Q, Li J, Wang J, Deng Y, et al. Widely targeted Metabolomic analysis reveals dynamic changes in non-volatile and volatile metabolites during green tea processing. *Food Chem*. (2021) 363:363. doi: 10.1016/j.foodchem.2021.130131

41. Wang H, Cao X, Yuan Z, Guo G. Untargeted metabolomics coupled with Chemometrics approach for Xinyang Maojian green tea with cultivar, elevation and processing variations. *Food Chem*. (2021) 352:352. doi: 10.1016/j.foodchem.2021.129359

42. Li J, Hua J, Yuan H, Deng Y, Zhou Q, Yang Y, et al. Investigation on green tea lipids and their metabolic variations during manufacturing by nontargeted Lipidomics. *Food Chem*. (2021) 339:339. doi: 10.1016/j.foodchem.2020.128114

43. Chen T, Ma J, Li H, Lin S, Dong C, Xie Y, et al. Csgdh2.1 negatively regulates Theanine accumulation in late-spring tea plants (*Camellia Sinensis Var. sinensis*). *Hortic Res*. (2023) 10:uhac245. doi: 10.1093/hr/uhac245

44. Lin J, Wilson IW, Ge G, Sun G, Xie F, Yang Y, et al. Whole transcriptome analysis of three leaf stages in two cultivars and one of their F1 hybrid of *Camellia Sinensis* L. with differing Egcg content. *Tree Genet Genomes*. (2017) 13:1089. doi: 10.1007/s11295-016-1089-5

45. Zhang LQ, Wei K, Cheng H, Wang LY, Zhang CC. Accumulation of Catechins and expression of Catechin synthetic genes in *Camellia Sinensis* at different developmental stages. *Bot Stud*. (2016) 57:31. Epub 2017/06/10. doi: 10.1186/s40529-016-0143-9

46. Wang Z, Gao C, Zhao J, Zhang J, Zheng Z, Huang Y, et al. The metabolic mechanism of flavonoid glycosides and their contribution to the flavor evolution of white tea during prolonged withering. *Food Chem*. (2024) 439:138133. doi: 10.1016/j.foodchem.2023.138133

47. Wang H, Hua J, Jiang Y, Yang Y, Wang J, Yuan H. Influence of fixation methods on the chestnut-like aroma of green tea and dynamics of key aroma substances. *Food Res Int*. (2020) 136:136. doi: 10.1016/j.foodres.2020.109479

48. Qiao D, Mi X, An Y, Xie H, Cao K, Chen H, et al. Integrated metabolic phenotypes and gene expression profiles revealed the effect of spreading on aroma volatiles formation in postharvest leaves of green tea. *Food Res Int*. (2021) 149:149. doi: 10.1016/j.foodres.2021.110680

49. Zhu J, Zhu Y, Wang K, Niu Y, Xiao Z. Characterization of key aroma compounds and enantiomer distribution in Longjing tea. *Food Chem*. (2021) 361:361. doi: 10.1016/j.foodchem.2021.130096

50. Peng Q, Li S, Zheng H, Meng K, Jiang X, Shen R, et al. Characterization of different grades of Jiuqu Hongmei tea based on flavor profiles using HS-SPME-GC-MS combined with E-nose and E-tongue. *Food Res Int*. (2023) 172:113198. doi: 10.1016/j.foodres.2023.113198

51. Yin X, Xiao Y, Wang K, Wu W, Huang J, Liu S, et al. Effect of shaking manners on floral aroma quality and identification of key floral-aroma-active compounds in Hunan black tea. *Food Res Int*. (2023) 174:174. doi: 10.1016/j.foodres.2023.113515

52. Wang H, Shen S, Wang J, Jiang Y, Li J, Yang Y, et al. Novel insight into the effect of fermentation time on quality of Yunnan congou black tea. *LWT*. (2022) 155:112939. doi: 10.1016/j.lwt.2021.112939

53. Wang M-Q, Ma W-J, Shi J, Zhu Y, Lin Z, Lv H-P. Characterization of the key aroma compounds in Longjing tea using stir Bar Sorptive extraction (Sbse) combined with gas chromatography-mass spectrometry (Gc–Ms), gas chromatography-Olfactometry (Gc-O), odor activity value (Oav), and aroma recombination. *Food Res Int*. (2020) 130:108908. doi: 10.1016/j.foodres.2019.108908

54. Cao Q-Q, Fu Y-Q, Wang J-Q, Zhang L, Wang F, Yin J-F, et al. Sensory and chemical characteristics of Tieguanyin oolong tea after roasting. *Food Chem*. (2021) 12:12. doi: 10.1016/j.fochx.2021.100178

55. Liao X, Yan J, Wang B, Meng Q, Zhang L, Tong H. Identification of key odorants responsible for cooked corn-like aroma of green teas made by tea cultivar 'Zhonghuang 1'. *Food Res Int*. (2020) 136:136. doi: 10.1016/j.foodres.2020.109355

A flavoromics approach to investigate the effect of Saskatoon berry powder on the sensory attributes, acceptability, volatile components, and electronic nose responses of a low-fat frozen yogurt

Donna Ryland[1], John Thoroski[1], Shiva Shariati-Ievari[2],
April McElrea[2], Alexandre Goertzen[2], Geraldine M. Dowling[3,4,5]
and Michel Aliani[1]*

[1]Department of Food and Human Nutritional Sciences, University of Manitoba, Winnipeg, MB, Canada,
[2]St. Boniface Hospital Research Centre, Winnipeg, MB, Canada, [3]Department of Life Sciences, School
of Science, Atlantic Technological University Sligo, Sligo, Ireland, [4]Department of Analytical,
Environmental, and Forensic Science, Faculty of Life Sciences and Medicine at Kings College London,
London, United Kingdom, [5]Cameron Forensic Medical Sciences at William Harvey Research Institute,
Barts and The London School of Medicine and Dentistry, Queen Mary University of London, London,
United Kingdom

Introduction: Saskatoon berries are grown in Canada and some northwestern states in the United States, and are notable for containing abundant antioxidant polyphenols, vitamins, metal elements, and fiber. To increase consumer interest in and accessibility to Saskatoon berries, some producers have begun to develop processes for refining Saskatoon berries into a powder with an extended shelf life that can be incorporated into a variety of value-added food products. To assess the desirability of this approach, this study sought to determine how the sensory attributes, consumer acceptability, and volatile and non-volatile composition of a plain, Greek-style frozen yogurt (PY) changed when fortified with 16% Saskatoon berry powder (SBP). Greek-style frozen yogurt was chosen as the food to be fortified for this study due to its low fat and relatively high calcium and protein content as well as its popularity among consumers.

Results: Descriptive analysis of the two yogurt formulations by 11 participants determined that SBY was higher in berry aroma, berry flavor, and sweetness, and lower in cream aroma, dairy aroma, and sourness compared to PY. SBY was lower in iciness and degree of smoothness and higher in viscosity and mouth coating compared to PY. Untrained participants ($n = 112$), found no significant differences in color, flavor, and overall acceptability between SBY and PY. However, SBY was significantly less acceptable than PY for texture and aroma. Iciness was the most influential variable related to texture acceptability. For aroma acceptability, berry flavor (negatively related) and berry aroma (positively related) were the most influential attributes. The exposure of Saskatoon berry powder (SBP), PY, and SBY to e-nose sensors showed consistencies in replicate analysis ($n = 25$ measurements/sample), and cross validation of the PCA showed that the model could sort samples into the correct class with 98.7% accuracy. Key volatile organic compounds (VOCs) responsible for berry

and fruity aroma in SBP were also found to be retained in the SBY. Several key phenolic compounds with therapeutic effects such as baicalein, chlorogenate, gallic acid, p-coumaric acid, and syringic acid were also identified in both SBP and SBY samples, potentially indicating that the SBY may retain some of the health benefits associated with the consumption of raw Saskatoon berries.

1 Introduction

The Saskatoon (*Amelanchier alnifolia*) also known as serviceberries, juneberries, or shadbush, is a perennial shrub belonging to the *Rosaceae* family, the fruits of which have historically been foraged for use both as a food and medicine by various Indigenous peoples of North America as well as early European settlers (1). Commercial Saskatoon orchards have also been established since the 1960s, with cultivated Canadian Saskatoon berry production now occupying 1,083 hectares as of 2023, and producing 695 metric tons of fruit with a farm gate value of approximately 3 million dollars (2). While these production numbers pale in comparison to production totals for some other Canadian-grown fruits, it is nevertheless notable that Saskatoon berry production numbers have also grown steadily over the last 5 years, indicating a stable or increasing commercial interest in these fruits (2).

Some of this interest could be attributed to the fact that Saskatoon berries are known for possessing a desirable nutritional profile that combines high levels of dietary fiber, vitamins A and C, manganese, and iron (3). Moreover, Saskatoon berries are also noteworthy for their high levels of antioxidants in the form of polyphenols (4), which in turn may confer various health benefits. In particular flavanol, anthocyanin, and proanthocyanin have all been identified as flavonoid compounds in Saskatoon berries that possess anti-inflammatory, antidiabetic, and antitumor effects (1, 5).

A consumer study conducted by Garg et al. (6) has revealed that potential exists for further investigations into value-added processing of Saskatoon berries. Developing powdered Saskatoon berry could be an option as Cedillos et al. (7) found that frozen yogurt with up to 500 mg/90 g hesperidin powder per serving, a polyphenolic functional ingredient, was of interest to health conscious consumers. Saskatoon berry powder fortification will be successful if it confers desirable sensory characteristics into the final product. To assess these characteristics a technique termed descriptive analysis is used. This approach involves identifying, describing, and then measuring the taste, aroma, textural, and potentially visual attributes of food, which may impact consumer acceptability of products fortified with Saskatoon berry.

In addition to sensory analysis, evaluating the volatile and non-volatile composition of these products can also prove valuable, as specific components within a food matrix may have a substantial impact on its overall sensory properties, and as such may be useful

targets for future product development activities. In terms of the volatile compounds identified with Saskatoon berries, Butorova et al. (8) identified various volatile organic compounds (VOCs), including 10 aldehydes, 13 alcohols, 4 esters, 3 ketones plus acetic acid from a gas chromatographic analysis of Saskatoon berries of different varieties grown in different years.

Electronic nose (e-nose) analysis is another method that can be used to analyze the volatile composition of products. These devices are designed to detect and recognize volatile compounds using arrays of sensors operating in parallel. When exposed to a volatile sample, these sensors produce a combined output that can be described as an 'odor fingerprint' which can then be compared with previous results from known samples to identify them or group together sets of samples which produce similar results. Moreover, if a consistent 'odor fingerprint' can be generated by a particular sample or set of samples, e-nose technology offers several advantages by being rapid, allowing non-destructive analyses, in addition to continuous monitoring potential. Within the context of Saskatoon berries, e-nose sensors have the capacity to simplify future product development, particularly if individual sensors can be strongly correlated with flavor or aroma attributes.

In addition to the sensory and volatile properties, assessing the nutritional composition of SBP is also important, as the original nutritional properties of Saskatoon berries may not necessairily be retained in the SBP. However, studies have found evidence of at least some of the health promoting effects of Saskatoon berries being preserved post-processing (9, 10). In particular, Nuclear Magnetic Resonance (NMR) spectroscopy is a powerful analytical technique that can be used to identify and quantify the concentrations of key phenolic compounds of Saskatoon berries. More directly, the oxygen radical absorbance capacity (ORAC) assay is another method that can be used for analyzing the antioxidant quenching capacity of foods.

Within this study, yogurt was chosen as a candidate for incorporation of SBP due to having relatively simple composition, being regularly consumed by approximately 20% of Canadians, and also being rich in protein, calcium and probiotics. Moreover, approximately 80% of the yogurt consumed in Canada is flavored, while 70% is fat-free or low-fat, indicating a general preference toward flavored, and health-promoting formulations – factors which would align well with a Saskatoon berry flavored product (11). Among consumers the frozen form of yogurt is popular (7). The objectives of this study therefore were to determine the consumer acceptability, sensory properties, and volatile and non-volatile chemical composition of Greek-style frozen yogurt fortified with SBP compared to its non-fortified counterpart, to provide a preliminary assessment of whether the nutritional

compounds associated with Saskatoon berries were retained in the frozen yogurt, and to provide guidance for future product development activities.

2 Materials and methods

2.1 Materials

SBP (Lot Code: 261115) contained only Saskatoon berry and was obtained from Interlake Saskatoon Inc., Warren MB. Nutrients contained in 10 g of SBP according to the Nutrition Facts label were as follows: fat 0.1 g, carbohydrate 9 g comprised of 5 g sugar and 2 g fiber, protein 0.2 g, 2% of daily value for calcium and 6% of daily value for iron, 30 calories.

2.2 Yogurt processing

All yogurt samples were processed in the Dairy Processing Pilot Plant, Department of Food and Human Nutritional Sciences, Faculty of Agricultural and Food Sciences at the University of Manitoba, Winnipeg MB, a facility licensed by the Canadian Food Inspection Agency under the Safe Food for Canadians Regulations for production and packaging of dairy products destined for human consumption.

The unflavored Greek style yogurt (PY) samples were prepared using milk (1% butter fat) obtained from the local supermarket, skim milk powder (Medallion Milk Co., Winnipeg MB) and bacterial culture, Danisco YoMix 495 (Danisco Canada, Mississauga ON) containing *Streptococcus Thermophilus* and *Lactobacillus delbrueckii subsp. Bulgaricus* bacteria in the amounts by weight of 95, 5 and 0.01%, respectively. The SBY was prepared by mixing 52% PY, with 16% SBP and 32% water (municipal water supply).

To make the PY the milk and skim milk powder were thoroughly mixed in a large sanitary steam kettle (Groen Manufacturing Company, Model # D 10). This was heated to 85°C and held for 5 min with constant agitation. The mixture was cooled to 42°C, and bacterial culture was added aseptically according to the recommended specification for the culture being used mixing for 3 to 5 min to thoroughly combine it into the milk products. This was transferred into sanitized pails with sanitary food liners and closed with sanitized lids which were placed in a custom-built sanitary room designed for incubating fermented dairy products at 42°C. The incubator contains a Caloritech heating system and a Coldstream cooling system with Omron temperature control. The dimensions are 2 m wide x 2.5 m long x 2.5 m high. Yogurt was incubated for approximately 5 h until the pH reached 4.6. Yogurt was cooled to 4°C after which time it was either used to make the SBY or 50 g was placed into 3.5 oz. (104 mL) solo cups covered with plastic lids (Dart Container Corporation, Mason MI) and frozen at −28°C. The SBP was combined with cold water in a clean sanitized vessel and mixed thoroughly. The powder/water mix was thoroughly combined with the plain yogurt in a clean sanitized vessel. It was packaged the same as the plain yogurt (50 g per 3.5 oz. portion cup) and frozen at −28°C. Microbiological testing of the final products yielded the following results:

SBY Lot # 17156 - Coliforms <10 CFU per gram, *E. coli* <10 CFU per gram; PY Lot # 17149 - Coliforms <10 CFU per gram, *E. coli* <10 CFU per gram. All values comply with the National Dairy Code of Standards Schedule III (12) for microbiologically safe fermented food products.

2.3 Preparation of samples for sensory evaluation

Yogurt samples were removed from the freezer (−28°C) about 18 h before the session and placed in a freezer at −15°C. One hour prior to the session, the samples were held at room temperature allowing them to thaw enough to penetrate with a plastic spoon. They were kept in thermal bags (Coleman, Chicago IL) to maintain the temperature at −3° ± 1°C for evaluation.

2.4 Sensory evaluation methods

Human Ethical Approval was obtained from the Joint Faculty Ethics Research Board of the University of Manitoba (Protocol # J2017:059) to conduct both the descriptive analysis and consumer acceptance panel. The criteria for participation were that the panelist be available, interested, have no allergies to any food products, and be 18 years of age or older. An honorarium was provided. Panelists were recruited via an e-mail invitation to students and staff members in the Faculty of Agricultural and Food Sciences at the University of Manitoba (Winnipeg MB).

2.5 Descriptive analysis panel— measurement of sensory attributes

The modified descriptive analysis sensory method (13) used was as described by Fahmi et al. 2019 (14). Eleven panelists agreed on the three aromas, two tastes, one flavor, and four texture attributes with the associated definition, evaluation procedure, and reference point (Table 1). Three replications were completed by panelists seated at partitioned computer workstations equipped with SIMS software (Sensory Integrated Management System, Berkeley Heights NJ). Samples were evaluated in random order under light from incandescent bulbs that were blocked with red transparent plastic to avoid the possibility of bias due to sample color. Filtered water at room temperature and an unsalted top cracker were available for cleansing the palate before and between sample evaluations.

2.6 Consumer acceptability panel

Demographics of the consumers (*n* = 112) were as follows: Female (*n* = 86), Male (*n* = 26); 37%:18 to 24 yr., 30% 25 to 34, 33% 35 yr. and over. Frequency of eating yogurt in any form: 44% at least two to three times a week, 30% at least once a week, 14% at least once a month, 6% a few times a year, 6% occasionally, 0% never; Frequency of eating frozen yogurt: 2% at least two to three times a week, 6% at least once a week, 27% at least once a month, 31% a few times a year, 30% occasionally, 5% never; Frequency of eating frozen Greek yogurt: 2% at least two to three times a week, 5% at least once a week, 18% at least once a month, 14% a few times a year, 29% occasionally, 32% never.

Consumers attended a single session (about 15 min) conducted in the same area as the descriptive analysis panel. However, the red transparent plastic was not used as acceptability testing requires samples to be presented as one would normally view them. The study was completed three days per week for two weeks to accommodate

TABLE 1 Attribute definitions, procedure for evaluation, reference standard and standard manufacturer for attributes found in SBY and PY.

Attribute	Definition	Procedure for evaluation of frozen yogurt	Reference (point on 15 cm line scale)	Manufacturer
Aroma		Remove the cap, take 3 short sniffs and replace the cap		
Cream aroma	Aroma similar to sour cream		Olympic Greek Plain Yogurt 2% fat (10.0)	Olympic, Division of Ultima Foods Inc. Delta BC
Dairy aroma	Aroma similar to milk		Olympic Greek Plain Yogurt 2% fat (12.0)	Olympic, Division of Ultima Foods Inc. Delta BC
Berry aroma	Aroma similar to typical Saskatoon berry which has been described as woody		25 g Saskatoon berry powder (SBP) in 100 g filtered water (10.5)	Interlake Saskatoon Inc. Warren MB Lot Code: 261115
Taste/Flavor		Take about 1/2 teaspoon (2 mL) of the sample making sure that the sample thoroughly covers all surfaces of the mouth.		
Sour taste	Taste similar to citric acid in solution		Liberté Greek Plain Yogurt 0% fat (9.0)	Liberté Canada, St-Hubert QC
Sweet taste	Taste similar to sucrose in solution		1.5 g sucrose in 100 g filtered water (6.5)	Rogers Fine Granulated Sugar, Lantic Inc. Montreal QC
Berry flavor	Flavor similar to Saskatoon berry which has been described as woody		25 g SBP in 100 g filtered water (9.5)	Interlake Saskatoon Inc. Warren MB Lot Code: 261115
Texture		Take about 1/2 teaspoon (2 mL) of sample		
Iciness	Sample that has low iciness melts immediately in the mouth with no ice crystals detected. Sample that is high in iciness does not melt immediately and ice crystals are detectable in large numbers.	Place the sample in the mouth and manipulate it to evaluate iciness.	4 parts Olympic Greek Plain Yogurt 2% fat to 1 part filtered water frozen (11.0)	Olympic, Division of Ultima Foods Inc. Delta BC
Degree of Smoothness	Sample that is not smooth is perceived as a gritty/sandy or rough texture. A high degree of smoothness means the sample has a smooth and uniform spread onto the palate and no rough texture is detectable.	Spread the sample onto the palate with the tongue and evaluate the smoothness.	25 g SBP in 100 g filtered water (4.0)	Interlake Saskatoon Inc. Warren MB Lot Code: 261115
Viscosity	High viscosity means the sample does not move easily within the mouth and may feel pasty offering some resistance during manipulation. Low viscosity means the sample offers little resistance during manipulation.	Gently manipulate the sample by slowly rotating the sample between the tongue and palate. During the melting process and immediately after the sample has melted assess the ease of movement within the mouth.	Chapman's Ice Cream Triple Berry Frozen Sorbet (2.5)	Chapman's Ice Cream, Markdale ON
Mouth coating	Evaluate the intensity of the mouth coating as the amount of film remaining in your mouth after swallowing.	Rinse with water to remove any residual coating within the mouth. Gently manipulate the sample by slowly rotating it between tongue and palate.	Real Dairy Frozen Greek Yogurt Lemon Meringue (5.5)	Lucerne Nestle Canada, North York ON

participants' schedules and workstation availability. Data collection for acceptability and frequency of eating the yogurt sample followed methods described previously (14). Consumers were also invited to comment regarding their thoughts about the samples before answering the demographic questions. Filtered water (20°C) was provided for rinsing before and between samples.

2.7 Proximate analysis

Proximate analysis for ash, fat hydrolysis, crude fibre, Calories (by calculation) carbohydrate (estimated, by calculation), crude protein and moisture of frozen yogurt was conducted by Central Testing Laboratories (Winnipeg MB) using methods previously reported (14).

2.8 Color measurement

The Hunterlab MiniScan (Hunter Associates Laboratory, Inc. Reston VA) with the D65 illuminant and 10° standard observer angle standardized to the white tile was used to measure L^*, a^*, and b^* values. Frozen yogurt samples were thawed overnight at 4°C. For each sample 22 g was taken from each of three cups and placed into a polystyrene Petri dish (60 mm dia x 15 mm ht.; Falcon Brand, Fisher Scientific, Ottawa ON) covered with a glass plate and placed on white paper.

2.9 Determination of pH

Measurements of pH values were taken using an Orion Star A211 pH meter calibrated using pH 4.01 and 7.00 buffers. For yogurt samples, approximately 25 mL of sample was thawed to room temperature, homogenized with a magnetic stirrer, and then transferred to a 100 mL beaker before measurement. The pH probe was inserted, and pH was monitored until a stable reading was obtained for at least 1 min. The pH meter was re-calibrated between each sample. For the SBP sample, 3.2 g of material was stirred into 17.2 g of MilliQ water.

2.10 Determination of oxygen radical absorbance capacity (ORAC) values

The oxygen radical absorbance capacity (ORAC) as an indicator of antioxidant capacity, was determined in four replicates for the SBP, PY, and SBY as previously described (15). The Trolox standard, fluorescein, potassium chloride, and sodium acetate were from Sigma-Aldrich (Oakville ON), and the 2,2′-azobis-2-methyl-propanimidamide dihydrochloride from Wako Chemicals (Richmond VA).

2.11 Electronic nose (E-nose) analysis of yogurt and powder samples

Both frozen yogurt samples (2.0 g), and SBP (2.0 g), were placed in 20 mL borosilicate headspace vials, which were then capped and frozen at -20°C for approximately 3 days before being removed from the freezer and allowed to thaw to room temperature. Measurements of the volatile produced by the samples were taken using an MSEM 160 E-nose (Sensigent LLC. Baldwin Park CA) equipped with a custom-built sampling apparatus consisting of a 16 cm long, 5 mm wide rubber tube attached to the sampling port of the device, which in turn was secured to a 1.28 diameter, 3.6 cm long needle that was used to pierce the septum of the headspace vial caps immediately prior to measurements. Five replicates of the sample were prepared, and each replicate was measured 5 times by the MSEM 160 while the needle remained inside the pierced vial. Sample measurement consisted of 90 s of pre-sampling purging of the device, followed by 90 s of sampling, and then 90 s of post-sampling purging using a 'low' pump speed. All measurements were performed on a single day in a non-random order and ambient air was used to calibrate measurements.

2.12 Analysis of volatile compounds in yogurt and powder samples using GC–MS

The extraction of volatile organic compounds (VOCs) was performed using solid phase microextraction (SPME) fibers (75 µm Carboxen. PDMS, Supelco) as previously described (16). In summary, 20 g of each of the two yogurts and 3.20 g of the SBP suspended in 17.2 g of Milli-Q water were prepared in a 100 mL PYREX™ bottle. These mixtures were spiked with 1,3-dichlorobenzene as an internal standard before extraction. The temperature of the Pyrex bottles was controlled by placing them in a water bath between 65–70°C (CORNING PC-420D heater/magnetic stirrer) to prevent clump formation. The SPME fiber was then inserted into the headspace above the mixture. The total extraction time was 60 min.

The collected volatiles were immediately analyzed using a 7890B GC with a 7,693 Auto-Sampler connected to a 7,000 GC/Triple Quadrupole mass spectrometry (MS) detector (Agilent Ltd., Santa Clara CA) as previously described (16). The semi-quantification of each volatile was calculated from the ratio of the base ion peak area for each VOC to the internal standard's (m/z 146) base ion peak. The identity of each peak was determined by matching their mass spectra with the mass spectra of authentic compounds analyzed and reported in the National Institute of Standards and Technology (NIST version 2.3, 2017) library. The relative linear retention indices (LRIs) of each of the compounds were also calculated using the retention time obtained for a series of n-alkanes (C8–C20, 40 mg/L in 150 µL of pentane) as described previously (17).

2.13 Extraction and analysis of selected compounds by nuclear magnetic resonance (NMR)

Approximately 1–1.2 g of sample was dissolved in 2 mL of methanol:water (3:2 v/v) in a 5 mL Eppendorf tube. The samples were vortexed for 1 min and then placed in a sonicator for 1 h. After sonicating they were centrifuged at 10,000 rpm for 30 min at 4°C. The supernatant was transferred to a clean tube and freeze-dried to remove all the liquid. The yogurt extracts were reconstituted in 550 mL of deuterated solvent mixture water: acetonitrile (4:1 v/v) using trimethylsilylpropanoic acid (TSP) as an internal standard. The SBP

was first reconstituted in 1 mL of the deuterated solvent mixture; 100 μL of this solution was then added to a clean tube with 450 μL of deuterated solvent using TSP as an internal standard. All the samples were then transferred to a 5 mm NMR tube for analysis.

The NMR experiments were conducted on a Bruker Ascend 600 spectrometer, operating at 600.27 MHz for proton nuclei and 150.938 MHz for carbon nuclei, and analyzed by 1D (NOESY) and 2D (COSY and HSQC) NMR methods. The spectra were processed using MestReNova version 12.0.0–20,080 as previously described (17).

2.14 Statistical analysis

For the descriptive analysis data, analysis of variance was performed with panelists and replicates as random factors and sample as a fixed effect. Two-way interactions of panelist and replicate, panelist and sample, and replicate and sample were included in the model. For consumer acceptability analysis of variance was performed with consumer as the random factor and sample, age, and gender as fixed effects. Interactions of 'sample by age' and 'sample by gender' were also included in the model. When interactions were not significant, the sums of squares were pooled with the error sums of squares, and the F value was recalculated as previously performed (15). One-way analysis of variance was performed for instrumental color, proximate analysis, pH, ORAC, e-nose sensor, and volatile data. All the above statistical procedures were carried out with SAS (2009 Version 9.2) software (Statistical Analysis System, Cary NC). The collected data by MSEM 160 were transferred into CDAnalysis software (Sensigent, Version 11.2), and processed using the specific parameters as follows: sensors ΔR/R as the data scaling, digital filtering and baseline correction of the raw data was performed using Savitsky-Golay and 'Adv min max' algorithms, respectively. The data were not normalized. Sensors 3, 5, 8–12, 14, 15, and 22 were identified as particularly significant in discriminating between the three sample categories; all other sensors were manually excluded from further processing. The processed sensor responses (.met file), were then used for statistical analysis. A PCA diagram was produced by CDAnalysis using selected sensors to graphically depict the combined sensor outputs for SBP, SBY, and PY.

A correlogram was generated using R statistical package (version 4.02) to correlate all statistically significant results obtained for VOCs, and selected sensors for SBP, SBY, and PY. Stepwise multiple linear regression was performed (SPSS, Version 25.0) using the significant attributes from the consumer acceptability study as the dependent variables and all the attributes measured as potential predictors.

3 Results and discussion

3.1 Descriptive analysis panel— measurement of sensory attributes

Aroma, taste/flavor, and texture/mouthfeel attributes showed no significant differences between the SBY and PY for replication indicating that day-to-day panelists were consistent in their evaluations (Table 2). However, the degree of smoothness did show a significant interaction. 'Sample by panelist' interaction was significant for most attributes. Investigation of the interaction plots revealed that

this was due to panelists using the line scales within different ranges, but the sample mean values were always consistent. Cream and dairy aromas were significantly higher for the PY whereas the berry aroma was consistently higher for the SBY sample rated at 9.5 on the 15 cm scale. Sour taste was significantly higher for the PY whereas the sweet taste and berry flavor were significantly higher for the SBY. It should be noted that the sweet taste is quite low (5.3) and can be attributed to the natural sugar in the SBP as no additional sugar was added to the formulation. For textural attributes, the SBY was significantly lower in iciness compared to PY. Frozen yogurt with 2.5% strawberry powder was also found to have significantly less iciness compared to the control when measured instrumentally (18). PY was higher in degree of smoothness than the SBY which could be due to the lack of soluble material in the PY. Viscosity and mouth coating were significantly higher in the SBY sample.

3.2 Consumer acceptability panel

The panelist effect was significant for all the attributes except aroma which is common as acceptability is based on individual experiences and familiarity with certain foods (Table 3). Overall acceptability was not shown to be significantly different between the PY and SBY. Lachowicz et al. (19) found that the overall acceptability of rye bread fortified with 3% Saskatoon berry powder was similar to the control bread. Consumer acceptability of frozen yogurt with 3.2% added functional jambolan fruit powder was found to be similar to the results of this study (20). Mean values on the 9-point hedonic scale were between 5.5 and 6 for the aroma and flavor of the frozen jambolan yogurt. A significant 'age by sample' interaction was found for texture. Consumers 35 years and older had the lowest acceptability mean value for texture for SBY corresponding to "neither like nor dislike" compared to those younger than 35 years with the highest mean value for SBY corresponding to "like slightly." The PY was significantly higher in acceptability for aroma with a mean value of 6.8 (like moderately) compared to the SBY sample with a mean value of 5.8 (like slightly). Females found the color acceptability significantly higher than the males (7.1 – like moderately vs. 6.4 – like slightly). For the flavor attribute females found it less acceptable than the males (4.9 – neither like nor dislike vs. 5.7 – like slightly). Females had a significantly lower frequency of eating the sample compared to males (4.1 – I do not like this but would eat it on an occasion vs. 4.7 – I would eat this if available but would not go out of my way). Age showed no significant differences for any of the attributes. The mean values of 5.1 and 5.3 for overall acceptability for SBY and PY samples, respectively, corresponded to "neither like nor dislike." For frequency of eating the sample, both yogurts had mean values corresponding to "I do not like this but would eat it on an occasion."

Approximately 10% of consumers made comments about the flavor of the samples. For SBY positive comments included "distinct berry taste' and "appreciate the reasonable sweetness" however negative comments were "not very sweet," "fake fruit," "wheat fibre flavor," "powdery aftertaste" and "mild taste not like yogurt." The PY received positive comments including "very creamy," "good yogurt taste" and "cultured real" while negative comments included "sour" and "prefer sweet." Adding a non-nutritive sweetener such as stevia to yogurt (21) or inulin and isomalt to frozen yogurt (22) may improve acceptability while keeping the glycemic index and caloric value low.

TABLE 2 *F*-value with associated probabilities and mean value (with standard deviation) for descriptive analysis of Saskatoon berry (SBY) and plain frozen yogurt (PY) from three-way analysis of variance [R, replication (*n* = 3); P, panelist (*n* = 11); S, Sample (*n* = 2)].

Attribute	Source of variation (*F*-value)						Mean[1] values	
	Replication	Panelist	Sample	P * S	P * R	R * S	SBY	PY
Aroma								
Cream aroma	0.25 NS[2]	1.75 NS	54.60 ***	5.76 ***	†	†	2.9[b] (2.6)	8.9[a] (2.3)
Dairy aroma	0.71 NS	2.94 NS	48.43 ***	5.77 ***	†	†	3.8[b] (2.8)	9.4[a] (2.8)
Berry aroma	0.70 NS	1.48 NS	292.06 ***	7.43 ***	†	†	9.5[a] (2.1)	0.2[b] (0.6)
Taste/Flavor								
Sour	0.35 NS	7.83 ***	43.44 ***	†	†	†	5.7[b] (2.8)	8.4[a] (1.7)
Sweet	2.20 NS	2.02 NS	39.36 ***	6.31 ***	†	†	5.3[a] (2.3)	1.3[b] (1.6)
Berry Flavor	0.42 NS	1.89 NS	301.11 ***	9.75 ***	†	†	9.3[a] (2.1)	0.2[b] (0.6)
Texture/Mouthfeel								
Iciness	0.49 NS	5.81 ***	15.07 ***	†	†	†	4.7[b] (3.5)	7.4[a] (4.0)
Degree of smoothness	0.14 NS	1.30 NS	17.27 **	10.97 ***	2.14 *	†	3.7[b] (2.7)	8.9[a] (4.1)
Viscosity	0.03 NS	3.59 *	9.14 **	3.62 **	†	†	5.6[a] (3.6)	3.3[b] (2.2)
Mouth coating	0.01 NS	0.99 NS	13.81 **	4.67 ***	†	†	6.1[a] (1.9)	3.4[b] (2.0)

[1]Mean intensity values were measured on a scale from 0 (low) to 15 (high).
[2]NS, not significant; $p \geq 0.05$; *$p < 0.05$; **$p < 0.01$; ***$p < 0.001$.
[ab]Mean intensity values with the same letter within the same row are not significantly different when a probability level of 0.05 is applied.
[†]Sums of squares pooled with error as the probability of the interaction effect was ≥ 0.05.

TABLE 3 *F*-value with associated probabilities and mean value (with standard deviation) for consumer acceptability of Saskatoon berry (SBY) and plain frozen yogurt (PY) from four-way analysis of variance [S, sample (*n* = 2); P, panelist (*n* = 112); G, gender (*n* = 2); A, age (*n* = 3)].

Attribute	Source of variation (*F* value)						Mean value			
	S	P	G	A	S * A	S * G	S		G	
							SBY	PY	Female	Male
Aroma[1]	33.06 ***[3]	1.39 *	0.35 NS	0.16 NS	†	†	5.8[b] (1.5)	6.8[a] (1.3)	6.3 (1.5)	6.1 (1.5)
Color[1]	0.00 NS	0.84 NS	13.04 ***	1.74 NS	†	†	7.0 (1.7)	7.0 (1.3)	7.1[a] (1.4)	6.4[b] (1.7)
Flavor[1]	0.10 NS	1.65 **	5.36 *	0.54 NS	†	†	5.1 (2.2)	5.0 (2.2)	4.9[b] (2.2)	5.7[a] (1.9)
Texture[1]	20.17 ***	1.84 ***	1.13 NS	0.55 NS	4.52 *	†	4.8[b] (2.2)	5.8[a] (1.9)	5.2 (2.1)	5.6 (2.0)
Overall acceptability[1]	0.82 NS	1.99 ***	3.58 NS	0.66 NS	†	†	5.1 (2.0)	5.3 (2.0)	5.0 (2.0)	5.7 (1.9)
FACT[2]	1.28 NS	2.26 ***	3.15 NS	1.10 NS	†	†	4.1 (2.0)	4.3 (2.0)	4.1 (2.0)	4.7 (1.9)

[1]1 = dislike extremely; 2 = dislike very much; 3 = dislike moderately; 4 = dislike slightly; 5 = neither like nor dislike; 6 = like slightly; 7 = like moderately; 8 = like very much; 9 = like extremely.
[2]1 = I would eat this only if forced; 2 = I would eat this if there were no other food choices; 3 = I would hardly ever eat this; 4 = I do not like this but would eat it on an occasion; 5 = I would eat this if available but would not go out of my way; 6 = I like this and would eat it now and then; 7 = I would frequently eat this; 8 = I would eat this very often; 9 = I would eat this every opportunity I had.
[3]NS, not significant; $p \geq 0.05$; *$p < 0.05$; **$p < 0.01$; ***$p < 0.001$.
[ab]Mean intensity values with the same letter within the same row within the same variable (S and G) are not significantly different when a probability level of 0.05 is applied.
[†]Sums of squares pooled with error as the probability of the interaction effect was ≥ 0.05.

TABLE 4 *F*-value with associated probabilities and mean value (with standard deviation) for proximate analysis, pH, color and ORAC results of frozen yogurt fortified with (SBY), and without (PY) Saskatoon berry powder (SBP).

Physicochemical properties	Source of Variation (*F*-value) [2, 5 df]	Mean values		
		SBY	PY	SBP
Moisture (%)	1611.43 ***[1]	79.6[b] (0.2)	87.2[a] (0.2)	N/A
Crude protein (%)	118.23 ***	3.1[b] (0.1)	4.3[a] (0.2)	N/A
Crude fibre (%)	562.37 ***	1.1[a] (0.1)	0.0[b] (0.0)	N/A
Fat (%)	0.03 NS	0.6 (0.0)	0.6 (0.1)	N/A
Ash (%)	11.85 *	0.9[b] (0.1)	1.1[a] (0.0)	N/A
CHO, by difference (%)	2877.04 ***	15.7[a] (0.3)	6.8[b] (0.1)	N/A
Calories (Cal/100 g)	763.23 ***	78.1[a] (0.9)	51.0[b] (1.4)	N/A
Color L*	14852.30 ***	30.7[b] (0.8)	86.4[a] (0.2)	N/A
Color a*	7456.03 ***	12.5[a] (0.3)	-3.0[b] (0.1)	N/A
Color b*	6002.50 ***	2.6[b] (0.2)	10.8[a] (0.1)	N/A
pH	1813.00 ***[2]	4.04[b] (0.00)	4.22[a] (0.00)	3.64[c] (0.02)
ORAC[3]	967.40 ***[4]	37593[a] (1178)	3608[b] (861)	39843[a] (1355)

[1]NS, not significant; $p \geq 0.05$; *$p < 0.05$; ***$p < 0.001$.
[2]Degrees of freedom (2, 8).
[3]ORAC values in μmole of Trolox/g of PY and SBY; μmole of Trolox/100 mg SBP.
[4]Degrees of freedom (2, 11).
[a,b,c]Mean values with the same letter within the same row are not significantly different when a probability level of 0.05 is applied.
All analyses were conducted in 3 or 4 replicates.

About 15% of consumers made comments regarding the texture of the samples. Positive comments (3%) for the SBY sample included "like frozen yogurt/ice cream," and "smooth." Negative comments (12%) included "coating on tongue," "crystallized ice crystals," "not smooth," "not appealing/good," "gritty, grainy, fibery." For PY positive comments (3%) included "smooth/creamy like ice cream" while the negative comment (12%) was "ice crystals." The texture could possibly be improved by reducing the particle size for the SBP and including a stabilizer such as xanthan gum to make the frozen yogurt creamier (23) and Arabic and guar gums to decrease iciness (24).

3.3 Stepwise linear regression

Aroma and texture were used as dependent variables in the models for the stepwise regression since the two frozen yogurts were found to be significantly different for these acceptability attributes. The 10 attributes measured by descriptive analysis were input as predictors. Aroma acceptability was related negatively to berry flavor (beta = −1.343;

$p = 0.004$) and positively to berry aroma (beta = 0.960; $p = 0.037$). The significant model ($F_{2, 63\,df} = 9.200$ $p = 0.000$) had an adjusted R square of 0.201, and a significant *R* square change when berry aroma was added ($F = 4.565$ $p = 0.037$). Texture acceptability was related positively to iciness (beta = 0.386; $p = 0.001$). The significant model ($F_{1, 64\,df} = 11.225$ $p = 0.001$) had an adjusted R square of 0.136. Masking the berry flavor and enhancing the berry aroma would be recommended to increase the aroma acceptability. Results showed that iciness was positively related to texture acceptability which may be associated with a desirable characteristic of a frozen yogurt.

3.4 Proximate analysis

SBY was found to have significantly lower moisture content, protein, and ash, and significantly higher crude fiber, carbohydrate, and Calories compared to PY (Table 4). Importantly, the significantly decreased moisture content in the SBY could be expected to have a relatively large impact on the textural properties of the SBY, and may
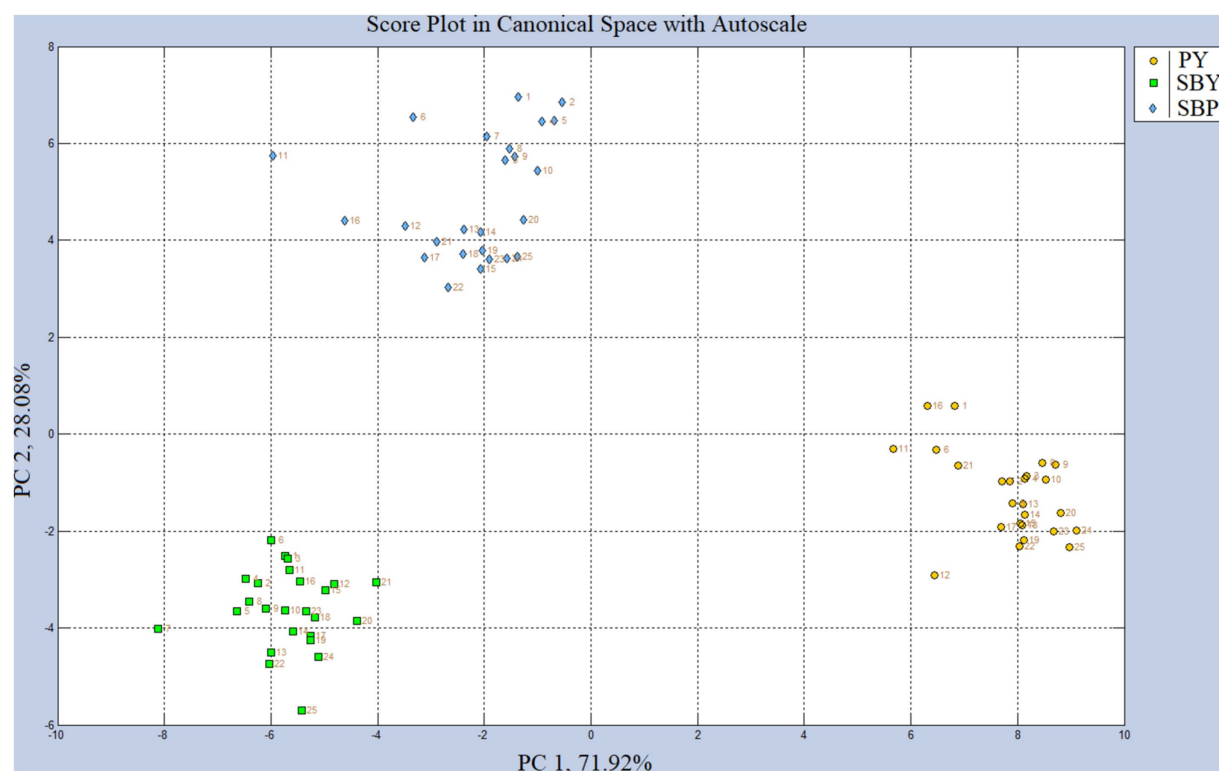
FIGURE 1
Score plot using principal component analysis (PCA) for Saskatoon berry powder (SBP), plain yogurt (PY) and yogurt with added Saskatoon berry powder (SBY) by 'SENSIGENT MSEM 160' portable odor and chemical monitor system.

therefore serve to explain some of the variation observed with respect to the textural properties analyzed. Fat content was 0.6% for both samples which is to be expected given that the SBP contained 0.1 g in 10 g as noted above.

3.5 Color measurement

SBY was significantly darker (lower L^* value), significantly redder (higher a^* value), and significantly less yellow (lower b^* value) compared to PY. As a result, consumers would easily be able to visually distinguish SBY from PY, though consumer testing did not indicate a preference with regard to color. Furthermore, it can also be concluded that at least part of natural pigments present in the Saskatoon berries survived undamaged following processing into SBP and SBY samples, some of which may have bioactive properties (Table 4).

3.6 Determination of pH

The pH of Saskatoon berry yogurt was 4.22. A model developed of functional yogurt containing clove determined that a pH range from 3.81 to 4.6 was acceptable with 3.86 being optimal (25). The pH of SBY was found to be significantly decreased compared to PY, while the measured pH of the SBP was even lower, indicating that the addition of the SBP had an acidifying effect on the yogurt matrix (Table 4).

3.7 Determination of oxygen radical absorbance capacity (ORAC) values

The ORAC results for PY and SBY were expressed in μmoles of Trolox /g and for SBP in μmoles of Trolox/100 mg (Table 4). These results showed ~10-fold differences in ORAC values for SBP compared to PY, with no significant changes ($p < 0.05$) when SBP was added to PY. The phenolic compounds present in SBP were likely to be responsible for the ORAC values obtained for these samples. The ORAC values obtained for SBP in this study were in a similar order to those obtained from Saskatoon berry syrup used to create a Rooibos tea beverage (15).

3.8 Electronic nose (E-nose) analysis of yogurt and powder samples

The exposure of the yogurt samples to the e-nose sensors showed consistencies both within individual samples and between samples in replicate analyses and produced distinct clustering of data when visualized using a Score Plot PCA (Figure 1). Cross-validation of the PCA produced by CDanalysis showed that the model would sort randomly selected samples into the appropriate class with 98.7% accuracy. Visually, SBP and SBY clusters appeared closer to each other than to PY suggesting that the e-nose was more sensitive toward VOCs related to Saskatoon berries, and less sensitive toward VOCs related to the Greek yogurt. Statistical analysis of values obtained for individual sensors (Table 5) showed very highly

TABLE 5 *F*-value with associated probabilities and mean value (with standard deviation) for e-nose sensor results for yogurt fortified with (SBY) and without (PY) Saskatoon berry powder (SBP).

E-nose sensor	Source of variation (F value) [2, 72 df]	Mean value		
		SBP	SBY	PY
S3	35.01***[1]	0.01[b] (0.00)	104.71[a] (88.47)	0.01[b] (0.00)
S5	28.89***	251.48[c] (15.18)	265.67[b] (11.28)	281.20[a] (14.70)
S8	49.29***	74307.77[b] (1224.41)	70235.52[c] (3205.99)	75882.14[a] (1068.53)
S9	408.75***	20214.91[b] (1306.91)	15489.61[c] (1553.35)	25447.43[a] (656.95)
S10	74.34***	336545.95[a] (8894.83)	312824.96[c] (8003.61)	321150.43[b] (1719.13)
S11	23.28***	29038.45[a] (690.45)	26738.67[b] (2018.14)	28509.17[a] (351.05)
S12	201.09***	40414.29[b] (741.70)	40388.01[b] (1169.28)	44668.79[a] (589.05)
S14	123.63***	38395.30[a] (352.06)	36868.33[b] (621.99)	38650.27[a] (229.25)
S15	86.01***	67832.00[b] (1790.24)	63404.76[c] (2148.90)	69394.67[a] (771.33)
S22	16.44***	1.13[b] (0.04)	1.15[b] (0.05)	1.20[a] (0.05)

[abc]Mean values (followed in brackets by the standard deviation) within the same row with the same letter are not significantly different when a probability level of 0.05 is applied. All analyses were conducted in 25 replicates. [1]***$p < 0.001$.

significant ($p < 0.001$) results for the processed data of 10 sensors. These sensors might be more sensitive to VOCs generated by SBP, yogurt, and or an interaction of both.

3.9 Analysis of volatile compounds in yogurt and powder samples using GC–MS

Sixty-two VOCs were successfully extracted, detected, identified, and quantified using the SPME method employed in this study (Table 6). These VOCs belonged to several major classes of organic chemicals including; aldehydes, alcohols, ketones and esters. The volatiles 2,3- pentanedione, butanoic acid and 2-undecanone were found exclusively in the PY which agrees with findings of Liu et al. (26). Butorova et al. (8) have previously reported the VOCs from different cultivars of chokeberries and Saskatoon berries using similar extraction methods (SPME) and analytical methods (GC–MS). They reported a high percentage of alcohols (40 to 52.6%, w:w) in their samples that was attributed to differences in varieties, different climatic and geographical conditions, post-harvest treatment, and conditions of storage (fresh vs. frozen fruits). The higher temperature used during SPME extraction in the present study could potentially have led to an oxidation of some of the alcohol contents, resulting in their conversion into aldehydes or acids, or otherwise modifying which and how many compounds were absorbed by the extraction fiber. However, our results may not be directly compared to the results reported for fresh and/or frozen berries.

Several VOCs were identified with known contributors to berry odor (pentanal, linalool, 3-nonen-2-one, *β*-damascenone and β-ionone); and fruity odor (acetic acid ethyl ester, pentanal, hexanal, butanoic acid, 2-heptanone, 2-butyl furan, furan, 2 -pentyl, 3,5-octadien-2-ol, 3,5-octadien-2-one, (E,E)-, 3-nonen-2-one, benzoic acid, ethyl ester, 2-undecanone, 2-undecenal, β-damascenone and β-ionone). These VOCs may have directly contributed to berry aroma and flavor described by trained panelists (Table 1) and to significantly higher mean values obtained for berry aroma and flavor in SBY compared to PY (Table 2).

A correlogram was prepared comparing signal variations obtained for both e-nose sensors and individual VOCs identified by GC–MS in order to determine if the former could be used as a proxy for the latter in subsequent studies (Figure 2). Using this model, it was noted that sensor 3, a mixed metal oxide semiconductor/nanocomposite sensor, was identified as particularly significantly correlated with several VOCs including benzaldehyde, 4-(1-methylethyl)-, hexanoicpyraz acid, heptanoic acid, nonanoic acid, and styrene, but also showed a positive correlation with most of the other VOCs identified in the study. This is unsurprising given that this sensor is expected to possess significant sensitivity toward hydrocarbons, VOCs generally, and reducing and oxidizing gases.

Sensor 5 meanwhile was found to be positively correlated with several VOCs including decanoic acid, butanone, 3-hydroxy, 2,3-pentanedione butanoic acid, and 2-undecanone. This was not expected, given that this sensor is an electrochemical sensor designed to be sensitive toward detecting ammonia, but also H_2S, SO_2, NO_2, and Cl_2. However the fact that all five of these correlated compounds were found

TABLE 6 *F*-value with associated probabilities and mean value (with standard deviation) for volatile organic compounds (μg/100 g) contained in Saskatoon berry powder (SBP), frozen yogurt with Saskatoon berry powder (SBY) and without (PY).

Volatile organic compound	Formula	Class[3]	Source of variation (*F* value) [2, 8 df]	Mean value			Odor descriptors[1]
				SBP	SBY	PY	
Acetic acid ethyl ester	$C_4H_8O_2$	Ester (est1)	8.28 *[2]	0.00[b] (0.00)	52.74[a] (26.19)	24.22[ab] (8.43)	ethereal, fruity, sweet, weedy, green
2,3-Pentanedione	$C_5H_8O_2$	Ketone (ket1)	11.19 **	0.00[b] (0.00)	0.00[b] (0.00)	5.17[a] (2.68)	pungent, sweet, buttery, creamy, caramellic, nutty, cheesy
Pentanal	$C_5H_{10}O$	Aldehyde	2.79 NS	39.27 (21.26)	41.09 (35.89)	0.00 (0.00)	Fermented, bready, fruity, nutty, berry
2-Butanone, 3-hydroxy	$C_4H_8O_2$	Ketone (ket2)	6.70 *	0.00[b] (0.00)	49.73[a] (31.47)	52.58[a] (13.56)	Sweet, buttery, creamy, dairy, milky, fatty
Disulfide, dimethyl	$C_2H_6S_2$	Sulfide (sul1)	8.78 *	0.00[b] (0.00)	6.71[a] (3.17)	3.72[ab] (1.23)	Sulfurous, vegetable, cabbage, onion
Toluene	C_7H_8	Hydrocarbon (hyd1)	13.41 **	16.87[ab] (6.79)	26.52[a] (7.09)	2.68[b] (0.40)	sweet
Hexanal	$C_6H_{12}O$	Aldehyde (ald1)	8.73 *	1110.45[a] (445.24)	1300.82[a] (536.44)	28.06[b] (9.74)	Fresh, green, fatty, aldehydic, grassy, leafy, fruity, sweaty
Butanoic acid	$C_4H_8O_2$	Fatty acid (faa1)	199.70 ***	0.00[b] (0.00)	0.00[b] (0.00)	30.13[a] (3.69)	Sharp, acetic, cheesy, buttery, fruity
Furfural	$C_5H_4O_2$	Aldehyde (ald2)	31.65 ***	829.45[a] (76.78)	1079.04[a] (290.74)	1.72[b] (0.52)	Sweet, woody, almond, baked bread
2-Hexenal, E	$C_6H_{10}O$	Aldehyde (ald3)	28.10 ***	18.19[a] (2.27)	18.70[a] (5.58)	0.00[b] (0.00)	Green, banana, aldehydic, fatty, cheesy
Styrene	C_8H_8	Hydrocarbon (hyd2)	84.06 ***	9.04[b] (1.01)	55.89[a] (5.95)	11.36[b] (6.19)	Sweet, balsamic, floral, plastic
2-Heptanone	$C_7H_{14}O$	Ketone (ket3)	11.38 **	36.61[b] (7.12)	126.61[a] (39.70)	13.86[b] (10.66)	Fruity, spicy, sweet, herbal, coconut, woody
2-Butyl Furan	$C_8H_{12}O$	Furan (fur1)	38.18 ***	63.25[b] (8.20)	100.46[a] (23.25)	0.00[c] (0.00)	Fruity, winey, sweet, spicy
Heptanal	$C_7H_{14}O$	Aldehyde (ald4)	19.67 **	109.73[a] (18.29)	111.24[a] (33.72)	11.83[b] (3.71)	Fresh, aldehydic, fatty, green, herbal, cognac, ozone
Acetylfuran (Ethanone, 1-(2-furanyl))	$C_6H_6O_2$	Furan (fur2)	51.75 ***	19.50[b] (1.63)	33.55[a] (6.60)	1.02[c] (0.31)	Sweet, balsamic, almond, cocoa, caramellic, coffee
Benzaldehyde	C_7H_6O	Aldehyde (ald5)	89.38 ***	1561.64[b] (109.45)	2320.13[a] (357.18)	10.36[c] (3.35)	Sharp, sweet, bitter, almond, cherry
Dimethyl trisulfide	$C_2H_6S_3$	Sulfide	1.73 NS	2.40 (0.55)	11.91 (10.19)	9.79 (5.05)	Sulfurous, onion-cooked, savory, meaty
1-Octen-3-one	$C_8H_{14}O$	Ketone (ket4)	100.92 ***	86.22[a] (6.77)	50.49[b] (11.02)	0.00[c] (0.00)	Herbal, mushroom, earthy, musty, dirty
1-Octen-3-ol	$C_8H_{16}O$	Alcohol (alc1)	235.64 ***	114.87[b] (2.58)	142.22[a] (14.52)	0.00[c] (0.00)	Mushroom, earthy, green, oily, fungal, raw chicken
5-Hepten-2-one, 6-methyl-	$C_8H_{14}O$	Ketone (ket5)	68.42 ***	43.26[a] (4.24)	50.89[a] (9.01)	0.00[b] (0.00)	Citrus, green, musty, lemongrass, apple

(Continued)

TABLE 6 (Continued)

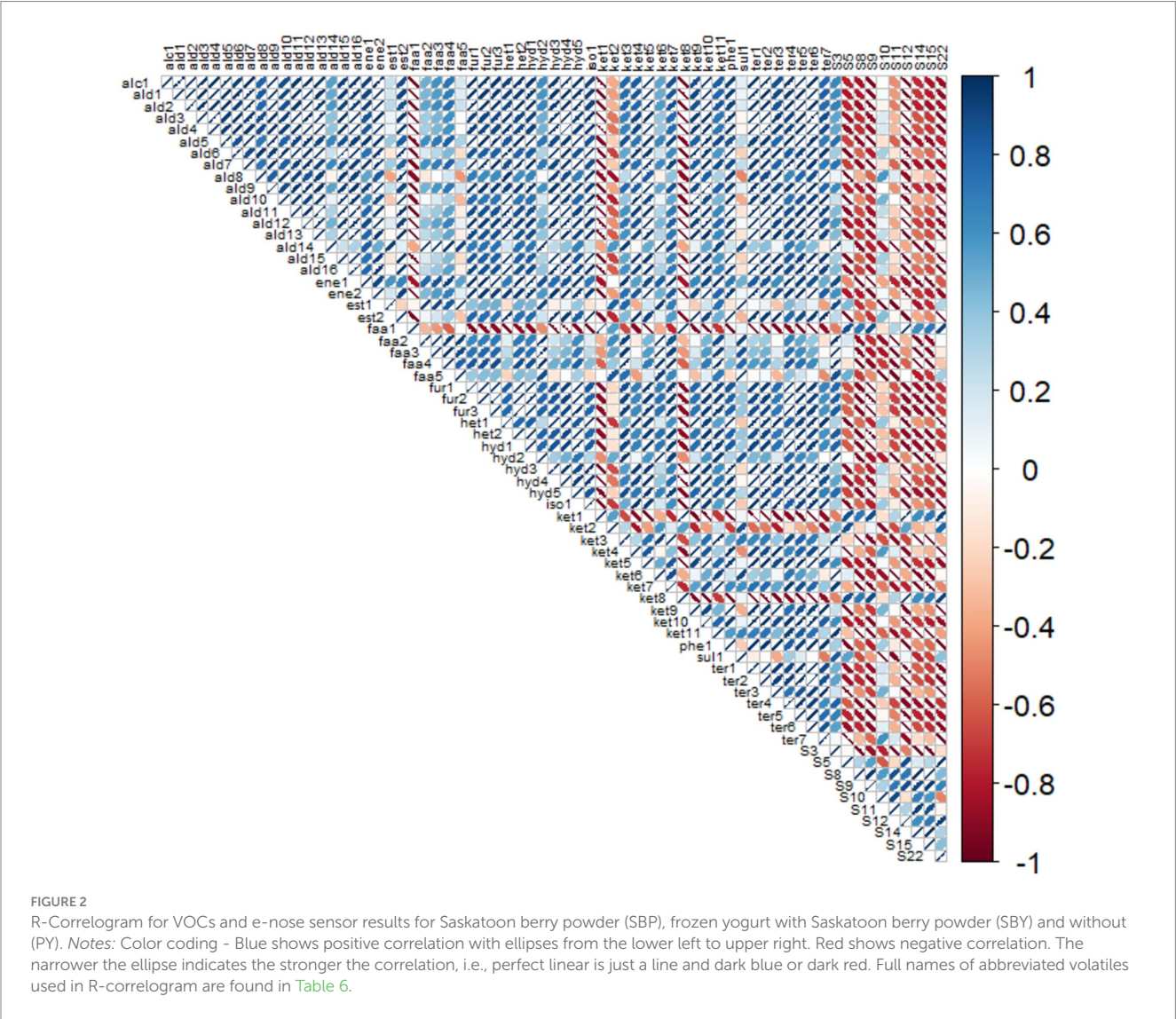| Volatile organic compound	Formula	Class[3]	Source of variation (F value) [2, 8 df]	Mean value			Odor descriptors[1]
				SBP	SBY	PY	
Furan, 2 -pentyl	$C_9H_{14}O$	Furan (fur3)	129.63 ***	513.05[b] (46.94)	909.83[a] (109.59)	7.06[c] (0.98)	Fruity, green, earthy, beany, vegetable, metallic
2,4-Heptadienal, (E,E)-	$C_7H_{10}O$	Aldehyde (ald6)	34.33 ***	107.58[a] (28.48)	88.13[a] (7.11)	0.00[b] (0.00)	Fatty, green, oily, aldehydic, vegetable cinnamon
Hexanoicpyraz acid	$C_6H_{12}O_2$	Fatty acid (faa2)	9.30 *	0.00[b] (0.00)	673.90[a] (348.10)	137.26[b] (39.50)	Sour, fatty, sweaty, cheesy
D-Limonene	$C_{10}H_{16}$	Hydrocarbon (hyd3)	181.89 **	21.95[a] (2.06)	19.02[a] (1.67)	0.00[b] (0.00)	Citrus, orange, fresh, sweet
1-Formyl-5-ethylcyclopentene	$C_8H_{12}O$	Aldehyde (ald7)	56.40 ***	76.97[b] (3.02)	111.21[a] (22.54)	0.00[c] (0.00)	Unknown
3,5-Octadien-2-ol	$C_8H_{12}O$	Enone (ene1)	352.72 ***	37.59[b] (1.09)	81.67[a] (6.39)	0.65[c] (0.10)	Fruity, fatty, mushroom
2-Octenal, (E)-	$C_8H_{14}O$	Aldehyde (ald8)	183.66 ***	399.30[a] (40.64)	226.51[b] (17.29)	1.41[c] (0.27)	Fresh, cucumber, fatty, green, herbal, banana, waxy, green, leafy
3,5-Octadien-2-one, (E,E)-	$C_8H_{12}O$	Enone (ene2)	192.18 ***	29.63[a] (1.92)	34.31[a] (3.40)	0.92[b] (0.27)	Fruity, green, grassy
Heptanoic acid	$C_7H_{14}O_2$	Fatty acid (faa3)	56.23 ***	0.00[b] (0.00)	19.95[a] (4.41)	1.55[b] (0.50)	Rancid, sour, cheesy, sweaty
2-Nonanone	$C_9H_{18}O$	Ketone (ket6)	1238.57***	4.31[c] (0.64)	47.29[a] (1.82)	11.10[b] (0.39)	Fresh, sweet, green, weedy, earthy, herbal
Linalool	$C_{10}H_{18}O$	Terpenoid (ter1)	135.98 ***	27.19[a] (1.85)	26.45[a] (3.53)	0.00[b] (0.00)	Citrus, floral, sweet, rose water, woody, green, blueberry
Nonanal	$C_9H_{18}O$	Aldehyde (ald9)	165.95 ***	111.09[a] (14.38)	134.43[a] (7.38)	4.13[b] (0.81)	Waxy, aldehydic, rose, fresh, orris, orange peel, fatty, peely
2,4-Octadienal, (E,E)	$C_8H_{12}O$	Aldehyde (ald10)	50.79 ***	40.05[a] (8.22)	27.57[a] (2.63)	0.00[b] (0.00)	Fatty, pear, vegetable, green
3-Nonen-2-one	$C_9H_{16}O$	Ketone (ket7)	419.72 ***	2.63[b] (0.28)	7.81[a] (0.51)	0.00[c] (0.00)	Fruity, berry, fatty, oily, ketonic, weedy, spicey, licorice
2-Nonenal, (E)-	$C_9H_{16}O$	Aldehyde (ald11)	46.63 ***	24.75[a] (5.55)	22.76[a] (1.24)	1.39[b] (0.20)	Fatty, green, cucumber, aldehydic, citrus
Benzoic acid, ethyl ester	$C_9H_{10}O_2$	Ester (est2)	97.29 ***	52.31[a] (8.09)	37.86[b] (1.44)	0.00[c] (0.00)	Fruity, dry, musty, sweet, wintergreen
α-Terpineol	$C_{10}H_{18}O$	Terpenoid (ter4)	59.99 ***	4.52[a] (0.94)	4.77[a] (0.44)	0.00[b] (0.00)	Pine, terpenic, lilac, citrus, woody, floral
Octanoic acid	$C_8H_{16}O_2$	Fatty acid	3.95 NS	0.00 (0.00)	287.27 (218.30)	111.31 (11.26)	Fatty, waxy, rancid, oily, vegetable, cheesy
Decanal	$C_{10}H_{20}O$	Aldehyde (ald12)	55.23 ***	11.14[a] (2.74)	12.49[a] (0.38)	0.00[b] (0.00)	Sweet, aldehydic, waxy, orange peel, citrus, floral

(Continued)

TABLE 6 (Continued)

Volatile organic compound	Formula	Class[3]	Source of variation (*F* value) [2, 8 df]	Mean value			Odor descriptors[1]
				SBP	SBY	PY	
2,4-Nonadienal, (E,E)-	$C_9H_{14}O$	Aldehyde (ald13)	49.87 ***	61.29[a] (13.32)	56.25[a] (5.24)	0.56[b] (0.03)	Fatty, melon, waxy, green, violet leaf, cucumber, fruit tropical, chicken fat
1-p-Menthene-9-al	$C_{10}H_{16}O$	Terpenoid (ter3)	51.74 ***	15.77[a] (3.28)	10.65[b] (0.70)	0.00[c] (0.00)	Spicy, herbal
β-Cyclocitral	$C_{10}H_{16}O$	Terpenoid (ter4)	25.13 **	4.40[a] (0.37)	6.54[a] (1.50)	1.31[b] (0.30)	Tropical, saffron, herbal, tobacco, medicinal, phenolic, leathery, green
Cyclohexane, hexyl-	$C_{12}H_{24}$	Hydrocarbon (hyd5)	40.88 ***	5.74[b] (1.10)	8.80[a] (1.78)	0.00[c] (0.00)	Not found
Benzaldehyde, 4-(1-methylethyl)-	$C_{10}H_{12}O$	Terpene (ald14)	128.72 ***	0.00[b] (0.00)	21.09[a] (1.56)	3.02[b] (2.58)	Spicy, cumin, green, herbal
Benzene, m-di-tert-butyl	$C_{10}H_{14}$	Hydrocarbon (hyd4)	35.76 ***	1640.00[a] (311.03)	1685.17[a] (367.56)	0.61[b] (0.13)	Not found
2-Decenal, (E)-	$C_{10}H_{18}O$	Aldehyde (ald15)	15.13 **	18.69[a] (7.36)	15.41[a] (1.48)	0.42[b] (0.05)	Waxy, fatty, earthy, green, cilantro, mushroom, aldehydic, fried chicken fat, tallow
Nonanoic acid	$C_9H_{18}O_2$	Fatty Acid (faa4)	9.49 *	1.00[b] (1.73)	6.85[a] (3.06)	0.24[b] (0.21)	Waxy, dirty, cheesy, dairy
Dihydroedulan II	$C_{13}H_{22}O$	Heterobicyclic (het1)	127.90 ***	3.25[a] (0.13)	2.54[b] (0.44)	0.00[c] (0.00)	Not found
2-Undecanone	$C_{11}H_{22}O$	Ketone (ket8)	263.01 ***	0.00[b] (0.00)	0.00[b] (0.00)	2.26[a] (0.24)	Waxy, fruity, creamy, fatty, orris, floral
2,4-Decadienal, (E,Z)-	$C_{10}H_{16}O$	Aldehyde	2.64 NS	95.43 (89.03)	59.56 (2.20)	0.00 (0.00)	Fried, fatty, geranium, green, waxy
2,4-Decadienal, (E,E)-	$C_{10}H_{16}O$	Aldehyde	3.19 NS	146.38 (156.99)	173.88 (5.73)	0.00 (0.00)	Oily, cucumber, melon, citrus, pumpkin, nutty
1-Methoxy-4-methylbicyclo[2.2.2]octane	$C_{10}H_{18}O$	Heterobicyclic (het2)	97.17 ***	14.74[a] (4.01)	26.43[a] (0.42)	0.00[b] (0.00)	Not found
α-Longipinene	$C_{15}H_{24}$	Terpenoid (ter5)	89.55 ***	5.15[a] (0.53)	6.62[a] (0.97)	0.00[b] (0.00)	Not found
Dehydro-ar-ionene	$C_{13}H_{16}$	Isoprenoid (iso1)	56.03 ***	9.24[a] (1.84)	7.35[a] (0.68)	0.00[b] (0.00)	Not found
2-Undecenal	$C_{11}H_{20}O$	Aldehyde (ald16)	12.20 **	6.30[a] (2.90)	5.81[a] (0.81)	0.00[b] (0.00)	Fresh, fruity, orange peel
n-Decanoic acid	$C_{10}H_{20}O_2$	Fatty acid (faa5)	36.65 ***	0.00[c] (0.00)	46.39[a] (9.80)	23.44[b] (6.00)	Rancid, sour, fatty, citrus
β-Damascenone	$C_{13}H_{18}O$	Ketone (ket9)	68.03 ***	19.36[a] (3.49)	13.55[b] (0.92)	0.00[c] (0.00)	Natural, sweet, fruity, rose plum, grape, raspberry, sugar
cis-Thujopsene	$C_{15}H_{24}$	Terpenoid (ter6)	119.48 ***	2.41[a] (0.15)	2.56[a] (0.36)	0.00[b] (0.00)	Not found
2,6-Di-tert-butylquinone	$C_{14}H_{20}O_2$	Terpenoid (ter7)	29.44 ***	23.75[a] (6.14)	12.77[b] (2.34)	0.00[c] (0.00)	Not found

(Continued)

TABLE 6 (Continued)

Volatile organic compound	Formula	Class[3]	Source of variation (F value) [2, 8 df]	Mean value			Odor descriptors[1]
				SBP	SBY	PY	
β-Ionone	$C_{13}H_{20}O$	Ketone (ket10)	15.75 **	4.49[a] (1.72)	5.24[a] (0.94)	0.41[b] (0.19)	Floral, woody, sweet, fruity, berry, tropical, beeswax
2-Tridecanone	$C_{13}H_{26}O$	Ketone (ket11)	11.56 **	4.71[b] (3.33)	16.06[a] (6.22)	0.63[b] (0.27)	Fatty, waxy, dairy, milky, coconut, nutty, herbal, earthy
2,4-Di-tert-butylphenol	$C_{14}H_{22}O$	Terpenoid (ter7)	17.49 **	61.09[a] (23.03)	49.34[a] (3.24)	0.00[b] (0.00)	Not found

[1]Odor descriptors obtained from the Good Scents Company (2009) https://www.thegoodscentscompany.com/.

[2]NS, not significant; $p \geq 0.05$; *$p < 0.05$; **$p < 0.01$; ***$p < 0.001$.

[3]Text in brackets are abbreviations used for Figure 2.

[abc]Mean values (followed in brackets by the standard deviation within the same row with the same letter are not significantly different when a probability level of 0.05 is applied).

All analyses were conducted in three replications.

FIGURE 2

R-Correlogram for VOCs and e-nose sensor results for Saskatoon berry powder (SBP), frozen yogurt with Saskatoon berry powder (SBY) and without (PY). Notes: Color coding – Blue shows positive correlation with ellipses from the lower left to upper right. Red shows negative correlation. The narrower the ellipse indicates the stronger the correlation, i.e., perfect linear is just a line and dark blue or dark red. Full names of abbreviated volatiles used in R-correlogram are found in Table 6.
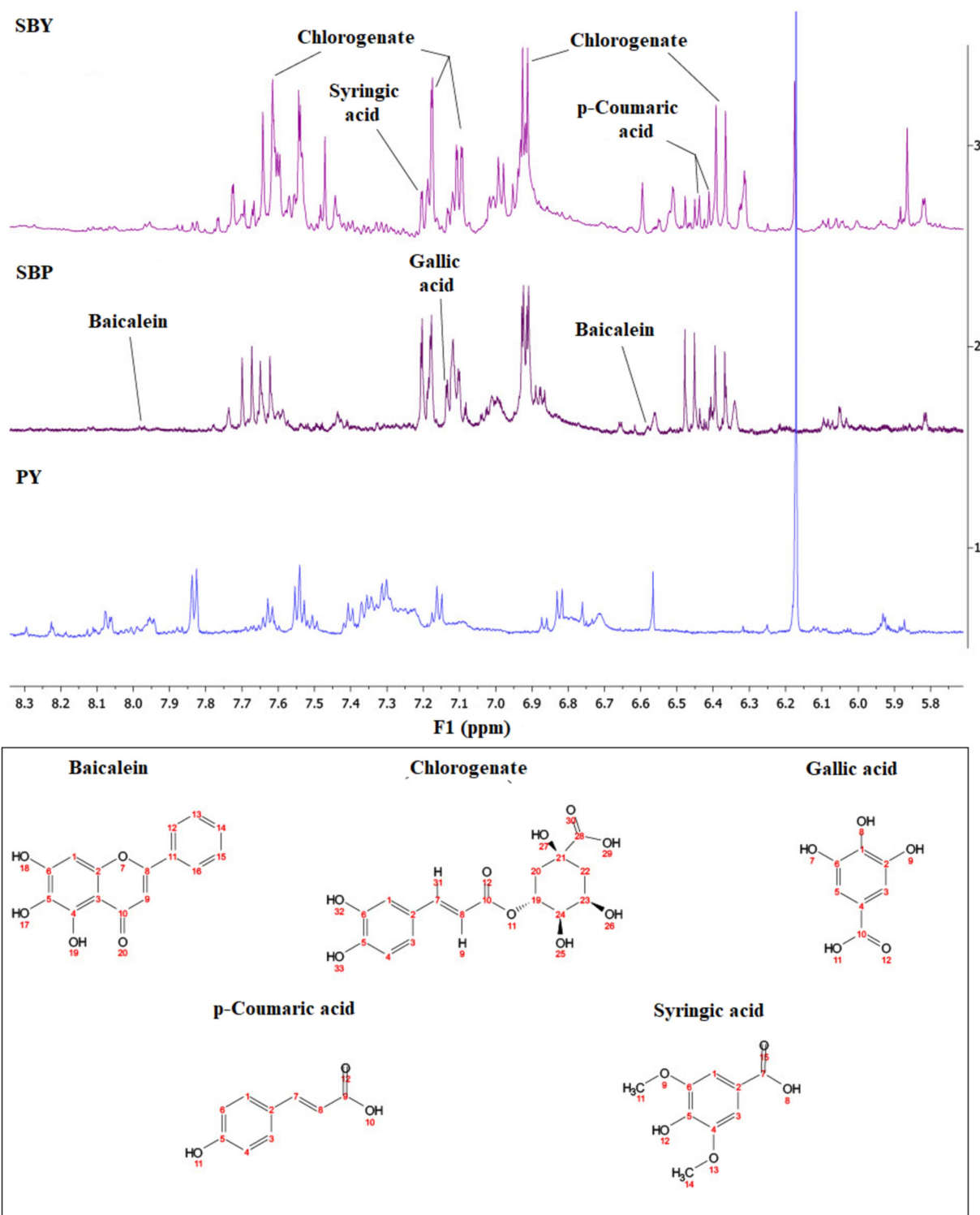
NMR Spectra for five selected phenolic compounds in Saskatoon berry powder (SBP), plain yogurt (PY) and yogurt with added Saskatoon berry powder (SBY). *Notes:* Concentration (mM) in SBP: Baicalein (0.101); Chlorogenate (0.305); Gallic acid (0.014); p-Coumaric acid (0.037) and Syringic acid (0.018).

in a higher concentration for either the PY or SBY samples compared to the SBP could imply that their increased sensor response owed to some other factor present within the yogurt and not the five compounds *per se*.

Sensors 8, 9, 12, 14, 15 and 22 were also all found to be positively correlated with 2,3 pentanedione, butanoic acid, and 2-undecanone and negatively correlated with most other VOCs analyzed. Again it is

somewhat difficult to imagine an explanation for this result that relies on molecular structure and composition given that the structures observed for these compounds also occur frequently in many of the negatively correlated compounds as well. An explanation for this result also cannot be easily speculated upon as these sensors are not identified as possessing any particular sensitivity by the manufacturer.

3.10 Extraction and analysis of selected compounds by nuclear magnetic resonance (NMR)

One of the key steps in developing functional foods is to ensure that the known bioactive compounds responsible for health effects are present and will remain stable and functional in the final developed product (27). Proton NMR (1D) and 2D NMR methods were used to identify the key bioactive compounds in these samples. Several phenolic compounds with known contribution to health were successfully extracted and identified in SBP and in yogurt enriched with SBP including baicalein, chlorogenate, gallic acid, p-coumaric acid, and syringic acid which is in the same class of compounds as gallic acid (Figure 3). Chlorogenate (28), gallic acid and p-coumaric acid (29) have been reported in Saskatoon berry. Baicalein has been shown to possess anti-inflammatory, antiviral, antitumor, antioxidant, and antibacterial effects, and is used to treat respiratory infections, enteritis, and dysentery (30). Chlorogenic acid has therapeutic effects related to neurodegenerative disorders, diabetic neuropathy, and exhibits anti-inflammatory, antioxidant, and antitumor activities (31). Gallic acid shows antioxidant, anti-inflammatory, and antitumor effects and has been reported to help with gastrointestinal, neuropsychological, metabolic, and cardiovascular disorders in animal studies (32). p-Coumaric acid possesses antioxidant, anti-cancer, antimicrobial, antiviral, anti-inflammatory, and anti-arthritis properties and has therapeutic effects on diabetes, obesity, and gout (33). Syringic acid, found in various fruits, exhibits therapeutic effects on diabetes, cardiovascular disease, and cancer, along with antioxidant, antimicrobial, anti-inflammatory, neuroprotective, and hepatoprotective activities (34). Despite concerns about the stability of these water-soluble compounds in the dehydrated material, their presence in the final flavored yogurt suggests that SBY may offer therapeutic benefits compared to PY.

4 Conclusion

Greek style frozen yogurt with SBP was significantly higher in berry aroma and flavor and sweetness and lower in cream and dairy aroma and sourness compared to PY. It was lower in iciness and degree of smoothness and higher in viscosity and mouth coating compared to PY. SBY was shown to be less acceptable for aroma and texture than PY although no significant differences were shown for color, flavor, overall acceptability, and frequency of eating the sample. Iciness was the most influential variable in terms of texture acceptability and berry flavor (negatively related) and berry aroma (positively related) to the acceptability of aroma. ORAC value for SBY showed about a 10 fold increase compared to the PY with no significant difference found between SBY and SBP. E-nose sensors were able to easily discriminate between the three sample types, and several strong correlations were observed between sensor 3 and some VOCs such as benzaldehyde 4-(1-methylethyl)-, hexanoicpyraz acid, heptanoic acid, nonanoic acid, and styrene. Of the 62 VOCs identified five were related to berry aroma and fifteen to fruity aroma perhaps accounting for the berry aroma and flavor perceived by the descriptive analysis panel. Bioactive phenolic compounds detected by NMR in the SBP and SBY included baicalein, chlorogenate, gallic acid, p-coumaric acid, and syringic acid confirming functional properties for the SBY.

This low fat functional dairy product with added phenolic contents and higher antioxidant capacity would be a nutritious dietary option for health-conscious consumers.

Data availability statement

The original contributions presented in the study are included in the article/supplementary material, further inquiries can be directed to the corresponding author/s.

Ethics statement

The studies involving humans were approved by the Joint Faculty Ethics Research Board of the University of Manitoba (Protocol # J2017:059) to conduct both the descriptive analysis and consumer acceptance panel. The studies were conducted in accordance with the local legislation and institutional requirements. The participants provided their written informed consent to participate in this study.

Author contributions

DR: Formal analysis, Investigation, Methodology, Project administration, Supervision, Validation, Visualization, Writing – original draft, Writing – review & editing. JT: Formal analysis, Methodology, Project administration, Validation, Writing – review & editing. SS-I: Methodology, Software, Validation, Writing – original draft. AM: Data curation, Formal analysis, Methodology, Software, Validation, Writing – review & editing. AG: Conceptualization, Data curation, Formal analysis, Investigation, Methodology, Validation, Visualization, Writing – original draft, Writing – review & editing. GD: Conceptualization, Formal analysis, Methodology, Validation, Writing – original draft, Writing – review & editing. MA: Conceptualization, Data curation, Formal analysis, Funding acquisition, Investigation, Methodology, Project administration, Resources, Software, Supervision, Validation, Visualization, Writing – original draft, Writing – review & editing.

Funding

Conflict of interest

The authors declare that the research was conducted in the absence of any commercial or financial relationships that could be construed as a potential conflict of interest.

Publisher's note

All claims expressed in this article are solely those of the authors and do not necessarily represent those of their affiliated organizations, or those of the publisher, the editors and the reviewers. Any product that may be evaluated in this article, or claim that may be made by its manufacturer, is not guaranteed or endorsed by the publisher.

References

1. Jurikova T, Balla S, Sochor J, Pohanka M, Mlcek J, Baron M. Flavonoid profile of Saskatoon berries (*Amelanchier alnifolia* Nutt.) and their health promoting effects. *Molecules*. (2013) 18:12571–86. doi: 10.3390/molecules181012571

2. Agriculture and Agri-Food Canada, (2023). Statistical overview of the Canadian fruit industry 2023. Available at: https://agriculture.canada.ca/en/sector/horticulture/reports/statistical-overview-canadian-fruit-industry-2023 (Accessed November 19, 2024).

3. Zhao L, Huang F, Hui AL, Shen GX. Bioactive components and health benefits of Saskatoon berry. *J Diabetes Res*. (2020) 2020:1–8. doi: 10.1155/2020/3901636

4. Szpadzik E, Krupa T. The yield, fruit quality and some of nutraceutical characteristics of Saskatoon berries (*Amelanchier alnifolia* Nutt.) in the conditions of eastern Poland. *Agriculture*. (2021) 11:824. doi: 10.3390/agriculture11090824

5. Ozga JA, Saeed A, Wismer W, Reinecke DM. Characterization of cyanidin-and quercetin-derived flavonoids and other phenolics in mature Saskatoon fruits (*Amelanchier alnifolia* Nutt.). *J Agric Food Chem*. (2007) 55:10414–24. doi: 10.1021/jf072949b

6. Garg S, Leisso R, Kim SH, Mayhew E, Song M, Jarrett B, et al. Market potential and value-added opportunities of cold-hardy berries and small fruits in the intermountain west, USA. *J Food Sci*. (2023) 88:860–76. doi: 10.1111/1750-3841.16426

7. Cedillos R, Aleman RS, Page R, Olson DW, Boeneke C, Prinyawiwatkul W, et al. Influence of hesperidin on the Physico-chemical, microbiological and sensory characteristics of frozen yogurt. *Food Secur*. (2024) 13:808. doi: 10.3390/foods13050808

8. Butorova L, Vitova E, Polovka M. Comparison of volatiles identified in Aronia melanocarpa and *Amelanchier alnifolia* using solid-phase microextraction coupled to gas chromatography-mass spectrometry. *J Food Nutri Res*. (2016) 55:57–68.

9. Zhao R, Xie X, Le K, Li W, Moghadasian MH, Beta T, et al. Endoplasmic reticulum stress in diabetic mouse or glycated LDL-treated endothelial cells: protective effect of Saskatoon berry powder and cyanidin glycans. *J Nutr Biochem*. (2015) 26:1248–53. doi: 10.1016/j.jnutbio.2015.05.015

10. Zhao R, Xiang B, Dolinsky VW, Xia M, Shen GX. Saskatoon berry powder reduces hepatic steatosis and insulin resistance in high fat-high sucrose diet-induced obese mice. *J Nutr Biochem*. (2021) 95:108778. doi: 10.1016/j.jnutbio.2021.108778

11. Vatanparast H, Islam N, Patil RP, Shamloo A, Keshavarz P, Smith J, et al. Consumption of yogurt in Canada and its contribution to nutrient intake and diet quality among Canadians. *Nutrients*. (2019) 11:1203. doi: 10.3390/nu11061203

12. Agriculture Canada. (2005). National Dairy Code-Production and processing requirements. Fourth edition amended July, 2005. Schedule III pg 28. Available at: https://agriculture.canada.ca/sites/default/files/legacy/resources/prod/dairy/pdf/National_Dairy_Code_Part_II-III_(2005)_e.pdf (Accessed November 15, 2023).

13. Stone H, Bleibaum RN, Thomas HA. "Descriptive analysis". In: Sensory evaluation practices. *5th* ed. London, UK: Academic Press (2021). 235–95.

14. Fahmi R, Ryland D, Sopiwnyk E, Aliani M. Sensory and physical characteristics of pan bread fortified with thermally treated split yellow pea (*Pisum sativum* L.) flour. *J Food Sci*. (2019) 84:3735–45. doi: 10.1111/1750-3841.14908

15. Grant J, Ryland D, Isaak CK, Prashar S, Siow YL, Taylor CG, et al. Effect of vitamin D-3 fortification and Saskatoon berry syrup addition on the flavor profile, acceptability, and antioxidant properties of rooibos tea (*Aspalathus linearis*). *J Food Sci*. (2017) 82:807–17. doi: 10.1111/1750-3841.13646

16. Bhowmik P, Yan W, Hodgins C, Polley B, Warkentin T, Nickerson M, et al. CRISPR/Cas 9-mediated lipoxygenase gene-editing in yellow pea leads to major changes in fatty acid and flavor profiles. *Front Plant Sci*. (2023) 14:1246905. doi: 10.3389/fpls.2023.1246905

17. Fahmi R, Ryland D, Sopiwnyk E, Malcolmson LJ, Ievari-Shariati S, McElrea A, et al. Effect of Revtech thermal processing on volatile organic compounds and chemical characteristics of split yellow pea (*Pisum sativum* L.) Flour. *J. Food Sci*. (2021) 86:4330–53. doi: 10.1111/1750-3841.15913

18. Bilbao-Sainz C, Sinrod AJG, Chiou BS, McHugh T. Functionality of strawberry powder on frozen dairy desserts. *J Texture Stud*. (2019) 50:556–63. doi: 10.1111/jtxs.12464

19. Lachowicz S, Swieca M, Pejcz E. Improvement of health-promoting functionality of rye bread by fortification with free and microencapsulated powders from *Amelanchier alnifolia* Nutt. *Antioxidants*. (2020) 9:614. doi: 10.3390/antiox9070614

20. Bezerra M, Araujo A, Santos K, Correia R, Bezerra M, Araujo A, et al. Caprine frozen yoghurt produced with fresh and spray dried jambolan fruit pulp (*Eugenia jambolana* lam) and *Bifidobacterium animalis* subsp. lactis BI-07. *LWT-Food Sci Tech*. (2015) 62:1099–104. doi: 10.1016/j.lwt.2015.01.049

21. Narayanan P, Chinnasamy B, Jin L, Clark S. Use of just-about-right scales and penalty analysis to determine appropriate concentrations of stevia sweeteners for vanilla yogurt. *J Dairy Sci*. (2014) 97:3262–72. doi: 10.3168/jds.2013-7365

22. Isik U, Boyacioglu D, Capanoglu E, Erdil DN. Frozen yogurt with added inulin and isomalt. *J Dairy Sci*. (2011) 94:1647–56. doi: 10.3168/jds.2010-3280

23. Soukoulis C, Tzia C. Impact of the acidification process, hydrocolloids and protein fortifiers on the physical and sensory properties of frozen yogurt. *Int J Dairy Tech*. (2008) 61:170–7. doi: 10.1111/j.1471-0307.2008.00385.x

24. Rezaei R, Khomeiri M, Kashaninejad M, Aalami M. Effects of guar gum and arabic gum on the physicochemical, sensory and flow behaviour characteristics of frozen yoghurt. *Inter J Dairy Tech*. (2011) 64:563–8. doi: 10.1111/j.1471-0307.2011.00705.x

25. Saleena LAK, Song AA, Yusof YA, In LLA, Lin NK, Pui LP. Development of optimized functional clove fortified probiotic yoghurt. *J Food Sci Technol*. (2024) 61:1343–54. doi: 10.1007/s13197-023-05904-y

26. Liu C, Yang P, Wang P, Song H. Identification of odor compounds and odor-active compounds of yogurt using DHS, SPME, SAFE, and SBSE/GC-O-MS. *Food Sci Tech*. (2022) 154:112689. doi: 10.1016/j.lwt.2021.112689

27. Goldberg E, Ryland D, Eskin MNA, Aliani M. "Functional foods and chronic diseases prevalent in North America and globally". In: M Aliani and MNA Eskin, editors. Functional foods and chronic disease: Role of sensory, chemistry and nutrition. London, UK: Academic Press (2024). p. 1–9.

28. Gorzelany J, Kapusta I, Zardzewialy M, Belcar J. Effects of ozone application on microbiological stability and content of sugars and bioactive compounds in the fruit of the Saskatoon berry (*Amelanchier alnifolia* Nutt.). *Molecules*. (2022) 27:6446. doi: 10.3390/molecules27196446

29. Dudonné S, Dubé P, Anhê F, Pilon G, Marette A, Lemire M, et al. Comprehensive analysis of phenolic compounds and abscisic acid profiles of twelve native Canadian berries. *J Food Comp Anal*. (2015) 44:214–24. doi: 10.1016/j.jfca.2015.09.003

30. Liao H, Ye J, Gao L, Liu Y. The main bioactive compounds of Scutellaria baicalensis Georgi. For alleviation of inflammatory cytokines: a comprehensive review. *Biomed Pharmacother*. (2021) 133:110917. doi: 10.1016/j.biopha.2020.110917

31. Nguyen V, Taine EG, Meng D, Cui T, Tan W. Chlorogenic acid: a systematic review on the biological functions, mechanistic actions, and therapeutic potentials. *Nutrients*. (2024) 16:924. doi: 10.3390/nu16070924

32. Kahkeshani N, Farzaei F, Fotouhi M, Alavi SS, Bahramsoltani R, Naseri R, et al. Pharmacological effects of gallic acid in health and diseases: a mechanistic review. *Iran J Basic Med Sci*. (2019) 22:225–37. doi: 10.22038/ijbms.2019.32806.7897

33. Pei K, Ou J, Huang J, Ou S. P-Coumaric acid and its conjugates: dietary sources, pharmacokinetic properties and biological activities. *J Sci Food Agric*. (2016) 96:2952–62. doi: 10.1002/jsfa.7578

34. Srinivasulu C, Ramgopal M, Ramanjaneyulu G, Anuradha CM, Suresh KC. Syringic acid (SA) – a review of its occurrence, biosynthesis, pharmacological and industrial importance. *Biomed Pharmacother*. (2018) 108:547–57. doi: 10.1016/j.biopha.2018.09.069

Frontiers in
Nutrition

Explores what and how we eat in the context
of health, sustainability and 21st century food
science

A multidisciplinary journal that integrates research
on dietary behavior, agronomy and 21st century
food science with a focus on human health.

Discover the latest
Research Topics

See more →

frontiers | Research Topics